

**Modelling the origin and fate of carbon in  
the aquatic continuum**

**WIM JOOST VAN HOEK**

**UTRECHT STUDIES IN EARTH SCIENCES**

**No. 262**

ISBN: 978-90-6266-631-7

Utrecht Studies in Earth Sciences (USES): 262

Cover formatting and placement: M. Stoete

Cover photo: W.J. van Hoek

Cover description: View on the Lower Rhine and his floodplains from “de  
Wageningse berg” in Wageningen, the Netherlands

Printed in the Netherlands by Ipskamp Enschede

Copyright © W.J van Hoek, 2022

All rights reserved. No part of this publication may be reproduced in any form, by  
print or photo print, microfilm or any other means, without written permission by  
the publishers

# **Modelling the origin and fate of carbon in the aquatic continuum**

## **Modellering van oorsprong en eindpunt van koolstof in het aquatisch continuüm**

(met een samenvatting in het Nederlands)

### **Proefschrift**

ter verkrijging van de graad van doctor aan de  
Universiteit Utrecht  
op gezag van de  
rector magnificus, prof.dr. H.R.B.M. Kummeling,  
ingevolge het besluit van het college voor promoties  
in het openbaar te verdedigen op

woensdag 21 december 2022 des middags te 12.15 uur

door

**Willem Johannes van Hoek**

geboren op 5 juli 1987  
te Vlaardingen

## **Promotors**

Prof. dr. J.B.M. Middelburg

Prof. dr. A.F. Bouwman

## **Members of the dissertation committee**

Prof. dr. S.C. Dekker

Universiteit Utrecht, GEO, Global Ecohydrology and Sustainability

Prof. dr. K.E.R. Soetaert

Universiteit Utrecht, GEO, Geochemistry

Prof. dr. P.A.G. Regnier

Université Libre de Bruxelles

Prof. dr. P. Friedlingstein

University of Exeter

Prof. dr. D.P. van Vuuren

Universiteit Utrecht, GEO, Environmental Sciences

Prof. dr. J.H.P. de Bresser

Universiteit Utrecht, GEO, Experimental rock deformation

This thesis was financially supported by the Dutch Research Council (NWO)  
by means of The New Delta 2014 ALW project no. 869.15.014

Voor mijn liefdevolle ouders



“All models are wrong, but some are useful”

George E.P. Box

# Contents

## Chapter 1

**General introduction and outline** 1

## Chapter 2

**Exploring spatially explicit changes in carbon budgets of global river basins during the 20th century** 15

Wim Joost van Hoek, Junjie Wang, Lauriane Vilmin, Arthur H.W. Beusen, José M. Mogollón, Gerrit Müller, Philip A. Pika, Xiaochen Liu, Joep J. Langeveld, Alexander F. Bouwman, Jack J. Middelburg  
*Environ. Sci. Technol.* (2021);  
<https://doi.org/10.1021/acs.est.1c04605>

## Chapter 3

**Global freshwater CO<sub>2</sub> emissions have increased as a result of rising terrestrial carbon inputs** 95

Wim Joost van Hoek, Joep J. Langeveld, Lauriane Vilmin, Xiaochen Liu, Arthur H.W. Beusen, José M. Mogollón, Alexander F. Bouwman, Jack J. Middelburg

## Chapter 4

**DISC-CARBON: A five decade (1950-2000) carbon cycle simulation of the stream network of the Rhine basin** 127

Wim Joost van Hoek, Lauriane Vilmin, Arthur H.W. Beusen, José M. Mogollón, Xiaochen Liu, Joep J. Langeveld, Alexander F. Bouwman, Jack J. Middelburg



|                         |  |            |
|-------------------------|--|------------|
| <b>Chapter 5</b>        |  |            |
|                         | <b>Carbon in inland waters; integrating freshwater systems into the global anthropogenic carbon budget</b> | <b>149</b> |
|                         | Wim Joost van Hoek, Joep J. Langeveld, Alexander F. Bouwman, Jack J. Middelburg                            |            |
| <b>Synthesis</b>        |  | <b>171</b> |
| <b>Synthese</b>         | <b>Dutch translation of summary</b>  | <b>179</b> |
| <b>Acknowledgements</b> |  | <b>189</b> |
| <b>Curriculum Vitae</b> |  | <b>191</b> |

## Chapter 1

### General introduction and outline

Greenhouse gas emissions induced by fossil fuel combustion, cement production, deforestation and other human activities, are likely to lead to additional global temperature rise over the 21st century between 0.3°C and 4.8° (Lee et al., 2021). Global temperature rise has far reaching consequences for the earth system, including sea level rise, biodiversity loss and changing weather patterns with increased risk of extreme events such as periods of intense precipitation, flooding, heat waves and drought periods.

Carbon dioxide (CO<sub>2</sub>) contributes 71% to total human-induced global warming potential (CO<sub>2</sub> equivalents) of all greenhouse gas emissions to the atmosphere (Crippa et al., 2021). The importance of CO<sub>2</sub> in the climate problem drives the interest in the global carbon (C) cycle. Global C cycle research focuses on identifying important C sources and sinks in the earth system, and how these fluxes change over time. Quantification of relevant fluxes supports improvement of climate change projections and more effective climate mitigation policies.

The earth system is traditionally considered as a system with an atmosphere, a land and an ocean component, being major reservoirs through which C circulates (Mackenzie and Lerman, 2006; Houghton, 2007; Ciais et al., 2013a; Canadell et al., 2021), see figure 1. Carbon is being exchanged among and transformed within these components through a wide range of biological, chemical and physical processes, interactions and feedbacks, occurring at time scales ranging from sub-daily to millennia.

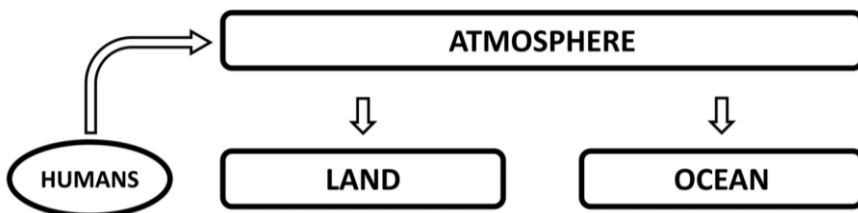


**Figure 1. Simplified conventional major budget components in global C cycling**

Large-scale and long-term quantifications of C fluxes largely rely on model simulations (Canadell et al., 2021). Conventional earth system models (ESM) are used to describe the C budget for each compartment and fluxes between them. However, ESM's have been omitting C transport and processing in inland waters despite the fact that we know that inland waters are active modulators of C and nutrients (Billen et al., 1991). Global C cycle assessments used to consider inland waters to be passive corridors, transporting water and dissolved and suspended matter from the terrestrial biosphere to the ocean (Bolin, 1981; Siegenthaler and Sarmiento, 1993).

Cole et al. (2007) were the first to identify C cycling in inland waters as the missing link between the terrestrial biosphere and the oceans. Inclusion of inland waters in global C cycle assessments better appreciates the inter-connected nature of global C cycling components. The simplest way to depict the C budget of freshwater systems, in the context of human interference is shown in figure 2. Carbon is delivered from the terrestrial biosphere to inland waters before it is either emitted to the atmosphere, exported to the sea or stored in sediments (geosphere).

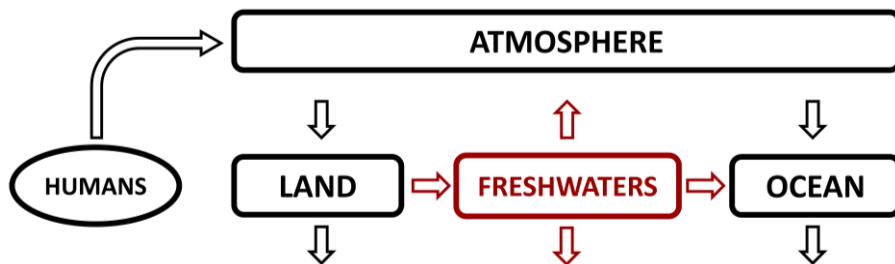


**Figure 2. Simplified conventional major budget components in global C cycling including freshwater systems**

The work of Cole et al. (2007) stimulated the C cycling research community to fill in the identified knowledge gaps. Cole et al. (2007) estimated an inland water outgassing flux of  $0.75 \text{ Pg C year}^{-1}$ . At the time, it was noticed that this estimate was “quite conservative” as a result of a lack of available gas transfer velocity data and a complexity induced uncertainty in seasonal dynamics of floodplains. These identified knowledge gaps were addressed by studies in the years that followed. Battin et al. (2009) stressed the importance of small streams, which increased the global inland water outgassing estimate to  $1.2 \text{ Pg C year}^{-1}$ . Tranvik et al. (2009) revised the global

lake emissions and hypothesized a global emission of 1.4 Pg C year<sup>-1</sup>. Raymond et al. (2013) were the first to report regional variations of CO<sub>2</sub> emissions from inland waters, by combining new estimates for inland water surface area and gas transfer velocities with calculated values of pCO<sub>2</sub> based on observational data from GloRiCh (Hartmann et al., 2014a). They reported a total global emission of 2.1 Pg C year<sup>-1</sup>.

**Table 1. Freshwater C budget estimates after Drake et al. (2018)**

|                                   |     |     |     |     |
|-----------------------------------|-----|-----|-----|-----|
| <i>Cole et al. 2007</i>           | 1.9 | 0.8 | 0.9 | 0.2 |
| <i>Battin et al. 2009</i>         | 2.7 | 1.2 | 0.9 | 0.6 |
| <i>Tranvik et al. 2009</i>        | 2.9 | 1.4 | 0.9 | 0.6 |
| <i>Regnier et al. 2013</i>        | 2.8 | 1.2 | 1.0 | 0.6 |
| <i>Raymond et al. 2013</i>        | 3.7 | 2.1 | 1.0 | 0.6 |
| <i>Borges et al. 2015</i>         | 4.3 | 2.8 | 1.0 | 0.6 |
| <i>Holgerson and Raymond 2016</i> | 4.5 | 3.0 | 1.0 | 0.6 |
| <i>Sawakuchi et al. 2017</i>      | 5.4 | 3.8 | 1.0 | 0.6 |

Borges et al. (2015) addressed a severe lack of observational data in the sub-Saharan region by reporting an extensive compilation of CO<sub>2</sub>-concentration data. Their work increased the global estimate by Raymond et al. (2013) by 0.6 Pg C year<sup>-1</sup> to a total CO<sub>2</sub> emission of 2.7 Pg C year<sup>-1</sup>. Further refinements were added by Holgerson & Raymond (2016) as they report emissions from small lakes to be 0.58 Pg C year<sup>-1</sup>, being 0.28 Pg C year<sup>-1</sup> higher than the estimate by Raymond et al. (2013), making total CO<sub>2</sub> from freshwaters 3 Pg C year<sup>-1</sup>. Sawakuchi et al. (2017) estimate that the Amazon basin upstream of Óbidos alone emits 1.4 Pg C year<sup>-1</sup>, which is 0.8 Pg C year<sup>-1</sup> more than the estimate by Raymond et al. (2013). With the inclusion of these insights, CO<sub>2</sub> emissions from inland waters worldwide would amount to 3.9 Pg C year<sup>-1</sup>.

The above estimates exclude methane (CH<sub>4</sub>) emission. Bastviken et al. (2011) estimate that freshwaters outgas ~0.075 Pg C year<sup>-1</sup>. From a C cycling perspective it is reasonable to neglect this flux. However, it is important to note that the greenhouse warming potential of CH<sub>4</sub> is a factor of 18 larger than that of CO<sub>2</sub> (Szopa et al., 2021) and should not be neglected when assessing the role of inland waters in the overall greenhouse gas budget of the atmosphere.

Global data on burial of organic carbon (OC) are limited. Cole et al. (2007) estimated a global burial flux of  $0.23 \text{ Pg C year}^{-1}$ , with a rather conservative  $0.18 \text{ Pg C year}^{-1}$  in reservoirs and  $0.05 \text{ Pg C year}^{-1}$  in lakes. Tranvik et al. (2009) showed for the first time that burial rates in inland waters exceed the sequestration rates on the ocean floor. Estimates vary from  $0.2 \text{ Pg C year}^{-1}$  to  $1.6 \text{ Pg C year}^{-1}$ ; most of this wide range is related to whether or not the sedimentation of particulate organic C in floodplains is included (Regnier et al., 2013). A global burial flux of  $0.6 \text{ Pg C year}^{-1}$  is adopted by most studies (Battin et al., 2009; Tranvik et al., 2009; Regnier et al., 2013; Drake et al., 2018).

Essentially, the global total C export of  $0.9 \text{ Pg C year}^{-1}$  estimate has not changed much over the past decades, although estimates of the total C flux and the different components are uncertain. Kempe (1979) estimated a flux of  $0.45 \text{ Pg C year}^{-1}$  as dissolved inorganic carbon (DIC).

A first estimate of OC export was conducted by Schlesinger & Melack (1981), which was  $0.37 \text{ Pg C year}^{-1}$ . A year later, Meybeck (1982) estimated a total of  $0.9 \text{ Pg C year}^{-1}$  being delivered to global coastal waters, with  $0.4 \text{ Pg C year}^{-1}$  as OC and  $0.5 \text{ Pg C year}^{-1}$  as DIC. Ludwig et al. (1996) used an empirical model to estimate global OC export of  $0.38 \text{ Pg C year}^{-1}$ . They refined the OC export by distinguishing dissolved OC (DOC) and particulate OC (POC). Aitkenhead & McDowell (2000) estimated a DOC export  $0.36 \text{ Pg C year}^{-1}$ . Reliable discharge monitoring and basin-scale nutrient export models (Beusen et al., 2005; Mayorga et al., 2010a) contributed to a robust and relatively well constrained global C export estimate.

The gross C fluxes through the interface of land/atmosphere (Gross photosynthesis  $113 \text{ Pg C year}^{-1}$  / Total respiration and fire  $111 \text{ Pg C year}^{-1}$  (Canadell et al., 2021)) and ocean/atmosphere (Gross photosynthesis  $54 \text{ Pg C year}^{-1}$  / Total respiration / outgassing  $54.6 \text{ Pg C year}^{-1}$  (Canadell et al., 2021)) are an order of magnitude larger than the flux between land and ocean (Ciais et al., 2013). However, net C fluxes between land/atmosphere and ocean/atmosphere, could be significantly offset by inland water C processing. The estimated net C flux from the atmosphere to the ocean is  $2.5 \pm 0.6 \text{ Pg C year}^{-1}$  (Friedlingstein et al., 2022), while that from atmosphere to land is  $3.4 \pm 0.9 \text{ Pg C year}^{-1}$  (Friedlingstein et al., 2022).

Drake et al. (2018) made an extensive overview of global or large-scale studies on freshwater C emissions (Table 1). With inland water C emissions estimates ranging from  $0.75 \text{ Pg C year}^{-1}$  to  $3.9 \text{ Pg C year}^{-1}$  and burial rates ranging from  $0.2 \text{ Pg C year}^{-1}$

---

to  $1.6 \text{ Pg C year}^{-1}$ , it is clear that freshwater C processing makes up a major component of the global C budget. Therefore, the effect of freshwater C cycling on global C cycling may be strongly underestimated.

A recent study on the changes in the land-ocean aquatic continuum carbon budget since the pre-industrial times (Regnier et al., 2013) acknowledges the importance of freshwaters system in the changing global C cycle. However, this book-keeping budget study did not account for the impact of many global changes such as climate change and human interference in the hydrology by dam construction. The fate of C in freshwater systems, either emission, burial or export, strongly depends on how C is processed after delivery to the water column.

There is a wide range of estimates of C export, emissions and burial, the numbers are poorly constrained and the long-term changes under several global change processes are only quantified but poorly understood. For example, the impact of massive land transformations such as forest conversion to grassland and arable land, and climate change on the delivery of C in different forms and via different pathways has not been investigated. At the scale of large river basins, it is not clear how dam construction influences the in-stream processing, burial and emission flux of C, both in the short term and longer term with ageing and progressing sediment and C burial of reservoirs.

A new process-based approach to describe the global freshwater C processing in river basins is helpful to identify key factors that act on global freshwater  $\text{CO}_2$  emissions, C burial or C export and can complement the existing budgeting approaches. There is a need for a method that integrates C delivery to freshwaters, in-stream processes and hydrological C transport from headwaters to downstream reaches and at the same time is applicable at the global scale.

In the past decades, major developments have been made in large scale freshwater biogeochemistry transport models. Nitrogen (N) and phosphorus (P) have been the focus of these types of models (Seitzinger et al., 2005; Mayorga et al., 2010b; Beusen et al., 2015a). Since transformations of nutrients and C are linked, the C/N ratio affects the denitrification rate (Her and Huang, 1995) and DOC affects the uptake of N and P from sediments (Stutter et al., 2020). Hence, in conceptual terms, model approaches could be akin. Three fundamentally different approaches to calculate export of a compound can be distinguished:

1. Lumped approach: uses a few empirical parameters to construct a statistical relationship between land factors and the export of any compound through the river mouth. The most well-known example is the Global NEWS framework (Seitzinger et al., 2005; Mayorga et al., 2010a). Here, regression models are used to mimic historical nutrient export and to forecast the export of nutrients into coastal oceans.
2. Distributed approach: calculates transport of any compound for each system component, soil, groundwater, riparian zones and lotic waters distinctly. Each subsystem requires a different calculation approach. Also, water is modeled explicitly as a medium for transport for dissolved and/or particulate compounds. Within this approach, processes can be described empirically, process-based or in a hybrid form. An example is the Riverstrahler model (Billen et al., 1994; Billen and Garnier, 2000; Garnier et al., 2000; Sferratore et al., 2005), which describes nutrient inputs in basin compartments, in-stream biological and chemical processes and riverine export.
3. Machine learning is an upcoming tool to simulate and predict biogeochemical components in historically well monitored freshwater/marine sites (Shen et al., 2019, Yu et al., 2020; Ludwig et al., 2022). Machine learning is helpful to obtain insights in complex interactions in dynamic systems, but their applications are heavily data-driven and therefore these methods can so far only be applied to thoroughly monitored sites.

Although statistical models have been useful to gain insights into orders of magnitudes of river export to global coastal waters and regional distributions of sources of nutrients, they have limits in some aspects. Lumped models are aggregated at the river basin scale and lump all retention processes in soils, groundwater and water bodies to estimate the export from the watershed. Distributed process-based models are generally spatially explicit, and can be applied to a variety of conditions, both temporally and spatially. Statistical relationships used in lumped approaches may not be applicable in future projections when conditions change to values outside the validity range of the regressions. This is an important disadvantage of lumped model approaches, especially because freshwater ecosystems have non-linear interactions and thresholds (Scheffer, 2004), or the relative importance of processes on the state of the system may change over time. Process-based, distributed models account better for the strongly integrated and spatial nature of biogeochemical interactions in freshwaters systems.

The basis of the modelling work presented in this thesis was established by Beusen et al. (2015), who presented the IMAGE 3.0 - GNM (Integrated Model to Assess the Global Environment - Global Nutrient Model) and more recently IMAGE 3.0 - DGNM (Dynamic Global Nutrient Model) was presented (Vilmin et al., 2020). The IMAGE 3.0 - GNM describes N and P delivery to lotic waters, retention, using the spiraling concept (Stream Solute Workshop, 1990) and export. Components of the environment were calculated in separate sub-modules; soil nutrient budget, nutrient delivery to lotic waters and finally water-column-biogeochemistry. The water as transport medium was calculated with the global hydrology model, PCR-GLOBWB (Van Beek et al., 2011).

The process-based IMAGE - DGNM presented by Vilmin et al. (2020) is the dynamic successor of IMAGE – GNM by replacing the strongly parameterized spiraling approach with an integrated explicit calculation of individual processes. The integrated calculation method is referred to as DISC (Dynamic In-Stream Chemistry). Separate DISC modules were developed for N, P, Silicon (Si; Liu, thesis, articles) and C (this thesis). DISC-CARBON is the principal tool developed in this thesis to address the main thesis objective to assess the spatial and temporal distribution of the global freshwater C budget as presented by Cole et al. (2007). More specifically, the objectives of this work are to:

- Quantify the spatial and temporal distribution of C delivery, emissions, burial and export for global freshwaters on the basis of consistent global datasets
- Identify key factors in the global freshwater C cycle
- Explore the long-term changes in global C delivery, emissions, burial and export in global freshwaters, and their role in the overall global C cycle during the 20<sup>th</sup> century

Chapter 2 presents a global implementation of DISC-CARBON in IMAGE – DGNM. The chapter presents in the main text the global freshwater C budget results that are being used throughout this thesis. In its extensive supplementary information, it presents the datasets used, the numerical scheme that is adopted to calculate interactions between forms of C in the water-column, deposition/resuspension processes and CO<sub>2</sub> emissions from the water surface. Validation results of the model for various basins are presented as well as an extensive sensitivity analysis for various major rivers worldwide.



Chapter 3 assesses global CO<sub>2</sub> emissions from freshwaters in more detail. It describes a 100 year global simulation with DISC-CARBON with a primary focus on CO<sub>2</sub> emissions. The study presented is different from existing global freshwater CO<sub>2</sub> emissions quantification studies because it is the first integrated approach to describe the long-term dynamics of the C fluxes along the river continuum. The delivery from the terrestrial soil-vegetation system, water-column primary production, carbon burial and processing leading to CO<sub>2</sub> exchange fluxes, and C export to the global coastal ocean over the course of the 20<sup>th</sup> century are calculated in a single numerical model framework with independent but consistent datasets.

Chapter 4 presents, as a proof of concept, the application of DISC-CARBON to the stream network of the Rhine basin for different computation schemes and evaluation of its characteristics through a sensitivity analysis.

Chapter 5 elaborates on the deeper consequences of assessing temporal changes in the freshwater C cycle as an integral contribution in temporal changes in the global C cycle. This work adds new insights in the global C cycle as it aims to reformulate the estimation of the global land and ocean C sink. By including the freshwater C budget in the global perspective, the work proposes to redefine the conventional approaches to estimating the land and ocean C sink.

Finally, chapter 6 wraps up all results of all previous chapters, compares results of DISC-CARBON with existing studies, and discusses the 20<sup>th</sup> century changes in the freshwater C cycle in the context of the overall global C cycle. Furthermore, chapter 6 discusses possible directions for further development of DISC-CARBON, directions of spatio-temporal freshwater quality modelling work in general and an outlook for future research regarding global freshwater C modelling and quantification.

## References

- Aitkenhead, J. A. and McDowell, W. H.: Soil C: N ratio as a predictor of annual riverine DOC flux at local and global scales, *Global Biogeochem. Cycles*, 14(1), 127–138, 2000.
- Bastviken, D., Tranvik, L. J., Downing, J. A., Crill, P. M. and Enrich-Prast, A.: Freshwater methane emissions offset the continental carbon sink, *Science* (80-. ), 331(6013), 50, 2011.
- Battin, T. J., Luyssaert, S., Kaplan, L. A., Aufdenkampe, A. K., Richter, A. and Tranvik, L. J.: The boundless carbon cycle, *Nat. Geosci.*, 2(9), 598–600, 2009.
- Van Beek, L. P. H., Wada, Y. and Bierkens, M. F. P.: Global monthly water stress: 1. Water balance and water availability, *Water Resour. Res.*, 47(7), 2011.
- Beusen, A. H. W., Dekkers, A. L. M., Bouwman, A. F., Ludwig, W. and Harrison, J.: Estimation of global river transport of sediments and associated particulate C, N, and P, *Global Biogeochem. Cycles*, 19(4), 2005.
- Beusen, A. H. W., Van Beek, L. P. H., Bouwman, L., Mogollón, J. M. and Middelburg, J. B. M.: Coupling global models for hydrology and nutrient loading to simulate nitrogen and phosphorus retention in surface water—description of IMAGE–GNM and analysis of performance, *Geosci. Model Dev.*, 8(12), 4045–4067, 2015.
- Billen, G. and Garnier, J.: Nitrogen transfers through the Seine drainage network: a budget based on the application of the ‘Riverstrahler’ model, *Hydrobiologia*, 139–150, 2000.
- Billen, G., Lancelot, C. and Meybeck, M.: N, P, and Si retention along the aquatic continuum from land and ocean, in *Dahlem workshop on ocean margin processes in global change*, pp. 19–44., 1991.
- Billen, G., Garnier, J. and Hanset, P.: Modelling phytoplankton development in whole drainage networks: the RIVERSTRAHLER Model applied to the Seine river system, *Hydrobiologia*, 289(1–3), 119–137, doi:10.1007/BF00007414, 1994.
- Bolin, B.: Carbon cycle modelling (SCOPE 16), 1981.
- Borges, A. V., Darchambeau, F., Teodoru, C. R., Marwick, T. R., Tamooh, F., Geeraert, N., Omengo, F. O., Guérin, F., Lambert, T., Morana, C., Okuku, E. and Bouillon, S.: Globally significant greenhouse-gas emissions from African inland waters, *Nat. Geosci.*, 8(8), 637–642, doi:10.1038/ngeo2486, 2015.
- Canadell, J. G., Monteiro, P. M. S., Costa, M. H., Da Cunha, L. C., Cox, P. M., Alexey, V., Henson, S., Ishii, M., Jaccard, S. and Koven, C.: Global carbon and other biogeochemical cycles and feedbacks, 2021.
- Ciais, P., Sabine, C., Bala, G., Bopp, L., Brovkin, V., Canadell, J., Chhabra, A., DeFries, R., Galloway, J. and Heimann, M.: Carbon and other biogeochemical cycles, in *Climate Change 2013 the Physical Science Basis: Working Group I Contribution*

- to the Fifth Assessment Report of the Intergovernmental Panel on Climate Change, vol. 9781107057, pp. 465–570, Cambridge University Press., 2013a.
- Ciais, P., Sabine, C., Bala, G., Bopp, L., Brovkin, V., Canadell, J., Chhabra, A., DeFries, R., Galloway, J. and Heimann, M.: Carbon and other biogeochemical cycles, in Climate Change 2013: The Physical Science Basis. Contribution of Working Group I to the Fifth Assessment Report of the Intergovernmental Panel on Climate Change, pp. 465–570, Cambridge University Press., 2013b.
- Cole, Prairie, Y. T., Caraco, N. F., McDowell, W. H., Tranvik, L. J., Striegl, R. G., Duarte, C. M., Kortelainen, P., Downing, J. A. and Middelburg, J. J.: Plumbing the global carbon cycle: integrating inland waters into the terrestrial carbon budget, *Ecosystems*, 10(1), 172–185, 2007.
- Crippa, M., Guizzardi, D., Solazzo, E., Muntean, M., Schaaf, E., Monforti-Ferrario, F., Banja, M., Olivier, J. G. J., Grassi, G. and Rossi, S.: GHG emissions of all world countries–2021 Report, Off. Eur. Union, Luxemb., 2021.
- Drake, T. W., Raymond, P. A. and Spencer, R. G. M.: Terrestrial carbon inputs to inland waters: A current synthesis of estimates and uncertainty, *Limnol. Oceanogr. Lett.*, 132–142, doi:10.1002/lol2.10055, 2018.
- Friedlingstein, P., Jones, M. W., O’Sullivan, M., Andrew, R. M., Bakker, D. C. E., Hauck, J., Le Quéré, C., Peters, G. P., Peters, W., Pongratz, J., Sitch, S., Canadell, J. G., Ciais, P., Jackson, R. B., Alin, S. R., Anthoni, P., Bates, N. R., Becker, M., Bellouin, N., Bopp, L., Chau, T. T. T., Chevallier, F., Chini, L. P., Cronin, M., Currie, K. I., Decharme, B., Djeutchouang, L. M., Dou, X., Evans, W., Feely, R. A., Feng, L., Gasser, T., Gilfillan, D., Gkritzalis, T., Grassi, G., Gregor, L., Gruber, N., Gürses, Ö., Harris, I., Houghton, R. A., Hurtt, G. C., Iida, Y., Ilyina, T., Luijckx, I. T., Jain, A., Jones, S. D., Kato, E., Kennedy, D., Klein Goldewijk, K., Knauer, J., Korsbakken, J. I., Körtzinger, A., Landschützer, P., Lauvset, S. K., Lefèvre, N., Lienert, S., Liu, J., Marland, G., McGuire, P. C., Melton, J. R., Munro, D. R., Nabel, J. E. M. S., Nakaoka, S.-I., Niwa, Y., Ono, T., Pierrot, D., Poulter, B., Rehder, G., Resplandy, L., Robertson, E., Rödenbeck, C., Rosan, T. M., Schwinger, J., Schwingshackl, C., Séférian, R., Sutton, A. J., Sweeney, C., Tanhua, T., Tans, P. P., Tian, H., Tilbrook, B., Tubiello, F., van der Werf, G. R., Vuichard, N., Wada, C., Wanninkhof, R., Watson, A. J., Willis, D., Wiltshire, A. J., Yuan, W., Yue, C., Yue, X., Zaehle, S. and Zeng, J.: Global Carbon Budget 2021, *Earth Syst. Sci. Data*, 14(4), 1917–2005, doi:10.5194/essd-14-1917-2022, 2022.
- Garnier, J., Billen, G. and Palfner, L.: Understanding the oxygen budget and related ecological processes in the river Mosel: The RIVERSTRAHLER approach, *Hydrobiologia*, 410, 151–166, doi:10.1023/A:1003894200796, 2000.
- Hartmann, J., Lauerwald, R. and Moosdorf, N.: A brief overview of the GLObal River CHemistry Database, GLORICH, *Procedia Earth Planet. Sci.*, 10, 23–27, 2014.

- Her, J.-J. and Huang, J.-S.: Influences of carbon source and C/N ratio on nitrate/nitrite denitrification and carbon breakthrough, *Bioresour. Technol.*, 54(1), 45–51, 1995.
- Holgerson, M. A. and Raymond, P. A.: Large contribution to inland water CO<sub>2</sub> and CH<sub>4</sub> emissions from very small ponds, *Nat. Geosci.*, 9(3), 222–226, doi:10.1038/ngeo2654, 2016.
- Houghton, R. A.: Balancing the global carbon budget, *Annu. Rev. Earth Planet. Sci.*, 35, 313–347, 2007.
- Kempe, S.: Carbon in the freshwater cycle, SCOPE 13. Glob. carbon cycle, (January 1979), 317 [online] Available from: <http://www.scopenvironment.org/downloadpubs/scope13/chapter12.html>, 1979.
- Lee, J.-Y., Marotzke, J., Bala, G., Cao, L., Corti, S., Dunne, J. P., Engelbrecht, F., Fischer, E., Fyfe, J. C. and Jones, C.: Future global climate: scenario-based projections and near-term information, IPCC., 2021.
- Ludwig, S. M., Natali, S. M., Mann, P. J., Schade, J. D., Holmes, R. M., Powell, M., Fiske, G. and Commane, R.: Using Machine Learning to Predict Inland Aquatic CO<sub>2</sub> and CH<sub>4</sub> Concentrations and the Effects of Wildfires in the Yukon-Kuskokwim Delta, Alaska, *Global Biogeochem. Cycles*, 36(4), e2021GB007146, 2022.
- Ludwig, W., Probst, J. and Kempe, S.: Predicting the oceanic input of organic carbon by continental erosion, *Global Biogeochem. Cycles*, 10(1), 23–41, 1996.
- Mackenzie, F. T. and Lerman, A.: Carbon in the Geobiosphere:-Earth's Outer Shell, Springer Science & Business Media., 2006.
- Mayorga, E., Seitzinger, S. P., Harrison, J. A., Dumont, E., Beusen, A. H. W., Bouwman, A. F., Fekete, B. M., Kroeze, C. and van Drecht, G.: Global nutrient export from WaterSheds 2 (NEWS 2): model development and implementation, *Environ. Model. Softw.*, 25(7), 837–853, 2010a.
- Mayorga, E., Seitzinger, S. P., Harrison, J. A., Dumont, E., Beusen, A. H. W., Bouwman, A. F., Fekete, B. M., Kroeze, C. and van Drecht, G.: Global nutrient export from WaterSheds 2 (NEWS 2): model development and implementation, *Environ. Model. Softw.*, 25(7), 837–853, 2010b.
- Meybeck, M.: Carbon, nitrogen, and phosphorus transport by world rivers, *Am. J. Sci.*, 282(4), 401–450, 1982.
- Raymond, P. A., Hartmann, J., Lauerwald, R., Sobek, S., McDonald, C., Hoover, M., Butman, D., Striegl, R., Mayorga, E. and Humborg, C.: Global carbon dioxide emissions from inland waters, *Nature*, 503(7476), 355–359, 2013.
- Regnier, P., Friedlingstein, P., Ciais, P., Mackenzie, F. T., Gruber, N., Janssens, I. A., Laruelle, G. G., Lauerwald, R., Luysaert, S. and Andersson, A. J.: Anthropogenic

- perturbation of the carbon fluxes from land to ocean, *Nat. Geosci.*, 6(8), 597–607, 2013.
- Sawakuchi, H. O., Neu, V., Ward, N. D., Barros, M. D. L. C., Valerio, A., Gagnemaynard, W., Cunha, A. C., Fernanda, D., Diniz, J. E., Brito, D. C., Krusche, A. V and Richey, J. E.: Carbon dioxide emissions along the lower Amazon River, *Front. Mar. Sci.*, 4(March), 1–12, doi:10.3389/fmars.2017.00076, 2017.
- Scheffer, M.: *Ecology of shallow lakes*, Springer., 2004.
- Schlesinger, W. H. and Melack, J. M.: Transport of organic carbon in the world's rivers, *Tellus*, 33(2), 172–187, 1981.
- Seitzinger, S. P., Harrison, J. A., Dumont, E., Beusen, A. H. W. and Bouwman, A. F.: Sources and delivery of carbon, nitrogen, and phosphorus to the coastal zone: An overview of Global Nutrient Export from Watersheds (NEWS) models and their application, *Global Biogeochem. Cycles*, 19(4), 2005.
- Sferratore, A., Billen, G., Garnier, J. and Théry, S.: Modeling nutrient (N, P, Si) budget in the Seine watershed: Application of the Riverstrahler model using data from local to global scale resolution, *Global Biogeochem. Cycles*, 19(4), 2005.
- Shen, J., Qin, Q., Wang, Y. and Sisson, M.: A data-driven modeling approach for simulating algal blooms in the tidal freshwater of James River in response to riverine nutrient loading, *Ecol. Modell.*, 398, 44–54, 2019.
- Siegenthaler, U. and Sarmiento, J. L.: Atmospheric carbon dioxide and the ocean, *Nature*, 365(6442), 119–125, 1993.
- Stream Solute Workshop: Concepts and methods for assessing solute dynamics in stream ecosystems, *J. North Am. Benthol. Soc.*, 95–119, 1990.
- Stutter, M., Graeber, D. and Weigelhofer, G.: Available dissolved organic carbon alters uptake and recycling of phosphorus and nitrogen from river sediments, *Water*, 12(12), 3321, 2020.
- Szopa, S., Naik, V., Adhikary, B., Artaxo, P., Berntsen, T., Collins, W. D., Fuzzi, S., Gallardo, L., Kiendler-Scharr, A. and Klimont, Z.: Short-lived climate forcers Climate Change 2021: The Physical Science Basis. Contribution of Working Group I to the Sixth Assessment Report of the Intergovernmental Panel on Climate Change ed V Masson-Delmotte et al, 2021.
- Tranvik, L. J., Downing, J. A., Cotner, J. B., Loiselle, S. A., Striegl, R. G., Ballatore, T. J., Dillon, P., Finlay, K., Fortino, K., Knoll, L. B., Kortelainen, P. L., Kutser, T., Larsen, S., Laurion, I., Leech, D. M., McCallister, S. L., McKnight, D. M., Melack, J. M., Overholt, E., Porter, J. A., Prairie, Y., Renwick, W. H., Roland, F., Sherman, B. S., Schindler, D. W., Sobek, S., Tremblay, A., Vanni, M. J., Verschoor, A. M., von Wachenfeldt, E. and Weyhenmeyer, G. A.: Lakes and reservoirs as regulators of

carbon cycling and climate, *Limnol. Oceanogr.*, 54(6), 2298–2314, doi:10.4319/lo.2009.54.6\_part\_2.2298, 2009.

Vilmin, L., Mogollón, J. M., Beusen, A. H. W., Van Hoek, W. J., Liu, X., Middelburg, J. J. and Bouwman, A. F.: Modeling process-based biogeochemical dynamics in surface fresh waters of large watersheds with the IMAGE-DGNM framework, *J. Adv. Model. Earth Syst.*, 12(11), e2019MS001796, 2020.

Yu, X., Shen, J. and Du, J.: A machine-learning-based model for water quality in coastal waters, taking dissolved oxygen and hypoxia in Chesapeake Bay as an example, *Water Resour. Res.*, 56(9), e2020WR027227, 2020

---

---

## Chapter 2

### Exploring spatially explicit changes in carbon budgets of global river basins during the 20th century

Wim Joost van Hoek<sup>1</sup>, Junjie Wang<sup>1</sup>, Lauriane Vilmin<sup>1,2</sup>, Arthur H.W. Beusen<sup>1,3</sup>, José M. Mogollón<sup>4</sup>, Gerrit Müller<sup>1</sup>, Philip A. Pika<sup>5</sup>, Xiaochen Liu<sup>1</sup>, Joep J. Langeveld<sup>1,3</sup>, Alexander F. Bouwman<sup>1,3</sup>, Jack J. Middelburg<sup>1</sup>

<sup>1</sup> Department of Earth Sciences, Utrecht University, P.O. Box 80021, 3508TA Utrecht, the Netherlands.

<sup>2</sup> Deltares, P.O. Box 177, Delft, the Netherlands. Postcode: 2600 MH.

<sup>3</sup> PBL Netherlands Environmental Assessment Agency, P.O. Box 30314, 2500GH the Hague, the Netherlands.

<sup>4</sup> Department of Industrial Ecology, Leiden University, P.O. Box 9518, 2300RA Leiden, the Netherlands.

<sup>5</sup> Faculty of Science, Earth and Climate, Free University of Amsterdam, de Boelelaan 1105, Amsterdam, the Netherlands. Postcode: 1081 HV.

*published as:*

van Hoek, W., Wang, J., Vilmin, L., Beusen, A., Mogollon, J., Müller, G., Pika, P., Liu, X., Langeveld, J., Bouwman, A. and Middelburg, J.: Exploring spatially explicit changes in carbon budgets of global river basins during the 20th century, *Environ. Sci. Technol.*, 2021.



**ABSTRACT**

Rivers play an important role in the global carbon (C) cycle. However, it remains unknown how long-term river C fluxes change due to climate, land-use and other environmental changes. Here, we investigated the spatiotemporal variations in global freshwater C cycling in the 20th century using the mechanistic IMAGE-Dynamic Global Nutrient Model extended with the Dynamic In-stream Chemistry Carbon module (DISC-CARBON) that couples river basin hydrology, environmental conditions and C delivery with C flows from headwaters to mouths. The results show heterogeneous spatial distribution of dissolved inorganic carbon (DIC) concentrations in global inland waters with the lowest concentrations in the tropics and highest concentrations in the Arctic and semi-arid and arid regions. Dissolved organic carbon (DOC) concentrations are less than 10 mg C liter<sup>-1</sup> in most global inland waters and are generally high in high-latitude basins. Increasing global C inputs, burial and CO<sub>2</sub> emissions reported in the literature are confirmed by DISC-CARBON. Global river C export to oceans has been stable around 0.9 Pg year<sup>-1</sup>. The long-term changes and spatial patterns of concentrations and fluxes of different C forms in the global river network unfold the combined influence of the lithology, climate and hydrology of river basins, terrestrial and biological C sources, in-stream C transformations, and human interferences such as damming

## 1 Introduction

Rivers are an important component of the global carbon (C) cycle and have been identified as a significant source of carbon dioxide (CO<sub>2</sub>) (Cole et al., 2007). Estimates of global inland-water CO<sub>2</sub> emissions range from 0.7 to 3.3 Pg C year<sup>-1</sup> (Cole et al., 2007; Battin et al., 2009; Tranvik et al., 2009; Bastviken et al., 2011; Raymond et al., 2013; Regnier et al., 2013; Borges et al., 2015a; Holgerson and Raymond, 2016; Sawakuchi et al., 2017); this large range not only implies uncertainty in global C budgets, but also illustrates our limited understanding of governing factors.

C in freshwater originates from terrestrial (allochthonous or external) sources and *in situ* aquatic (autochthonous or within system) production (Prairie and Cole, 2009). Allochthonous C is delivered to surface water as dissolved organic carbon (DOC) and particulate organic carbon (POC) from plant litter, surface runoff or leaching, and as dissolved inorganic carbon (DIC) produced during weathering or soil respiration (Drake et al., 2018). After delivery to streams, rivers, lakes or reservoirs, organic C can be metabolized to DIC, buried in sediment or transported towards the oceans (Cole et al., 2007). The DIC delivered to or generated within the system is transported downstream or emitted to the atmosphere as CO<sub>2</sub>, since aquatic systems are predominantly supersaturated in CO<sub>2</sub> relative to the atmosphere (Kempe, 1984; Frankignoulle et al., 1998; Duarte and Prairie, 2005). These early studies on CO<sub>2</sub> partial pressure and effluxes have been an impetus to develop global assessments on the importance of freshwater systems in global C cycling (Cole et al., 2007; Raymond et al., 2013; Li et al., 2017; Maavara et al., 2017; Marx et al., 2017).

Most studies on C processing in streams, rivers, lakes, reservoirs and floodplains have focused on local processes and cycling, including their sensitivity to perturbations, such as dam construction, eutrophication, land-use change, and climate change (Barnes and Raymond, 2009; Tranvik et al., 2009; Huang et al., 2012; Crawford et al., 2013; Wallin et al., 2013; Zhang et al., 2013; Crawford et al., 2016; Regnier et al., 2013; Wollheim et al., 2015; Hotchkiss et al., 2015; Holgerson and Raymond, 2016; Sawakuchi et al., 2017; Prokushkin et al., 2018; Raymond and Hamilton, 2018). However, these available snap-shot estimates often cover one single river, one specific year, or one specific C flux (mainly CO<sub>2</sub> fluxes or river organic carbon export), and fail to describe the complete C budget. Moreover, these studies do not resolve how C cycling in aquatic systems has changed because of changes in hydrology, climate and land use. Recently, Ran et al., (2021) reported a decrease in CO<sub>2</sub> emissions from Chinese inland waters because of a combination of environmental factors and it is unknown whether such a change is specific to China or of global importance.

Modelling approaches are useful to describe long-term changes in the C cycle that occurred in the past and to generate projections into the future. Many existing river biogeochemistry models use regressions by lumping data at the river-basin scale to quantify C export to coastal waters or CO<sub>2</sub> emission to the atmosphere for specific years (Ludwig et al., 1996a; Harrison et al., 2005; Beusen et al., 2005; Mayorga et al., 2010a; Aufdenkampe et al., 2011; Raymond et al., 2013; Massicotte et al., 2017; Liu et al., 2019; Baronas et al., 2020; Fabre et al., 2020; Rouhani et al., 2021). These lumped regression approaches are often based on a priori assumptions on the controlling factors or pre-selected datasets (Ludwig et al., 1996b; Beusen et al., 2005; Harrison et al., 2005; Mayorga et al., 2010a; Aufdenkampe et al., 2011; Raymond et al., 2013; Massicotte et al., 2017; Liu et al., 2019; Baronas et al., 2020; Fabre et al., 2020; Rouhani et al., 2021). Such models lack spatiotemporal inputs and dynamic hydrological constraints, thus fail to reflect temporal changes and only improve our understanding of the underlying processes at highly aggregated levels (e.g. at river-basin level or at one point in time). A few semi-mechanistic models that use some distributed inputs and in-stream processes have attempted to simulate the long-term changes in the riverine fluxes of certain C forms. For example, in the regional Terrestrial Ecosystem Model (TEM), the annual river DOC export to oceans in Arctic regions is simulated as leaching of DOC from soil in spring based on a series of environmental factors, which causes huge uncertainties in estimates and inapplicability to other rivers (Kicklighter et al., 2013). The TRIPLEX-hydrological routing algorithm model (TRIPLEX-HYDRA) couples natural organic C inputs from soil and river hydrology and uses DOC observations from literature to estimate the global riverine DOC export during 1951-2015, but the crucial in-stream C biogeochemical processes and all anthropogenic impacts including land-use change, wastewater discharge, dam construction, etc., are not considered (Li et al., 2019). The Dynamic Land Ecosystem Model (DLEM) includes multiple C forms and in-stream processes, and has been applied to some rivers in North America, but the potentially important processes of aquatic production, C burial, sediment dynamics, CO<sub>2</sub> exchange with the atmosphere in large waterbodies, and the impacts of floodplains and construction of dams and reservoirs are not included (Ren et al., 2015; Tian et al., 2015b, 2015a). The regional model Integrated Catchments Model for Carbon (INCA-C) is designed to simulate the processes of dissolved C, especially DOC, in boreal and temperate river basins, but sediment dynamics, POC dynamics and, anthropogenic impacts other than land cover are not considered (Futter et al., 2007; Xu et al., 2020).

The regional model ORCHILEAK simulates terrestrial C inputs, in-stream respiration and DOC decomposition, and transport of DOC and CO<sub>2</sub> along the terrestrial-aquatic continuum of the Amazon basin, but other C forms and dynamic processes are not included (Lauerwald et al., 2017a, 2020). The regional model Organic matter Removal and Export for Dissolved Organic Carbon (MORE-DOC) simulates riverine DOC processes in the Yangtze River for 1980-2015, but it relies on numerous observational data for calibration, and does not include other C forms and relevant processes (Lv et al., 2019). The regional process-based model National Integrated Catchment-based Ecohydrology (NICE)-BGC was recently applied to simulate the in-stream processing for DIC, DOC and POC in global 153 river basins for the period 1980-2015 with a 1°×1° spatial resolution, but the land-use change before the year 1992, impacts of dams and reservoirs, and processes relevant to sediment and C burial were not considered (Nakayama, 2017, 2020). Since these process-based models do not fully consider multiple C forms and their associated in-stream dynamic processes including C production, consumption, transformation, lateral transport and interaction at the water-sediment and water-air interfaces, they have limited capabilities of hindcasting the historical spatially-explicit riverine fluxes and concentration of multiple C forms on the global scale.

To describe the changing riverine C cycling resulting from the long-term interactions between land-use changes, interventions in hydrology (dam construction, reservoirs, water extraction), and wastewater discharge, we need a spatially explicit integrated model that describes biogeochemical processes coupled to hydrology and the terrestrial C cycle. In this paper, we implement freshwater C cycling in the process-based Dynamic In-stream Chemistry module (DISC) (i.e. DISC-CARBON), which is part of the Integrated Model to Assess the Global Environment (IMAGE (Stehfest et al., 2014)) - Dynamic Global Nutrient Model (IMAGE-DGNM (Vilmin et al., 2020)). This new model describes the spatial and temporal variability of C concentrations, transformations and fluxes based on the river basin hydrology, environmental conditions and C delivery from headwaters to mouths. The model calculates pCO<sub>2</sub>, CO<sub>2</sub> emissions, organic carbon burial and export of DIC, POC and DOC resulting from the balance of inputs, transfers and transformations, and observational data are only used for performance assessment and not for calibration. We employ DISC-CARBON to investigate long-term changes in concentrations and fluxes for DIC, DOC and POC, in the world's river network over the 20th century and via a sensitivity analysis identify the major drivers of C fluxes (export, burial and emission) for 5 major river basins.

## 2 Model and data used

### 2.1 DGNM framework

The DISC-CARBON module, part of the IMAGE-DGNM framework (Figure 1a), is an extension of the recently published DISC module (Vilmin et al., 2020) with a description of the riverine C cycle. IMAGE-DGNM builds on the IMAGE-GNM that uses the spiraling approach for describing global annual in-stream nitrogen (N) and phosphorus (P) retention for long time series (20<sup>th</sup> century). With defined sub-annual variations and speciation of C and nutrient delivery to river networks (Vilmin et al., 2018), and the integration of the new process-based DISC module which replaces the spiraling approach, the IMAGE-DGNM framework allows for the global simulation of transfers of multiple nutrient and C forms from land to coastal waters. IMAGE-DGNM provides a long-term global perspective on C and nutrient accumulation and consumption processes in landscapes within river basins. Apart from the sub-annual temporal scale and the representation of different nutrient and C forms, the description of re-mobilization processes of accumulated matter is a major innovation at this scale of analysis (with more details in Text SI1 in the Supporting Information). In the current version of the framework, input and output time steps range from monthly to yearly. In this paper, we used an annual temporal resolution at the global scale and compared results for annual and monthly resolution for the Rhine River basin. The spatial resolution of 0.5-by-0.5 degree matches that of the PCR-GLOBWB hydrology model which is part of the IMAGE-DGNM framework (Figure 1a). PCR-GLOBWB dynamically simulates the volumes, surface areas and discharges of the different waterbodies of river networks, including lakes, reservoirs and high-order ( $\geq 6$ ) streams (Van Beek et al., 2011; Sutanudjaja et al., 2018). Floodplains are assumed to exchange water in Strahler orders  $\geq 6$  and have a flow velocity of 10% of that in the mainstream. The discharge and characteristics of smaller streams are estimated for each 0.5 by 0.5-degree continental grid cell, based on runoff and the properties of high-order streams using the parameterization proposed by Wollheim et al. (2008).

Within the IMAGE-DGNM framework, the IMAGE model provides land cover data to PCR-GLOBWB and C delivery fluxes to DISC-CARBON. Climate data from ERA-40 re-analysis (Uppala et al., 2005) are used in PCR-GLOBWB for computing the water balance, runoff and discharge for each year. Carbon delivery includes POC, DOC, DIC (the sum of dissolved  $\text{CO}_2$ ,  $\text{HCO}_3^-$  and  $\text{CO}_3^{2-}$ ) and alkalinity (ALK) from wastewater, surface runoff, weathering, eroded soil material, and litterfall from vegetation in flooded areas (Figure 1a). The calculation of each of these input fluxes is described in Table SI1.

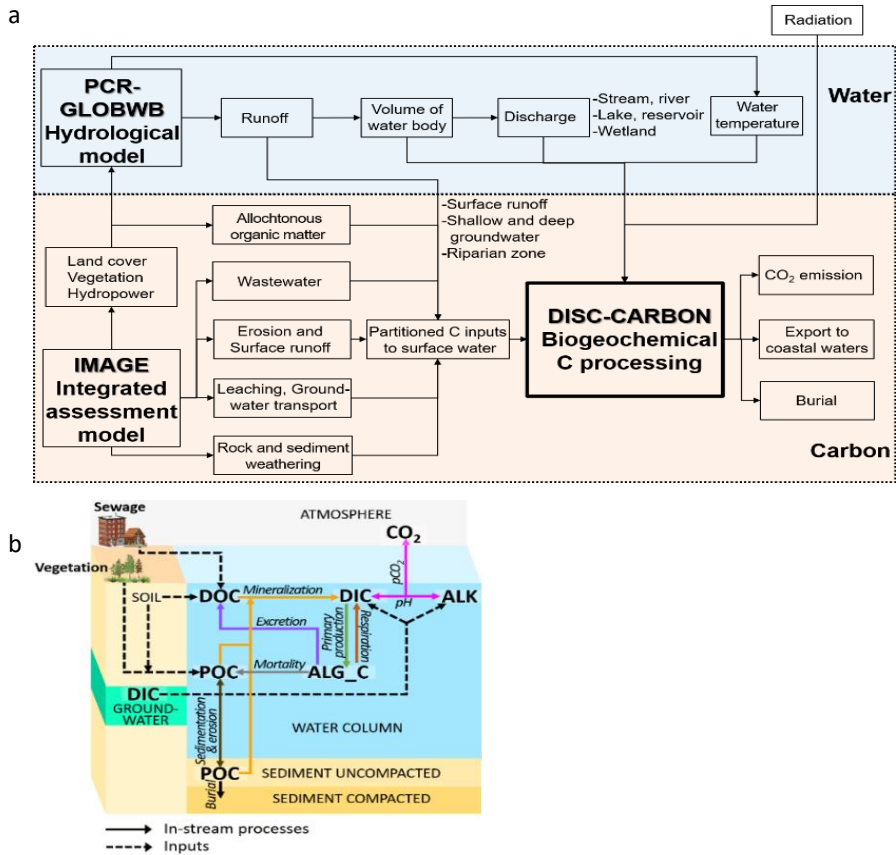


Figure 1. (a) Scheme of the IMAGE-DGNM framework including the DISC-CARBON module for the in-stream biogeochemical C transformation processes and (b) scheme of C sources, forms and biogeochemical transformations in all simulated waterbodies in the DISC-CARBON module. The formulae for each transformation process are listed in Table S12.

## 2.2 DISC-CARBON

After delivery of C to streams and rivers, the DISC-CARBON model calculates in-stream biogeochemistry, uptake by pelagic and benthic algae (ALG), burial, mineralization, CO<sub>2</sub> emission, and transport for all waterbodies from upstream grid cells down to the river mouth for each river basin at the global scale (Figure 1b). Particulate inorganic carbon (PIC), primarily calcium carbonate, is ignored in DISC-CARBON for simplification considering that PIC mainly originates from detrital old carbonates (Probst et al., 1994), that PIC transport flux is relatively limited compared with those of other C species (Huang et al., 2012, 2017; Li et al., 2017), and that its relocation within river basins does generally not affect the short-term biogeochemical C fluxes (Ciais et al., 2008). DISC-CARBON calculates the concentration of C species  $i$  for each time step, in each waterbody type (i.e. rivers of different stream orders, lake, reservoir or floodplain) of every cell, as an effect of biogeochemical ( $bgc$ ) interactions between C species and as a result of hydrological ( $hyd$ ) transport (between cells or waterbodies within the same grid cell), as follows:

$$\frac{dC_i}{dt_{tot}} = \begin{cases} \frac{dC_i}{dt_{bgc}} + \frac{dC_i}{dt_{hyd}} & \text{if species is dissolved or suspended in water column} \\ \frac{dC_i}{dt_{bgc}} & \text{if species is incorporated or attached to bed surface} \end{cases} \quad (1)$$

Hydrological advection of any dissolved or particulate C species  $i$  in the water column, being DIC, DOC, POC and ALG, is calculated as follows:

$$\frac{dC_i}{dt_{hyd}} = L_i - Q * [C_i] \quad (2)$$

where  $L_i$  is the upstream load (Mmol year<sup>-1</sup>) of species  $i$ ,  $Q$  is the water discharge (km<sup>3</sup> year<sup>-1</sup>) and  $[C_i]$  is the concentration of C species  $i$  (Mmol km<sup>-3</sup>). POC, when sedimented, is not transported until it is resuspended. Benthic algae are assumed to be attached to the streambed and are not transported downstream.

Model equations for C dynamics are listed in Table SI2, and model constants and parameters are listed in Tables SI3 and SI4. Subsequently, we briefly discuss the simulation of light limitation, primary production, DIC and DOC dynamics.

The biogeochemical transformations among DOC, POC and DIC depend on hydrology, temperature and radiation. Light limitation for primary production is calculated using a spatiotemporal distribution of solar radiation reaching the surface of the waterbody and water turbidity, caused by particulate matter, which controls light penetration through the water column (equations 1-7 in Table SI2). Primary production (equations 8-19 in Table SI2) depends on the biomass of the producers, their growth rates, temperature, and light and DIC availability. Similarly, respiration and excretion (biomass to DOC) are modeled as a fraction of primary producer biomass and depend on temperature.

POC dynamics is affected by delivery fluxes from erosion and litterfall, sedimentation and resuspension, primary production and mineralization. The mineralization of terrestrial organic matter with structural carbohydrates and lignins is slower than that of aquatic organic matter, which is rich in N and P (Middelburg, 2019). The role of associations with protective mineral surfaces is ignored (see e.g. (Lynch and Cotnoir Jr, 1956; Vogel et al., 2015; Freymond et al., 2018)). However, to account for the diversity in POC reactivity (Middelburg, 1989; Bianchi, 2011), DISC-CARBON distinguishes (1) allochthonous, terrestrial POC (with slow mineralization) and (2) aquatic, autochthonous POC (with fast mineralization) (Table SI2 equations 27-30).

The dynamics of DIC is described by equations 20-25 in Table SI2. External input of DIC in the DISC-CARBON module originates from weathering (Table SI1) and DIC is produced in-stream through mineralization of organic C forms and respiration of living biomass. DIC consumption occurs through primary production. Finally, DIC is added to or removed from the waterbody through CO<sub>2</sub> exchange with the atmosphere. Alkalinity (ALK) is generated by weathering of sediments and rocks and delivered to streams. ALK production and consumption by primary production, respiration, nitrification and calcium carbonate precipitation and dissolution within the stream network (Soetaert et al., 2007) are assumed to be negligible compared to the ALK inputs from weathering; the spatial and temporal resolution of the model does not allow calculating hyporheic ALK production and removal (Boulton et al., 1998a). Although ALK is the sum of excess bases in solution in natural environments, carbonate alkalinity (i.e. the bicarbonate and carbonate ions) tends to make up most alkalinity. In DISC-CARBON, ALK delivered to surface water is combined with DIC to calculate pCO<sub>2</sub> and pH.



Surface runoff and wastewater constitute external DOC sources (Table SI1). In-stream DOC production occurs through excretion by pelagic and benthic algae and DOC consumption occurs through mineralization. DOC dynamics is described by equations 26-46 in Table SI2.

## **2.3 Sensitivity analysis**

For a selection of the world's largest rivers (Amazon, Lena, Mississippi, Nile, and Yangtze), we calculated the sensitivity of the DISC-CARBON modeled average CO<sub>2</sub> emissions, C burial and C export (DOC, POC, DIC, ALG and their sum (total carbon, TC)) to the variation of 52 parameters, 8 environmental and 8 C delivery forcings. We used the Latin Hypercube Sampling method (Saltelli, 2000) and carried out 750 runs. Model sensitivity is expressed as the standardized regression coefficient (SRC). More details on this approach are provided in Text SI2.

## **2.4 Model performance assessment strategy**

The model performance is evaluated by comparing simulated concentrations of DIC, DOC and TC with measurements-based annual and 0.5-by-0.5 degree grid averages for a range of global rivers calculated from GloRiSe (Müller et al., 2021), GLORICH (Hartmann et al., 2019) and GEMS-GLORI (Meybeck and Ragu, 1997) databases. Available data have been selected for stations and years with at least 6 observations per year to represent the annual mean, while these measurements may include different sampling and analytical methods (which are not always recorded in the databases).

# **3 Results and discussion**

## **3.1 Model performance**

### **3.1.1 Model estimates and observations**

The comparison of the simulated concentrations of DIC, DOC and TC with available observational data in river basins since the 1940s shows that the concentrations of different C forms simulated by DISC-CARBON are in fair agreement with observations (Figures 2a-c). Most simulated DIC (89%) and DOC (90%) concentrations are within a factor of 2 of the observations at various stations in a range of global river basins, irrespective of the basin size (Figures 2a,b,e and SI1a). The simulated TC concentrations agree with the measurements for major rivers; for small rivers, 83%

of the simulated TC concentrations are within a factor of 2 of those measured, with a slight general overestimation (Figures 2c and SI1b). For data from river mouths, the simulated DIC ( $R^2 = 0.519$ ,  $p < 0.001$ ) and DOC concentrations ( $R^2 = 0.562$ ,  $p < 0.001$ ) show an even better agreement with observations, with over 97% of both within a factor of 2 (Figure SI2a-b). DISC-CARBON predictions of POC river export are consistent with observations for large global rivers ( $R^2 = 0.462$ ,  $p < 0.001$ ) (Figure 2d). Despite the limited available measurements of TC (i.e. all C forms measured simultaneously at the same location) at global river mouths compared with those of DIC and DOC, 97% of the simulated TC concentrations are within a factor of 2 of the measurements (Figure SI2c). Freshwaters are heavily under-sampled and the lack of representativeness of the few TC measurements available may also contribute to the minor mismatch. DISC-CARBON results are closer to the observations for river mouths than for upstream stations, because the simulation results at river mouths integrate the effect of processes over the entire river basins: the quality of input data is better at basin than single grid cell scale. For upstream stations, the spatial input data of DISC-CARBON can be uncertain due to the coarse resolution and available observational data may not be representative due to incomplete temporal coverage within each year.

We also tested the model performance with the Bland-Altman approach (Bland and Altman, 1986), i.e. examining the difference between the observation and prediction (residual) with the mean of the predicted and observed values. The results show that the predictions agree with observations (Figures 2e, SI1a-b) and there is no systematic error for DIC (Figure 2f), DOC (Figure SI1c) and TC (Figure SI1d).

This fair agreement between model predictions and independent observations gives confidence to the overall approach because DISC-CARBON is a mechanistic model and not a regression model aiming to reduce differences between observations and estimates.

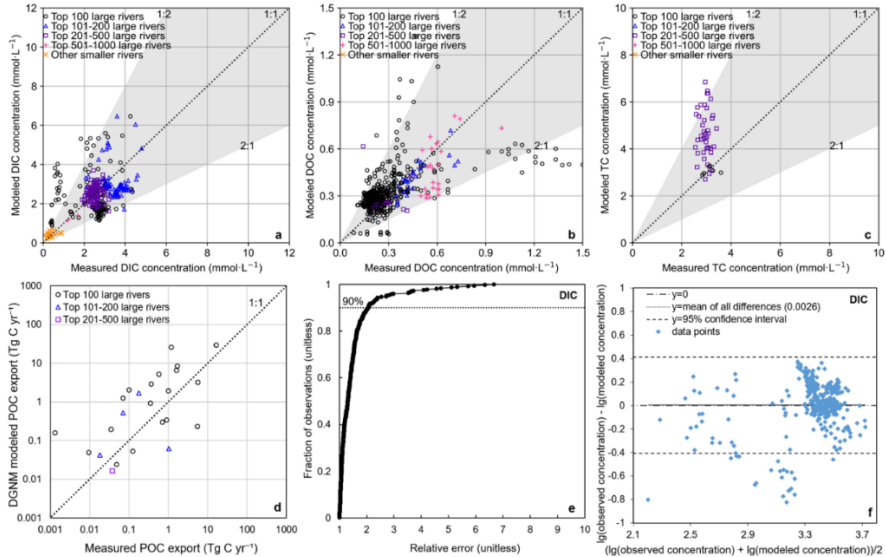


**Figure 2.** Validation of DISC-CARBON against observed concentrations of (a) DIC, (b) DOC and (c) TC (DIC + DOC + POC) at different stations with at least 6 measurements within the year considered for numerous global rivers of various sizes; when more than one station occurs within a grid cell, the mean of their annual average concentrations is used for comparison; (d) validation of DISC-CARBON simulated POC export to the coastal oceans against observation data from the late 1980s to early 1990s; (e) fraction of observations plotted against the ratio of prediction: observation (relative error) for DIC; (f) comparison of the difference between predicted and observed DIC concentrations (in  $\mu\text{mol liter}^{-1}$ ) with the mean of predicted and observed values according to Bland and Altman (1986). Similar figures for DOC and TC to (e) and (f) for DIC are in Figures SI1a-d, respectively. DIC data covering 1942-2000, DOC data covering 1973-2000 and TC data (for Rhine and Weser Rivers) covering 1978-1998 are from GloRiSe (Müller et al., 2021) and GLORICH (Hartmann et al., 2019); POC observation data are from GEMS-GLORI (Meybeck and Ragu, 1997). Rivers are sorted based on their catchment areas.

### 3.1.2 Sensitivity analysis

Since our model is based on mass conservation, the modeled global C fluxes are internally consistent and temporal changes are the combined result of the changes in hydrology, climate and C inputs from the land. However, the uncertainties in the fluxes can be as large as their temporal changes, which calls for an analysis of the sensitivity of modelled fluxes to variation of model parameters. The results of this sensitivity analysis for those parameters with a significant and important influence on the simulated CO<sub>2</sub> efflux, C burial and export of different C forms are presented in Table S15 for the Amazon (a), Lena (b), Mississippi (c), Nile (d), and Yangtze (e). These rivers represent a range in climates, hydrology and human activity (land use, dam construction, etc.). In this way, not only the variations of parameters driving changes in C cycling but also their differences among river basins are examined. We present values of the Standard Regression Coefficient (SRC), which quantify the sensitivity of the model to parameters (see Tables S15). Results for 32 input parameters are shown that have a significant and important effect on one of the output variables listed in Table S15 in any of the five rivers analyzed.

For the five rivers analyzed, the role of discharge (Q) is important for almost all C fluxes as it influences the flow velocity and time available for transformations, with a commonly negative influence of increasing discharge on CO<sub>2</sub> efflux and C burial, and a positive influence (though limited in some cases) on the export of the various C forms (because there is less burial and less CO<sub>2</sub> efflux), which is consistent with the findings in other studies (Gao et al., 2012; Sun et al., 2017; Lv et al., 2019; Fabre et al., 2020; Lauerwald et al., 2020; Xu et al., 2020). An increase in temperature positively influences CO<sub>2</sub> efflux (SRC of 0.28 for the Amazon to 0.39 in the Yangtze and 0.65 in the Nile) and lowers C burial (not important in the Lena due to low temperatures and low production rates, and SRC values of -0.43 to -0.83 in the other rivers); it also negatively impacts export of primarily DOC (high negative values of -0.43 for the Lena and -0.73 for the Amazon) and POC (-0.22 for the Nile to -0.73 for the Amazon). The parameters related to phytoplankton growth (e.g. solar radiation, maximum rates of phytoplankton growth or mortality) are important in most of the rivers for export of POC and algal biomass (SRC values of 0.22-0.30, Tables S15a-e), but also exert an influence on DOC export, C burial and CO<sub>2</sub> emission in rivers heavily controlled by dams and reservoirs, such as the Mississippi (Bianchi et al., 2007; Maavara et al., 2017) and Yangtze (Li et al., 2015; Wu et al., 2018; Ran et al., 2021). Maximum algal growth rates influence CO<sub>2</sub> exchange negatively (SRC of -0.36 for Mississippi and Yangtze) and burial positively (SRC of 0.48 for Mississippi and 0.43 for

Yangtze); the sensitivity to variation of parameter values for algal growth is much smaller in the other rivers considered (Tables SI5c and e).

Terrestrial organic inputs generally have a small positive effect on the POC export (highest SRC values of 0.41-0.43 for the Mississippi, Nile and Yangtze, Tables SI5c,d,e). Differences in geomorphology play a role in the importance of autochthonous phytoplankton growth. For the Amazon River and its tributaries, floodplains are major components (Quay et al., 1992; Moreira-Turcq et al., 2003; Melack et al., 2009) and have large standing stocks of biomass and limited agricultural land use, which cause large C inputs to the water during flooding periods in forested areas (POC input from litterfall, with high SRC of 0.85 for CO<sub>2</sub> emission). In contrast, the Mississippi and Yangtze Rivers have extensive agricultural areas (Chen and Simons, 1986; Liu et al., 2020), and floodplain processes are less important (SRC of 0.39 and 0.2 for CO<sub>2</sub>, respectively, Tables SI5c and e) than in the Amazon. With its extensive forested area in upstream areas, the Nile basin also has a high SRC of 0.58 for CO<sub>2</sub> emission due to variation in litterfall (Table SI5d). Finally, alkalinity inputs from groundwater have a significant and important influence on DIC export in all analyzed rivers (with SRC values ranging from 0.77 for the Amazon to 1.0 for the Rhine), and in most cases, there is also a large influence on total C export, especially where DIC is the major component of total C in the rivers.

**Table 1. Average yearly CO<sub>2</sub> emission, total C burial and total C export in Tg C year<sup>-1</sup> by the Amazon, Lena, Mississippi, Nile and Yangtze Rivers over the period 1995-2000 simulated by DISC-CARBON with the ranges covering 95% of the outcomes (between brackets in %) based on the assumed ranges in input parameters listed in Text SI2.**

| <i>Rivers</i>      | <i>CO<sub>2</sub> emission</i> | <i>TC burial</i> | <i>TC export</i> |
|--------------------|--------------------------------|------------------|------------------|
| <i>Amazon</i>      | 975.2 (±5%)                    | 33.2 (±15%)      | 89.9 (±13%)      |
| <i>Lena</i>        | 2.6 (±11%)                     | 0.03 (±13%)      | 4.9 (±4%)        |
| <i>Mississippi</i> | 20.7 (±11%)                    | 18.1 (±8%)       | 19.1 (±5%)       |
| <i>Nile</i>        | 1.6 (±11%)                     | 0.1 (±11%)       | 2.7 (±5%)        |
| <i>Yangtze</i>     | 2.6 (±16%)                     | 0.1 (±21%)       | 13.4 (±13%)      |

Although the small parameter ranges used to calculate the model sensitivity are by no means uncertainty ranges, the approach allows for calculating the ranges covering 95% of the outcomes. We illustrate the model behaviour with the estimates and their ranges for the five rivers in Table 1. Results indicate that the ranges vary among rivers and also among output variables. The CO<sub>2</sub> emissions vary less in the Amazon River than in the other rivers, the variation in C burial is largest for the Yangtze River, and that of C export is largest in the Amazon and Yangtze Rivers. However, our analysis demonstrates that relatively narrow ranges of 5% for all inputs and parameters except temperature (Text SI2) can lead to large variations in the model output.

### **3.2 DIC and DOC concentrations in global inland waters**

After the above performance evaluation, we simulated C cycling in global river basins for the period 1900-2000 at a yearly time step. The results of dissolved C concentrations in global inland waters with a 0.5°×0.5° spatial resolution are shown in Figures 4 and SI3.

#### **3.2.1 DIC concentration patterns**

In 2000, simulated DIC concentrations in global inland waters show a wide range with distinct regions having high or low concentrations (Figure 3a). The lowest simulated DIC concentrations are in the equatorial region between 10°N and 10°S, with a range of 10-30 mg C liter<sup>-1</sup> in the island area of Oceania and southern Asia and even lower levels (minimum values <10 mg C liter<sup>-1</sup>) in the continental areas of Africa and South America. These results agree with the observed mean DIC concentrations of 8 mg C liter<sup>-1</sup> in the Amazon River and 3 mg C liter<sup>-1</sup> in the Congo River (Probst et al., 1994). Huang et al. (2012) reported a mean DIC concentration of 8 mg C liter<sup>-1</sup> for 175 equatorial rivers. Our results are also consistent with mean DIC concentrations of 5 mg C liter<sup>-1</sup> in Africa and Americas, 13 mg C liter<sup>-1</sup> in Asia and 21 mg C liter<sup>-1</sup> in Oceania. The slightly higher DIC concentration in the equatorial region of Asia than in South America is mainly because of the more widespread presence of carbonate rock in Asia (Amiotte Suchet et al., 2003; Liu et al., 2019).

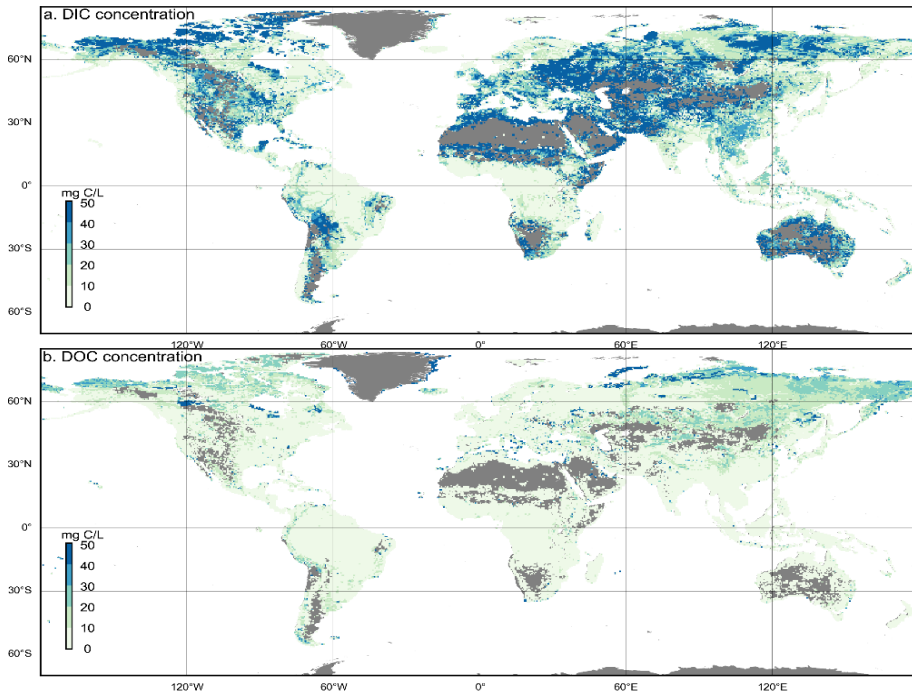


**Figure 3. Concentrations of DIC (a) and DOC (b) in global inland waters simulated by DISC-CARBON for the year 2000. Grey colours indicate grid cells with precipitation excess lower than 3mm per year. Maps showing the concentration difference between 1950 and 2000 are presented in Figure S13**

The highest predicted DIC concentrations (generally over  $40 \text{ mg C liter}^{-1}$ ) in global inland waters are mostly in the Arctic river basins (in eastern Asia, Europe and North America), which are regions with carbonate and volcanic rocks and regions with calcareous soils (mainly loess) (Amiotte Suchet et al., 2003; Dürr et al., 2005; Striegl et al., 2007; Huang et al., 2012; Raymond and Hamilton, 2018). The simulated spatial distribution of DIC concentration in global inland waters thus seems closely related to lithology, which is consistent with the early study by Meybeck and Helmer (1989) and with the consensus that DIC in rivers primarily originates from rock and sediment weathering (Richey, 2006; Berner and Berner, 2012). Therefore, driven by weathering of carbonate (in North America) and silicate rocks (in Siberian watersheds) (Dürr et al., 2005), the high DIC loadings of Arctic rivers may be an important source of DIC to the Arctic Ocean. The simulated high DIC concentrations

in Arctic rivers also agree with observations (Tank et al., 2012). Simulated DIC concentrations are also high in rivers in semi-arid and arid regions due to the high evaporation and low water discharge, including the Niger and Nile River basins (in northern Africa), Limpopo and Orange River basins (in southern Africa), Darling River basin (in Oceania), and Indus, Ural, Volga, Tigris and Euphrates River basins (in eastern Europe and western Asia).

### 3.2.2 DOC concentration patterns

In 2000, simulated DOC concentrations in inland waters are usually lower than 10 mg C liter<sup>-1</sup> (Figure 3b), which is consistent with the mean DOC concentration in global rivers of 6 mg C liter<sup>-1</sup> (Huang et al., 2012), and reports of 6 mg C liter<sup>-1</sup> in Oubangui River, 5 mg C liter<sup>-1</sup> in Mpoko River, 10 mg C liter<sup>-1</sup> in Ngoko-Sangha River and 11 mg C liter<sup>-1</sup> in Congo-Zaire River during 1990-1996 (Huang et al., 2012). The DOC concentrations tend to be higher at high latitudes, especially in the Northern Hemisphere, and the highest DOC concentrations are in Arctic river basins. This agrees with the reported high DOC concentrations for the Yenisey (2-13 mg C liter<sup>-1</sup>), Ob' (4-17 mg C liter<sup>-1</sup>), Lena (3-24 mg C liter<sup>-1</sup>), Yukon (3-16 mg C liter<sup>-1</sup>), Porcupine (2-12 mg C liter<sup>-1</sup>), and Kolyma (3-18 mg C liter<sup>-1</sup>) rivers (Raymond et al., 2007; Striegl et al., 2007; Huang et al., 2019). The latitudinal distribution of river DOC concentrations is mainly due to the spatial heterogeneity of soil C inputs (Raymond et al., 2007; Holmes et al., 2012). High-latitude soils and peatlands account for about half of the global soil C stock, much of which is in the Arctic watersheds that extend as far south as 45°N on the Eurasian continent (Raymond et al., 2007; Holmes et al., 2012). With substantial inputs from the large soil C stocks (Raymond et al., 2007; Striegl et al., 2007; Holmes et al., 2012; Prokushkin et al., 2018; Huang et al., 2019), the DOC concentrations in Arctic rivers are among the highest. The DOC concentrations for tropical rivers are low because high DOC inputs (from vegetation and soils) to rivers are balanced by high DOC decomposition rates at high temperatures.

This consistency between model predictions and observations for DOC and DIC at the various sites discussed above, indicates that DISC-CARBON sufficiently incorporates the combined influence of the lithology, climate and hydrology of basins, terrestrial and biological sources, and in-stream transformations on the distributions of DIC and DOC in global rivers.



### 3.3 Global river C budget and export

To evaluate the simulations of global C fluxes in inland waters and export to coastal waters, it is important not only to understand the governing factors at the global scale and how well they are represented in our models, but also to assess how simulated global C fluxes compare with data-based estimates. No direct observations are available to validate the C input from terrestrial ecosystems and there are few observations for C burial and CO<sub>2</sub> emissions. Moreover, these observations are only available for the last part of the twentieth century. We therefore evaluate the flux estimates, their changes and uncertainties by comparison with estimates based on data, models and other approaches from literature.

The literature inventory shows that the temporal changes simulated by DISC-CARBON (Figure 4a) are generally consistent with the trends from earlier data-based and model-based assessments (Table 2). A direct comparison of our model predictions with these assessments is not straightforward, because in these studies (1) “static” C fluxes are based on merging data covering long periods, (2) the data usually did not cover all global inland waters, and (3) the whole C budget was rarely fully quantified with a consistent approach, as done in our study. Literature estimates of C inputs from terrestrial ecosystems are

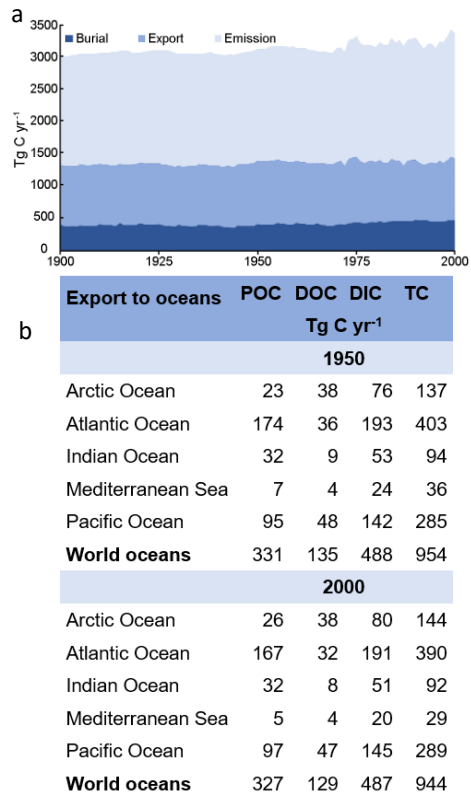


**Figure 4. (a) Aggregated C burial, export and emission (i.e. CO<sub>2</sub> emission) in global river basins for the period 1900-2000 and (b) export of POC, DOC, DIC and TC to world oceans in 1950 and 2000. Carbon input is the sum of burial, emission and export.**

basically the resultant of the overall C budget, and are consequently subject to substantial uncertainty. Our estimate of the C input to global inland waters for the year 2000 (Figure 4a) is in the middle of the range of previous estimates for the 2000s of 1.9 Pg C year<sup>-1</sup> by Cole et al., (2007) to 5.1 Pg C year<sup>-1</sup> by Sawakuchi et al. (2017) and Drake et al. (2018), and is very close to the 2.7 Pg C year<sup>-1</sup> estimated by Battin et al. (2009) and (Regnier et al., 2013) and the 2.9 Pg C year<sup>-1</sup> estimated by Tranvik et al. (2009) (Table 2). These estimates have been derived in multiple ways, and are generally based on extrapolation of independent C burial, CO<sub>2</sub> emission and river C transport data, unlike our integrated model results. Our estimated 3.0 Pg C year<sup>-1</sup> of C input to inland waters for the year 1900 is higher than the 1.7 Pg C year<sup>-1</sup> for the pre-industrial era estimated by Regnier et al. (2013). This difference is likely due to multiple factors: e.g., we included, while they ignored, the decline of natural inputs due to land-use changes over the past century (Figure SI4).

The increase in C burial during the past century reported by existing studies (Table 2) is well captured by DISC-CARBON (Table 2 and Figure 4a). This is mainly the result of increasing C inputs (Figure 4a). Our estimated 0.5 Pg C year<sup>-1</sup> of C burial for the year 2000 is very close to the 0.6 Pg C year<sup>-1</sup> for 1990-2016 reported in recent studies (Battin et al., 2009; Tranvik et al., 2009; Regnier et al., 2013; Drake et al., 2018) and obviously higher than the earlier estimate of 0.2-0.3 Pg C year<sup>-1</sup> for the pre-industrial era and the 1970s-2000s (Mulholland and Elwood, 1982; Meybeck, 1993; Dean and Gorham, 1998; Cole et al., 2007). Our simulated C burial of 0.37 Pg C year<sup>-1</sup> in 1900 is higher than the 0.04 Pg C year<sup>-1</sup> for the 1920s-1930s estimated by Mulholland and Elwood (1982) because they only counted C burial in lakes and reservoirs, and ignored the decline of lake area since the 1920s-1930s when using the estimate for the 1970s as the basis to trace back the C burial during the 1920s-1930s. Our estimate of 1.9 Pg C year<sup>-1</sup> of the CO<sub>2</sub> emission from global inland waters for the year 2000 is in the middle of the range of 0.8 Pg C year<sup>-1</sup> by Cole et al. (2007) and 3.3 Pg C year<sup>-1</sup> by Aufdenkampe et al. (2011) for the 1990s-2000s, and is very close to the CO<sub>2</sub>-partial-pressure-data-based estimate of Raymond et al. (2013) for 1990-2010 (2.1 Pg C year<sup>-1</sup>). The estimated CO<sub>2</sub> emission for the Amazon (Table 1) is consistent with the estimate of 0.8 Pg C year<sup>-1</sup> by Rasera et al. (2013), but twice the estimate of 0.5 Pg C year<sup>-1</sup> by Richey et al. (2002). The estimate 1.4 Pg C year<sup>-1</sup> Sawakuchi et al. (2017) includes emissions from the many tidal floodplains in the lower Amazonian basin. This suggests that the lower estimates for global CO<sub>2</sub> emissions in Table 2 may be underestimates as they are close to the estimated emissions attributed to the Amazon River alone.

**Table 2. Comparison with existing estimates of global freshwater carbon fluxes in Pg C year<sup>-1</sup>**

| <i>Study</i>                            | <i>Period</i> | <i>TC export</i> | <i>CO<sub>2</sub> emission</i> | <i>TC burial</i> | <i>Terrestrial TC delivery</i> |
|---|---------------|------------------|--------------------------------|------------------|--------------------------------|
| <i>Mulholland &amp; Elwood (1982)</i>   | 1920s-1930s   |                  |                                | 0.04             |                                |
| <i>Mulholland &amp; Elwood (1982)</i>   | 1977-1979     |                  |                                | 0.3              |                                |
| <i>Sarmiento &amp; Sundquist (1992)</i> | 1970s-1980s   | 0.8-0.9          |                                |                  |                                |
| <i>Degens et al. (1991)</i>             | 1980s         | 0.7-0.8          |                                |                  |                                |
| <i>Meybeck (1982)</i>                   | 1970s-1980s   | 1.0              |                                |                  |                                |
| <i>Dean &amp; Gorham (1998)</i>         | 1970s-1990s   |                  |                                | 0.2              |                                |
| <i>Meybeck (1993)</i>                   | 1992          | 1.0              |                                | 0.2              |                                |
| <i>Aumont et al. (2001)</i>             | 1980s-1990s   | 0.8              |                                |                  |                                |
| <i>Schlünz &amp; Schneider (2000)</i>   | 1980s-1990s   | 0.8-0.9          |                                |                  |                                |
| <i>Cole et al. (2007)</i>               | 1990s-2000s   | 0.9              | 0.8                            | 0.2              | 1.9                            |
| <i>Battin et al. (2009)</i>             | 1990s-2000s   | 0.9              | 1.2                            | 0.6              | 2.7                            |
| <i>Tranvik et al. (2009)</i>            | 1990s-2000s   | 0.9              | 1.4                            | 0.6              | 2.9                            |
| <i>Aufdenkampe et al. (2011)</i>        | 1990s-2000s   |                  | 3.3                            |                  |                                |
| <i>Regnier et al. (2013)</i>            | 1750          | 0.8              | 0.7                            | 0.2              | 1.7                            |
| <i>Regnier et al. (2013)</i>            | 2000-2010     | 1.0              | 1.2                            | 0.6              | 2.7                            |
| <i>Raymond et al. (2013)</i>            | 1990-2010     |                  | 2.1                            |                  |                                |
| <i>Deemer et al. (2016)</i>             | 1990-2010     |                  | 2.7                            |                  |                                |
| <i>Sawakuchi et al. (2017)</i>          | 1990-2016     |                  | 2.5                            |                  | 5.1                            |
| <i>Drake et al. (2018)</i>              | 1990-2016     | 1.0              | 2.5                            | 0.6              | 5.1                            |
| <i>This study</i>                       | 1900          | 0.9              | 1.6                            | 0.4              | 3.0                            |
| <i>This study</i>                       | 2000          | 0.9              | 1.9                            | 0.5              | 3.3                            |

Our CO<sub>2</sub> emission estimate for the year 2000 is somewhat lower than the 2.5 Pg C year<sup>-1</sup> reported by Sawakuchi et al. (2017) and Drake et al. (2018) for the period 1990-2016. This temporal increase (between the periods 1990s-2000s and 1990-2016) and the increase from 0.7 Pg C year<sup>-1</sup> to 1.2 Pg C year<sup>-1</sup> between the pre-industrial era and the 2000s observed by Regnier et al. (2013) are consistent with the increasing trend in the global freshwater CO<sub>2</sub> emission from DISC-CARBON (Figure 4a). Our estimated 1.6 Pg C year<sup>-1</sup> of CO<sub>2</sub> emission from inland waters for the year 1900 is higher than the 0.7 Pg C year<sup>-1</sup> for the pre-industrial era estimated by Regnier et al. (2013), because of the increasing trend in the CO<sub>2</sub> emission during 1750-1900 and the possible underestimation of historical emissions by Regnier et al. (2013) due to ignoring the change in natural C inputs.

These increasing C inputs to the global inland waters have been accompanied by increasing C retention and in particular emission to the atmosphere, with the consequence that the river C export to the world's oceans has remained stable (Figures 4a-b). Our simulated global TC export of 0.9 Pg C year<sup>-1</sup> in 2000 almost equals the estimates of 0.9-1.0 Pg C year<sup>-1</sup> for the period 1990-2016 in previous studies (Cole et al., 2007; Battin et al., 2009; Tranvik et al., 2009; Regnier et al., 2013; Drake et al., 2018) (Table 2). This lack of change in TC export was also observed in previous estimates of 0.8 Pg C year<sup>-1</sup> for the pre-industrial era (Regnier et al., 2013), 0.7-1.0 Pg C year<sup>-1</sup> for the 1970s-1980s (Meybeck, 1982; Degens et al., 1991; Sarmiento and Sundquist, 1992) and the 0.9-1.0 Pg C year<sup>-1</sup> for the most recent decade (Drake et al., 2018) (Table 2).

Although our simulation results show that the global export of TC remained rather constant (in terms of quantity and forms), there are regional differences. For instance, C export into the Mediterranean Sea and Black Sea showed a decline (Figure 4b). The river DOC export from Arctic rivers simulated by DISC-CARBON is 38 Tg C year<sup>-1</sup> for the period 1950-2000 (Figure 4b), which is in good agreement with the estimates of 25-36 Tg C year<sup>-1</sup> based on observations in other studies (Raymond et al., 2007; Holmes et al., 2012). Our simulated global DOC export of 129 Tg C year<sup>-1</sup> is ~20% lower than the regression result by Global NEWS for the year 2000 (Seitzinger et al., 2010), while our simulated global POC export exceeds the previous regression-based estimates by ~50% for the 1990s (Ludwig et al., 1996a; Beusen et al., 2005). One reason for the difference between our model and these regression-based estimates of POC export is related to the large uncertainties in the regressions used for calculating total suspended sediments (TSS), which was the basis for their POC calculation. In this study, sediment dynamics is tightly linked with C cycling along the entire aquatic continuum and is thoroughly described in the DISC-CARBON module (Text SI1), which reduces the uncertainty. Another reason is that the Beusen et al. (2005) estimate is based on data for 19 European rivers, which may have induced a bias.

Overall, the temporal changes simulated by DISC-CARBON are consistent with the trends from earlier data-based and model-based assessments (Table 2). In DISC-CARBON, the simulated long-term trends of the annual freshwater C fluxes indicate that global river basins have been balancing the increased inputs through more in-stream retention and emission to the atmosphere. The increasing C retention in inland waters may be closely related to the increasing global dam construction and thus increasing reservoir volume, which has increased from 7 to 3800 km<sup>3</sup> parallel to

dramatic land-use changes between 1950 and 2000 (Figure S14). The result of C budget from Regnier et al. (2013) also shows similar increases in C input, emission and burial and a relatively stable C export between the pre-industrial era and the 2000s and the increase in C burial is mainly attributed to that in reservoirs.

### **3.4 Future improvements and outlooks**

This paper provides an integrated view and consistent quantification of the spatiotemporal changes in global freshwater C cycling over long time series, which can only be achieved with (i) a full and form-explicit process-representation and (ii) spatially-explicit and dynamic C inputs and environmental forcings. The long-term simulations of DISC-CARBON show good agreement with available observations covering the second half of the 20th century (with close to 90% within a factor of 2, and no systematic errors), and the simulated trends for the full 20th century agree with results of other studies based on various approaches.

However, our model assessment and sensitivity analysis demonstrate that improvement in some formulations and model input parameters could result in an improved description of the C fluxes in river basins and a better match of simulations with observations. Such an improved model would lead to not only a better understanding of the role of rivers in the global C cycle, but also better information for policy makers about the influence of human interferences on emissions of greenhouse gases from inland waters to the atmosphere.

The sensitivity analysis clearly points to some parameters that have an overall influence on the model results. The first is the discharge, which affects several biological and physical processes important for C dynamics in river basins. To improve this, a better description of the hydrology in low-order streams to replace the current parameterization will improve our C cycle model in headwaters. The HydroSheds dataset (Lehner and Grill, 2013) is a good candidate to improve our PCR-GLOBWB model. The HydroLakes dataset (Messenger et al., 2016) can be useful to improve the current data on lake and reservoir water volume.

Secondly, the sensitivity analysis pointed to the importance of C inputs from terrestrial systems and alkalinity and DIC inputs via groundwater. These C inputs are an important source of uncertainty in terms of their spatial distribution, organic/inorganic ratios and forms (dissolved or particulate). For example, an

improved estimate of terrestrial POC input from litterfall and its variation from headwaters to mainstreams is necessary to provide a more robust quantification and spatial estimate of CO<sub>2</sub> emissions from freshwaters. Similarly, alkalinity input from groundwater is important but uncertain and can be improved by a better model for weathering and DOC input to aquifers and transformation to DIC. Furthermore, accounting for PIC dynamics will form a necessary extension of the model (Müller et al., 2021).

Furthermore, a future major challenge to be tackled in global biogeochemical modeling frameworks is to include nutrient limitations to primary production (N, P and silicon) and oxygen availability for respiration and C burial, in particular in reservoirs. Apart from advancing our capabilities to simulate freshwater C dynamics, this will allow extending the applications to other important issues such as global emissions of greenhouse gases (nitrous oxide, methane) from inland waters.

Finally, the current model simulates annual fluxes, while for many processes it may be important to analyze fluxes at shorter time scales. A shorter time step (e.g. monthly) would allow the simulation of seasonal C fluxes in river basins and export to coastal waters, to better understand the impacts on coastal marine ecosystems. A first experiment for the Rhine River basin (Text S13) showed that the model with annual and monthly settings yields similar results.

## Associated content

### Supporting Information

Description of Sediment dynamics in IMAGE-DGNM; method of sensitivity analysis; comparison of the simulation results of the three process-representation schemes in DISC-CARBON for the river Rhine; testing monthly and annual temporal resolution; sources of C in inland waters and description of their calculation in the model; model equations; model constants, their units, values and references; model parameters and units; sensitivity analysis results for Amazon, Lena, Mississippi, Nile, and Yangtze Rivers; fraction of observations plotted against relative error and Bland-Altman test for DGNM-prediction and observation for DOC and TC concentrations; validation of DISC-CARBON simulations against observed DIC, DOC and TC concentrations at the river mouths for a range of global rivers of various sizes; difference between the DISC-CARBON simulated dissolved carbon concentrations in global inland waters for the years 2000 and 1950: DIC and DOC; global areas of agricultural land and natural ecosystems and global reservoir volume for the years 1900, 1950, and 2000; DISC-CARBON simulations with yearly and monthly time steps for the river Rhine Basin (pdf).

### Author contributions

W.J.V.H. developed the DISC-CARBON module and ran the model simulations, W.J.V.H., A.F.B., J.J.M. and J.W. prepared the manuscript, A.H.W.B., L.V. and J.M.M. developed the DISC framework, J.W., G.M. and P.A.P. performed the model validation, J.J.M., X.L. and J.J.L. contributed model components, A.F.B., J.J.M. and J.W. designed research.

### Code and data availability

Code and data of DISC-CARBON 1.0 is available on reasonable request from Alexander F. Bouwman ([lex.bouwman@pbl.nl](mailto:lex.bouwman@pbl.nl)).

## **Acknowledgement**

This work is part of The New Delta 2014 ALW project no. 869.15.014, which is financed by the Netherlands Organisation for Scientific Research (NWO). Alexander F. Bouwman and Arthur H. W. Beusen received support from PBL Netherlands Environmental Assessment Agency through in-kind contributions to The New Delta 2014 ALW project. Lauriane Vilmin and Junjie Wang received funding from part of the Earth and life sciences (ALW) Open Programme 2016 project no. ALWOP.230, which is financed by the Netherlands Organisation for Scientific Research (NWO). Joep J. Langeveld received funding from The New Delta 2014 ALW project no. 869.15.015, which is financed by the Netherlands Organisation for Scientific Research (NWO). Jack J. Middelburg and Gerrit Müller are funded by the Dutch Ministry of Education, Culture and Science through the Netherlands Earth System Science Center (NESSC) and Philip A. Pika by the European Research Council Starting Grant (THAWSOME) no. 676982.



---

## References

- Amiotte Suchet, P., Probst, J. and Ludwig, W.: Worldwide distribution of continental rock lithology: Implications for the atmospheric/soil CO<sub>2</sub> uptake by continental weathering and alkalinity river transport to the oceans, *Global Biogeochem. Cycles*, 17(2), 2003.
- Aufdenkampe, A. K., Mayorga, E., Raymond, P. A., Melack, J. M., Doney, S. C., Alin, S. R., Aalto, R. E. and Yoo, K.: Riverine coupling of biogeochemical cycles between land, oceans, and atmosphere, *Front. Ecol. Environ.*, 9(1), 53–60, 2011.
- Aumont, O., Orr, J. C., Monfray, P., Ludwig, W., Amiotte-Suchet, P. and Probst, J.: Riverine-driven interhemispheric transport of carbon, *Global Biogeochem. Cycles*, 15(2), 393–405, 2001.
- Barnes, R. T. and Raymond, P. A.: The contribution of agricultural and urban activities to inorganic carbon fluxes within temperate watersheds, *Chem. Geol.*, 266(3–4), 327–336, doi:10.1016/j.chemgeo.2009.06.018, 2009.
- Baronas, J. J., Stevenson, E. I., Hackney, C. R., Darby, S. E., Bickle, M. J., Hilton, R. G., Larkin, C. S., Parsons, D. R., Myo Khaing, A. and Tipper, E. T.: Integrating suspended sediment flux in large alluvial river channels: Application of a synoptic Rouse-based model to the Irrawaddy and Salween rivers, *J. Geophys. Res. Earth Surf.*, 125(9), e2020JF005554, 2020.
- Bastviken, D., Tranvik, L. J., Downing, J. A., Crill, P. M. and Enrich-Prast, A.: Freshwater methane emissions offset the continental carbon sink, *Science* (80-. ), 331(6013), 50, 2011.
- Battin, T. J., Luysaert, S., Kaplan, L. A., Aufdenkampe, A. K., Richter, A. and Tranvik, L. J.: The boundless carbon cycle, *Nat. Geosci.*, 2(9), 598–600, 2009.
- Van Beek, L. P. H., Wada, Y. and Bierkens, M. F. P.: Global monthly water stress: 1. Water balance and water availability, *Water Resour. Res.*, 47(7), 2011.
- Berner, E. K. and Berner, R. A.: *Global environment: water, air, and geochemical cycles*, Princeton University Press., 2012.
- Beusen, A. H. W., Dekkers, A. L. M., Bouwman, A. F., Ludwig, W. and Harrison, J.: Estimation of global river transport of sediments and associated particulate C, N, and P, *Global Biogeochem. Cycles*, 19(4), 2005.
- Bianchi, T. S.: The role of terrestrially derived organic carbon in the coastal ocean: A changing paradigm and the priming effect, *Proc. Natl. Acad. Sci.*, 108(49), 19473–19481, doi:10.1073/pnas.1017982108, 2011.
- Bianchi, T. S., Wysocki, L. A., Stewart, M., Filley, T. R. and McKee, B. A.: Temporal variability in terrestrially-derived sources of particulate organic carbon in the

- lower Mississippi River and its upper tributaries, *Geochim. Cosmochim. Acta*, 71(18), 4425–4437, 2007.
- Bland, J. M. and Altman, D.: Statistical methods for assessing agreement between two methods of clinical measurement, *Lancet*, 327(8476), 307–310, 1986.
- Borges, A. V., Abril, G., Darchambeau, F., Teodoru, C. R., Deborde, J., Vidal, L. O., Lambert, T. and Bouillon, S.: Divergent biophysical controls of aquatic CO<sub>2</sub> and CH<sub>4</sub> in the World's two largest rivers, *Sci. Rep.*, 5, 1–10, doi:10.1038/srep15614, 2015.
- Boulton, A. J., Findlay, S., Marmonier, P., Stanley, E. H. and Valett, H. M.: The functional significance of the hyporheic zone in streams and rivers, *Annu. Rev. Ecol. Syst.*, 59–81, 1998.
- Chen, Y. H. and Simons, D. B.: Hydrology, hydraulics, and geomorphology of the Upper Mississippi River System, *Hydrobiologia*, 136(1), 5–19, 1986.
- Ciais, P., Borges, A., Abril, G., Meybeck, M., Folberth, G., Hauglustaine, D. and Janssens, I. A.: The impact of lateral carbon fluxes on the European carbon balance, *Biogeosciences*, 5, 1259–1271, 2008.
- Cole, Prairie, Y. T., Caraco, N. F., McDowell, W. H., Tranvik, L. J., Striegl, R. G., Duarte, C. M., Kortelainen, P., Downing, J. A. and Middelburg, J. J.: Plumbing the global carbon cycle: integrating inland waters into the terrestrial carbon budget, *Ecosystems*, 10(1), 172–185, 2007.
- Crawford, J. T., Striegl, R. G., Wickland, K. P., Dornblaser, M. M. and Stanley, E. H.: Emissions of carbon dioxide and methane from a headwater stream network of interior Alaska, *J. Geophys. Res. Biogeosciences*, 118(2), 482–494, doi:10.1002/jgrg.20034, 2013.
- Crawford, J. T., Loken, L. C., Stanley, E. H., Stets, E. G., Dornblaser, M. M. and Striegl, R. G.: Basin scale controls on CO<sub>2</sub> and CH<sub>4</sub> emissions from the Upper Mississippi River, *Geophys. Res. Lett.*, 1–7, doi:10.1002/2015GL067599. Received, 2016.
- Dean, W. E. and Gorham, E.: Magnitude and significance of carbon burial in lakes, reservoirs, and peatlands, *Geology*, 26(6), 535–538, 1998.
- Dean Walter E. and Gorham, E.: Magnitude and Significance of Carbon Burial in Lakes, Reservoirs, and Peatlands, *Geology*, 26(6), 535–538, doi:10.1130/0091-7613(1998)026<0535, 1998.
- Deemer, B. R., Harrison, J. A., Li, S., Beaulieu, J. J., Delsontro, T., Barros, N., Bezerra-Neto, J. F., Powers, S. M., Dos Santos, M. A. and Vonk, J. A.: Greenhouse Gas Emissions from Reservoir Water Surfaces: A New Global Synthesis Manuscript, *Bioscience*, 66(11), 949–964, doi:10.1093/biosci/biw117, 2016.

- Degens, E. T., Kempe, S. and Richey, J. E.: Summary: biogeochemistry of major world rivers, in *Biogeochemistry of major world rivers*. SCOPE 42, pp. 323–347., 1991.
- Drake, T. W., Raymond, P. A. and Spencer, R. G. M.: Terrestrial carbon inputs to inland waters: A current synthesis of estimates and uncertainty, *Limnol. Oceanogr. Lett.*, 132–142, doi:10.1002/lol2.10055, 2018.
- Duarte, C. M. and Prairie, Y. T.: Prevalence of heterotrophy and atmospheric CO<sub>2</sub> emissions from aquatic ecosystems, *Ecosystems*, 8(7), 862–870, doi:10.1007/s10021-005-0177-4, 2005.
- Dürr, H. H., Meybeck, M. and Dürr, S. H.: Lithologic composition of the Earth's continental surfaces derived from a new digital map emphasizing riverine material transfer, *Global Biogeochem. Cycles*, 19(4), 1–23, doi:10.1029/2005GB002515, 2005.
- Fabre, C., Sauvage, S., Probst, J.-L. and Sanchez-Pérez, J. M.: Global-scale daily riverine DOC fluxes from lands to the oceans with a generic model, *Glob. Planet. Change*, 194, 103294, 2020.
- Frankignoulle, M., Abril, G., Borges, A., Bourge, I., Canon, C., Delille, B., Libert, E. and Théate, J.-M.: Carbon Dioxide Emission from European Estuaries, *Science* (80-. ), 282(5388), 434–436, doi:10.1126/science.282.5388.434, 1998.
- Freymond, C. V., Kündig, N., Stark, C., Peterse, F., Buggle, B., Lupker, M., Plötze, M., Blattmann, T. M., Filip, F. and Giosan, L.: Evolution of biomolecular loadings along a major river system, *Geochim. Cosmochim. Acta*, 223, 389–404, 2018.
- Futter, M. N., Butterfield, D., Cosby, B. J., Dillon, P. J., Wade, A. J. and Whitehead, P. G.: Modeling the mechanisms that control in-stream dissolved organic carbon dynamics in upland and forested catchments, *Water Resour. Res.*, 43(2), 1–16, doi:10.1029/2006WR004960, 2007.
- Gao, L., Li, D. and Zhang, Y.: Nutrients and particulate organic matter discharged by the Changjiang (Yangtze River): Seasonal variations and temporal trends, *J. Geophys. Res. Biogeosciences*, 117(G4), 2012.
- Harrison, J. A., Caraco, N. and Seitzinger, S. P.: Global patterns and sources of dissolved organic matter export to the coastal zone: Results from a spatially explicit, global model, *Global Biogeochem. Cycles*, 19(4), 2005.
- Hartmann, J., Lauerwald, R. and Moosdorf, N.: GLORICH-Global river chemistry database, PANGAEA <https://doi.org/10.1594/PANGAEA.902360>, 520, 2019.
- Holgerson, M. A. and Raymond, P. A.: Large contribution to inland water CO<sub>2</sub> and CH<sub>4</sub> emissions from very small ponds, *Nat. Geosci.*, 9(3), 222–226, doi:10.1038/ngeo2654, 2016.

- Holmes, R. M., McClelland, J. W., Peterson, B. J., Tank, S. E., Bulygina, E., Eglinton, T. I., Gordeev, V. V., Gurtovaya, T. Y., Raymond, P. A. and Repeta, D. J.: Seasonal and annual fluxes of nutrients and organic matter from large rivers to the Arctic Ocean and surrounding seas, *Estuaries and Coasts*, 35(2), 369–382, 2012.
- Hotchkiss, E. R., Hall Jr, R. O., Sponseller, R. A., Butman, D., Klaminder, J., Laudon, H., Rosvall, M. and Karlsson, J.: Sources of and processes controlling CO<sub>2</sub> emissions change with the size of streams and rivers, *Nat. Geosci.*, 8(9), 696–699, 2015.
- Huang, J., Wu, M., Cui, T. and Yang, F.: Quantifying DOC and its controlling factors in major Arctic rivers during ice-free conditions using Sentinel-2 data, *Remote Sens.*, 11(24), 2904, 2019.
- Huang, T. H., Fu, Y. H., Pan, P. Y. and Chen, C. T. A.: Fluvial carbon fluxes in tropical rivers, *Curr. Opin. Environ. Sustain.*, 4(2), 162–169, doi:10.1016/j.cosust.2012.02.004, 2012.
- Huang, T. H., Chen, C. T. A., Tseng, H.-C., Lou, J. Y., Wang, S. L., Yang, L., Kandasamy, S., Gao, X., Wang, J. T. and Aldrian, E.: Riverine carbon fluxes to the South China Sea, *J. Geophys. Res. Biogeosciences*, 122(5), 1239–1259, 2017.
- Kempe, S.: Sinks of the anthropogenically enhanced carbon cycle in surface fresh waters, *J. Geophys. Res.*, 89(D3), 4657, doi:10.1029/JD089iD03p04657, 1984.
- Kicklighter, D. W., Hayes, D. J., McClelland, J. W., Peterson, B. J., McGuire, A. D. and Melillo, J. M.: Insights and issues with simulating terrestrial DOC loading of Arctic river networks, *Ecol. Appl.*, 23(8), 1817–1836, 2013.
- Lauerwald, R., Regnier, P., Camino-Serrano, M., Guenet, B., Guimberteau, M., Ducharne, A., Polcher, J. and Ciais, P.: ORCHILEAK (revision 3875): A new model branch to simulate carbon transfers along the terrestrial-aquatic continuum of the Amazon basin, *Geosci. Model Dev.*, 10(10), 3821–3859, doi:10.5194/gmd-10-3821-2017, 2017.
- Lauerwald, R., Regnier, P., Guenet, B., Friedlingstein, P. and Ciais, P.: How simulations of the land carbon sink are biased by ignoring fluvial carbon transfers: A case study for the Amazon Basin, *One Earth*, 3(2), 226–236, 2020.
- Lehner, B. and Grill, G.: Global river hydrography and network routing: Baseline data and new approaches to study the world's large river systems, *Hydrol. Process.*, 27(15), 2171–2186, doi:10.1002/hyp.9740, 2013.
- Li, G., Wang, X. T., Yang, Z., Mao, C., West, A. J. and Ji, J.: Dam-triggered organic carbon sequestration makes the Changjiang (Yangtze) river basin (China) a significant carbon sink, *J. Geophys. Res. Biogeosciences*, 120(1), 39–53, 2015.
- Li, M., Peng, C., Wang, M., Xue, W., Zhang, K., Wang, K., Shi, G. and Zhu, Q.: The carbon flux of global rivers: A re-evaluation of amount and spatial patterns, *Ecol. Indic.*, 80(April), 40–51, doi:10.1016/j.ecolind.2017.04.049, 2017.

- Li, M., Peng, C., Zhou, X., Yang, Y., Guo, Y., Shi, G. and Zhu, Q.: Modeling global riverine DOC flux dynamics from 1951 to 2015, *J. Adv. Model. Earth Syst.*, 11(2), 514–530, 2019.
- Liu, T., Wang, X. f, Yuan, X., Gong, X., Hou, C. and Yang, H.: Review on N<sub>2</sub>O emission from lakes and reservoirs, *J. Lake Sci*, 31, 319–335, 2019.
- Liu, X., Joost van Hoek, W., Vilmin, L., Beusen, A., Mogollón, J. M., Middelburg, J. J. and Bouwman, A. F.: Exploring long-term changes in silicon biogeochemistry along the river continuum of the Rhine and Yangtze (Changjiang), *Environ. Sci. Technol.*, 54(19), 11940–11950, 2020.
- Ludwig, W., Probst, J. and Kempe, S.: Predicting the oceanic input of organic carbon by continental erosion, *Global Biogeochem. Cycles*, 10(1), 23–41, 1996a.
- Ludwig, W., Amiotte Suchet, P. and Probst, J.-L.: River discharges of carbon to the world's oceans: determining local inputs of alkalinity and of dissolved and particulate organic carbon, *Sci. la terre des planètes (Comptes rendus l'Académie des Sci.)*, 323, 1007–1014, 1996b.
- Lv, S., Yu, Q., Wang, F., Wang, Y., Yan, W. and Li, Y.: A synthetic model to quantify dissolved organic carbon transport in the Changjiang River system: Model structure and spatiotemporal patterns, *J. Adv. Model. Earth Syst.*, 11(9), 3024–3041, 2019.
- Lynch, D. L. and Cotnoir Jr, L. J.: The influence of clay minerals on the breakdown of certain organic substrates, *Soil Sci. Soc. Am. J.*, 20(3), 367–370, 1956.
- Maavara, T., Lauerwald, R., Regnier, P. and Cappellen, P. Van: Global perturbation of organic carbon cycling by river damming, *Nat. Commun.*, accepted(May), 1–10, doi:10.1038/ncomms15347, 2017.
- Marx, A., Dusek, J., Jankovec, J., Sanda, M., Vogel, T., Geldern, R., Hartmann, J. and Barth, J. A. C.: A review of CO<sub>2</sub> and associated carbon dynamics in headwater streams: a global perspective, *Rev. Geophys.*, 2017.
- Massicotte, P., Asmala, E., Stedmon, C. and Markager, S.: Global distribution of dissolved organic matter along the aquatic continuum: Across rivers, lakes and oceans, *Sci. Total Environ.*, 609, 180–191, 2017.
- Mayorga, E., Seitzinger, S. P., Harrison, J. A., Dumont, E., Beusen, A. H. W., Bouwman, A. F., Fekete, B. M., Kroeze, C. and van Drecht, G.: Global nutrient export from WaterSheds 2 (NEWS 2): model development and implementation, *Environ. Model. Softw.*, 25(7), 837–853, 2010.
- Melack, J. M., Novo, E., Forsberg, B. R., Piedade, M. T. F. and Maurice, L.: Floodplain ecosystem processes, *Amaz. Glob. Chang.*, 186, 525–542, 2009.

- Messenger, M. L., Lehner, B., Grill, G., Nedeva, I. and Schmitt, O.: Estimating the volume and age of water stored in global lakes using a geo-statistical approach, *Nat. Commun.*, 7, 1–11, doi:10.1038/ncomms13603, 2016.
- Meybeck, M.: Carbon, nitrogen, and phosphorus transport by world rivers, *Am. J. Sci.*, 282(4), 401–450, 1982.
- Meybeck, M.: Riverine transport of atmospheric carbon: Sources, global typology and budget, *Water, Air, Soil Pollut.*, 70(1–4), 443–463, doi:10.1007/BF01105015, 1993.
- Meybeck, M. and Helmer, R.: The quality of rivers: from pristine stage to global pollution, *Palaeogeogr. Palaeoclimatol. Palaeoecol.*, 75(4), 283–309, 1989.
- Meybeck, M. and Ragu, A.: River discharges to the oceans: an assessment of suspended solids, major ions and nutrients, UNEP Nairobi, Kenya., 1997.
- Middelburg, J. J.: A simple rate model for organic matter decomposition in marine sediments, *Geochim. Cosmochim. Acta*, 53(7), 1577–1581, doi:https://doi.org/10.1016/0016-7037(89)90239-1, 1989.
- Middelburg, J. J.: Organic Matter is more than CH<sub>2</sub>O BT - Marine Carbon Biogeochemistry : A Primer for Earth System Scientists, edited by J. J. Middelburg, pp. 107–118, Springer International Publishing, Cham., 2019.
- Moreira-Turcq, P., Seyler, P., Guyot, J. L. and Etcheber, H.: Exportation of organic carbon from the Amazon River and its main tributaries, *Hydrol. Process.*, 17(7), 1329–1344, 2003.
- Mulholland, P. J. and Elwood, J. W.: the Role of Lake and Reservoir Sediments As Sinks in the Perturbed Global Carbon-Cycle, *Tellus*, 34(5), 490–499, 1982.
- Müller, G., Middelburg, J. J. and Sluijs, A.: Introducing GloRiSe—a global database on river sediment composition, *Earth Syst. Sci. Data*, 13(7), 3565–3575, 2021.
- Nakayama, T.: Development of an advanced eco-hydrologic and biogeochemical coupling model aimed at clarifying the missing role of inland water in the global biogeochemical cycle, *J. Geophys. Res. Biogeosciences*, 122(4), 966–988, 2017.
- Nakayama, T.: Inter-annual simulation of global carbon cycle variations in a terrestrial–aquatic continuum, *Hydrol. Process.*, 34(3), 662–678, 2020.
- Prairie, Y. T. and Cole, J. J.: Carbon , Unifying Currency, *Encycl. Inl. Waters*, 2(December), 743–746, doi:http://dx.doi.org/10.1016/B978-012370626-3.00107-1, 2009.
- Probst, J.-L., Mortatti, J. and Tardy, Y.: Carbon river fluxes and weathering CO<sub>2</sub> consumption in the Congo and Amazon river basins, *Appl. Geochemistry*, 9(1), 1–13, 1994.

- 
- Prokushkin, A. S., Pokrovsky, O. S., Korets, M. A., Rubtsov, A. V., Titov, S. V., Tokareva, I. V., Kolosov, R. A. and Amon, R. M. W.: Sources of dissolved organic carbon in rivers of the Yenisei River Basin, in *Doklady Earth Sciences*, vol. 480, pp. 763–766, Springer., 2018.
- Quay, P. D., Wilbur, D. O., Richey, J. E., Hedges, J. I., Devol, A. H. and Victoria, R.: Carbon cycling in the Amazon River: implications from the  $^{13}\text{C}$  compositions of particles and solutes, *Limnol. Oceanogr.*, 37(4), 857–871, 1992.
- Ran, L., Butman, D. E., Battin, T. J., Yang, X., Tian, M., Duvert, C., Hartmann, J., Geeraert, N. and Liu, S.: Substantial decrease in  $\text{CO}_2$  emissions from Chinese inland waters due to global change, *Nat. Commun.*, 12(1), 1–9, 2021.
- Rasera, M. de F. F. L., Krusche, A. V., Richey, J. E., Ballester, M. V. R. and Victória, R. L.: Spatial and temporal variability of  $\text{pCO}_2$  and  $\text{CO}_2$  efflux in seven Amazonian Rivers, *Biogeochemistry*, 116(1–3), 241–259, 2013.
- Raymond, P. A. and Hamilton, S. K.: Anthropogenic influences on riverine fluxes of dissolved inorganic carbon to the oceans, *Limnol. Oceanogr. Lett.*, 3(3), 143–155, 2018.
- Raymond, P. A., McClelland, J. W., Holmes, R. M., Zhulidov, A. V., Mull, K., Peterson, B. J., Striegl, R. G., Aiken, G. R. and Gurtovaya, T. Y.: Flux and age of dissolved organic carbon exported to the Arctic Ocean: A carbon isotopic study of the five largest arctic rivers, *Global Biogeochem. Cycles*, 21(4), 2007.
- Raymond, P. A., Hartmann, J., Lauerwald, R., Sobek, S., McDonald, C., Hoover, M., Butman, D., Striegl, R., Mayorga, E. and Humborg, C.: Global carbon dioxide emissions from inland waters, *Nature*, 503(7476), 355–359, 2013.
- Regnier, P., Friedlingstein, P., Ciais, P., Mackenzie, F. T., Gruber, N., Janssens, I. A., Laruelle, G. G., Lauerwald, R., Luysaert, S. and Andersson, A. J.: Anthropogenic perturbation of the carbon fluxes from land to ocean, *Nat. Geosci.*, 6(8), 597–607, 2013.
- Ren, W., Tian, H., Tao, B., Yang, J., Pan, S., Cai, W., Lohrenz, S. E., He, R. and Hopkinson, C. S.: Large increase in dissolved inorganic carbon flux from the Mississippi River to Gulf of Mexico due to climatic and anthropogenic changes over the 21st century, *J. Geophys. Res. Biogeosciences*, 120(4), 724–736, 2015.
- Richey, J. E.: Global river carbon biogeochemistry, *Encycl. Hydrol. Sci.*, 2006.
- Richey, J. E., Melack, J. M., Aufdenkampe, A. K., Ballester, V. M. and Hess, L. L.: Outgassing from Amazonian rivers and wetlands as a large tropical source of atmospheric  $\text{CO}_2$ , *Nature*, 416(6881), 617–620, doi:10.1038/416617a, 2002.

- Rouhani, S., Schaaf, C. L., Huntington, T. G. and Choate, J.: Simulation of dissolved organic carbon flux in the Penobscot Watershed, Maine, *Ecohydrol. Hydrobiol.*, 21(2), 256–270, 2021.
- Saltelli, A.: Chan. K., Scott EM (ed.), *Sensitivity Analysis*, 2000.
- Sarmiento, J. L. and Sundquist, E. T.: Revised budget for the oceanic uptake of anthropogenic carbon dioxide, *Nature*, 356(6370), 589–593, 1992.
- Sawakuchi, H. O., Neu, V., Ward, N. D., Barros, M. D. L. C., Valerio, A., Gagne-maynard, W., Cunha, A. C., Fernanda, D., Diniz, J. E., Brito, D. C., Krusche, A. V and Richey, J. E.: Carbon dioxide emissions along the lower Amazon River, *Front. Mar. Sci.*, 4(March), 1–12, doi:10.3389/fmars.2017.00076, 2017.
- Schlünz, B. and Schneider, R. R.: Transport of terrestrial organic carbon to the oceans by rivers: re-estimating flux and burial rates, *Int. J. Earth Sci.*, 88, 599–606, doi:10.1007/s005310050290, 2000.
- Seitzinger, S. P., Mayorga, E., Bouwman, A. F., Kroeze, C., Beusen, A. H. W., Billen, G., Van Drecht, G., Dumont, E., Fekete, B. M. and Garnier, J.: Global river nutrient export: A scenario analysis of past and future trends, *Global Biogeochem. Cycles*, 24(4), 2010.
- Soetaert, K., Hofmann, A. F., Middelburg, J. J., Meysman, F. J. R. and Greenwood, J.: Reprint of “The effect of biogeochemical processes on pH,” *Mar. Chem.*, 106(1), 380–401, doi:https://doi.org/10.1016/j.marchem.2007.06.008, 2007.
- Stehfest, E., van Vuuren, D., Kram, T., Bouwman, L., Alkemade, R., Bakkenes, M., Biemans, H., Bouwman, A., den Elzen, M., Janse, J., Lucas, P., van Minnen, J., Muller, C. and Prins, A. G.: *Integrated Assessment of Global Environmental Change with IMAGE 3.0. Model description and policy applications.* [online] Available from: <http://www.pbl.nl/en/publications/integrated-assessment-of-global-environmental-change-with-IMAGE-3.0>, 2014.
- Striegl, R. G., Dornblaser, M. M., Aiken, G. R., Wickland, K. P. and Raymond, P. A.: Carbon export and cycling by the Yukon, Tanana, and Porcupine rivers, Alaska, 2001–2005, *Water Resour. Res.*, 43(2), 2007.
- Sun, H., Han, J., Li, D., Lu, X., Zhang, H. and Zhao, W.: Organic carbon transport in the Songhua River, NE China: Influence of land use, *Hydrol. Process.*, 31(11), 2062–2075, 2017.
- Sutanudjaja, E. H., Beek, R. van, Wanders, N., Wada, Y., Bosmans, J. H. C., Drost, N., Ent, R. J., De Graaf, I. E. M., Hoch, J. M. and Jong, K. de: PCR-GLOBWB 2: a 5 arcmin global hydrological and water resources model, *Geosci. Model Dev.*, 11(6), 2429–2453, 2018.



- Tank, S. E., Raymond, P. A., Striegl, R. G., McClelland, J. W., Holmes, R. M., Fiske, G. J. and Peterson, B. J.: A land-to-ocean perspective on the magnitude, source and implication of DIC flux from major Arctic rivers to the Arctic Ocean, *Global Biogeochem. Cycles*, 26(4), 2012.
- Tian, H., Yang, Q., Najjar, R. G., Ren, W., Friedrichs, M. A. M., Hopkinson, C. S. and Pan, S.: Anthropogenic and climatic influences on carbon fluxes from eastern North America to the Atlantic Ocean: A process-based modeling study, *Geophys. Res. Biogeosciences*, 120, 752–772, doi:10.1002/2014JG002760. Received, 2015a.
- Tian, H., Ren, W., Yang, J., Tao, B., Cai, W., Lohrenz, S. E., Hopkinson, C. S., Liu, M., Yang, Q. and Lu, C.: Climate extremes dominating seasonal and interannual variations in carbon export from the Mississippi River Basin, *Global Biogeochem. Cycles*, 29(9), 1333–1347, 2015b.
- Tranvik, L. J., Downing, J. A., Cotner, J. B., Loiselle, S. A., Striegl, R. G., Ballatore, T. J., Dillon, P., Finlay, K., Fortino, K., Knoll, L. B., Kortelainen, P. L., Kutser, T., Larsen, S., Laurion, I., Leech, D. M., McCallister, S. L., McKnight, D. M., Melack, J. M., Overholt, E., Porter, J. A., Prairie, Y., Renwick, W. H., Roland, F., Sherman, B. S., Schindler, D. W., Sobek, S., Tremblay, A., Vanni, M. J., Verschoor, A. M., von Wachenfeldt, E. and Weyhenmeyer, G. A.: Lakes and reservoirs as regulators of carbon cycling and climate, *Limnol. Oceanogr.*, 54(6), 2298–2314, doi:10.4319/lo.2009.54.6\_part\_2.2298, 2009.
- Uppala, S. M., Kållberg, P. W., Simmons, A. J., Andrae, U., Bechtold, V. D. C., Fiorino, M., Gibson, J. K., Haseler, J., Hernandez, A. and Kelly, G. A.: The ERA-40 re-analysis, *Q. J. R. Meteorol. Soc. A J. Atmos. Sci. Appl. Meteorol. Phys. Oceanogr.*, 131(612), 2961–3012, 2005.
- Vilmin, L., Mogollón, J. M., Beusen, A. H. W. and Bouwman, A. F.: Forms and subannual variability of nitrogen and phosphorus loading to global river networks over the 20th century, *Glob. Planet. Change*, 163(February), 67–85, doi:10.1016/j.gloplacha.2018.02.007, 2018.
- Vilmin, L., Mogollón, J. M., Beusen, A. H. W., Van Hoek, W. J., Liu, X., Middelburg, J. J. and Bouwman, A. F.: Modeling process-based biogeochemical dynamics in surface fresh waters of large watersheds with the IMAGE-DGNM framework, *J. Adv. Model. Earth Syst.*, 12(11), e2019MS001796, 2020.
- Vogel, N., Retsch, M., Fustin, C.-A., Del Campo, A. and Jonas, U.: Advances in colloidal assembly: the design of structure and hierarchy in two and three dimensions, *Chem. Rev.*, 115(13), 6265–6311, 2015.

- Wallin, M. B., Grabs, T., Buffam, I., Laudon, H., Ågren, A., Öquist, M. G. and Bishop, K.: Evasion of CO<sub>2</sub> from streams - The dominant component of the carbon export through the aquatic conduit in a boreal landscape, *Glob. Chang. Biol.*, 19(3), 785–797, doi:10.1111/gcb.12083, 2013.
- Wollheim, W. M., Vörösmarty, C. J., Bouwman, A. F., Green, P., Harrison, J., Linder, E., Peterson, B. J., Seitzinger, S. P. and Syvitski, J. P. M.: Global N removal by freshwater aquatic systems using a spatially distributed, within-basin approach, *Global Biogeochem. Cycles*, 22(2), 1–14, doi:10.1029/2007GB002963, 2008.
- Wollheim, W. M., Stewart, R. J., Aiken, G. R., Butler, K. D., Morse, N. B. and Salisbury, J.: Removal of terrestrial DOC in aquatic ecosystems of a temperate river network, *Geophys. Res. Lett.*, 42(16), 6671–6679, 2015.
- Wu, Y., Eglinton, T. I., Zhang, J. and Montluçon, D. B.: Spatiotemporal variation of the quality, origin, and age of particulate organic matter transported by the Yangtze River (Changjiang), *J. Geophys. Res. Biogeosciences*, 123(9), 2908–2921, 2018.
- Xu, J., Morris, P. J., Liu, J., Ledesma, J. L. J. and Holden, J.: Increased dissolved organic carbon concentrations in peat-fed UK water supplies under future climate and sulfate deposition scenarios, *Water Resour. Res.*, 56(1), e2019WR025592, 2020.
- Zhang, L. J., Wang, L., Cai, W. J., Liu, D. M. and Yu, Z. G.: Impact of human activities on organic carbon transport in the Yellow River, *Biogeosciences*, 10(4), 2513–2524, doi:10.5194/bg-10-2513-2013, 2013.

---

---

## **Supporting Information: Exploring spatially explicit changes in carbon budgets of global river basins during the 20th century**

Wim Joost van Hoek<sup>1</sup>, Junjie Wang<sup>1</sup>, Lauriane Vilmin<sup>1,2</sup>, Arthur H.W. Beusen<sup>1,3</sup>, José M. Mogollón<sup>4</sup>, Gerrit Müller<sup>1</sup>, Philip A. Pika<sup>5</sup>, Xiaochen Liu<sup>1</sup>, Joep J. Langeveld<sup>1,3</sup>, Alexander F. Bouwman<sup>1,3</sup>, Jack J. Middelburg<sup>1</sup>

<sup>1</sup> Department of Earth Sciences, Utrecht University, P.O. Box 80021, 3508TA Utrecht, the Netherlands.

<sup>2</sup> Deltares, P.O. Box 177, Delft, the Netherlands. Postcode: 2600 MH.

<sup>3</sup> PBL Netherlands Environmental Assessment Agency, P.O. Box 30314, 2500GH the Hague, the Netherlands.

<sup>4</sup> Department of Industrial Ecology, Leiden University, P.O. Box 9518, 2300RA Leiden, the Netherlands.

<sup>5</sup> Faculty of Science, Earth and Climate, Free University of Amsterdam, de Boelelaan 1105, Amsterdam, the Netherlands. Postcode: 1081 HV.

### **Text S11. Sediment dynamics in IMAGE-DGNM**

Sediment dynamics play an important role in river biogeochemistry. Total suspended solids (TSS) is an important factor by influencing the transport of sediment-bound compounds (Watson et al., 2018), light attenuation in the water column (Kirk, 2011) and vertical sedimentation, re-mobilization and accumulation of particles in river beds (Alekseevskiy et al., 2008). TSS, in turn, can be influenced by river biogeochemistry and erosion. IMAGE-DGNM explicitly resolves the mass and fluxes of sedimentation and re-mobilization of TSS and particulate forms of C and nutrients (e.g. POC in Figure 1) as is described by (Vilmin et al., 2020). The pool of sedimented particles represents the mass of particles that have settled. While the upper sedimented particles exposed to the flow can be re-mobilized, the accumulated sediment in the benthic layer is compacted when a threshold is exceeded (Vilmin et al., 2020). The TSS inputs delivered from land to surface waters are assumed to originate from soil erosion and litterfall by terrestrial vegetation; during riverine transport, TSS is also produced within the water column through primary production. TSS consists of particulate inorganic matter (PIM, assumed to be inert) and particulate organic matter (e.g. POC for DISC-CARBON). Calcium carbonate particles (particulate inorganic carbon, PIC) are not resolved as a distinct unit in the current version of DISC-CARBON.

**Text SI2. Method of sensitivity analysis**

The method used to compute the model sensitivity is expressed as standardized Regression Coefficient (SRC) and allows to quantify the sensitivity of model results to varying parameters values with a relatively limited number of runs. We ran the model 750 times with a uniformly randomized combined set of all model parameters, external constraints and external inputs.

In each run, values of 68 model parameters, constraints and inputs are randomly multiplied with a factor between 0.95 and 1.05. For temperature, the randomization is applied between -1K and +1K of the default temperature. Values used for the parameters, constraints and inputs are presented in Tables SI2 and SI3. The output parameter Y can be simulated with a combination of input parameters ( $X_i$ ) using a linear regression approach (Saltelli, 2000):

$$Y = \beta_0 + \beta_1 X_1 + \beta_2 X_2 \dots + \beta_n X_n + e \quad (S1)$$

with  $\beta_i$  as the ordinary regression coefficient of parameter i and e the error of the approximation of Y. The linear regression model can be evaluated for parameter contribution analysis if the coefficient of determination ( $R^2$ ) is close to 1, i.e., when there is no variation of Y that is not explained with the linear regression model. A standardized regression coefficient ( $SRC_i$ ) is used to scale  $\beta_i$  to the relative contribution of variation of Y, by using the standard deviations  $\sigma$  of  $X_i$  and Y as follows:

$$SRC_i = \beta_i \frac{\sigma_{X_i}}{\sigma_Y} \quad (S2)$$

$SRC_i$  is independent of units and scale of parameters. The  $SRC_i$  has a value between -1 and 1. A positive  $SRC_i$  value indicates that an increased parameter value leads to an increased output Y. A negative  $SRC_i$  indicates a decreased output Y with an increased parameter value.  $SRC_i^2 / R^2$  yields the contribution of each parameter  $X_i$  to model outcome Y. SRC values that are considered to exert an important influence on model results have values smaller than -0.2 or larger than +0.2, since this implies an contribution larger than 4%.

We present results for the following output parameters (Y): average yearly CO<sub>2</sub> emission, total C burial, and export of TC, DIC, DOC, POC and ALG, for the rivers Amazon, Lena, Mississippi, Nile and Yangtze over the period 1995-2000. We present results for 32 out of the 68 input parameters that have a significant and important effect on the output variable considered in any of the five rivers analyzed (Table SI5a-f).

### **Text S13. Testing monthly and annual temporal resolution**

To examine the effects of annual versus monthly temporal resolution for DISC-CARBON, we simulated the River Rhine with two temporal resolutions for the period 1950-2000. The simulated TC budgets of the river Rhine with monthly and yearly time steps differ on average 8% for the 50-year period 1950-2000 (Figure S15). The simulated C inputs to the Rhine Basin, CO<sub>2</sub> emission to the atmosphere and export to the coastal waters with a monthly time step exceed those with a yearly time step by on average 1%, 14% and 5%, respectively. The simulated C burial in the Rhine Basin with a monthly time step is on average 13% higher than that with a yearly time step. Considering that the long-term trends of different C fluxes in the river Rhine during the period 1950-2000 are well captured with both time steps (Figure S15), and that the C export, which reflects the integrated effect of the C biogeochemistry over the entire river basin, differs only  $\leq 5\%$  for the two time steps, it is reasonable and representative to use a yearly time step to examine the fate of C in the global river basins on the long term.

**Table SI1. Sources of C in inland waters and description of their calculation in DISC-CARBON.**

| <i>Source</i>   | <i>Description</i>  |
|---|---|
| <i>DOC input from wastewater (WAS<sub>DOC</sub>)</i>                        | Global organic carbon from wastewater obtained from estimates by Prairie and Duarte (2006) is combined with the spatiotemporal estimates of P in wastewater based on Vilmin et al. (2018) to obtain DOC in wastewater. All organic carbon in wastewater is assumed to be in dissolved form.   |
| <i>DOC input via groundwater and surface runoff (SRO<sub>DOC</sub>)</i>     | DOC delivery via surface runoff and groundwater discharge to surface water was obtained from the model developed by (Langeveld et al., 2020)  |
| <i>POC<sub>terre</sub> input from soil loss (SOI<sub>POC</sub>)</i>         | Soil erosion delivers terrestrial POC in freshwaters parallel to an approach proposed by Cerdan et al. (2010) based on slope, soil texture and land cover type. Country aggregated soil loss rates for arable land, grassland and natural vegetation were applied to all grid cells with each their own areal fraction of arable land, grassland and natural vegetation. The soil loss enters the surface waters as SPM. To account for the POC <sub>terre</sub> , SPM input is multiplied with fSOC from Batjes (2016) to obtain the fPOC by eroded soil.  |
| <i>POC<sub>terre</sub> input from litterfall (LIT<sub>POC</sub>)</i>        | Terrestrial POC input from litterfall is based on IMAGE estimates of C production with NPP for wetlands and floodplains from the LPJ model (Sitch et al., 2003). In the DISC module, POC <sub>terre</sub> from litterfall enters surface waters in two ways: <ol style="list-style-type: none"> <li>1) via riparian zones of small streams 50% of total NPP within the areal fraction of riparian zones (of 1 meter wide) is assumed to end in the stream;</li> <li>2) via floodplains along the mainstream 100% of total NPP within the floodplain area is considered to end up in the floodplain surface waters.</li> </ol> |
| <i>DIC/ALK input from weathering (WEA<sub>DIC</sub>; WEA<sub>ALK</sub>)</i> | Lithology and runoff are the strongest controls of annual bicarbonate fluxes for 338 catchment basins across North America (Jansen, 2010; Moosdorf et al., 2011; Lauerwald et al., 2013). Here we apply the empirical parameterization for annual bicarbonate fluxes from Jansen (2010). We use lithological data from (Dürr et al., 2005). All the DIC input from this source is assumed to be bicarbonate.  |



**Table S12. Model equations**

| <i>Model equations and descriptions</i> | <i>Equation number</i> |
|---|------------------------|
| <i>Light limitation</i>                 |                        |

Light limitation for both pelagic and benthic primary producers is calculated using a spatial and temporal distribution of solar radiation reaching the surface of the water body and the water turbidity ( $\eta_{tot}$ ) that affects light penetration through the water column. Cloudless average solar radiation per month of the year (MOY) per latitude (lat) is calculated by dividing the month-integral solar radiation by the number of hours per month (HPM) as below:

$$I_0(\text{MOY}, \text{lat}) = \frac{\int_0^t I_0(t, \text{lat}) dt}{\text{HPM}} \quad 1$$

where  $I_0$ , the solar radiation above the water surface, is integrated over time. Light limitation ( $I_{\text{lim}}$ ) is calculated separately for benthic primary producers ( $\text{ALG}_{\text{benth}}$ ) and pelagic primary producers (ALG).

Light limitation for pelagic primary producers is integrated over the water column from surface to bottom at depth  $z$ , whereas for the benthic primary producers, production only takes place at the bottom (depth  $z$ ). This is formulated as follows:

$$I_{\text{lim}}(\text{MOY}, \text{lat}) = \begin{cases} \frac{I_z}{\left( I_z + k_{I_{\text{ALG}_{\text{benth}}}} \right)} & \text{for } \text{ALG}_{\text{benth}} \\ \frac{\int_0^z I_0(\text{MOY}, \text{lat})}{\left( \int_0^z I_0(\text{MOY}, \text{lat}) + k_{I_{\text{ALG}_C}} \right)} & \text{for } \text{ALG} \end{cases} \quad 2$$

**Table S12 (continuation). Model equations**

Model equations and descriptions

*Equation  
number*

The light intensity  $I_z$  at depth  $z$  is calculated with the Lambert-Beer equation:

3

$$I_z = I_0(\text{MOY}, \text{lat}) * e^{-\eta_{tot} * z}$$

The turbidity  $\eta_{tot}$  is calculated by adding all contributions to light attenuation. The turbidity  $\eta_{tot}$ , with  $\eta_{water}=0.8$  and  $\eta_{PIM}=0.03$ , is calculated according to:

4

$$\eta_{tot} = \eta_{water} + \eta_{POC_{terre}} * [POC_{terre}] + \eta_{POC_{auto}} * [POC_{auto}] + \eta_{ALG} * [ALG] + \eta_{DOC} * [DOC] + \eta_{PIM} * [PIM]$$

The solar radiation above the water surface  $I_0$  is calculated according to:

$$I_0(t, \text{lat}) = \theta_s(t, \text{lat}) * tt * I_{solar\_constant}$$

5

with  $\theta_s(t, \text{lat})$  as the solar zenith angle. Zenith is the hemispheric point above the location of reference. Transmissivity ( $tt$ ) is fixed at 0.8 [-] and the solar constant ( $I_{solar\_constant}$ ) fixed at 1367 W m<sup>-2</sup>.

The solar zenith angle  $\theta_s(t, \text{lat})$  is calculated from:

$$\theta_s(t, \text{lat}) = \arccos((\sin(\text{lat}) * \sin(\delta(t)) + \cos(\text{lat}) * \cos(\delta(t))) * \cos(h(t, \text{lat})))$$

6

with  $\delta$  as the solar declination angle (the angle the sun makes with the Earth's equatorial plane),  $h$  is the hour angle (the radian angle the earth has turned around since the previous midnight at the location of reference at time  $t$ )

**Table S12 (continuation). Model equations**

| <i>Model equations and descriptions</i>   | <i>Equation number</i> |
|---|------------------------|
| <p>The solar declination is calculated as follows:</p> $\delta(t) = 23.45 * \pi/180 * \sin(2\pi*(284+DOY(t))/362.5)$  | 7                      |
| <i>Primary production</i>   |                        |
| <p>ALG and ALG<sub>benth</sub> represent carbon in suspended and stream-bed attached primary producers, respectively. Primary producer biomass increases through fixation of DIC and decreases via respiration (to DIC), mortality (to POC<sub>auto</sub>) or excretion (to DOC):</p> | 8                      |
| $dALG/dt = ALG\_PRIMARY\_PRODUCTION - ALG\_RESPIRATION - ALG\_MORTALITY - ALG\_EXCRETION$   |                        |
| $dALG_{benth}/dt = ALG_{benth}\_PRIMARY\_PRODUCTION - ALG_{benth}\_RESPIRATION - ALG_{benth}\_MORTALITY - ALG_{benth}\_EXCRETION$   | 9                      |
| <p>Primary production depends on the biomass of the producers, their maximal growth rates, temperature, and light and DIC availability.</p>   | 10                     |
| $ALG\_PRIMARY\_PRODUCTION = fALG\_pp(T) * ALG\_I\_lim * ALG\_DIC\_lim * kALG\_pp * ALG$   |                        |
| $ALG_{benth}\_PRIMARY\_PRODUCTION = fALG_{benth}\_pp(T) * ALG_{benth}\_I\_lim * ALG_{benth}\_DIC\_lim * kALG_{benth}\_pp * ALG_{benth}$   | 11                     |

**Table S12 (continuation). Model equations**

| <i>Model equations and descriptions</i>  | <i>Equation number</i> |
|--|------------------------|
| Similarly, respiration and excretion are modeled as a fraction of primary producer biomass and depend on temperature via the function after Garnier et al. (2000) (see Eq. 16).  | 12                     |
| $ALG\_RESPIRATION = fALG\_resp(T) * kALG\_resp * ALG\_C$   |                        |
| $ALG_{benth\_RESPIRATION} = fALG_{benth\_resp}(T) * kALG_{benth\_resp} * ALG_{benth}$  | 13                     |
| $ALG\_EXCRETION = fALG\_excr(T) * kALG\_excr * ALG$  | 14                     |
| $ALG_{benth\_EXCRETION} = fALG_{benth\_excr}(T) * kALG_{benth\_excr} * ALG_{benth}$  | 15                     |
| The temperature response $f(T)$ function is applied to respiration, excretion and mortality. Parameter values $T_{opt}$ and $\sigma$ are after Garnier et al. (2000) in Table S13. $f(T)$ is calculated as follows:  | 16                     |
| $f(T) = e^{\frac{(T_{opt}-T)^2}{\sigma^2}}$  |                        |
| Mortality of ALG and ALG <sub>benth</sub> is attributed to viral lysis and modeled with a parasitic lysis factor (vf) of 20 when a threshold concentration of ALG and ALG <sub>benth</sub> of 19 $\mu\text{mol C liter}^{-1}$ ( $\approx 65 \mu\text{g liter}^{-1}$ Chl a (Garnier et al., 2000)) is exceeded. For algae this is as follows: | 17                     |
| $ALG\_MORTALITY = (fALG\_mort(T) * kALG\_mort) * (1+vf) * ALG$   |                        |

**Table SI2 (continuation). Model equations*****Model equations and descriptions******Equation  
number***

And for benthic algae:

$$\text{ALG}_{\text{benth\_MORTALITY}} = (\text{fALG}_{\text{benth\_mort}}(T) * \text{kALG}_{\text{benth\_mort}}) * (1 + \text{vf}) * \text{ALG}_{\text{benth}}$$

18

Primary production of ALG and ALG<sub>benth</sub> includes a DIC limitation (DIC<sub>lim</sub>) term that is calculated with a Michaelis-Menten function as follows:

19

$$\text{ALG}_{\text{DIC\_lim}} = \frac{[\text{DIC}]}{k_{\text{DIC}} + [\text{DIC}]}$$

***DIC dynamics***

The external input of DIC in the DISC module is from weathering (Table SI1). In-stream production of DIC comes from mineralization of organic carbon forms and respiring living biomass. DIC is consumed through primary production. Finally, DIC is added to or removed from the water body in the form of CO<sub>2</sub> as a result of atmospheric exchange:

$$\begin{aligned} \text{dDIC/dt} = & \text{WEADIC} + \text{DOC\_MINERALIZATION} + \\ & \text{POC}_{\text{terre\_MINERALIZATION}} + \text{POC}_{\text{auto\_MINERALIZATION}} + \\ & \text{SEDO}_{\text{terre\_MINERALIZATION}} + \text{SEDO}_{\text{auto\_MINERALIZATION}} + \\ & \text{ALG\_RESPIRATION} + \text{ALG}_{\text{benth\_RESPIRATION}} - \text{ALG} \\ & \text{\_PRIMARY\_PRODUCTION} - \text{ALG}_{\text{benth\_PRIMARY\_PRODUCTION}} - \\ & \text{DIC\_ATMOSPHERIC\_EXCHANGE} \end{aligned}$$

20

**Table S12 (continuation). Model equations*****Model equations and descriptions******Equation  
number***

Atmospheric exchange is calculated from the difference in CO<sub>2</sub> concentrations between the surface water and the atmosphere:

$$\text{DIC\_ATMOSPHERIC\_EXCHANGE} = k_{\text{air}} * (\text{CO}_{2\_water} - \text{CO}_{2\_atmosphere})$$

Where CO<sub>2\_atmosphere</sub> is the atmospheric concentration, fixed at 0.0136 mmol liter<sup>-1</sup> (equivalent of 400 ppmv). CO<sub>2\_water</sub> is the dissolved CO<sub>2</sub> concentration that is calculated (together with pH) from [DIC] [# volume<sup>-1</sup>], [ALK] [# volume<sup>-1</sup>] and temperature with the MOCSY2.0 scheme from Orr and Epitalon (2015). Here, alkalinity delivery to surface waters is the same as DIC delivery, from WEA<sub>DIC</sub>.

21

Alkalinity is transported downstream without biogeochemical modifications.  $k_{\text{air}}$  is the atmospheric exchange coefficient [h<sup>-1</sup>] calculated as follows:

$$k_{\text{air}} = k600 / (600/\text{ScT}) - 0.5$$

22

where k600 is the normalized  $k_{\text{air}}$  at 20°C and ScT is the Schmidt number at temperature T [C°] (Wanninkhof, 2014).

$k_{\text{air}}$  above floodplains is strongly reduced with factor  $F_{u10\_veg}$  (0.001) when there is vegetation ( $F_{\text{high\_veg}}$ ) coverage. Vegetation types from IMAGE (Stehfest et al., 2014) are classified as either high or low vegetation. A spatial fraction of high vegetation ( $F_{\text{high\_veg}}$ ) per 30-minute grid cell was obtained from 5-minutes resolution IMAGE output. Equation 22 is modified for floodplains as follows:

23

$$k_{\text{air\_floodplains}} = (k600 / (600/\text{ScT}) - 0.5) * F_{\text{high\_veg}} * F_{u10\_veg} + (k600 / (600/\text{ScT}) - 0.5) * (1 - F_{\text{high\_veg}})$$

**Table S12 (continuation). Model equations**

***Model equations and descriptions*** ***Equation number***

The Schmidt number is obtained from:

$$Sc_T = 1911.1 - 118.11T + 3.4527T^2 - 0.04132T^3 \quad 24$$

where T is represented by air temperature (Mitchell and Jones, 2005).

$k_{600}$  is estimated from flow velocity ( $v$  [L / t]) (L=length) for small rivers or from windspeed ( $\bar{u}_{10}$  [L / t]) for large rivers:

$$k_{600} = \begin{cases} a_1 + b_1 \bar{u}_{10} & \text{if stream width} > 100 \text{ meters} \\ a_2 + b_2 * v & \text{if stream width} < 100 \text{ meters} \end{cases} \quad 25$$

Values for  $a_1$ ,  $b_1$ ,  $a_2$  and  $b_2$  are by default set to respectively 4.46, 7.11, 13.82 and 0.35 (Alin et al., 2011).

---

***DOC and POC dynamics***

---

In-stream DOC production occurs through excretion by pelagic and benthic algae. DOC is consumed by mineralization.

26

$$dDOC/dt = SRO_{DOC} + WAS_{DOC} + ALG\_EXCRETION + ALG_{benth\_EXCRETION} - DOC\_MINERALIZATION$$

$POC_{terre}$  has a terrestrial origin and originates from litterfall and soil erosion (Table 1). There is resuspension through in-stream erosion and sedimentation. Finally,  $POC_{terre}$  can be consumed by mineralization:

27

$$dPOC_{terre}/dt = LIT_{POC} + SOI_{POC} + SEDOC_{terre\_INSTREAM\_EROSION} - POC_{terre\_SEDIMENTATION} - POC_{terre\_MINERALIZATION}$$

**Table S12 (continuation). Model equations****Model equations and descriptions****Equation  
number**

POC<sub>auto</sub> is the in-stream autochthonous particulate organic carbon from dead primary producers. Similar to POC<sub>terre</sub>, POC<sub>auto</sub> can be resuspended (erosion), deposited, or mineralized.

28

$$d\text{POC}_{\text{auto}}/dt = \text{ALG\_C\_MORTALITY} + \text{ALG\_C\_benth\_MORTALITY} + \text{SEDOC}_{\text{auto\_INSTREAM\_EROSION}} - \text{POC}_{\text{auto\_SEDIMENTATION}} - \text{POC}_{\text{auto\_MINERALIZATION}}$$

Particulate organic matter that has settled from the water column (SEDOC<sub>terre</sub> and SEDOC<sub>auto</sub>) can either be resuspended to the water column, transformed into DIC via mineralization or become buried, according to equations 29 and 30:

29

$$d\text{SEDOC}_{\text{terre}}/dt = \text{POC}_{\text{terre\_SEDIMENTATION}} - \text{SEDOC}_{\text{terre\_INSTREAM\_EROSION}} - \text{SEDOC}_{\text{terre\_MINERALIZATION}} - \text{SEDOC}_{\text{terre\_BURIAL}}$$

$$d\text{SEDOC}_{\text{auto}}/dt = \text{POC}_{\text{auto\_SEDIMENTATION}} - \text{SEDOC}_{\text{auto\_INSTREAM\_EROSION}} - \text{SEDOC}_{\text{auto\_MINERALIZATION}} - \text{SEDOC}_{\text{auto\_BURIAL}} \quad 30$$

Erosion of the individual sedimented C species is a fraction of the total erosion  $\Phi_{\text{ero\_tot}}$  [g year<sup>-1</sup>].  $\Phi_{\text{ero\_tot}}$  is calculated from the total mass of sediment in the water body (SED<sub>tot</sub> [g], bed area A (m<sup>2</sup>), flow velocity v [m / s], slope S [m / m], a fixed erosion coefficient  $k_{\text{ero}}$  [g m<sup>-2</sup>] of 2\*10<sup>4</sup> and a half-saturation constant  $k_{\text{sed}}$  [m] of 1\*10<sup>-6</sup>:

31

$$\Phi_{\text{ero\_tot}} = k_{\text{ero}} * (\text{SED}_{\text{tot}} / A) / (k_{\text{sed}} + \text{SED}_{\text{tot}}/A) * S * v * A$$



**Table S12 (continuation). Model equations**

| <i>Model equations and descriptions</i>   | <i>Equation number</i> |
|---|------------------------|
| <p>SED<sub>tot</sub> is calculated as:</p> $\text{SED}_{\text{tot}} = \text{SEDIM} + \text{SEDOM}_{\text{terre}} + \text{SEDOM}_{\text{auto}}$  | 32                     |
| <p>SEDIM represents the mass [g] of sedimented inorganic matter and SEDOM<sub>terre</sub> and SEDOM<sub>auto</sub> represent the masses [g] of organic matter in the sediment of terrestrial and in-stream origin, respectively. Their masses are calculated from SEDOC<sub>terre</sub> and SEDOC<sub>auto</sub> as:</p> $\text{SEDOM}_{\text{terre}} = \text{SEDOC}_{\text{terre}} / \text{fc\_SEDOC}_{\text{terre}} * \text{MMC}$ | 33                     |
| $\text{SEDOM}_{\text{auto}} = \text{SEDOC}_{\text{auto}} / \text{fc\_SEDOC}_{\text{auto}} * \text{MMC}$ <p>where fc_SEDOC<sub>terre</sub> and fc_SEDOC<sub>auto</sub> are the mass fractions of C in SEDOM<sub>terre</sub> and SEDOM<sub>auto</sub>, respectively, assumed to be 0.5. MMC is the molar mass of C (12 g/mol).</p>  | 34                     |
| <p>To calculate erosion of individual particulate species we use:</p> $\text{SEDOC}_{\text{terre\_INSTREAM\_EROSION}} = (\text{SEDOC}_{\text{terre}} / \text{SED}_{\text{tot}}) * \Phi_{\text{ero\_tot}}$   | 35                     |
| $\text{SEDOC}_{\text{auto\_INSTREAM\_EROSION}} = (\text{SEDOC}_{\text{auto}} / \text{SED}_{\text{tot}}) * \Phi_{\text{ero\_tot}}$   | 36                     |
| <p>Sedimentation of POC (terre and auto) is calculated with:</p> $\text{POC}_{\text{terre\_SEDIMENTATION}} = v_{\text{sed}} \text{POC}_{\text{terre}} / D * \text{POC}_{\text{terre}}$  | 37                     |

**Table SI2 (continuation). Model equations*****Model equations and descriptions******Equation  
number***

$$POC_{\text{auto\_SEDIMENTATION}} = v_{\text{sed}} POC_{\text{auto}} / D * POC_{\text{auto}}$$

where  $v_{\text{sed}} POC$  is the sediment deposition velocity which is assumed to be  $0.5 \text{ m h}^{-1}$  (Vilmin et al., 2020) for both the terrestrial and autochthonous POC. D is the stream depth [m].

38

The temperature-dependent mineralization rates for DOC, POC (terre and auto) and SEDOC (terre and auto) are formulated as follows:

39

$$DOC_{\text{MINERALIZATION}} = f_{\text{min}}(T) * k_{\text{DOC}_{\text{min}}} * DOC$$

$$POC_{\text{terre\_MINERALIZATION}} = f_{\text{min}}(T) * k_{\text{POC}_{\text{terre\_min}}} * POC_{\text{terre}}$$

40

$$POC_{\text{auto\_MINERALIZATION}} = f_{\text{min}}(T) * k_{\text{POC}_{\text{auto\_min}}} * POC_{\text{auto}}$$

41

$$SEDOC_{\text{terre\_MINERALIZATION}} = f_{\text{min}}(T) * k_{\text{SEDOC}_{\text{terre\_min}}} * SEDOC_{\text{terre}}$$

42

$$SEDOC_{\text{auto\_MINERALIZATION}} = f_{\text{min}}(T) * k_{\text{SEDOC}_{\text{auto\_min}}} * SEDOC_{\text{auto}}$$

43

**Table S12 (continuation). Model equations**

| <i>Model equations and descriptions</i>   | <i>Equation number</i> |
|---|------------------------|
| <p>The temperature dependency is described with a standard Q10 function:</p> $f_{\min}(T) = \exp\left(\frac{T - T_{ref}}{10}\right) \ln(Q10)$ <p>where <math>T_{ref} = 15^{\circ}</math> Celsius and Q10 set to 2 for all non-living organic species (Soetaert and Herman, 2008).</p> | 44                     |
| <p>Burial occurs when the <math>SED_{tot}</math> per bed area is more than 50 kg/m<sup>2</sup> and is calculated with:</p> $SED_{\text{terre\_BURIAL}} = k_{\text{burial}} * SED_{\text{terre}}$  | 45                     |
| $SED_{\text{auto\_BURIAL}} = k_{\text{burial}} * SED_{\text{auto}}$   | 46                     |

**Table S13. Model constants, their units, values and literature references**

| <i>Parameter</i>                            | <i>Unit</i>                                | <i>Value</i> | <i>Reference/note</i>     |
|---|--|--------------|---------------------------|
| <i>Catmosphere</i>                          | mmol liter <sup>-1</sup>                   | 0.0136       | 400 ppm                   |
| <i>a1</i>                                   | -  | 4.46         | Alin et al., 2011         |
| <i>b1</i>                                   | -  | 7.11         | Alin et al., 2011         |
| <i>a2</i>                                   | -  | 13.82        | Alin et al., 2011         |
| <i>b2</i>                                   | -  | 0.35         | Alin et al., 2011         |
| <i>kDOC<sub>min</sub></i>                   | day <sup>-1</sup>                          | 0.04         | Richardson et al., 2013   |
| <i>η<sub>doc</sub></i>                      | meter <sup>-1</sup> mg <sup>-1</sup> liter | 0.01         | Scheffer, 2004            |
| <i>kPOC<sub>terre<sub>min</sub></sub></i>   | day <sup>-1</sup>                          | 0.01         | Richardson et al., 2013   |
| <i>Q10POC<sub>terre</sub></i>               | -  | 2            | Soetaert and Herman, 2008 |
| <i>ηPOC<sub>terre</sub></i>                 | meter <sup>-1</sup> mg <sup>-1</sup> liter | 0.05         | Scheffer, 2004            |
| <i>vsedPOC<sub>terre</sub></i>              | km year <sup>-1</sup>                      | 4.38         | Vilmin et al. (2020a)     |
| <i>kSEDOC<sub>terre<sub>min</sub></sub></i> | day <sup>-1</sup>                          | 0.001        | Richardson et al., 2013   |
| <i>Q10SEDOC<sub>terre</sub></i>             | -  | 2            | Soetaert and Herman, 2008 |
| <i>kPOC<sub>auto<sub>min</sub></sub></i>    | day <sup>-1</sup>                          | 0.02         | Richardson et al., 2013   |
| <i>Q10POC<sub>auto</sub></i>                | -  | 2            | Soetaert and Herman, 2008 |
| <i>ηPOC<sub>auto</sub></i>                  | meter <sup>-1</sup> mg <sup>-1</sup> liter | 0.03         | Scheffer, 2004            |
| <i>vsedPOC<sub>auto</sub></i>               | km year <sup>-1</sup>                      | 4.38         | Vilmin et al. (2020a)     |
| <i>kSEDOC<sub>auto<sub>min</sub></sub></i>  | day <sup>-1</sup>                          | 0.02         | Richardson et al., 2013   |
| <i>Q10SEDOC<sub>auto</sub></i>              | -  | 2            | Soetaert and Herman, 2008 |
| <i>k<sub>burial</sub></i>                   | day <sup>-1</sup>                          | 0.024        | -                         |
| <i>kALG<sub>pp</sub></i>                    | day <sup>-1</sup>                          | 4.8          | Garnier et al. (2000)     |
| <i>kl<sub>ALG</sub></i>                     | Watt meter <sup>-2</sup>                   | 25           | Garnier et al. (2000)     |
| <i>kDIC<sub>ALG</sub></i>                   | mmol liter <sup>-1</sup>                   | 0.001        | Riesebell et al. (1993)   |
| <i>kALG<sub>resp</sub></i>                  | day <sup>-1</sup>                          | 0.072        | Garnier et al. (2000)     |
| <i>kALG<sub>mort</sub></i>                  | day <sup>-1</sup>                          | 0.096        | Garnier et al. (2000)     |
| <i>kALG<sub>excr</sub></i>                  | day <sup>-1</sup>                          | 0.072        | Garnier et al. (2000)     |

**Table S13 (continuation). Model constants, their units, values and literature references**

| <i>Parameter</i>   | <i>Unit</i>                | <i>Value</i> | <i>Reference/note</i>  |
|--|----------------------------|--------------|--|
| <i>vf</i> <sub>ALG</sub> ( <i>parasitic lysis amplification</i> )              | -                          | 20           | Garnier et al. (2000)  |
| <i>P</i> <sub>thresholdALG</sub>   | mmol C liter <sup>-1</sup> | 0.019        | Garnier et al. (2000)  |
| <i>k</i> <sub>ALG</sub> <i>benth</i> <sub>pp</sub>                             | day <sup>-1</sup>          | 1.5          | Garnier et al. (2000)  |
| <i>k</i> <sub>ALG</sub> <i>benth</i>   | Watt meter <sup>-2</sup>   | 12.5         | Garnier et al. (2000)  |
| <i>k</i> <sub>DICALG</sub> <i>benth</i>  | mmol liter <sup>-1</sup>   | 0.001        | Riesebell et al. (1993)  |
| <i>k</i> <sub>ALG</sub> <i>benth</i> <sub>resp</sub>                           | day <sup>-1</sup>          | 0.072        | Garnier et al. (2000)  |
| <i>k</i> <sub>ALG</sub> <i>benth</i> <sub>mort</sub>                           | day <sup>-1</sup>          | 0.096        | Garnier et al. (2000)  |
| <i>k</i> <sub>ALG</sub> <i>benth</i> <sub>excr</sub>                           | day <sup>-1</sup>          | 0.072        | Garnier et al. (2000)  |
| <i>vf</i> <sub>ALG</sub> <i>benth</i> ( <i>parasitic lysis amplification</i> ) | -                          | 20           | Garnier et al. (2000)  |
| <i>p</i> <sub>thresholdALG</sub> <i>benth</i>                                  | mmol C liter <sup>-1</sup> | 0.019        | Garnier et al. (2000)  |
| <i>T</i> <sub>opt</sub> <sub>ALG</sub>   | K                          | 18           | Garnier et al. (2000)  |
| $\sigma$ <sub>ALG</sub>  | K                          | 13           | Garnier et al. (2000)  |
| <i>T</i> <sub>opt</sub> <sub>ALG</sub> <i>benth</i>                            | K                          | 18           | Garnier et al. (2000)  |
| $\sigma$ <sub>ALG</sub> <i>benth</i>   | K                          | 13           | Garnier et al. (2000)  |
| <i>Ratio</i> <sub>v</sub> <i>flood</i>   | -                          | 0.1          | Flow velocity in flooded areas, 0.1 of that in the main branch   |
| <i>Sed</i> <sub>threshold</sub>  | kg meter <sup>-2</sup>     | 5            | Accumulated sediment in the benthic layer is compacted when this threshold of sediment stock is exceeded (Billen et al., 2015) |
| <i>COMP</i> <sub>max</sub>   | hour <sup>-1</sup>         | 0.001        | Maximal compaction rate of the sediment (Billen et al., 2015)  |

**Table S14. Model parameters and their units**

| <i>Parameter</i>  | <i>Full name [unit]</i>   |
|-------------------|---|
| $WAS_{DOC}$       | Dissolved organic carbon in wastewater [Mmol year <sup>-1</sup> ]                                     |
| $LIT_{POC}$       | Particulate organic carbon in litterfall [Mmol year <sup>-1</sup> ]                                   |
| $WEA_{DIC}$       | Dissolved organic carbon in weathering [Mmol year <sup>-1</sup> ]                                     |
| $SOI_{POC}$       | Particulate organic carbon in soil loss [Mmol year <sup>-1</sup> ]                                    |
| $LEA_{DOC}$       | Dissolved organic carbon in soil leaching water [Mmol year <sup>-1</sup> ]                            |
| $f_{DOC}$         | Mass fraction of dissolved organic carbon [-]   |
| $f_{SOC}$         | Mass fraction of soil organic carbon [-]  |
| $\rho_b$          | Soil dry bulk density [kg dm <sup>-3</sup> ]  |
| $soil_{ro}$       | Soil runoff [mm year <sup>-1</sup> ]  |
| $TSS$             | Total suspended solids [Mmol]   |
| $NPP$             | Net primary production [Mmol year <sup>-1</sup> ]   |
| $f_{wetlands}$    | Areal fraction of wetlands [-]  |
| $f_{floodplains}$ | Areal fraction of floodplains [-]   |
| $b_0$             | Empirical parameter used to calculate alkalinity discharge  |
| $A_L$             | Area with lithological class L [km <sup>2</sup> ]   |
| $Q$               | Discharge [km <sup>3</sup> year <sup>-1</sup> ]   |
| $b_L$             | Empirical parameter accounting for the effect of lithological class L on alkalinity discharge         |
| $v_I$             | Flow velocity in order I [cm s <sup>-1</sup> ]  |
| $A_b$             | Stream bed area [km <sup>2</sup> ]  |
| $D$               | Stream depth [meter]  |
| $w$               | Stream width [meter]  |
| $u_{10}$          | Windspeed at 10 meters above water surface [meter s <sup>-1</sup> ]                                   |
| $F_{high_{veg}}$  | High vegetation fraction  |
| $Fu_{10_{veg}}$   | Wind speed reduction under high vegetation  |
| $k_{600}$         | Gas exchange rate at 20°C [cm h <sup>-1</sup> ]   |
| $Sc_T$            | Schmidt number for temperature T  |
| $H$               | Parameter to represent the effect of a biogeochemical species on light extinction in the water column |
| $T$               | Water temperature [°C]  |

**Table S14 (continuation). Model parameters and their units**

| <i>Parameter</i> | <i>Full name [unit]</i>  |
|------------------|--|
| $I_0$            | Solar radiation at water surface [Watt meter <sup>-2</sup> ]                           |
| $I_z$            | Light at depth z in the water column [Watt meter <sup>-2</sup> ]                       |
| $k_I$            | Half saturation for light limitation with Michaelis-Menten [Watt meter <sup>-2</sup> ] |
| $k_{DIC}$        | Half saturation for DIC limitation with Michaelis-Menten [mmol liter <sup>-1</sup> ]   |

**Table SI5a. Sensitivity results for Amazon River to variation in model parameters, expressed as the standard regression coefficient**

| <i>Parameter description</i>                                     | <i>Symbol</i>                         | <i>CO<sub>2</sub> flux</i> | <i>TC burial</i> | <i>TC export</i> | <i>DIC export</i> | <i>DOC export</i> | <i>POC export</i> | <i>ALG export</i> |
|--|---------------------------------------|----------------------------|------------------|------------------|-------------------|-------------------|-------------------|-------------------|
| <i>Discharge (main text eq. 2)</i>                               | Q                                     | -0.06                      | -0.13            | 0.30             | 0.23              | 0.21              | 0.32              | 0.36              |
| <i>Temperature (eq. 10-18. 39-44)</i>                            | T                                     | 0.28                       | -0.66            | -0.77            | -0.42             | -0.73             | -0.73             | 0.00              |
| <i>Width (eq. 25)</i>  | W                                     | 0.00                       | 0.00             | 0.00             | 0.00              | 0.00              | 0.00              | 0.00              |
| <i>Depth (eq. 25)</i>  | D                                     | 0.00                       | 0.00             | 0.00             | 0.00              | 0.00              | 0.00              | 0.00              |
| <i>Floodplain velocity relative to main branch</i>               | Ratio_Vflood                          | 0.01                       | -0.10            | 0.02             | 0.02              | -0.01             | 0.02              | 0.00              |
| <i>Solar radiation at water surface (eq. 1-3)</i>                | I <sub>0</sub>                        | -0.04                      | 0.07             | 0.11             | 0.00              | 0.12              | 0.04              | 0.22              |
| <i>Slope (eq. 31)</i>  | S                                     | 0.01                       | -0.11            | 0.02             | 0.02              | 0.00              | 0.03              | 0.00              |
| <i>Minimum mineralization rate for DOC (eq. 39)</i>              | k <sub>DOCmin</sub>                   | 0.00                       | 0.00             | 0.00             | -0.01             | -0.21             | 0.00              | 0.00              |
| <i>Temperature dependency DOC mineralization (Eq. 39)</i>        | Q10                                   | 0.00                       | 0.00             | -0.01            | 0.00              | -0.26             | 0.00              | 0.00              |
| <i>Light sensitivity algae growth (eq. 2; 10)</i>                | ALG <sub>i_lim</sub>                  | 0.02                       | 0.00             | -0.09            | 0.03              | -0.11             | -0.02             | -0.22             |
| <i>Maximum growth rate algae (eq. 10)</i>                        | k <sub>ALG_pp</sub>                   | -0.07                      | 0.01             | 0.26             | -0.07             | 0.31              | 0.04              | 0.59              |
| <i>Maximum mortality rate algae (eq. 17)</i>                     | k <sub>ALG_mort</sub>                 | 0.03                       | 0.01             | -0.10            | 0.04              | -0.24             | -0.01             | -0.46             |
| <i>Parasitic lysis threshold for mortality of algae (eq. 17)</i> | p <sub>threshold</sub> <sub>ALG</sub> | -0.03                      | 0.00             | 0.11             | -0.03             | 0.19              | 0.01              | 0.36              |
| <i>Parasitic lysis of algae (eq. 17)</i>                         | v <sub>FALG</sub>                     | 0.02                       | 0.01             | -0.07            | 0.02              | -0.17             | -0.01             | -0.31             |



**Table SI5a (continuation). Sensitivity results for Amazon River to variation in model parameters, expressed as the standard regression coefficient**

| <i>Parameter description</i>  | <i>Symbol</i>                     | <i>CO<sub>2</sub><br/>flux</i> | <i>TC<br/>burial</i> | <i>TC<br/>export</i> | <i>DIC<br/>export</i> | <i>DOC<br/>export</i> | <i>POC<br/>export</i> | <i>ALG<br/>export</i> |
|---|-----------------------------------|--------------------------------|----------------------|----------------------|-----------------------|-----------------------|-----------------------|-----------------------|
| <i>Minimum mineralization rate allochthonous POC in sediment (eq. 42)</i>               | <i>k<sub>SEDOCTerre_min</sub></i> | 0.02                           | -0.08                | -0.04                | -0.04                 | 0.00                  | -0.03                 | 0.00                  |
| <i>Temperature dependency allochthonous POC mineralization in sediment (eq. 42; 44)</i> | <i>Q<sub>10</sub></i>             | 0.02                           | -0.09                | -0.05                | -0.05                 | 0.00                  | -0.03                 | 0.00                  |
| <i>Sedimentation velocity of autochthonous POC (eq. 38)</i>                             | <i>v<sub>SEDOPOCauto</sub></i>    | 0.00                           | 0.08                 | -0.04                | -0.03                 | 0.00                  | -0.08                 | 0.00                  |
| <i>Minimum mineralization rate autochthonous POC (eq. 43)</i>                           | <i>k<sub>SEDOCauto_min</sub></i>  | 0.03                           | -0.04                | -0.11                | -0.05                 | 0.00                  | -0.24                 | 0.00                  |
| <i>Temperature dependency POC mineralization in sediment (eq. 43; 44)</i>               | <i>Q<sub>10</sub></i>             | 0.04                           | -0.04                | -0.14                | -0.05                 | 0.00                  | -0.30                 | 0.00                  |
| <i>Minimum mineralization rate allochthonous POC in sediment (eq. 41)</i>               | <i>k<sub>POCauto_min</sub></i>    | 0.05                           | -0.21                | -0.11                | -0.13                 | 0.00                  | -0.19                 | 0.00                  |
| <i>Temperature dependency autochthonous POC mineralization in sediment (eq. 43;44)</i>  | <i>Q<sub>10</sub></i>             | 0.06                           | -0.23                | -0.14                | -0.16                 | 0.00                  | -0.22                 | 0.00                  |
| <i>Sedimentation velocity of allochthonous POC (eq. 37)</i>                             | <i>v<sub>SEDOPOCTerre</sub></i>   | 0.01                           | 0.36                 | -0.18                | -0.20                 | 0.00                  | -0.25                 | 0.00                  |
| <i>Erosion coefficient (eq. 31)</i>   | <i>k<sub>ero</sub></i>            | 0.01                           | -0.10                | 0.02                 | 0.02                  | 0.00                  | 0.03                  | 0.00                  |

**Table S15a (continuation). Sensitivity results for Amazon River to variation in model parameters, expressed as the standard regression coefficient**

| <i>Parameter description</i>   | <i>Symbol</i>       | <i>CO<sub>2</sub><br/>flux</i> | <i>TC<br/>burial</i> | <i>TC<br/>export</i> | <i>DIC<br/>export</i> | <i>DOC<br/>export</i> | <i>POC<br/>export</i> | <i>ALG<br/>export</i> |
|--|---------------------|--------------------------------|----------------------|----------------------|-----------------------|-----------------------|-----------------------|-----------------------|
| <i>Compaction of<br/>sediment after burial</i>                                 | COMP <sub>max</sub> | -0.03                          | 0.33                 | -0.01                | -0.02                 | 0.00                  | -0.02                 | 0.00                  |
| <i>Sedimentation<br/>threshold (eq. 45-46)</i>                                 | Sed_thresho<br>ld   | 0.03                           | -0.32                | 0.01                 | 0.01                  | 0.00                  | 0.01                  | 0.00                  |
| <i>POC input from soil<br/>erosion (eq. 27)</i>                                | SOI <sub>POC</sub>  | 0.00                           | 0.00                 | 0.00                 | 0.00                  | 0.00                  | 0.00                  | 0.00                  |
| <i>DOC input from<br/>surface runoff (eq.<br/>26)</i>                          | SRO <sub>DOC</sub>  | 0.02                           | 0.00                 | 0.00                 | 0.00                  | 0.00                  | 0.00                  | 0.00                  |
| <i>Alkalinity in<br/>weathering flow from<br/>groundwater (eq. 20;<br/>21)</i> | ALK <sub>wea</sub>  | -0.06                          | 0.00                 | 0.22                 | 0.77                  | 0.00                  | 0.00                  | 0.00                  |
| <i>DIC in weathering<br/>flow from<br/>groundwater (eq. 20;<br/>21)</i>        | DIC <sub>wea</sub>  | 0.42                           | 0.00                 | 0.00                 | 0.01                  | 0.01                  | 0.00                  | 0.00                  |
| <i>POC input from<br/>litterfall in floodplains</i>                            | LIT <sub>POC</sub>  | 0.85                           | 0.27                 | 0.18                 | 0.22                  | 0.00                  | 0.27                  | 0.00                  |
| <i>POC from litterfall in<br/>streams/ivers (Table<br/>S11)</i>                | LIT <sub>POC</sub>  | 0.01                           | 0.00                 | 0.00                 | 0.00                  | 0.00                  | 0.00                  | 0.00                  |
| <i>DOC in wastewater<br/>(eq. 26)</i>  | WAS <sub>DOC</sub>  | 0.00                           | 0.00                 | 0.00                 | 0.00                  | 0.00                  | 0.00                  | 0.00                  |

\*SRC values that are not significant are not shown. An SRC value smaller than -0.2 or larger than +0.2 means the corresponding parameter has a significant and important influence on the model results of the C output (i.e. larger than 4%).

**Table SI5b. Sensitivity results for Lena River to variation in model parameters, expressed as the standard regression coefficient**

| <i>Parameter description</i>                                     | <i>Symbol</i>                         | <i>CO<sub>2</sub><br/>flux</i> | <i>TC<br/>burial</i> | <i>TC<br/>export</i> | <i>DIC<br/>export</i> | <i>DOC<br/>export</i> | <i>POC<br/>export</i> | <i>ALG<br/>export</i> |
|--|---------------------------------------|--------------------------------|----------------------|----------------------|-----------------------|-----------------------|-----------------------|-----------------------|
| <i>Discharge (main text eq. 2)</i>                               | Q                                     | -0.30                          | -0.60                | 0.63                 | 0.05                  | 0.36                  | 0.59                  | 0.01                  |
| <i>Temperature (eq. 10-18. 39-44)</i>                            | T                                     | 0.20                           | -0.08                | -0.21                | -0.14                 | -0.43                 | -0.25                 | 0.69                  |
| <i>Width (eq. 25)</i>  | W                                     | 0.08                           | 0.32                 | -0.23                | -0.12                 | 0.00                  | -0.26                 | 0.01                  |
| <i>Depth (eq. 25)</i>  | D                                     | 0.02                           | 0.08                 | -0.06                | -0.01                 | -0.01                 | -0.01                 | -0.04                 |
| <i>Floodplain velocity relative to main branch</i>               | Ratio_Vflood                          | -0.05                          | -0.05                | 0.09                 | 0.03                  | -0.01                 | 0.11                  | -0.01                 |
| <i>Solar radiation at water surface (eq. 1-3)</i>                | I <sub>0</sub>                        | -0.06                          | 0.04                 | 0.06                 | -0.01                 | 0.01                  | 0.00                  | 0.29                  |
| <i>Slope (eq. 31)</i>  | S                                     | -0.04                          | -0.31                | 0.17                 | -0.05                 | 0.00                  | 0.26                  | -0.01                 |
| <i>Minimum mineralization rate for DOC (eq. 39)</i>              | k <sub>DOCmin</sub>                   | 0.11                           | 0.00                 | -0.13                | 0.05                  | -0.36                 | 0.00                  | 0.00                  |
| <i>Temperature dependency DOC mineralization (Eq. 39)</i>        | Q <sub>10</sub>                       | -0.16                          | 0.00                 | 0.20                 | -0.08                 | 0.54                  | 0.00                  | 0.00                  |
| <i>Light sensitivity algae growth (eq. 2; 10)</i>                | ALG <sub>lim</sub>                    | 0.02                           | 0.00                 | -0.02                | 0.01                  | 0.00                  | 0.00                  | -0.29                 |
| <i>Maximum growth rate algae (eq. 10)</i>                        | k <sub>ALG_pp</sub>                   | -0.03                          | 0.02                 | 0.02                 | -0.02                 | 0.00                  | 0.00                  | 0.54                  |
| <i>Maximum mortality rate algae (eq. 17)</i>                     | k <sub>ALG_mort</sub>                 | 0.01                           | 0.00                 | -0.01                | 0.00                  | 0.00                  | 0.00                  | -0.28                 |
| <i>Parasitic lysis threshold for mortality of algae (eq. 17)</i> | p <sub>threshold</sub> <sub>ALG</sub> | -0.01                          | 0.01                 | 0.00                 | 0.00                  | 0.00                  | 0.00                  | 0.15                  |
| <i>Parasitic lysis of algae (eq. 17)</i>                         | v <sub>FALG</sub>                     | 0.00                           | 0.00                 | 0.00                 | 0.00                  | 0.00                  | 0.00                  | -0.12                 |

**Table S15b (continuation). Sensitivity results for Lena River to variation in model parameters, expressed as the standard regression coefficient**

| <i>Parameter description</i>  | <i>Symbol</i>                     | <i>CO<sub>2</sub> flux</i> | <i>TC burial</i> | <i>TC export</i> | <i>DIC export</i> | <i>DOC export</i> | <i>POC export</i> | <i>ALG export</i> |
|---|-----------------------------------|----------------------------|------------------|------------------|-------------------|-------------------|-------------------|-------------------|
| <i>Minimum mineralization rate allochthonous POC in sediment (eq. 42)</i>               | <i>k<sub>SEDOCTerre_min</sub></i> | 0.02                       | -0.03            | -0.01            | 0.00              | 0.00              | 0.00              | 0.00              |
| <i>Temperature dependency allochthonous POC mineralization in sediment (eq. 42; 44)</i> | <i>Q<sub>10</sub></i>             | -0.03                      | 0.04             | 0.02             | 0.00              | 0.00              | 0.00              | 0.00              |
| <i>Sedimentation velocity of autochthonous POC (eq. 38)</i>                             | <i>v<sub>SEDOPOCauto</sub></i>    | 0.05                       | 0.16             | -0.13            | 0.02              | 0.00              | -0.21             | 0.01              |
| <i>Minimum mineralization rate autochthonous POC (eq. 43)</i>                           | <i>k<sub>SEDOCauto_min</sub></i>  | 0.03                       | -0.03            | -0.03            | 0.02              | 0.00              | -0.05             | 0.00              |
| <i>Temperature dependency POC mineralization in sediment (eq. 43; 44)</i>               | <i>Q<sub>10</sub></i>             | -0.05                      | 0.03             | 0.05             | -0.04             | 0.00              | 0.09              | 0.00              |
| <i>Minimum mineralization rate allochthonous POC in sediment (eq. 41)</i>               | <i>k<sub>POCauto_min</sub></i>    | 0.12                       | -0.17            | -0.07            | 0.02              | 0.00              | -0.11             | 0.00              |
| <i>Temperature dependency autochthonous POC mineralization in sediment (eq. 43;44)</i>  | <i>Q<sub>10</sub></i>             | -0.17                      | 0.23             | 0.11             | -0.03             | 0.00              | 0.18              | 0.00              |
| <i>Sedimentation velocity of allochthonous POC (eq. 37)</i>                             | <i>v<sub>SEDOPOCTerre</sub></i>   | 0.07                       | 0.08             | -0.12            | -0.01             | 0.00              | -0.16             | 0.01              |
| <i>Erosion coefficient (eq. 31)</i>   | <i>k<sub>Kero</sub></i>           | -0.03                      | -0.31            | 0.17             | -0.05             | 0.00              | 0.26              | -0.01             |

**Table SI5b (continuation). Sensitivity results for Lena River to variation in model parameters, expressed as the standard regression coefficient**

| <i>Parameter description</i>                                       | <i>Symbol</i>                | <i>CO<sub>2</sub> flux</i> | <i>TC burial</i> | <i>TC export</i> | <i>DIC export</i> | <i>DOC export</i> | <i>POC export</i> | <i>ALG export</i> |
|--|------------------------------|----------------------------|------------------|------------------|-------------------|-------------------|-------------------|-------------------|
| <i>Compaction of sediment after burial</i>                         | COMP <sub>max</sub>          | -0.04                      | 0.16             | -0.02            | -0.01             | 0.00              | -0.02             | 0.00              |
| <i>Sedimentation threshold (eq. 45-46)</i>                         | Sed <sub>thres</sub><br>hold | 0.03                       | -0.14            | 0.02             | 0.01              | 0.00              | 0.03              | 0.00              |
| <i>POC input from soil erosion (eq. 27)</i>                        | SOI <sub>POC</sub>           | 0.03                       | 0.10             | 0.21             | 0.03              | 0.00              | 0.29              | 0.00              |
| <i>DOC input from surface runoff (eq. 26)</i>                      | SRO <sub>DOC</sub>           | 0.13                       | 0.00             | 0.20             | 0.08              | 0.39              | 0.00              | 0.00              |
| <i>Alkalinity in weathering flow from groundwater (eq. 20; 21)</i> | ALK <sub>wea</sub>           | -0.25                      | 0.00             | 0.31             | 0.96              | 0.00              | 0.00              | 0.00              |
| <i>DIC in weathering flow from groundwater (eq. 20; 21)</i>        | DIC <sub>wea</sub>           | 0.82                       | 0.00             | 0.00             | 0.01              | 0.00              | 0.00              | 0.00              |
| <i>POC input from litterfall in floodplains</i>                    | LIT <sub>POC</sub>           | 0.14                       | 0.27             | 0.18             | 0.02              | 0.00              | 0.25              | 0.00              |
| <i>POC from litterfall in streams/rivers (Table SI1)</i>           | LIT <sub>POC</sub>           | 0.03                       | 0.10             | 0.19             | 0.02              | 0.00              | 0.27              | 0.00              |
| <i>DOC in wastewater (eq. 26)</i>                                  | WAS <sub>DOC</sub>           | 0.00                       | 0.00             | 0.00             | 0.00              | 0.00              | 0.00              | 0.00              |

\*SRC values that are not significant are not shown. An SRC value smaller than -0.2 or larger than +0.2 means the corresponding parameter has a significant and important influence on the model results of the C output (i.e. larger than 4%).

**Table SI5c. Sensitivity results for Mississippi River to variation in model parameters, expressed as the standard regression coefficient**

| <i>Parameter description</i>                                     | <i>Symbol</i>                             | <i>CO<sub>2</sub> flux</i> | <i>TC burial</i> | <i>TC export</i> | <i>DIC export</i> | <i>DOC export</i> | <i>POC export</i> | <i>ALG export</i> |
|--|---|----------------------------|------------------|------------------|-------------------|-------------------|-------------------|-------------------|
| <i>Discharge (main text eq. 2)</i>                               | Q   | -0.10                      | -0.02            | 0.27             | 0.09              | 0.34              | 0.66              | 0.35              |
| <i>Temperature (eq. 10-18. 39-44)</i>                            | T   | 0.34                       | -0.43            | -0.15            | -0.04             | -0.60             | -0.29             | 0.00              |
| <i>Width (eq. 25)</i>  | W   | 0.02                       | 0.04             | -0.10            | -0.05             | 0.01              | -0.23             | 0.00              |
| <i>Depth (eq. 25)</i>  | D   | -0.06                      | 0.07             | 0.03             | -0.02             | -0.02             | 0.18              | -0.01             |
| <i>Floodplain velocity relative to main branch</i>               | Ratio_V <sub>flood</sub>                  | -0.02                      | 0.01             | 0.04             | 0.02              | -0.03             | 0.09              | 0.00              |
| <i>Solar radiation at water surface (eq. 1-3)</i>                | I <sub>0</sub>                            | -0.18                      | 0.26             | 0.05             | 0.01              | 0.15              | -0.02             | 0.24              |
| <i>Slope (eq. 31)</i>  | S   | -0.01                      | -0.04            | 0.07             | 0.02              | 0.00              | 0.23              | 0.00              |
| <i>Minimum mineralization rate for DOC (eq. 39)</i>              | k <sub>DOCmin</sub>                       | 0.00                       | 0.00             | -0.01            | 0.00              | -0.34             | 0.00              | 0.00              |
| <i>Temperature dependency DOC mineralization (Eq. 39)</i>        | Q <sub>10</sub>                           | 0.00                       | 0.00             | -0.01            | 0.00              | -0.18             | 0.00              | 0.00              |
| <i>Light sensitivity algae growth (eq. 2; 10)</i>                | ALG <sub>lim</sub>                        | 0.15                       | -0.20            | -0.05            | 0.00              | -0.14             | 0.02              | -0.24             |
| <i>Maximum growth rate algae (eq. 10)</i>                        | k <sub>ALG_pp</sub>                       | -0.36                      | 0.48             | 0.12             | 0.01              | 0.34              | -0.03             | 0.59              |
| <i>Maximum mortality rate algae (eq. 17)</i>                     | k <sub>ALG_mort</sub>                     | 0.14                       | -0.18            | -0.06            | 0.00              | -0.27             | 0.02              | -0.46             |
| <i>Parasitic lysis threshold for mortality of algae (eq. 17)</i> | p <sub>thresh</sub><br>old <sub>ALG</sub> | -0.14                      | 0.18             | 0.05             | 0.00              | 0.20              | -0.01             | 0.35              |
| <i>Parasitic lysis of algae (eq. 17)</i>                         | v <sub>fALG</sub>                         | 0.09                       | -0.11            | -0.04            | 0.00              | -0.17             | 0.01              | -0.30             |

**Table SI5c (continuation). Sensitivity results for Mississippi River to variation in model parameters, expressed as the standard regression coefficient**

| <i>Parameter description</i>  | <i>Symbol</i>                     | <i>CO<sub>2</sub> flux</i> | <i>TC burial</i> | <i>TC export</i> | <i>DIC export</i> | <i>DOC export</i> | <i>POC export</i> | <i>ALG export</i> |
|---|-----------------------------------|----------------------------|------------------|------------------|-------------------|-------------------|-------------------|-------------------|
| <i>Minimum mineralization rate allochthonous POC in sediment (eq. 42)</i>               | <i>k<sub>SEDOCTerre_min</sub></i> | 0.13                       | -0.19            | -0.01            | 0.00              | 0.00              | 0.01              | 0.00              |
| <i>Temperature dependency allochthonous POC mineralization in sediment (eq. 42; 44)</i> | <i>Q<sub>10</sub></i>             | -0.01                      | 0.02             | -0.01            | 0.00              | 0.00              | 0.00              | 0.00              |
| <i>Sedimentation velocity of autochthonous POC (eq. 38)</i>                             | <i>v<sub>sedPOCauto_o</sub></i>   | 0.01                       | 0.03             | -0.08            | -0.01             | 0.00              | -0.43             | 0.00              |
| <i>Minimum mineralization rate autochthonous POC (eq. 43)</i>                           | <i>k<sub>SEDOCauto_min</sub></i>  | 0.03                       | -0.04            | -0.02            | 0.00              | 0.00              | -0.07             | 0.00              |
| <i>Temperature dependency POC mineralization in sediment (eq. 43; 44)</i>               | <i>Q<sub>10</sub></i>             | 0.01                       | 0.00             | -0.01            | 0.00              | 0.00              | -0.03             | 0.00              |
| <i>Minimum mineralization rate allochthonous POC in sediment (eq. 41)</i>               | <i>k<sub>POCauto_min</sub></i>    | 0.18                       | -0.26            | -0.02            | 0.00              | 0.00              | -0.17             | 0.00              |
| <i>Temperature dependency autochthonous POC mineralization in sediment (eq. 43;44)</i>  | <i>Q<sub>10</sub></i>             | -0.02                      | 0.03             | -0.01            | 0.00              | 0.00              | -0.08             | 0.00              |
| <i>Sedimentation velocity of allochthonous POC (eq. 37)</i>                             | <i>v<sub>sedPOCTerre</sub></i>    | 0.03                       | -0.03            | -0.02            | -0.01             | 0.00              | -0.05             | 0.00              |
| <i>Erosion coefficient (eq. 31)</i>   | <i>k<sub>ero</sub></i>            | -0.01                      | -0.04            | 0.07             | 0.02              | -0.01             | 0.24              | 0.00              |

**Table SI5c (continuation). Sensitivity results for Mississippi River to variation in model parameters, expressed as the standard regression coefficient**

| <i>Parameter description</i>                                       | <i>Symbol</i>       | <i>CO<sub>2</sub> flux</i> | <i>TC burial</i> | <i>TC export</i> | <i>DIC export</i> | <i>DOC export</i> | <i>POC export</i> | <i>ALG export</i> |
|--|---------------------|----------------------------|------------------|------------------|-------------------|-------------------|-------------------|-------------------|
| <i>Compaction of sediment after burial</i>                         | COMP <sub>max</sub> | -0.17                      | 0.26             | 0.00             | -0.01             | 0.00              | 0.06              | 0.00              |
| <i>Sedimentation threshold (eq. 45-46)</i>                         | Sed_thres hold      | 0.11                       | -0.17            | -0.01            | 0.00              | 0.00              | -0.04             | 0.00              |
| <i>POC input from soil erosion (eq. 27)</i>                        | SOI <sub>POC</sub>  | 0.05                       | 0.11             | 0.00             | 0.00              | 0.00              | 0.01              | 0.00              |
| <i>DOC input from surface runoff (eq. 26)</i>                      | SRO <sub>DOC</sub>  | 0.05                       | 0.00             | 0.00             | 0.00              | 0.04              | 0.00              | 0.00              |
| <i>Alkalinity in weathering flow from groundwater (eq. 20; 21)</i> | ALK <sub>wea</sub>  | -0.40                      | 0.00             | 0.91             | 0.99              | 0.00              | 0.00              | 0.00              |
| <i>DIC in weathering flow from groundwater (eq. 20; 21)</i>        | DIC <sub>wea</sub>  | 0.50                       | 0.00             | 0.00             | 0.00              | 0.01              | 0.00              | 0.00              |
| <i>POC input from litterfall in floodplains</i>                    | LIT <sub>POC</sub>  | 0.39                       | 0.30             | 0.06             | 0.03              | 0.00              | 0.23              | 0.00              |
| <i>POC from litterfall in streams/rivers (Table SI1)</i>           | LIT <sub>POC</sub>  | 0.05                       | 0.08             | 0.00             | 0.00              | 0.00              | 0.01              | 0.00              |
| <i>DOC in wastewater (eq. 26)</i>                                  | WAS <sub>DOC</sub>  | 0.01                       | 0.00             | 0.00             | 0.00              | 0.01              | 0.00              | 0.00              |

\*SRC values that are not significant are not shown. An SRC value smaller than -0.2 or larger than +0.2 means the corresponding parameter has a significant and important influence on the model results of the C output (i.e. larger than 4%).



**Table SI5d. Sensitivity results for Nile River to variation in model parameters, expressed as the standard regression coefficient**

| <i>Parameter description</i>  | <i>Symbol</i>                             | <i>CO<sub>2</sub> flux</i> | <i>TC burial</i> | <i>TC export</i> | <i>DIC export</i> | <i>DOC export</i> | <i>POC export</i> | <i>ALG export</i> |
|---|---|----------------------------|------------------|------------------|-------------------|-------------------|-------------------|-------------------|
| <i>Discharge (main text eq. 2)</i>  | Q   | -0.02                      | 0.02             | 0.15             | 0.03              | 0.32              | 0.53              | 0.38              |
| <i>Temperature (eq. 10-18, 39-44)</i>                                     | T   | 0.65                       | -0.83            | -0.16            | 0.02              | -0.69             | -0.22             | 0.01              |
| <i>Width (eq. 25)</i>   | W   | -0.01                      | 0.01             | -0.01            | 0.00              | 0.02              | -0.14             | 0.00              |
| <i>Depth (eq. 25)</i>   | D   | 0.22                       | -0.28            | -0.06            | 0.00              | -0.39             | 0.32              | -0.06             |
| <i>Floodplain velocity relative to main branch</i>                        | Ratio_V <sub>flood</sub>                  | 0.00                       | 0.00             | 0.01             | 0.00              | 0.05              | 0.05              | 0.02              |
| <i>Solar radiation at water surface (eq. 1-3)</i>                         | I <sub>0</sub>                            | -0.16                      | 0.20             | 0.08             | -0.02             | 0.20              | -0.02             | 0.24              |
| <i>Slope (eq. 31)</i>   | S   | 0.01                       | -0.01            | 0.01             | 0.00              | -0.02             | 0.14              | 0.00              |
| <i>Minimum mineralization rate for DOC (eq. 39)</i>                       | k <sub>DOCmin</sub>                       | 0.00                       | 0.00             | -0.03            | 0.01              | -0.34             | 0.00              | 0.00              |
| <i>Temperature dependency DOC mineralization (Eq. 39)</i>                 | Q <sub>10</sub>                           | 0.00                       | 0.00             | -0.02            | 0.00              | -0.20             | 0.00              | 0.00              |
| <i>Light sensitivity algae growth (eq. 2; 10)</i>                         | ALG <sub>lim</sub>                        | -0.03                      | 0.04             | -0.04            | 0.01              | 0.02              | -0.02             | -0.24             |
| <i>Maximum growth rate algae (eq. 10)</i>                                 | k <sub>ALG_pp</sub>                       | 0.05                       | -0.07            | 0.11             | -0.04             | -0.03             | 0.05              | 0.56              |
| <i>Maximum mortality rate algae (eq. 17)</i>                              | k <sub>ALG_mort</sub>                     | -0.09                      | 0.12             | -0.06            | 0.01              | 0.02              | -0.03             | -0.46             |
| <i>Parasitic lysis threshold for mortality of algae (eq. 17)</i>          | p <sub>thresh</sub><br>old <sub>ALG</sub> | 0.06                       | -0.09            | 0.05             | -0.01             | -0.03             | 0.03              | 0.36              |
| <i>Parasitic lysis of algae (eq. 17)</i>                                  | v <sub>fALG</sub>                         | -0.06                      | 0.09             | -0.04            | 0.01              | 0.02              | -0.02             | -0.31             |
| <i>Minimum mineralization rate allochthonous POC in sediment (eq. 42)</i> | k <sub>SEDOCTerre_min</sub>               | 0.18                       | -0.23            | -0.01            | 0.01              | 0.00              | 0.02              | 0.00              |

**Table SI5d (continuation). Sensitivity results for Nile River to variation in model parameters, expressed as the standard regression coefficient**

| <i>Parameter description</i>  | <i>Symbol</i>           | <i>CO<sub>2</sub> flux</i> | <i>TC burial</i> | <i>TC export</i> | <i>DIC export</i> | <i>DOC export</i> | <i>POC export</i> | <i>ALG export</i> |
|---|-------------------------|----------------------------|------------------|------------------|-------------------|-------------------|-------------------|-------------------|
| <i>Temperature dependency allochthonous POC mineralization in sediment (eq. 42; 44)</i> | $Q_{10}$                | 0.17                       | -0.22            | -0.01            | 0.00              | 0.00              | 0.01              | 0.00              |
| <i>Sedimentation velocity of autochthonous POC (eq. 38)</i>                             | $v_{sed_{POC_{auto}}}$  | 0.00                       | 0.00             | 0.00             | 0.00              | 0.00              | -0.43             | 0.00              |
| <i>Minimum mineralization rate autochthonous POC (eq. 43)</i>                           | $k_{SEDO_{Cauto\_min}}$ | 0.01                       | -0.01            | 0.00             | 0.00              | 0.00              | -0.03             | 0.00              |
| <i>Temperature dependency POC mineralization in sediment (eq. 43; 44)</i>               | $Q_{10}$                | 0.00                       | 0.00             | 0.00             | 0.00              | 0.00              | -0.01             | 0.00              |
| <i>Minimum mineralization rate allochthonous POC in sediment (eq. 41)</i>               | $k_{POC_{auto\_min}}$   | 0.07                       | -0.10            | 0.00             | 0.00              | 0.00              | -0.16             | 0.00              |
| <i>Temperature dependency autochthonous POC mineralization in sediment (eq. 43;44)</i>  | $Q_{10}$                | 0.08                       | -0.10            | 0.00             | 0.00              | 0.00              | -0.10             | 0.00              |
| <i>Sedimentation velocity of allochthonous POC (eq. 37)</i>                             | $v_{sed_{POC_{terr}}}$  | -0.01                      | 0.01             | -0.02            | 0.00              | 0.00              | -0.10             | 0.00              |
| <i>Erosion coefficient (eq. 31)</i>   | $k_{ero}$               | 0.01                       | -0.01            | 0.01             | 0.00              | -0.02             | 0.14              | 0.00              |
| <i>Compaction of sediment after burial</i>  | $COMP_{max}$            | -0.14                      | 0.19             | 0.00             | 0.00              | 0.00              | 0.02              | 0.00              |
| <i>Sedimentation threshold (eq. 45-46)</i>  | $Sed\_thres_{hold}$     | 0.12                       | -0.16            | 0.00             | 0.00              | 0.00              | -0.02             | 0.00              |
| <i>POC input from soil erosion (eq. 27)</i>   | $SOL_{POC}$             | 0.05                       | 0.03             | 0.00             | 0.00              | 0.00              | 0.19              | 0.00              |

**Table SI5d (continuation). Sensitivity results for Nile River to variation in model parameters, expressed as the standard regression coefficient**

| <i>Parameter description</i>                                       | <i>Symbol</i>      | <i>CO<sub>2</sub><br/>flux</i> | <i>TC<br/>burial</i> | <i>TC<br/>export</i> | <i>DIC<br/>export</i> | <i>DOC<br/>export</i> | <i>POC<br/>export</i> | <i>ALG<br/>export</i> |
|--|--------------------|--------------------------------|----------------------|----------------------|-----------------------|-----------------------|-----------------------|-----------------------|
| <i>DOC input from surface runoff (eq. 26)</i>                      | SRO <sub>DOC</sub> | 0.02                           | 0.00                 | 0.00                 | 0.00                  | 0.00                  | 0.00                  | 0.00                  |
| <i>Alkalinity in weathering flow from groundwater (eq. 20; 21)</i> | ALK <sub>wea</sub> | -0.06                          | 0.00                 | 0.96                 | 0.99                  | 0.00                  | 0.00                  | 0.00                  |
| <i>DIC in weathering flow from groundwater (eq. 20; 21)</i>        | DIC <sub>wea</sub> | 0.14                           | 0.00                 | 0.00                 | 0.00                  | 0.00                  | 0.00                  | 0.00                  |
| <i>POC input from litterfall in floodplains</i>                    | LIT <sub>POC</sub> | 0.58                           | 0.08                 | 0.01                 | 0.00                  | 0.00                  | 0.15                  | 0.00                  |
| <i>POC from litterfall in streams/rivers (Table SI1)</i>           | LIT <sub>POC</sub> | 0.03                           | 0.02                 | 0.01                 | 0.00                  | 0.00                  | 0.39                  | 0.00                  |
| <i>DOC in wastewater (eq. 26)</i>                                  | WAS <sub>DOC</sub> | 0.01                           | 0.00                 | 0.05                 | 0.01                  | 0.30                  | 0.00                  | 0.00                  |

\*SRC values that are not significant are not shown. An SRC value smaller than -0.2 or larger than +0.2 means the corresponding parameter has a significant and important influence on the model results of the C output (i.e. larger than 4%).

**Table SI5e. Sensitivity results for Yangtze River to variation in model parameters, expressed as the standard regression coefficient**

| <i>Parameter description</i>  | <i>Symbol</i>                         | <i>CO<sub>2</sub> flux</i> | <i>TC burial</i> | <i>TC export</i> | <i>DIC export</i> | <i>DOC export</i> | <i>POC export</i> | <i>ALG export</i> |
|---|---------------------------------------|----------------------------|------------------|------------------|-------------------|-------------------|-------------------|-------------------|
| <i>Discharge (main text eq. 2)</i>  | Q                                     | -0.11                      | -0.04            | 0.31             | 0.04              | 0.46              | 0.63              | 0.35              |
| <i>Temperature (eq. 10-18. 39-44)</i>                                     | T                                     | 0.39                       | -0.54            | -0.17            | -0.03             | -0.59             | -0.27             | 0.00              |
| <i>Width (eq. 25)</i>   | W                                     | 0.00                       | 0.00             | 0.00             | 0.00              | 0.00              | 0.00              | 0.00              |
| <i>Depth (eq. 25)</i>   | D                                     | 0.00                       | 0.00             | 0.00             | 0.00              | 0.00              | 0.00              | 0.00              |
| <i>Floodplain velocity relative to main branch</i>                        | Ratio_Vflood                          | -0.02                      | -0.01            | 0.06             | 0.02              | -0.03             | 0.22              | 0.00              |
| <i>Solar radiation at water surface (eq. 1-3)</i>                         | I <sub>0</sub>                        | -0.18                      | 0.23             | 0.11             | -0.03             | 0.11              | -0.02             | 0.24              |
| <i>Slope (eq. 31)</i>   | S                                     | -0.01                      | -0.05            | 0.10             | 0.00              | 0.00              | 0.29              | 0.00              |
| <i>Minimum mineralization rate for DOC (eq. 39)</i>                       | k <sub>DOCmin</sub>                   | 0.02                       | 0.00             | -0.06            | -0.01             | -0.47             | 0.00              | 0.00              |
| <i>Temperature dependency DOC mineralization (Eq. 39)</i>                 | Q <sub>10</sub>                       | 0.00                       | 0.00             | -0.01            | 0.00              | -0.08             | 0.00              | 0.00              |
| <i>Light sensitivity algae growth (eq. 2; 10)</i>                         | ALG <sub>L</sub> <sub>lim</sub>       | 0.15                       | -0.17            | -0.10            | 0.03              | -0.10             | 0.02              | -0.24             |
| <i>Maximum growth rate algae (eq. 10)</i>                                 | k <sub>ALG</sub> <sub>pp</sub>        | -0.36                      | 0.43             | 0.26             | -0.07             | 0.25              | -0.04             | 0.59              |
| <i>Maximum mortality rate algae (eq. 17)</i>                              | k <sub>ALG</sub> <sub>mort</sub>      | 0.14                       | -0.15            | -0.13            | 0.03              | -0.20             | 0.02              | -0.46             |
| <i>Parasitic lysis threshold for mortality of algae (eq. 17)</i>          | p <sub>thresh</sub> <sub>oldALG</sub> | -0.14                      | 0.16             | 0.12             | -0.03             | 0.15              | -0.01             | 0.35              |
| <i>Parasitic lysis of algae (eq. 17)</i>                                  | v <sub>fALG</sub>                     | 0.09                       | -0.10            | -0.08            | 0.02              | -0.12             | 0.01              | -0.30             |
| <i>Minimum mineralization rate allochthonous POC in sediment (eq. 42)</i> | k <sub>SEDOCTerre_min</sub>           | 0.11                       | -0.18            | -0.02            | 0.01              | 0.00              | 0.01              | 0.00              |

**Table SI5e (continuation). Sensitivity results for Yangtze River to variation in model parameters, expressed as the standard regression coefficient**

| <i>Parameter description</i>  | <i>Symbol</i>              | <i>CO<sub>2</sub> flux</i> | <i>TC burial</i> | <i>TC export</i> | <i>DIC export</i> | <i>DOC export</i> | <i>POC export</i> | <i>ALG export</i> |
|---|----------------------------|----------------------------|------------------|------------------|-------------------|-------------------|-------------------|-------------------|
| <i>Temperature dependency allochthonous POC mineralization in sediment (eq. 42; 44)</i> | $Q_{10}$                   | 0.01                       | -0.02            | 0.00             | 0.00              | 0.00              | 0.00              | 0.00              |
| <i>Sedimentation velocity of autochthonous POC (eq. 38)</i>                             | $v_{sed_{POC_{auto}}}$     | 0.01                       | 0.04             | -0.07            | 0.00              | 0.00              | -0.41             | 0.00              |
| <i>Minimum mineralization rate autochthonous POC (eq. 43)</i>                           | $k_{SEDO_{C_{auto\_min}}}$ | 0.03                       | -0.04            | -0.01            | 0.00              | 0.00              | -0.07             | 0.00              |
| <i>Temperature dependency POC mineralization in sediment (eq. 43; 44)</i>               | $Q_{10}$                   | 0.00                       | 0.00             | 0.00             | 0.00              | 0.00              | -0.01             | 0.00              |
| <i>Minimum mineralization rate allochthonous POC in sediment (eq. 41)</i>               | $k_{POC_{auto\_min}}$      | 0.15                       | -0.24            | -0.02            | 0.00              | 0.00              | -0.15             | 0.00              |
| <i>Temperature dependency autochthonous POC mineralization in sediment (eq. 43;44)</i>  | $Q_{10}$                   | 0.02                       | -0.03            | 0.00             | 0.00              | 0.00              | -0.02             | 0.00              |
| <i>Sedimentation velocity of allochthonous POC (eq. 37)</i>                             | $v_{sed_{POC_{terr}}}$     | 0.02                       | -0.03            | -0.01            | 0.00              | 0.00              | -0.02             | 0.00              |
| <i>Erosion coefficient (eq. 31)</i>   | $k_{ero}$                  | -0.01                      | -0.05            | 0.10             | 0.00              | 0.00              | 0.29              | 0.00              |

**Table SI5e (continuation). Sensitivity results for Yangtze River to variation in model parameters, expressed as the standard regression coefficient**

| <i>Parameter description</i>                                       | <i>Symbol</i>       | <i>CO<sub>2</sub><br/>flux</i> | <i>TC<br/>burial</i> | <i>TC<br/>export</i> | <i>DIC<br/>export</i> | <i>DOC<br/>export</i> | <i>POC<br/>export</i> | <i>ALG<br/>export</i> |
|--|---------------------|--------------------------------|----------------------|----------------------|-----------------------|-----------------------|-----------------------|-----------------------|
| <i>Compaction of sediment after burial</i>                         | COMP <sub>max</sub> | -0.17                          | 0.28                 | 0.02                 | -0.01                 | 0.00                  | 0.07                  | 0.00                  |
| <i>Sedimentation threshold (eq. 45-46)</i>                         | Sed_thres hold      | 0.07                           | -0.12                | -0.01                | 0.01                  | 0.00                  | -0.04                 | 0.00                  |
| <i>POC input from soil erosion (eq. 27)</i>                        | SOI <sub>POC</sub>  | 0.12                           | 0.28                 | 0.02                 | 0.00                  | 0.00                  | 0.10                  | 0.00                  |
| <i>DOC input from surface runoff (eq. 26)</i>                      | SRO <sub>DOC</sub>  | 0.14                           | 0.00                 | 0.02                 | 0.01                  | 0.09                  | 0.00                  | 0.00                  |
| <i>Alkalinity in weathering flow from groundwater (eq. 20; 21)</i> | ALK <sub>wea</sub>  | -0.35                          | 0.00                 | 0.83                 | 0.99                  | 0.00                  | 0.00                  | 0.00                  |
| <i>DIC in weathering flow from groundwater (eq. 20; 21)</i>        | DIC <sub>wea</sub>  | 0.59                           | 0.00                 | 0.01                 | 0.01                  | 0.00                  | 0.00                  | 0.00                  |
| <i>POC input from litterfall in floodplains</i>                    | LIT <sub>POC</sub>  | 0.20                           | 0.20                 | 0.05                 | 0.01                  | 0.00                  | 0.27                  | 0.00                  |
| <i>POC from litterfall in streams/rivers (Table S11)</i>           | LIT <sub>POC</sub>  | 0.03                           | 0.06                 | 0.01                 | 0.00                  | 0.00                  | 0.04                  | 0.00                  |
| <i>DOC in wastewater (eq. 26)</i>                                  | WAS <sub>DOC</sub>  | 0.03                           | 0.00                 | 0.01                 | 0.00                  | 0.07                  | 0.00                  | 0.00                  |

\*SRC values that are not significant are not shown. An SRC value smaller than -0.2 or larger than +0.2 means the corresponding parameter has a significant and important influence on the model results of the C output (i.e. larger than 4%).

**Figure S11. Fraction of rivers with observations plotted against relative error and Bland-Altman test for DGNM-prediction and observation for DOC and TC concentrations**

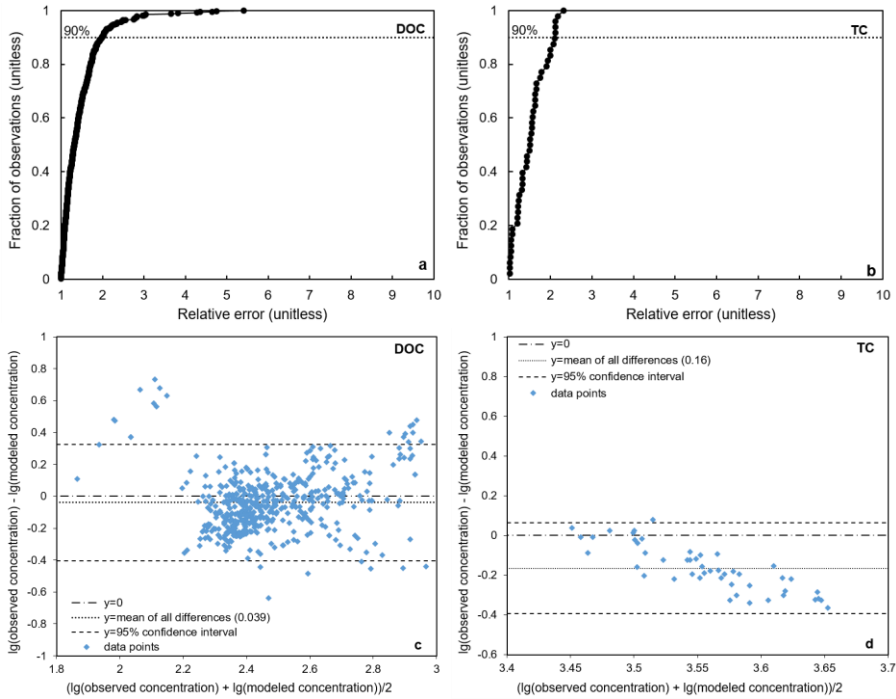


**Figure S11. Fraction of rivers with observations plotted against the ratio prediction: observation (relative error) for DOC (a) and TC (b) concentrations and comparison of the difference between DGNM-predicted and observed DOC (c) and TC (d) concentrations (in  $\mu\text{mol liter}^{-1}$ ) with the mean of predicted and observed values according to Bland and Altman (1986) similar to Figure 2f in main text for DIC concentrations. DOC data covering 1973-2000 and TC data covering 1978-1998 are from GloRiSe v. 1.0 (Müller et al., 2021) and GLORICH (Hartmann et al., 2019).**

**Figure S12. Validation of DISC-CARBON simulations against observations at the river mouths**

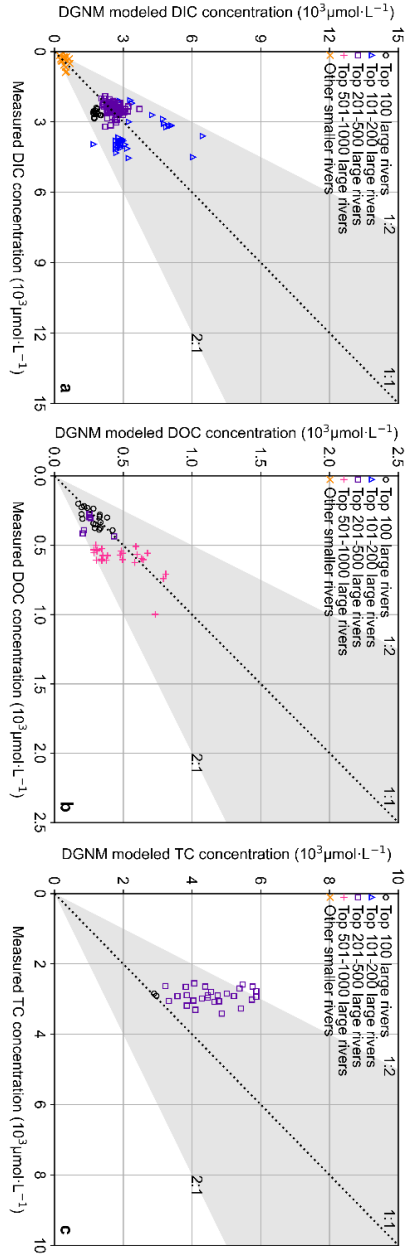


**Figure S12. Validation of DISC-CARBON simulations against observed DIC concentrations (a), DOC concentrations (b), and TC (DOC + DIC + POC) concentrations (c) at the river mouths (here defined as 50-250 km upstream from the coastline) for a range of global rivers of various sizes, where more than one station occurs within a grid cell, the mean of annual average concentrations is presented. DIC data covering 1942-2000, DOC data covering 1980-2000 and TC data covering 1979-1998 are from GLORISe v. 1.0 (Müller et al., 2021) and GLOTRICH (Hartmann et al., 2019). Rivers are sorted on the basis of their catchment areas.**



**Figure S13. Difference between simulated dissolved C concentrations between the years 2000 and 1950**

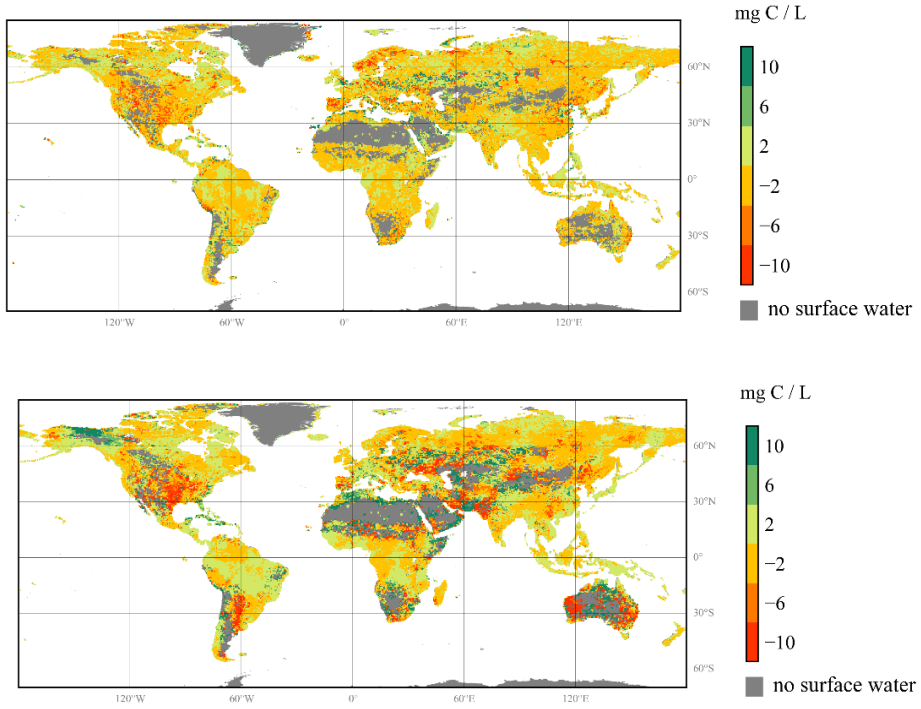
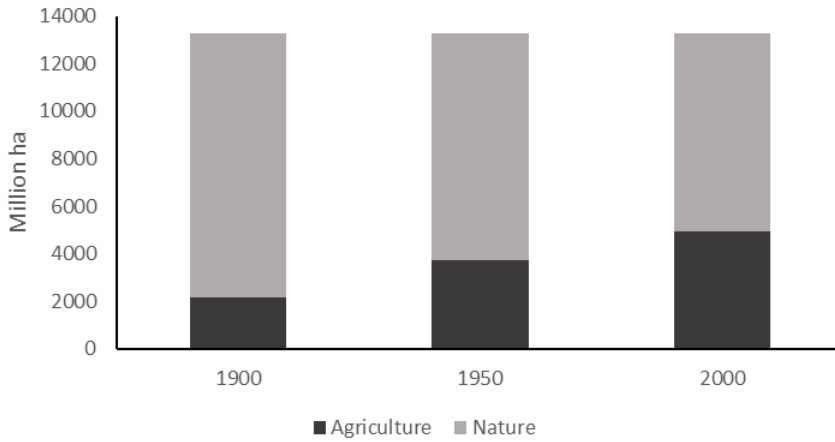


**Figure S13. Difference between the DISC-CARBON simulated dissolved carbon concentrations in global inland waters between the years 2000 and 1950: DIC (top) and DOC (bottom). Grey colors indicate grid cells with precipitation excess lower than 3mm per year.**

**Figure SI4. Global areas of agricultural land and natural ecosystems and global reservoir volume for the years 1900, 1950, and 2000**

a. Land use



b. Reservoir volume

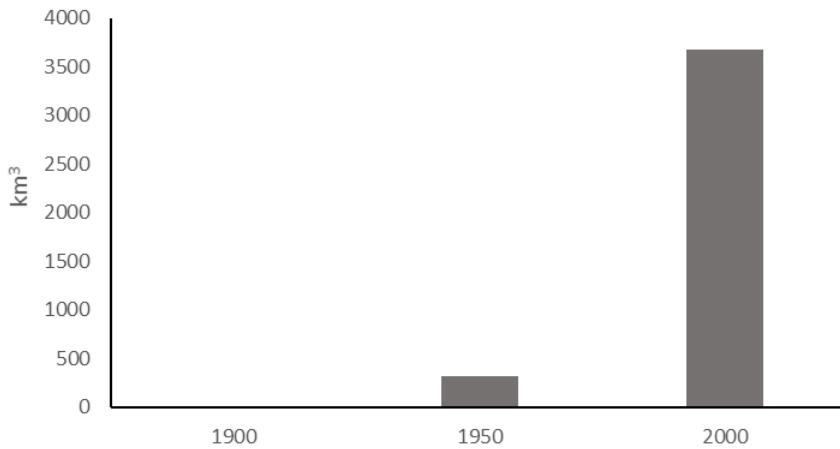
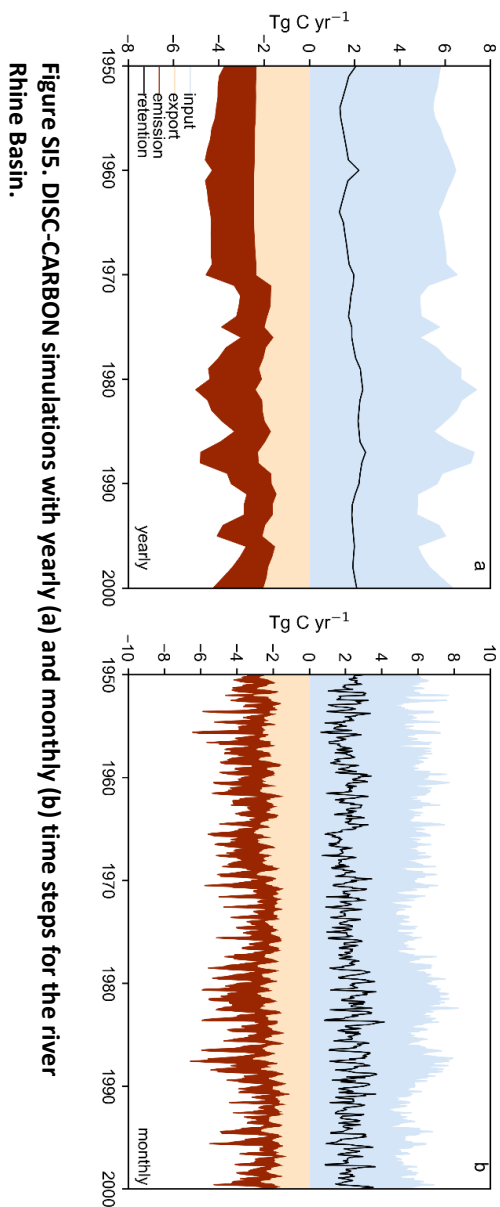


**Figure SI4. a) Global areas of agricultural land and natural ecosystems and b) global reservoir volume for the years 1900, 1950, and 2000 (Beusen et al., 2015b).**

Figure S15. DISC-CARBON simulations with yearly (a) and monthly (b) time steps for the river Rhine Basin



## References

- Alekseevskiy, N. I., Berkovich, K. M. and Chalov, R. S.: Erosion, sediment transportation and accumulation in rivers, *Int. J. Sediment Res.*, 23(2), 93–105, 2008.
- Alin, S. R., Rasera, M. D. F. F. L., Salimon, C. I., Richey, J. E., Holtgrieve, G. W., Krusche, A. V. and Snidvongs, A.: Physical controls on carbon dioxide transfer velocity and flux in low-gradient river systems and implications for regional carbon budgets, *J. Geophys. Res. Biogeosciences*, 116(1), doi:10.1029/2010JG001398, 2011.
- Batjes, N. H.: Harmonized soil property values for broad-scale modelling (WISE30sec) with estimates of global soil carbon stocks, *Geoderma*, 269, 61–68, 2016.
- Beusen, A. H. W., Bouwman, A. F., Van Beek, L. P. H., Mogollón, J. M. and Middelburg, J. J.: Global riverine N and P transport to ocean increased during the twentieth century despite increased retention along the aquatic continuum, *Biogeosciences Discuss.*, 12(23), 20123–20148, doi:10.5194/bgd-12-20123-2015, 2015.
- Billen, G., Garnier, J. and Silvestre, M.: A simplified algorithm for calculating benthic nutrient fluxes in river systems, in *Annales de Limnologie-International Journal of Limnology*, vol. 51, pp. 37–47, EDP Sciences., 2015.
- Bland, J. M. and Altman, D.: Statistical methods for assessing agreement between two methods of clinical measurement, *Lancet*, 327(8476), 307–310, 1986.
- Cerdan, O., Govers, G., Le Bissonnais, Y., Van Oost, K., Poesen, J., Saby, N., Gobin, A., Vacca, A., Quinton, J., Auerswald, K., Klik, A., Kwaad, F. J. P. M., Raclot, D., Ionita, I., Rejman, J., Rousseva, S., Muxart, T., Roxo, M. J. and Dostal, T.: Rates and spatial variations of soil erosion in Europe: A study based on erosion plot data, *Geomorphology*, 122(1–2), 167–177, doi:10.1016/j.geomorph.2010.06.011, 2010.
- Dürr, H. H., Meybeck, M. and Dürr, S. H.: Lithologic composition of the Earth's continental surfaces derived from a new digital map emphasizing riverine material transfer, *Global Biogeochem. Cycles*, 19(4), 1–23, doi:10.1029/2005GB002515, 2005.
- Garnier, J., Billen, G. and Palfner, L.: Understanding the oxygen budget and related ecological processes in the river Mosel: The RIVERSTRAHLER approach, *Hydrobiologia*, 410, 151–166, doi:10.1023/A:1003894200796, 2000.
- Hartmann, J., Lauerwald, R. and Moosdorf, N.: GLORICH-Global river chemistry database, PANGAEA <https://doi.org/10.1594/PANGAEA.902360>, 520, 2019.
- Jansen, N.: Chemical rock weathering as source of dissolved silica and sink of atmospheric CO<sub>2</sub>, *Intitute Biogeochem. Mar. Chem., Dr rer. na*, 125, 2010.

- Kirk, J. T. O.: Light and photosynthesis in aquatic ecosystems, Third Edit., Cambridge University Press., 2011.
- Langeveld, J., Bouwman, A. F., van Hoek, W. J., Vilmin, L., Beusen, A. H. W., Mogollón, J. M. and Middelburg, J. J.: Estimating dissolved carbon concentrations in global soils: a global database and model, *SN Appl. Sci.*, 2(10), 1–21, 2020.
- Lauerwald, R., Hartmann, J., Moosdorf, N., Kempe, S. and Raymond, P. A.: What controls the spatial patterns of the riverine carbonate system? - A case study for North America, *Chem. Geol.*, 337–338, 114–127, doi:10.1016/j.chemgeo.2012.11.011, 2013.
- Mitchell, T. D. and Jones, P. D.: An improved method of constructing a database of monthly climate observations and associated high-resolution grids, *Int. J. Climatol.*, 25(6), 693–712, doi:10.1002/joc.1181, 2005.
- Moosdorf, N., Hartmann, J., Lauerwald, R., Hagedorn, B. and Kempe, S.: Atmospheric CO<sub>2</sub> consumption by chemical weathering in North America, *Geochim. Cosmochim. Acta*, 75(24), 7829–7854, doi:10.1016/j.gca.2011.10.007, 2011.
- Müller, G., Middelburg, J. J. and Sluijs, A.: Introducing GloRiSe—a global database on river sediment composition, *Earth Syst. Sci. Data*, 13(7), 3565–3575, 2021.
- Orr, J. C. and Epitalon, J. M.: Improved routines to model the ocean carbonate system: Mocsy 2.0, *Geosci. Model Dev.*, 8(3), 485–499, doi:10.5194/gmd-8-485-2015, 2015.
- Prairie, Y. T. and Duarte, C. M.: Direct and indirect metabolic CO<sub>2</sub> release by humanity, *Biogeosciences Discuss.*, 3(6), 1781–1789, doi:10.5194/bgd-3-1781-2006, 2006.
- Richardson, D. C., Newbold, J. D., Aufdenkampe, A. K., Taylor, P. G. and Kaplan, L. A.: Measuring heterotrophic respiration rates of suspended particulate organic carbon from stream ecosystems, *Limnol. Oceanogr. Methods*, 11(5), 247–261, 2013.
- Riesebell, U., Wolf-Gladrow, D. A. and Smetacek, V.: Carbon dioxide limitation of marine phytoplankton growth rates, *Nature*, 361, 249–251, 1993.
- Saltelli, A.: Chan. K., Scott EM (ed.), *Sensitivity Analysis*, 2000.
- Scheffer, M.: *Ecology of shallow lakes*, Springer., 2004.
- Sitch, S., Smith, B., Prentice, I. C., Arneth, A., Bondeau, A., Cramer, W., Kaplan, J. O., Levis, S., Lucht, W. and Sykes, M. T.: Evaluation of ecosystem dynamics, plant geography and terrestrial carbon cycling in the LPJ dynamic global vegetation model, *Glob. Chang. Biol.*, 9(2), 161–185, 2003.

- Soetaert, K. and Herman, P. M. J.: A practical guide to ecological modelling: using R as a simulation platform, Springer Science & Business Media., 2008.
- Stehfest, E., van Vuuren, D., Kram, T., Bouwman, L., Alkemade, R., Bakkenes, M., Biemans, H., Bouwman, A., den Elzen, M., Janse, J., Lucas, P., van Minnen, J., Muller, C. and Prins, A. G.: Integrated Assessment of Global Environmental Change with IMAGE 3.0. Model description and policy applications. [online] Available from: <http://www.pbl.nl/en/publications/integrated-assessment-of-global-environmental-change-with-IMAGE-3.0>, 2014.
- Vilmin, L., Mogollón, J. M., Beusen, A. H. W. and Bouwman, A. F.: Forms and subannual variability of nitrogen and phosphorus loading to global river networks over the 20th century, *Glob. Planet. Change*, 163(February), 67–85, doi:10.1016/j.gloplacha.2018.02.007, 2018.
- Vilmin, L., Mogollón, J. M., Beusen, A. H. W., Van Hoek, W. J., Liu, X., Middelburg, J. J. and Bouwman, A. F.: Modeling process-based biogeochemical dynamics in surface fresh waters of large watersheds with the IMAGE-DGNM framework, *J. Adv. Model. Earth Syst.*, 12(11), e2019MS001796, 2020.
- Wanninkhof, R.: Relationship between wind speed and gas exchange over the ocean revisited, *Limnol. Oceanogr. Methods*, 12(JUN), 351–362, doi:10.4319/lom.2014.12.351, 2014.
- Watson, S. J., Cade-Menun, B. J., Needoba, J. A. and Peterson, T. D.: Phosphorus forms in sediments of a river-dominated estuary, *Front. Mar. Sci.*, 5, 302, 2018.

---

---

## Chapter 3

### **Global freshwater CO<sub>2</sub> emissions have increased as a result of rising terrestrial carbon inputs**

Wim Joost van Hoek<sup>1</sup>, Joep J. Langeveld<sup>1</sup>, Lauriane Vilmin<sup>1,2</sup>, Xiaochen Liu<sup>1</sup>, Arthur H.W. Beusen<sup>1,3</sup>, José M. Mogollón<sup>1,4</sup>, Alexander F. Bouwman<sup>1,3</sup>, Jack J. Middelburg<sup>1</sup>

<sup>1</sup> Department of Earth Sciences, Utrecht University, P.O. Box 80021, 3508TA Utrecht, the Netherlands.

<sup>2</sup> Deltares, P.O. Box 177, Delft, the Netherlands. Postcode: 2600 MH.

<sup>3</sup> PBL Netherlands Environmental Assessment Agency, P.O. Box 30314, 2500GH the Hague, the Netherlands.

<sup>4</sup> Department of Industrial Ecology, Leiden University, P.O. Box 9518, 2300RA Leiden, the Netherlands.



**ABSTRACT**

In this study we discuss the spatio-temporal simulation results of the DISC-CARBON model of global CO<sub>2</sub> emissions from inland water systems that reveal an increase from an average of 2.09 Pg C year<sup>-1</sup> in the 1900's to an average of 2.24 Pg C year<sup>-1</sup> in the 1990's, mainly as a result of an increase in terrestrial carbon (C) delivery. Most CO<sub>2</sub> emissions originate from floodplains (1.36 Pg C year<sup>-1</sup>), where CO<sub>2</sub> is produced through mineralization of terrestrial organic C. Streaming waters contribute 0.75 Pg C year<sup>-1</sup> (major streams: 379 Tg C year<sup>-1</sup>; small streams: 386 Tg C year<sup>-1</sup>) of the total CO<sub>2</sub> emissions mainly due to the influx of CO<sub>2</sub> supersaturated groundwater. Lakes and reservoirs emit 0.13 Pg C year<sup>-1</sup>. Although during the 20th century the delivery of organic C through soil erosion increased from 106 Tg C year<sup>-1</sup> to 168 Tg C year<sup>-1</sup> and the volume of reservoirs from nearly 0 to more than 3500 km<sup>3</sup>, DISC-CARBON simulations do not indicate a major influence of these changes on global CO<sub>2</sub> emissions from freshwaters.

## 1 Introduction

Global freshwaters emit between 0.75 and 3.9 Pg carbon (C)year<sup>-1</sup> in the form of carbon dioxide (CO<sub>2</sub>) (Cole et al., 2007; Aufdenkampe et al., 2011; Raymond et al., 2013; Lauerwald et al., 2015; Drake et al., 2018). This total CO<sub>2</sub> emission from freshwaters is of a similar magnitude as net terrestrial and oceanic uptake of anthropogenic CO<sub>2</sub> (Quéré et al., 2018). Terrestrial ecosystems currently act as a sink for anthropogenic C, with a net uptake of 3.2 ±0.6 Pg C year<sup>-1</sup> (Friedlingstein et al., 2022). Nevertheless, only recently the riverine C flux has been placed in the context of the global carbon (C) cycle in assessment reports such as the Intergovernmental Panel on Climate Change (IPCC, 2021)

Carbon is transferred via streams, rivers, lakes and reservoirs from the terrestrial system to the coastal ocean. A substantial proportion of C delivered to freshwaters is emitted as CO<sub>2</sub> during its transport to the coastal ocean. This implies that part of the terrestrial sink is counterbalanced by the lateral transport of C through soils, groundwater, and via other allochthonous inputs to inland waters, and eventual outgassing of CO<sub>2</sub> from surface waters (Cole et al., 2007). However, it is unclear how freshwater CO<sub>2</sub> effluxes are affected by various global change processes. The dynamics in response to global change processes have only been tacitly investigated. For example, the CO<sub>2</sub> emissions from inland waters stem largely from decomposition of organic material from terrestrial vegetation, and may be changing due to climate warming, human induced changes in land-use and hydrology.

Estimates of present-day total CO<sub>2</sub> emissions from global freshwaters range between 0.75 Pg C year<sup>-1</sup> and 3.9 Pg C year<sup>-1</sup> (Cole et al., 2007; Aufdenkampe et al., 2011; Raymond et al., 2013; Regnier et al., 2013; Lauerwald et al., 2015; Sawakuchi et al., 2017; Drake et al., 2018). This wide range is due to differences in data sets, approaches, system boundaries and upscaling procedures. Cole et al. (2007), as part of a literature-based inventory of the C budget of global freshwaters, made a global lumped estimate of 0.75 Pg C year<sup>-1</sup>. More recently, Aufdenkampe et al. (2011) distinguished various waterbody types (including wetlands) in 3 climate zones (tropical, temperate and boreal) and presented a global estimate for the riverine CO<sub>2</sub> efflux of 3.3 Pg C year<sup>-1</sup>. Subsequently, regional CO<sub>2</sub> emissions with a global total of 2.1 Pg C year<sup>-1</sup> were estimated by Raymond et al. (2013), by quantifying emissions from observed partial CO<sub>2</sub> pressure for the global coastal segmentation and its river catchment contributors (COSCAT) of Meybeck et al. (2006).

These studies have been helpful to better constrain total CO<sub>2</sub> emission from global freshwaters. Apart from the inconsistencies in the approaches used, these studies (1) do not address the temporal dynamics of the CO<sub>2</sub> emission in the terrestrial-aquatic continuum (seasonal or longer term) and (2) only provide estimates for the present-day total CO<sub>2</sub> emission but possible impacts due to human-induced global changes are not known. Global freshwaters are strongly affected by human activities, by interference in the hydrology (Van Beek et al., 2011), carbon delivery and in-stream biogeochemistry (Regnier et al., 2013; Beusen et al., 2015b). An estimate of the anthropogenic perturbation of CO<sub>2</sub> emissions from freshwater systems is needed to understand the global carbon budget.

Carbon dioxide emissions from rivers and other freshwater systems are governed by the balance between multiple terrestrial inputs, in-stream primary production and internal C processing. In order to improve our understanding of the freshwater C cycle, we use the Dynamic-In-Stream-Chemistry model for Carbon (DISC-CARBON) model presented by van Hoek et al. (2021) that (i) links terrestrial and aquatic ecosystems in the river continuum via the hydrological cycle; and (ii) describes the seasonal dynamics of the C cycle, as well as the long-term changes, by integrating key processes involved in transformations of different C forms in a single framework.

Here we present global CO<sub>2</sub> emissions from river networks over the 20th century, and identify major emission hotspots and drivers, with the goal to better understand how interacting global changes have been affecting the global C budget in inland waters and to estimate the anthropogenic component of freshwater CO<sub>2</sub> emission.

## **2 Model description**

DISC-CARBON simulates the in-stream C biogeochemistry within the Integrated Model to Assess the Global Environment -Dynamic Global Nutrient Model (IMAGE-DGNM) framework (Figure 1a). DISC-CARBON has been described in detail by van Hoek et al. (2021). Here we present a brief outline. DISC consistently couples climate, hydrology, soils, groundwater and vegetation and land use to simulate in-stream biogeochemistry in a single process-based modelling framework. It simulates the C-cycle and CO<sub>2</sub> dynamics in the river continuum at the global scale with a spatiotemporal resolution of 0.5 by 0.5 degrees and a yearly timestep from 1900-2000. As such our study is the first integrated approach to describe the long-term dynamics of the C fluxes along the river continuum, i.e. delivery from the terrestrial soil-vegetation system, in-stream primary production, carbon burial and processing leading to CO<sub>2</sub> exchange fluxes, and C export to the global coastal ocean over the course of the 20<sup>th</sup> century.

DGNM uses the climate and hydrological constraints from PCR-GLOBWB, a global hydrological model (Van Beek et al., 2011), to calculate water flows and volumes. Organic C inputs include litterfall from LPJml (Sitch et al., 2003), and soil erosion, surface runoff and waste water inputs from IMAGE (Stehfest et al., 2014). Weathering and surface run-off provide both dissolved inorganic carbon (*DIC*) and alkalinity (*ALK*), weathering input is based on (Hartmann et al., 2014; Langeveld et al., 2019). From the hydrological constraints and C inputs follows a lateral transport of dissolved organic carbon (*DOC*), particulate organic carbon (*POC*), *DIC* and *ALK* in each waterbody within a river basin from lower order to the river mouth, including lakes, reservoirs, wetlands and floodplains. Transport is calculated within 0.5 by 0.5 spatial degree grid cells (transfer from lower stream orders to higher orders and exchanges between floodplain and main stem) as well as from upstream to downstream grid cells along the main branch of rivers. After its delivery to freshwaters and along its transport, C transformations, atmospheric exchange, resuspension/deposition dynamics and primary production are numerically resolved (Figure 1b). We apply DISC-CARBON with time series of data covering the 20<sup>th</sup> century.

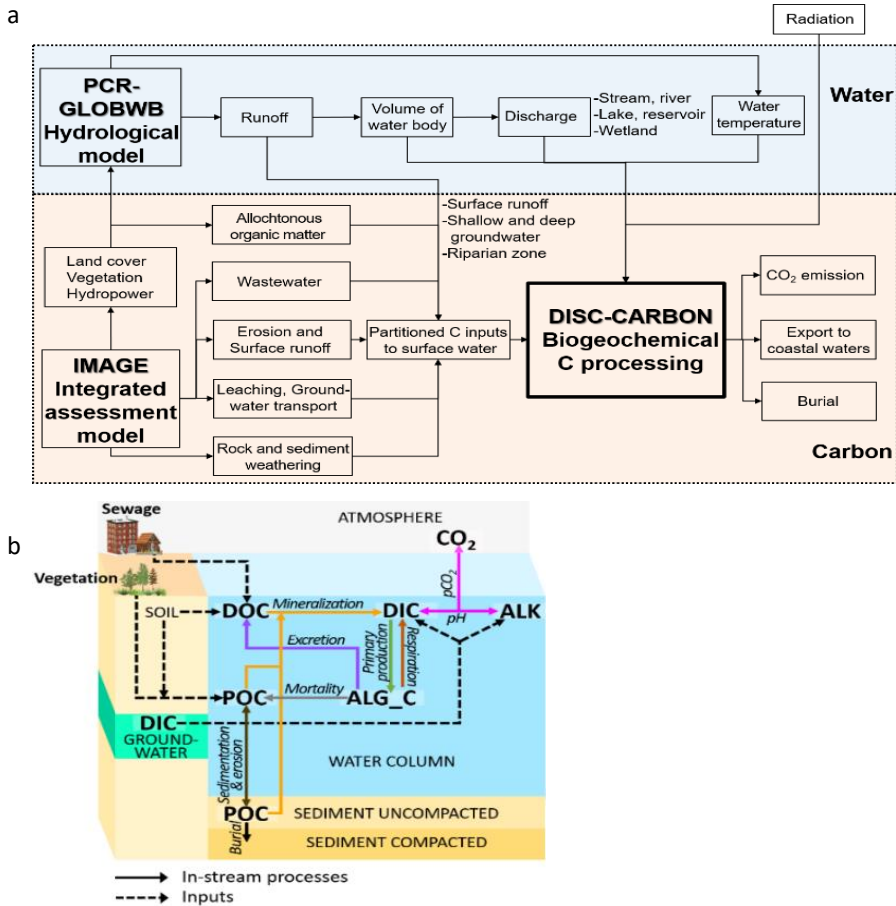


Figure 2. (a) Scheme of the IMAGE-DGNM framework including the DISC-CARBON module for the in-stream biogeochemical C transformation processes and (b) scheme of C sources, forms and biogeochemical transformations in all simulated waterbodies in the DISC-CARBON module. The formulae for each transformation process are listed in Table S12.

In DISC-CARBON, *DIC* originates from three main pathways:

(1) *DIC* is produced through temperature depending mineralization  $M$  of organic carbon  $OC$  ( $M_{OC}$ ). The organic carbon can either be imported or locally produced and be in dissolved, suspended particulate or sedimented particulate form (*DOC*,  $POC_{terre}$ ,  $POC_{auto}$ ,  $SEDOC_{terre}$  or  $SEDOC_{auto}$ ). A standard  $Q_{10}$  formulation is used for the temperature dependence:

$$M_{OC} = x * M_{ref} * Q_{10}^{\frac{(T-T_{ref})}{10}} \quad (1)$$

where  $x$  is the quantity of organic form  $OC$ ,  $M_{ref}$  is the reference mineralization rate for that form of  $OC$ ,  $Q_{10}$  is a unitless quantity (fixed at 2 for all  $OC$  forms),  $T$  is the water temperature,  $T_{ref}$  is the reference temperature at which  $M_{ref}$  is  $M_c$  (fixed at 15 °C for all  $OC$  forms). Values of  $M_{ref}$  for each  $OC$  form are provided in the SI.

(2) *DIC* is also produced by respiration of algae ( $R_{AC}$ ) and includes both phytoplankton  $ALG\_C$  and benthic primary producers  $ALG\_Cbenthic$ ):

$$R_{AC} = x * R_{ref} * e^{-\frac{(T_{opt} - T)^2}{\sigma^2}} \quad (2)$$

with  $x$  is the algal biomass for either phytoplankton or benthic primary producers,  $R_{ref}$  is the reference respiration rate for the primary producer involved,  $T_{opt}$  is the optimal respiration temperature and  $\sigma$  represents a range of temperatures.

(3) *DIC* is also coming from groundwater (GRW) and surface runoff (SRO), where hydrology is a function of land use, soil properties, lithology and net evapotranspiration (Beusen et al., 2015a). The *DIC* concentration in SRO is constrained by atmospheric  $pCO_2$  and soil pH (Batjes, 2015). The *DIC* and *ALK* fluxes from GRW are a function of hydrology, soil respiration, soil and hydraulic properties, lithology, weathering and residence time-dependent processing of *DOC* to *DIC* (see Text S1 for an extensive description and discussion).

From  $ALK$ ,  $DIC$  and  $T$ , DISC-CARBON calculates  $CO_{2water}$  and  $pCO_2$  using Mocsy 2.0 (Orr and Epitalon, 2015). Subsequently,  $CO_2$  emission or the exchange of  $DIC$  with the atmosphere ( $DIC_{exch}$ ) is calculated:

$$DIC_{exch} = k_{air} * (CO_{2water} - CO_{2atmosphere}) \quad (3)$$

with  $CO_{2atmosphere} = 400$  ppm and

$$k_{air} = k_{600} / \left(\frac{600}{Sc_T}\right)^{-0.5} \quad (4)$$

where  $k_{600}$  is the normalized  $k_{air}$  at 20°C and  $Sc_T$  is the Schmidt number at  $T$  [C°] (Wanninkhof, 2014), calculated from:

$$Sc_T = 1911.1 - 118.11T + 3.4527 * T^2 - 0.04132 * T^3 \quad (5)$$

The atmospheric exchange coefficient  $k_{600}$  is estimated from flow velocity ( $v$  [ $cm\ s^{-1}$ ]) for small rivers or from windspeed ( $\bar{u}_{10}$  [ $m\ s^{-1}$ ]) for large rivers (Alin et al., 2011):

$$k_{600} = \begin{cases} a_1 + b_1 \bar{u}_{10} & \text{if stream width} > 100 \text{ meters} \\ a_2 + b_2 * v & \text{if stream width} < 100 \text{ meters} \end{cases} \quad (6)$$

Values for  $a_1$ ,  $b_1$ ,  $a_2$  and  $b_2$  are by default set to respectively 4.46, 7.11, 13.82 and 0.35 (Alin et al., 2011).

The full model has been presented in (van Hoek et al., 2021) and the most relevant interactions for this paper are shown in Figure 1. The DISC-CARBON model uses the same equations and parameters for each individual grid cell and for the entire period. In other words, the model is not tuned to specific observations and the performance needs to be assessed by comparing model results with observations for specific large rivers. A previous version of the model has been extensively tested against various stations along the river Rhine (Chapter 4 of this thesis). Here we present an additional performance test by comparing model results with measured time series of different C forms from the USGS for the Mississippi river at St. Francisville (Aulenbach et al., 2007); the most downstream station without tidal influence. Furthermore, we compare observed  $pCO_2$  values for river end-members of 14 estuaries around the world (Abril and Borges, 2005). The performance is expressed in terms of root-mean-square-error (RMSE).

Lastly, to further evaluate the performance of DISC-CARBON and to identify the main governing factors, we examine the sensitivity of the modelled 5-year average (1995-2000) for five watersheds. The sensitivity of CO<sub>2</sub> emissions for the Amazon, Mississippi, Nile, Lena and Yangtze river was evaluated using a Latin Hypercube Sampling approach (see Text S2 for an extensive description and discussion). The five watersheds are considered to represent a large proportion of worlds' climates.

### 3 Results

#### 3.1 Observations and simulations

Measurements of alkalinity, pCO<sub>2</sub>, pH and total organic carbon (TOC=DOC+POC) in the main branch of the Mississippi basin at station St Francisville are compared to DISC-CARBON simulation results (Figure 4), because multiyear timeseries data are available for this station. The observed concentrations were aggregated to yearly values (years with <6 observations are excluded).

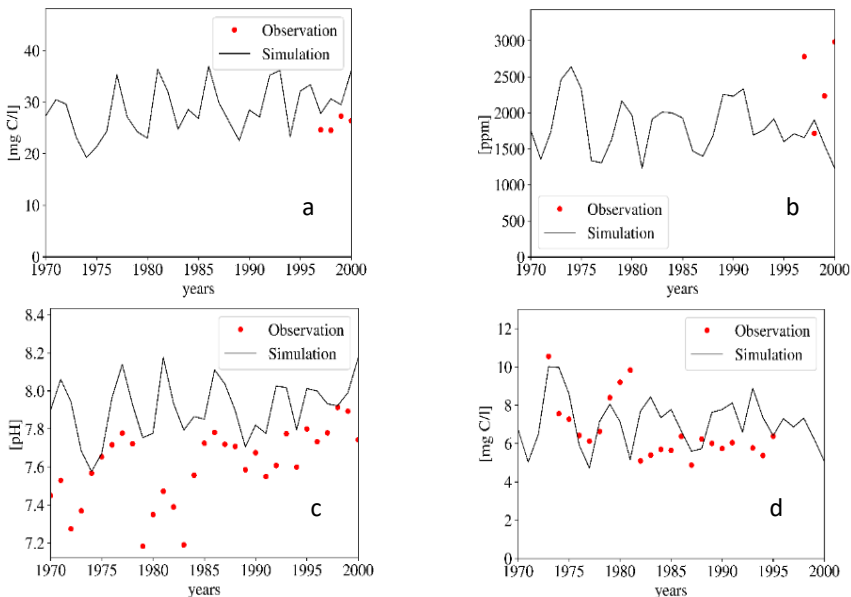


**Figure 2. Yearly observations and simulations of (a) alkalinity (RMSE = 23%), (b) pCO<sub>2</sub> (RMSE = 45%), (c) pH and (d) TOC (RMSE = 30%)**



Correspondence between model results and observations for alkalinity and TOC are acceptable for this global model with RMSE values of 23% and 30%, respectively. Moreover, there appears to be no systematic over- or underestimation. Predictions and observations for  $p\text{CO}_2$  are of the same order of magnitude as the measurements, but the RMSE is higher (45%). The data for pH cover a longer timespan; the model slightly overestimates this variable, but simulates its trends realistically. The model overestimates pH values likely because acid generating processes such as nitrification (ammonia oxidation) are not included in our simple model (Soetaert et al., 2007; Middelburg, 2019). RMSE values below 50% indicate that DISC-CARBON based on local forcings and generic, globally uniform parameters adequately captures the main trend. Model-data comparisons for other Mississippi stations are presented in the SI.

Table 1 presents another performance test based on  $p\text{CO}_2$  observations. Abril & Borges (2005) presented observed river end-member  $p\text{CO}_2$  values for 14 estuaries in Europe and North America. Their observed  $p\text{CO}_2$  values show a reasonable agreement with DISC simulations given that sub-grid, small-scale observations are compared with grid scale simulation outcomes.

**Table 1. Observed pCO<sub>2</sub> values in estuaries (Abril and Borges, 2005) compared to DISC simulations of pCO<sub>2</sub> in the most downstream grid cell of the corresponding basins. Simulated values are shown in green if values are within range of measurements, shown in red if out of the observed values range.**

| <i>River</i>    | <i>Country / State</i> | <i>Observed pCO<sub>2</sub> range<br/>(max - min)</i> |      | <i>DISC<br/>simulation<br/>values pCO<sub>2</sub></i> |
|-----------------|------------------------|---|------|---|
| <i>Altamaha</i> | US/Georgia             | 7800  | 380  | 3332  |
| <i>Columbia</i> | US/Oregon              | 950   | 560  | 1954  |
| <i>Douro</i>    | Portugal               | 2200  | 1330 | 824   |
| <i>Elbe</i>     | Germany                | 1100  | 580  | 829   |
| <i>Gironde</i>  | France                 | 3535  | 500  | 1101  |
| <i>Hudson</i>   | US/NY                  | 1795  | 515  | 2103  |
| <i>James</i>    | US/Virginia            | 1361  | 284  | 1784  |
| <i>Loire</i>    | France                 | 2780  | 770  | 1128  |
| <i>Potomac</i>  | US/Maryland            | 878   | 646  | 1322  |
| <i>Rhine</i>    | The Netherlands        | 1870  | 570  | 1450  |
| <i>Satilla</i>  | US/Georgia             | 5475  | 420  | 4400  |
| <i>Scheldt</i>  | Belgium                | 6650  | 495  | 1263  |
| <i>Seine</i>    | France                 | 5345  | 826  | 1818  |
| <i>Thames</i>   | UK                     | 3755  | 560  | 2997  |

### 3.2 CO<sub>2</sub> emissions, sources and spatial distribution

Decadal average global emissions of CO<sub>2</sub> from freshwaters have increased between 1900 and 2000 from 2.09 Pg C year<sup>-1</sup> to 2.24 Pg C year<sup>-1</sup> (+7%) (Figure 3a). In the first half of the 20<sup>th</sup> century, emissions have been rather stable, around 2.1 Pg C year<sup>-1</sup>. After 1970, CO<sub>2</sub> emissions increased not only in magnitude, but also their variability increased. The global average CO<sub>2</sub> emission rates from surface freshwaters have gone up from 428 g C meter<sup>-2</sup> year<sup>-1</sup> in the first decade to 459 g C meter<sup>-2</sup> year<sup>-1</sup> in the last decade of the 20<sup>th</sup> century. This increase, similar to the global CO<sub>2</sub> emission, occurred after 1970 (Figure 3b).

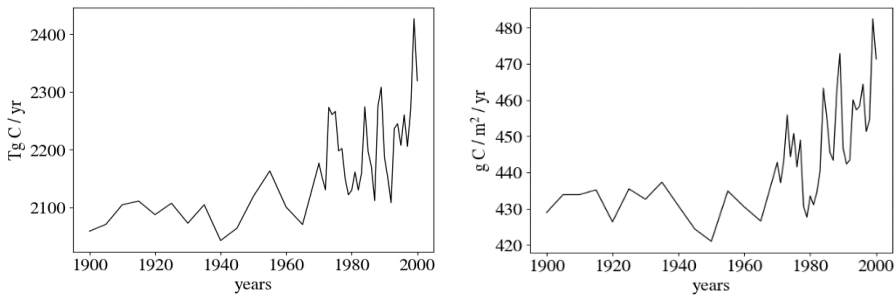


**Figure 3. (a) Total global CO<sub>2</sub> emission and (b) surficial emission rates from global**

Figure 4a shows that throughout the century most CO<sub>2</sub> emissions (60% or 1.36 Pg C year<sup>-1</sup> in 1990's) came from flooded areas. Wide streams (>60 m wide), small streams, reservoirs and major lakes contributed 17% (379 Tg C year<sup>-1</sup>), 17% (386 Tg C year<sup>-1</sup>), 3% and 2% to the total emission, respectively (Figure 4a). The CO<sub>2</sub> emission rates showed a different pattern. Small streams showed high CO<sub>2</sub> emission rates of 3476 g C meter<sup>-2</sup> year<sup>-1</sup>, followed by wide streams emitting 2487 g C meter<sup>-2</sup> year<sup>-1</sup>. Lower emissions rates occurred in flooded areas (401 g C meter<sup>-2</sup> year<sup>-1</sup>), reservoirs (174 g C meter<sup>-2</sup> year<sup>-1</sup>) and lakes (62 g C meter<sup>-2</sup> year<sup>-1</sup>). The total change in global freshwater CO<sub>2</sub> emissions throughout the 20<sup>th</sup> century was +160 Tg C year<sup>-1</sup>. Figure 4a shows that most of the CO<sub>2</sub> emission increase during the 20<sup>th</sup> century occurred in reservoirs (69 Tg C year<sup>-1</sup>, or 44% of the change). Floodplains contributed another 43 Tg C year<sup>-1</sup> (27%) to the total increase. Wide streams, small streams and lakes contributed 14%, 8% and 7% to the emissions increase respectively.

The global freshwater CO<sub>2</sub> emission rates increased by +31 g C meter<sup>-2</sup> year<sup>-1</sup> on average, but there are large differences between waterbody types (Figure 4b). Wide streams and small streams showed the strongest acceleration of the C cycling, with

an increase of +366 g C meter<sup>-2</sup> year<sup>-1</sup> and +349 g C meter<sup>-2</sup> year<sup>-1</sup> respectively. Reservoir emission rates decreased by 134 g C meter<sup>-2</sup> year<sup>-1</sup>. Nevertheless, their global CO<sub>2</sub> emission has increased (+69 Tg C year<sup>-1</sup>) because of their areal increase (+0.4 million km<sup>2</sup>).

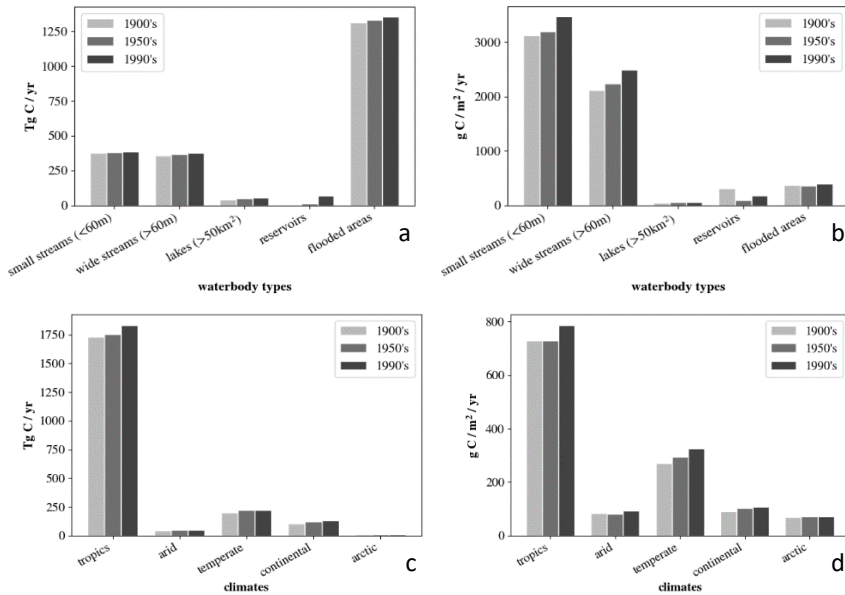


**Figure 4. (a) Total CO<sub>2</sub> emissions, (b) CO<sub>2</sub> emission rates by waterbody type, (c) total CO<sub>2</sub> emissions and (d) emission rates by climate zone, 10 year average fluxes for 1900's, 1950's and the 1990's.**

Figure 4c and d present the freshwater CO<sub>2</sub> emissions by climate type. Tropical freshwaters were the largest freshwater CO<sub>2</sub> emission source throughout the 20<sup>th</sup> century, with 1.8 Pg C year<sup>-1</sup> or 82% of global emission from freshwaters in the 1990's. They also showed the highest emission rates (787 g C meter<sup>-2</sup> year<sup>-1</sup>) (Figure 4c,b). Freshwaters in temperate climates emitted 221 Tg C year<sup>-1</sup> (10%), with rates of 325 g C meter<sup>-2</sup> year<sup>-1</sup>. Continental (132 Tg C year<sup>-1</sup> or 6%), arid (50 Tg C year<sup>-1</sup>, or 2%) and arctic (7 Tg C year<sup>-1</sup> which is <<1%) had a small contribution to total CO<sub>2</sub> emissions.

The tropics also contributed most to the increase of freshwater CO<sub>2</sub> emissions (100 Tg C year<sup>-1</sup>, 63% of the total change). CO<sub>2</sub> emissions from continental and temperate climates increased by 28 Tg C year<sup>-1</sup> and 22 Tg C year<sup>-1</sup>, respectively. Absolute emissions from other climates only changed marginally.

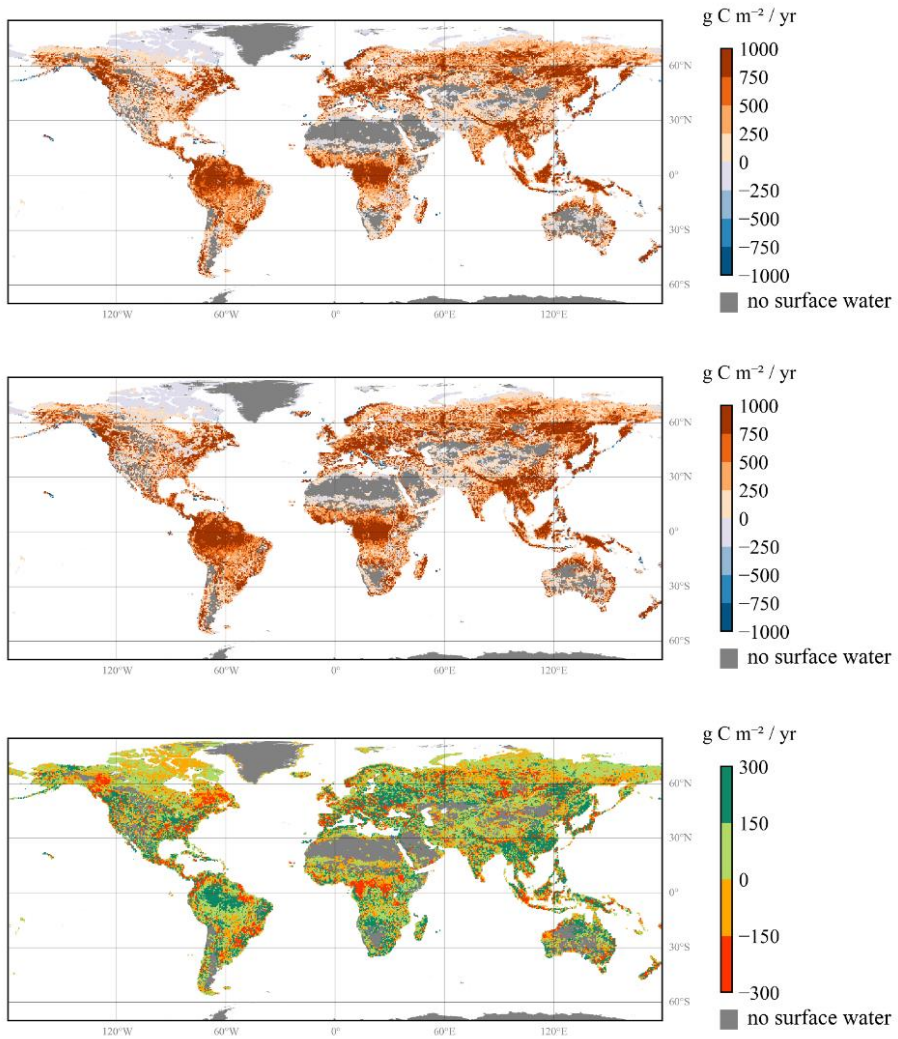


**Figure 5.** Decade average CO<sub>2</sub> emissions from freshwaters in 1900's (a) and 1990's (b); (c) Difference in CO<sub>2</sub> emission between 1900's and 1990's

The spatial patterns of emissions around 1900 and 1990 are similar (Figure 5a,b). Many south American, tropical African, central Asian, South-east Asian and European freshwaters show emission rates of more than 1000 g C meter<sup>-2</sup> year<sup>-1</sup>. In these regions, most CO<sub>2</sub> emissions originate from flooded areas. CO<sub>2</sub> emission rates are high in Central-America, India, southeast Asia, central Europe and eastern Asia; here most emissions originate from CO<sub>2</sub> saturated groundwater. DISC-CARBON simulates an uptake of CO<sub>2</sub> by freshwaters in the northern parts of Canada and the northern Eurasian continent; generally as a result of low OC delivery and low OC decomposition rates as a result of low temperatures. Figure 9c shows that the CO<sub>2</sub> emissions from freshwaters have increased slightly, most strongly in the central Amazon. In contrast, Central African freshwaters, western and eastern Canadian freshwaters and patches of Siberian freshwaters show large areas with decreases in CO<sub>2</sub> emissions rates of more than 300 g C meter<sup>-2</sup> year<sup>-1</sup>. The spatio-temporal variability of these differences is related to variable delivery of CO<sub>2</sub> supersaturated groundwater.

#### 4 Sensitivity analysis

Amazon CO<sub>2</sub> emissions strongly respond to variability in POC delivery in flooded areas (SRC=0.85) (Table SI2). The reason for this high responsiveness is that emissions from flooded areas in the Amazon basin are primarily responsive to POC delivery in flooded areas, combined with a contribution of 70% of the basin total CO<sub>2</sub> emissions from flooded areas makes the basin as a whole responsive to the POC delivery in flooded areas.

In contrast to the Amazon, the CO<sub>2</sub> emissions from the Mississippi, Lena and Yangtze respond most strongly to DIC delivery from groundwater with SRC's of 0.50, 0.62 and 0.59 respectively (Table SI2). For the Lena and Yangtze, groundwater DIC delivery is the dominant driver of variability because their CO<sub>2</sub> content mostly originates from groundwater. The fraction of DIC delivery of the total C delivery in these rivers is 40% and 40% (versus 17% and 23% for POC delivery respectively). For the Mississippi, the dominant source of C delivery is litterfall in flooded areas (43% of total C delivery versus 36% for groundwater DIC) and also 70% of the total CO<sub>2</sub> emissions originate from flooded areas, but basin total CO<sub>2</sub> emissions are still most sensitive to DIC delivery from groundwater. In the Mississippi and the Yangtze, we see a negative response of basin total CO<sub>2</sub> emissions to the maximum primary production rate. Furthermore, the Mississippi, the Yangtze and the Lena show an important negative response to increased alkalinity inputs from groundwater. In general, increased alkalinity reduces the pCO<sub>2</sub> and as such less CO<sub>2</sub> is emitted.

The Nile shows a clear response of basin CO<sub>2</sub> emissions to temperature variability (SRC=0.65) (Table S12), although CO<sub>2</sub> variability is also regulated by POC delivery in flooded areas. The emission response to temperature occurs in small streams (<60m), wide streams (>60m) as well as in flooded areas. Finally, CO<sub>2</sub> emissions are strongly influenced by the depth of the water column.

## 5 Discussion

Our dynamic and spatially resolved freshwater carbon model links hydrology, carbon inputs and biogeochemical transformations to CO<sub>2</sub> emission from freshwaters. DISC-CARBON calculations show that CO<sub>2</sub> emissions from global freshwaters have increased in the second half of the 20<sup>th</sup> century from 2.09 Pg C year<sup>-1</sup> to 2.24 Pg C year<sup>-1</sup>.

The sensitivity analysis (Table S12) showed that CO<sub>2</sub> emission is particularly sensitive to C inputs from land to freshwaters. More specifically, CO<sub>2</sub> emissions are sensitive to the delivery of terrestrial organic C to flooded areas and to the input of DIC from groundwater. There are clear differences between the rivers studied. The CO<sub>2</sub> emissions from the Amazon and Nile rivers are most sensitive to POC inputs in flooded areas, while Mississippi, Yangtze and Lena are most sensitive to DIC inputs from groundwater, reflecting the different nature and geohydrological setting of these rivers. This has important consequences for the way CO<sub>2</sub> emissions from freshwater systems should be considered in a globally changing C cycle; changes in the terrestrial C cycle (e.g. due to N or CO<sub>2</sub> fertilization of vegetation or land-use change) are directly reflected in CO<sub>2</sub> emissions from freshwaters. The increase in CO<sub>2</sub> emission and emission variability since 1970 (Figure 3) can be attributed to the increased and more variable terrestrial carbon cycle since then (Friedlingstein et al., 2022). Hence, improved understanding of C delivery to freshwater systems is key for a robust quantification of their CO<sub>2</sub> emissions.

The recognition that freshwaters represent a key component in the global C cycle (Cole et al., 2007) has stimulated many research efforts to quantify CO<sub>2</sub> emissions from freshwater systems. Table 2 shows that estimates have increased drastically from 0.75 Pg C year<sup>-1</sup> (Cole et al., 2007) to 3.9 Pg C year<sup>-1</sup> (Sawakuchi et al., 2017) due to an increase in the availability of pCO<sub>2</sub> data for rivers, lakes and reservoirs (Hartmann et al., 2014b) and improved spatial and environmental constraints in major tropical basins such as the Amazon and the Congo (Borges et al., 2015b; Sawakuchi et al., 2017).

Literature suggests that tropical basins account for 75% of total emissions while they only account for 35% of the land surface (Ward et al., 2017). DISC-CARBON simulations revealed a similar tropical contribution to freshwater CO<sub>2</sub> emissions (82% or 1.84 Pg C year<sup>-1</sup>) throughout the 20<sup>th</sup> century. The Amazon has the largest contribution with 943 Tg C year<sup>-1</sup>, which is consistent with the 800 Tg C year<sup>-1</sup> estimated by Rasera et al. (2013), but twice the estimate of 470 Tg C year<sup>-1</sup> by Richey et al. (2002). The most recent CO<sub>2</sub> emission estimate for Amazon freshwaters (1.39 Pg C year<sup>-1</sup>) is even higher (Sawakuchi et al., 2017), but this number includes contributions from the many tidal floodplains in the lower Amazonian basin. We note that our global estimates and those of Raymond et al. (2013) are very similar for global C delivery (3.5 vs. 3.4 Pg C year<sup>-1</sup>) and CO<sub>2</sub> emissions (2.24 vs. 2.18 Pg C year<sup>-1</sup>). This consistency strengthens the accuracy of these estimates because the Raymond et al. (2013) results are based on a spatially resolved large database of observed pCO<sub>2</sub> values, while our pCO<sub>2</sub> estimates are calculated from a carbon balance model. However, both DISC-CARBON and Raymond et al. (2013) do not explicitly resolve wetlands that may contribute substantially to riverine pCO<sub>2</sub> values (Borges et al., 2015a)

**Table 2. Inventory of global studies on current freshwater C inputs and CO<sub>2</sub> emissions (after Drake et al., 2018), including this study in Pg C year<sup>-1</sup>.**

\* Emissions as fraction of the input

| <i>Studies</i>                      | <i>Inputs</i> | <i>Emissions (*)</i> |
|-------------------------------------|---------------|----------------------|
| <i>Cole et al. (2007)</i>           | 1.9           | 0.75 (39%)           |
| <i>Battin et al. (2009)</i>         | 1.9           | 1.2 (63%)            |
| <i>Tranvik et al. (2009)</i>        | 2.1           | 1.4 (66%)            |
| <i>Bastviken et al. (2011)</i>      | 2.2           | 1.5 (68%)            |
| <i>Regnier et al. (2013)</i>        | 2.5           | 1.2 (48%)            |
| <i>Raymond et al. (2013)</i>        | 3.4           | 2.1 (62%)            |
| <i>Borges et al. (2015)</i>         | 4             | 2.78 (70%)           |
| <i>Holgerson and Raymond (2016)</i> | 4.3           | 3.1 (72%)            |
| <i>Sawakuchi et al (2017)</i>       | 5.1           | 3.9 (76%)            |
| <i>This study</i>                   | 3.5           | 2.24 (64%)           |



DISC-CARBON simulations indicate that total CO<sub>2</sub> emissions increased by 0.15 Pg C year<sup>-1</sup> (i.e. 7 % from 2.09 Pg C year<sup>-1</sup> to 2.24 Pg C year<sup>-1</sup>) over the last century. This is primarily because the delivery of C to freshwater systems has increased from 3.3 Pg year<sup>-1</sup> to 3.5 Pg year<sup>-1</sup> (+6%). This 200 Tg C year<sup>-1</sup> increase includes +102 Tg C year<sup>-1</sup> from increased *POC* delivery, +77 Tg C year<sup>-1</sup> from increased groundwater *DIC* delivery and +25 Tg C year<sup>-1</sup> from increased *DOC* delivery. The increased *POC* input (+102 Tg C year<sup>-1</sup>) can be attributed to the increased terrestrial NPP (+40 Tg C year<sup>-1</sup>) (Stehfest et al., 2014) and inputs through soil erosion due to land-use change (+62 Tg C year<sup>-1</sup>). About 50% of the increase enters floodplains, the other 50% originates from increased delivery to small streams (<60m) via riparian zones.

Accordingly, the anthropogenic contribution to freshwater CO<sub>2</sub> emissions is about 0.15 Pg C year<sup>-1</sup> and this additional CO<sub>2</sub> emission should be included in the future anthropogenic carbon assessments. However, Regnier et al. (2013) reported a much stronger anthropogenic perturbation in global freshwater C cycling. In their study terrestrial inputs to the hydrosphere increased by 1 Pg C year<sup>-1</sup>, primarily because of a 0.8±0.4 Pg C year<sup>-1</sup> increase through soil erosion. Of this perturbation in C delivery, ~0.4 Pg C year<sup>-1</sup> returns to the atmosphere as CO<sub>2</sub>, ~0.5 Pg C year<sup>-1</sup> is stored in aquatic ecosystems and ~0.1 Pg C year<sup>-1</sup> is exported to the ocean. This difference in the anthropogenic perturbation of the aquatic C cycle between our study (~0.2 Pg C year<sup>-1</sup>) and that of Regnier et al. (2013) of ~1 Pg C year<sup>-1</sup> is due differences in methodology (spatio-temporal simulation vs. literature assessment) and estimates of soil erosion. Our relatively conservative perturbation estimate is due to our low estimate for soil erosion (+0.062 Pg C year<sup>-1</sup>) vs ~0.8 Pg C year<sup>-1</sup> of Regnier et al. (2013). A recent study on soil erosion arrived at a global organic carbon loss through soil erosion of 0.13 Pg C year<sup>-1</sup> for the last century (Sanderman et al., 2017), which corresponds fairly well with our century average estimate of 0.13 Pg C year<sup>-1</sup>.

DISC-CARBON resolves different waterbody types and their role in carbon cycling can thus be identified. Flooded areas dominate the global CO<sub>2</sub> emissions from freshwaters and their changes (+0.18 Pg C year<sup>-1</sup>, from 1.29 to 1.47 Pg C year<sup>-1</sup>), with minor contributions from reservoirs (+0.07 Pg C year<sup>-1</sup>, from 0 to 0.07 Pg C year<sup>-1</sup>), small streams (+0.06, from 0.44 to 0.5 Pg C year<sup>-1</sup>) and rivers (+0.03, from 0.28 to 0.31 Pg C year<sup>-1</sup>). Lakes have a small contribution to the rise in CO<sub>2</sub> emissions from freshwaters. Tropical flooded areas are the dominant CO<sub>2</sub> source in the global river continuum in terms of total CO<sub>2</sub> emissions, because they receive high OC inputs (1.7 Pg C year<sup>-1</sup>, which is 48% of the total C delivery to global freshwaters).

Globally, 64% or 1.4 Tg C year<sup>-1</sup> of the 2.2 Pg C year<sup>-1</sup> of organic litter C input from terrestrial vegetation that is directly delivered to floodplains is mineralized to CO<sub>2</sub>. Additional CO<sub>2</sub> in flooded areas is produced by mineralization of DOC (0.21 Pg C year<sup>-1</sup>) and autochthonous organic C production (1.8 Pg C year<sup>-1</sup>). Total CO<sub>2</sub> production in floodplains is 3.4 Pg C year<sup>-1</sup>; about 45% or 1.4 Pg C year<sup>-1</sup> of it escapes to the atmosphere as CO<sub>2</sub>, while the other half is consumed by primary production (2 Pg C year<sup>-1</sup>) or transported downstream (<1%).

Many other studies identify tropical freshwaters as global hotspots for CO<sub>2</sub> emissions (e.g. Richey et al., 2002; Abril et al., 2014; Borges et al., 2015). Floodplains are highly dynamic, complex systems that, in the tropics, cover large areas that show a strong seasonal variation (Melack et al., 2009). Floodplains exert a strong influence on the hydrology, ecology and biogeochemistry of many lowland tropical rivers, such as some of the world's largest rivers in the tropics (Amazon, Congo and Mekong). Other studies report that wetlands are the most important CO<sub>2</sub> source in these river systems (Belger et al., 2011; Miguez-Macho and Fan, 2012; Abril et al., 2014; Sjögersten et al., 2014). We note that CO<sub>2</sub> emissions associated with wetlands in literature may overlap the flooded areas in DISC-CARBON. Also, the hydrological representation of the water exchange between flooded areas and river could be refined. The current simple approach, assuming that flow velocity in flooded areas is a fraction of the flow velocity in the main stream, is possibly not sufficient to describe the complex interplay between floodplain and main stream.

The CO<sub>2</sub> emissions that originate from rivers (>60m) and streams (<60m) remained relatively stable throughout the 20<sup>th</sup> century and are 0.3 and 0.45 Pg C year<sup>-1</sup>, respectively, similar to estimates by Aufdenkampe et al. (2011) (0.3 and 0.26 Pg C year<sup>-1</sup>, respectively) and Lauerwald et al. (2015) (0.33 and 0.32 Pg C year<sup>-1</sup>, respectively), but lower than the 1.8 Pg C year<sup>-1</sup> of Raymond et al. (2013) who lumped flooded areas and rivers. These CO<sub>2</sub> emissions from rivers and streams are primarily fueled by import of CO<sub>2</sub>-supersaturated groundwater, which confirms earlier results based on pCO<sub>2</sub> data (Raymond et al., 2013).

Simulated CO<sub>2</sub> emissions from lakes (>50 km<sup>2</sup>) and reservoirs together sum up to 0.12 Pg C year<sup>-1</sup> at the end of the 20<sup>th</sup> century. Large waterbodies are often subject to strong DIC consumption by primary producers (due to their long residence times) or to low DIC formation from organic C mineralization (due to low organic carbon inputs), which results in an undersaturation with respect to the atmosphere and an uptake of CO<sub>2</sub>. Lake areas and volumes as used in PCR-GLOBWB are obtained from

GLWD (Lehner and Döll, 2004), and represent only lakes larger than 50 km<sup>2</sup> and only those that are connected to the river network. Estimated CO<sub>2</sub> emissions from global lakes range from 0.55 to 0.64 Pg C year<sup>-1</sup> (Tranvik et al., 2009; Aufdenkampe et al., 2011; Holgerson and Raymond, 2016). Excluding small lakes, which are a critical component of the global freshwater C cycle (Holgerson and Raymond, 2016), would lead to a significant underestimation of global freshwater CO<sub>2</sub> emissions, although there is large uncertainty with respect to their areal extent (Verpoorter et al., 2014). Due to the methodology used to describe low Strahler orders (<5), part of the CO<sub>2</sub> emissions that DISC-CARBON attributes to small streams may actually originate from small lakes. To refine our current estimates of freshwater CO<sub>2</sub> emissions, future work should aim at improving the hydrological representation of lakes and reservoirs, for example by including spatial lake distribution data from Verpoorter et al. (2014).

CO<sub>2</sub> emissions from global endoreic lakes amount to ~0.3 Pg C year<sup>-1</sup> (Duarte et al., 2008). Endoreic lakes, including the Caspian Sea, show high CO<sub>2</sub> emissions resulting from carbonate precipitation/dissolution reactions. Moreover, exchange rates in these lakes are impacted by chemical enhancement as a result of the hydration of atmospheric CO<sub>2</sub> directly to bicarbonates (Wanninkhof and Knox, 1996). In the current version of DISC-CARBON these processes are not represented. To account for CO<sub>2</sub> emissions from endoreic lakes, a process-based simulation of carbonate precipitation/dissolution reactions and chemical enhancement of exchange rates should be included. We focused here on the land-ocean continuum, but bear in mind that our global estimates for emissions from surface freshwaters are most likely underestimated by ~10%.

In the latest global C cycle assessment, Friedlingstein et al., (2022) reported a net disturbed terrestrial uptake of 3.2 Pg C year<sup>-1</sup> as a result of the perturbation of the global C cycle. It is important to note that in their assessment, C transfers from terrestrial to freshwater systems and subsequent freshwater C cycling, burial and emissions are not explicitly taken into account, because these processes are not included in global vegetation and oceanic biogeochemistry models. Given that reported net disturbed terrestrial C uptake (3.2 Pg C year<sup>-1</sup>; Friedlingstein et al., (2022)), and our estimates of lateral C transfers to freshwater systems (3.5 Pg C year<sup>-1</sup>) and freshwater CO<sub>2</sub> emissions (2.2 Pg C year<sup>-1</sup>) are in the same order of magnitude, it is critical to distinguish the natural and perturbed components of the freshwater C flows.

## Conclusions

The presented study aimed to explore large scale spatio-temporal dynamics of the global CO<sub>2</sub> emissions from the terrestrial-aquatic continuum during the 20<sup>th</sup> century. Our results indicate that global CO<sub>2</sub> emissions from freshwaters have been increasing since the 1970s, from 2.09 Pg C year<sup>-1</sup> to 2.24 Pg C year<sup>-1</sup>, mainly as a result of increased C delivery from groundwater (*DIC*) and soil erosion (*POC*). DISC-CARBON provides complementary knowledge of large-scale dynamic C cycling in freshwater systems, as it simulates the origin of CO<sub>2</sub> emissions from river systems by integrating a terrestrial C model with a hydrological model. For this purpose, we quantify spatially and temporally distributed C delivery from land to rivers, specify interactions between different C forms and account for hydrology from headwaters to river mouths. Simulations indicate that, on basin scale, there is a strong coupling between terrestrial delivery and freshwater CO<sub>2</sub> emissions. The link of CO<sub>2</sub> emissions from freshwaters to the terrestrial C cycle highlights the necessity of integrating the aquatic C cycle in the global C cycle.

## Associated content

### Acknowledgments

This work is part of The New Delta 2014 ALW project project nr 869.15.014, which is financed by the Netherlands Organisation for Scientific Research (NWO). Alexander F. Bouwman and Arthur H. W. Beusen received support from PBL Netherlands Environmental Assessment Agency through in-kind contributions to The New Delta 2014 ALW project. Lauriane Vilmin received funding from part of the Earth and life sciences (ALW) Open Programme 2016 project no. ALWOP.230, which is financed by the Netherlands Organisation for Scientific Research (NWO). Joep J. Langeveld received funding from The New Delta 2014 ALW project project nr 869.15.015, which is financed by the Netherlands Organisation for Scientific Research (NWO).

---

## References

- Abril, G. and Borges, A. V.: Carbon dioxide and methane emissions from estuaries, in *Greenhouse gas emissions—fluxes and processes*, pp. 187–207, Springer., 2005.
- Abril, G., Martinez, J.-M., Artigas, L. F., Moreira-Turcq, P., Benedetti, M. F., Vidal, L., Meziane, T., Kim, J.-H., Bernardes, M. C., Savoye, N., Deborde, J., Souza, E. L., Albéric, P., Landim de Souza, M. F. and Roland, F.: Amazon River carbon dioxide outgassing fuelled by wetlands., *Nature*, 505(7483), 395–398, doi:10.1038/nature12797, 2014.
- Alin, S. R., Rasera, M. D. F. L., Salimon, C. I., Richey, J. E., Holtgrieve, G. W., Krusche, A. V. and Snidvongs, A.: Physical controls on carbon dioxide transfer velocity and flux in low-gradient river systems and implications for regional carbon budgets, *J. Geophys. Res. Biogeosciences*, 116(1), doi:10.1029/2010JG001398, 2011.
- Aufdenkampe, A. K., Mayorga, E., Raymond, P. A., Melack, J. M., Doney, S. C., Alin, S. R., Aalto, R. E. and Yoo, K.: Riverine coupling of biogeochemical cycles between land, oceans, and atmosphere, *Front. Ecol. Environ.*, 9(1), 53–60, 2011.
- Aulenbach, B. T., Buxton, H. T., Battaglin, W. A. and Coupe, R. H.: Streamflow and nutrient fluxes of the Mississippi-Atchafalaya River Basin and subbasins for the period of record through 2005., 2007.
- Bastviken, D., Tranvik, L. J., Downing, J. A., Crill, P. M. and Enrich-Prast, A.: Freshwater methane emissions offset the continental carbon sink, *Science* (80-. ), 331(6013), 50, 2011.
- Batjes, N. H.: World soil property estimates for broad-scale modelling (WISE30sec), *ISRIC-World Soil Information.*, 2015.
- Battin, T. J., Luyssaert, S., Kaplan, L. A., Aufdenkampe, A. K., Richter, A. and Tranvik, L. J.: The boundless carbon cycle, *Nat. Geosci.*, 2(9), 598–600, 2009.
- Van Beek, L. P. H., Wada, Y. and Bierkens, M. F. P.: Global monthly water stress: 1. Water balance and water availability, *Water Resour. Res.*, 47(7), 2011.
- Belger, L., Forsberg, B. R. and Melack, J. M.: Carbon dioxide and methane emissions from interfluvial wetlands in the upper Negro River basin, Brazil, *Biogeochemistry*, 105(1–3), 171–183, 2011.
- Beusen, A. H. W., Van Beek, L. P. H., Bouwman, L., Mogollón, J. M. and Middelburg, J. B. M.: Coupling global models for hydrology and nutrient loading to simulate nitrogen and phosphorus retention in surface water—description of IMAGE–GNM and analysis of performance, *Geosci. Model Dev.*, 8(12), 4045–4067, 2015a.

- Beusen, A. H. W., Bouwman, A. F., Van Beek, L. P. H., Mogollón, J. M. and Middelburg, J. J.: Global riverine N and P transport to ocean increased during the twentieth century despite increased retention along the aquatic continuum, *Biogeosciences Discuss.*, 12(23), 20123–20148, doi:10.5194/bgd-12-20123-2015, 2015b.
- Borges, A. V., Abril, G., Darchambeau, F., Teodoru, C. R., Deborde, J., Vidal, L. O., Lambert, T. and Bouillon, S.: Divergent biophysical controls of aquatic CO<sub>2</sub> and CH<sub>4</sub> in the World's two largest rivers, *Sci. Rep.*, 5, 1–10, doi:10.1038/srep15614, 2015a.
- Borges, A. V., Darchambeau, F., Teodoru, C. R., Marwick, T. R., Tamooh, F., Geeraert, N., Omengo, F. O., Guérin, F., Lambert, T., Morana, C., Okuku, E. and Bouillon, S.: Globally significant greenhouse-gas emissions from African inland waters, *Nat. Geosci.*, 8(8), 637–642, doi:10.1038/ngeo2486, 2015b.
- Ciais, P., Sabine, C., Bala, G., Bopp, L., Brovkin, V., Canadell, J., Chhabra, A., DeFries, R., Galloway, J. and Heimann, M.: Carbon and other biogeochemical cycles, in *Climate Change 2013: The Physical Science Basis. Contribution of Working Group I to the Fifth Assessment Report of the Intergovernmental Panel on Climate Change*, pp. 465–570, Cambridge University Press., 2013.
- Cole, Prairie, Y. T., Caraco, N. F., McDowell, W. H., Tranvik, L. J., Striegl, R. G., Duarte, C. M., Kortelainen, P., Downing, J. A. and Middelburg, J. J.: Plumbing the global carbon cycle: integrating inland waters into the terrestrial carbon budget, *Ecosystems*, 10(1), 172–185, 2007.
- Drake, T. W., Raymond, P. A. and Spencer, R. G. M.: Terrestrial carbon inputs to inland waters: A current synthesis of estimates and uncertainty, *Limnol. Oceanogr. Lett.*, 132–142, doi:10.1002/lol2.10055, 2018.
- Duarte, C. M., Prairie, Y. T., Montes, C., Cole, J. J., Striegl, R., Melack, J. and Downing, J. A.: CO<sub>2</sub> emissions from saline lakes: A global estimate of a surprisingly large flux, *J. Geophys. Res. Biogeosciences*, 113(G4), 2008.
- Friedlingstein, P., Jones, M. W., O'Sullivan, M., Andrew, R. M., Bakker, D. C. E., Hauck, J., Le Quéré, C., Peters, G. P., Peters, W., Pongratz, J., Sitch, S., Canadell, J. G., Ciais, P., Jackson, R. B., Alin, S. R., Anthoni, P., Bates, N. R., Becker, M., Bellouin, N., Bopp, L., Chau, T. T. T., Chevallier, F., Chini, L. P., Cronin, M., Currie, K. I., Decharme, B., Djeutchouang, L. M., Dou, X., Evans, W., Feely, R. A., Feng, L., Gasser, T., Gilfillan, D., Gkritzalis, T., Grassi, G., Gregor, L., Gruber, N., Gürses, Ö., Harris, I., Houghton, R. A., Hurtt, G. C., Iida, Y., Ilyina, T., Luijckx, I. T., Jain, A., Jones, S. D., Kato, E., Kennedy, D., Klein Goldewijk, K., Knauer, J., Korsbakken, J. I., Körtzinger, A., Landschützer, P., Lauvset, S. K., Lefèvre, N., Lienert, S., Liu, J., Marland, G., McGuire, P. C., Melton, J. R., Munro, D. R., Nabel, J. E. M. S., Nakaoka, S.-I., Niwa, Y., Ono, T., Pierrot, D., Poulter, B., Rehder, G., Resplandy, L., Robertson, E., Rödenbeck, C., Rosan, T. M., Schwinger, J., Schwingshackl, C.,

- Séférian, R., Sutton, A. J., Sweeney, C., Tanhua, T., Tans, P. P., Tian, H., Tilbrook, B., Tubiello, F., van der Werf, G. R., Vuichard, N., Wada, C., Wanninkhof, R., Watson, A. J., Willis, D., Wiltshire, A. J., Yuan, W., Yue, C., Yue, X., Zaehle, S. and Zeng, J.: Global Carbon Budget 2021, *Earth Syst. Sci. Data*, 14(4), 1917–2005, doi:10.5194/essd-14-1917-2022, 2022.
- Hartmann, J., Lauerwald, R. and Moosdorf, N.: A Brief Overview of the GLObal River Chemistry Database, GLORICH, *Procedia Earth Planet. Sci.*, 10, 23–27, doi:10.1016/j.proeps.2014.08.005, 2014.
- van Hoek, W., Wang, J., Vilmin, L., Beusen, A., Mogollon, J., Müller, G., Pika, P., Liu, X., Langeveld, J., Bouwman, A. and Middelburg, J.: Exploring spatially explicit changes in carbon budgets of global river basins during the 20th century, *Environ. Sci. Technol.*, 2021.
- Holgerson, M. A. and Raymond, P. A.: Large contribution to inland water CO<sub>2</sub> and CH<sub>4</sub> emissions from very small ponds, *Nat. Geosci.*, 9(3), 222–226, doi:10.1038/ngeo2654, 2016.
- IPCC, 2021: Climate Change 2021: The Physical Science Basis. Contribution of Working Group I to the Sixth Assessment Report of the Intergovernmental Panel on Climate Change [Masson-Delmotte, V., P. Zhai, A. Pirani, S.L. Connors, C. Péan, S. Berger, N. Caud, Y. Chen, L. Goldfarb, M.I. Gomis, M. Huang, K. Leitzell, E. Lonnoy, J.B.R. Matthews, T.K. Maycock, T. Waterfield, O. Yelekçi, R. Yu, and B. Zhou (eds.)]. Cambridge University Press, Cambridge, United Kingdom and New York, NY, USA, In press, doi:10.1017/9781009157896
- Langeveld, J., Bouwman, A. F., van Hoek, W. J., Vilmin, L., Beusen, A. H. W., Mogollón, J. M. and Middelburg, J. J.: Estimating dissolved carbon concentrations in global soils: a global database and model (submitted), *Springer Nat. Appl. Sci.*, 2019.
- Lauerwald, R., Laruelle, G. G., Hartmann, J., Ciais, P. and Regnier, P. A. G.: Spatial patterns in CO<sub>2</sub> evasion from the global river network, *Global Biogeochem. Cycles*, 29(5), 534–554, doi:10.1002/2014GB004941. Received, 2015.
- Lehner, B. and Döll, P.: Development and validation of a global database of lakes, reservoirs and wetlands, *J. Hydrol.*, 296(1–4), 1–22, doi:10.1016/j.jhydrol.2004.03.028, 2004.
- Melack, J. M., Novo, E., Forsberg, B. R., Piedade, M. T. F. and Maurice, L.: Floodplain ecosystem processes, *Amaz. Glob. Chang.*, 186, 525–542, 2009.
- Meybeck, M., Dürr, H. H. and Vörösmarty, C. J.: Global coastal segmentation and its river catchment contributors: A new look at land-ocean linkage, *Global Biogeochem. Cycles*, 20(1), 1–15, doi:10.1029/2005GB002540, 2006.

- Middelburg, J. J.: Organic Matter is more than CH<sub>2</sub>O BT - Marine Carbon Biogeochemistry : A Primer for Earth System Scientists, edited by J. J. Middelburg, pp. 107–118, Springer International Publishing, Cham., 2019.
- Miguez-Macho, G. and Fan, Y.: The role of groundwater in the Amazon water cycle: 1. Influence on seasonal streamflow, flooding and wetlands, *J. Geophys. Res. Atmos.*, 117(D15), 2012.
- Orr, J. C. and Epitalon, J. M.: Improved routines to model the ocean carbonate system: Mocsy 2.0, *Geosci. Model Dev.*, 8(3), 485–499, doi:10.5194/gmd-8-485-2015, 2015.
- Le Quéré, C., Andrew, R. M., Friedlingstein, P., Sitch, S., Pongratz, J., Manning, A. C., Korsbakken, J. I., Peters, G. P., Canadell, J. G., Jackson, R. B., Boden, T. A., Tans, P. P., Andrews, O. D., Arora, V. K., Bakker, D. C. E., Van Der Laan-Luijkx, I. T., Van Der Werf, G. R., Van Heuven, S., Viovy, N., Vuichard, N., Walker, A. P., Watson, A. J., Wiltshire, A. J., Zaehle, S. and Zhu, D.: Global Carbon Budget 2017, *Earth Syst. Sci. Data* Etsushi Kato Markus Kautz Ralph F. Keeling Kees Klein Goldewijk Nathalie Lefèvre Andrew Lent. Danica Lomb. Nicolas Metzl Yukihiko Nojiri Antonio Padin Janet Reimer, 1010333739(10), 405–448, doi:10.5194/essd-10-405-2018, 2018.
- Rasera, M. de F. F. L., Krusche, A. V., Richey, J. E., Ballester, M. V. R. and Victória, R. L.: Spatial and temporal variability of pCO<sub>2</sub> and CO<sub>2</sub> efflux in seven Amazonian Rivers, *Biogeochemistry*, 116(1–3), 241–259, 2013.
- Raymond, P. A., Hartmann, J., Lauerwald, R., Sobek, S., McDonald, C., Hoover, M., Butman, D., Striegl, R., Mayorga, E. and Humborg, C.: Global carbon dioxide emissions from inland waters, *Nature*, 503(7476), 355–359, 2013.
- Regnier, P., Friedlingstein, P., Ciais, P., Mackenzie, F. T., Gruber, N., Janssens, I. A., Laruelle, G. G., Lauerwald, R., Luysaert, S. and Andersson, A. J.: Anthropogenic perturbation of the carbon fluxes from land to ocean, *Nat. Geosci.*, 6(8), 597–607, 2013.
- Richey, J. E., Melack, J. M., Aufdenkampe, A. K., Ballester, V. M. and Hess, L. L.: Outgassing from Amazonian rivers and wetlands as a large tropical source of atmospheric CO<sub>2</sub>, *Nature*, 416(6881), 617–620, doi:10.1038/416617a, 2002.
- Sanderman, J., Hengl, T. and Fiske, G. J.: Soil carbon debt of 12,000 years of human land use, *Proc. Natl. Acad. Sci. U. S. A.*, 114(36), 9575–9580, doi:10.1073/pnas.1706103114, 2017.
- Sawakuchi, H. O., Neu, V., Ward, N. D., Barros, M. D. L. C., Valerio, A., Gagnemaynard, W., Cunha, A. C., Fernanda, D., Diniz, J. E., Brito, D. C., Krusche, A. V. and Richey, J. E.: Carbon dioxide emissions along the lower Amazon River, *Front. Mar. Sci.*, 4(March), 1–12, doi:10.3389/fmars.2017.00076, 2017.



- Sitch, S., Smith, B., Prentice, I. C., Arneeth, A., Bondeau, A., Cramer, W., Kaplan, J. O., Levis, S., Lucht, W. and Sykes, M. T.: Evaluation of ecosystem dynamics, plant geography and terrestrial carbon cycling in the LPJ dynamic global vegetation model, *Glob. Chang. Biol.*, 9(2), 161–185, 2003.
- Sjögersten, S., Black, C. R., Evers, S., Hoyos-Santillan, J., Wright, E. L. and Turner, B. L.: Tropical wetlands: A missing link in the global carbon cycle?, *Global Biogeochem. Cycles*, 28(12), 1371–1386, 2014.
- Soetaert, K., Hofmann, A. F., Middelburg, J. J., Meysman, F. J. R. and Greenwood, J.: Reprint of “The effect of biogeochemical processes on pH,” *Mar. Chem.*, 106(1), 380–401, doi:<https://doi.org/10.1016/j.marchem.2007.06.008>, 2007.
- Stehfest, E., van Vuuren, D., Kram, T., Bouwman, L., Alkemade, R., Bakkenes, M., Biemans, H., Bouwman, A., den Elzen, M., Janse, J., Lucas, P., van Minnen, J., Muller, C. and Prins, A. G.: Integrated Assessment of Global Environmental Change with IMAGE 3.0. Model description and policy applications. [online] Available from: <http://www.pbl.nl/en/publications/integrated-assessment-of-global-environmental-change-with-IMAGE-3.0>, 2014.
- Tranvik, L. J., Downing, J. A., Cotner, J. B., Loiselle, S. A., Striegl, R. G., Ballatore, T. J., Dillon, P., Finlay, K., Fortino, K., Knoll, L. B., Kortelainen, P. L., Kutser, T., Larsen, S., Laurion, I., Leech, D. M., McCallister, S. L., McKnight, D. M., Melack, J. M., Overholt, E., Porter, J. A., Prairie, Y., Renwick, W. H., Roland, F., Sherman, B. S., Schindler, D. W., Sobek, S., Tremblay, A., Vanni, M. J., Verschoor, A. M., von Wachenfeldt, E. and Weyhenmeyer, G. A.: Lakes and reservoirs as regulators of carbon cycling and climate, *Limnol. Oceanogr.*, 54(6), 2298–2314, doi:10.4319/lo.2009.54.6\_part\_2.2298, 2009.
- Verpoorter, C., Kutser, T., Seekell, D. A. and Tranvik, L. J.: A global inventory of lakes based on high-resolution satellite imagery, *Geophys. Res. Lett.*, 41(18), 6396–6402, doi:10.1002/2014GL060641, 2014.
- Wanninkhof, R.: Relationship between wind speed and gas exchange over the ocean revisited, *Limnol. Oceanogr. Methods*, 12(JUN), 351–362, doi:10.4319/lom.2014.12.351, 2014.
- Wanninkhof, R. and Knox, M.: Chemical enhancement of CO<sub>2</sub> exchange in natural waters, *Limnol. Oceanogr.*, 41(4), 689–697, 1996.
- Ward, N. D., Bianchi, T. S., Medeiros, P. M., Seidel, M., Richey, J. E., Keil, R. G. and Sawakuchi, H. O.: Where Carbon Goes When Water Flows : Carbon Cycling across the Aquatic Continuum, , 4(January), 1–27, doi:10.3389/fmars.2017.00007, 2017.

## Supporting information: Global freshwater CO<sub>2</sub> emissions have increased as a result of rising terrestrial carbon inputs

Table SI1 Global freshwaters CO<sub>2</sub> emissions per climate region

|             |                         | Area<br>(10 <sup>3</sup> km <sup>2</sup> ) |                   | Emission<br>(Tg C year <sup>-1</sup> ) |                   | Areal emission<br>(g m <sup>2</sup> year <sup>-1</sup> ) |                   |
|-------------|-------------------------|--|-------------------|--|-------------------|--|-------------------|
|             |                         | 1990's                                     | Century<br>change | 1990's                                 | Century<br>change | 1990's   | Century<br>change |
| Global      | Total                   | 4891                                       | 15                | 2243                                   | 157               | 459  | 31                |
|             | Wide streams<br>(>60m)  | 152  | -16               | 379                                    | 22                | 2487   | 366               |
|             | Small streams<br>(<60m) | 111  | -9                | 386                                    | 11                | 3476   | 349               |
|             | Lakes                   | 848  | -164              | 53                                     | 13                | 62   | 23                |
|             | Reservoirs              | 402  | 399               | 70                                     | 69                | 174  | -134              |
|             | Flooded areas           | 3378                                       | -196              | 1356                                   | 43                | 401  | 34                |
| Tropical    | Total                   | 2329                                       | -50               | 1833                                   | 100               | 787  | 58                |
|             | Wide streams<br>(>60m)  | 67   | -2                | 321                                    | 27                | 4793   | 558               |
|             | Small streams<br>(<60m) | 34   | -2                | 293                                    | 16                | 8636   | 887               |
|             | Lakes                   | 126  | -69               | 42                                     | 5                 | 334  | 144               |
|             | Reservoirs              | 111  | 110               | 20                                     | 20                | 178  | -1311             |
|             | Flooded areas           | 1992                                       | -88               | 1158                                   | 32                | 581  | 40                |
| Arid        | Total                   | 544  | 31                | 50                                     | 7                 | 92   | 8                 |
|             | Wide streams<br>(>60m)  | 8  | -1                | 3                                      | -1                | 331  | -57               |
|             | Small streams<br>(<60m) | 10   | 0                 | 5                                      | 1                 | 506  | 146               |
|             | Lakes                   | 16   | -1                | 1                                      | 0                 | 53   | 4                 |
|             | Reservoirs              | 33   | 33                | 7                                      | 7                 | 206  | -214              |
|             | Flooded areas           | 477  | 0                 | 35                                     | 0                 | 73   | 0                 |
| Continental | Total                   | 1239                                       | 92                | 132                                    | 28                | 107  | 16                |
|             | Wide streams<br>(>60m)  | 49   | -6                | 25                                     | -3                | 523  | 12                |
|             | Small streams<br>(<60m) | 37   | -2                | 40                                     | -1                | 1086   | 34                |
|             | Lakes                   | 589  | -85               | -1                                     | 7                 | -1   | 10                |
|             | Reservoirs              | 201  | 199               | 17                                     | 17                | 86   | -104              |
|             | Flooded areas           | 364  | -13               | 50                                     | 8                 | 139  | 25                |

**Table SI1 (continuation) Global freshwaters CO<sub>2</sub> emissions per climate region**

|                  |                         | <i>Area<br/>(10<sup>3</sup> km<sup>2</sup>)</i> |                           | <i>Emission<br/>(Tg C year<sup>-1</sup>)</i> |                           | <i>Areal emission<br/>(g m<sup>2</sup> year<sup>-1</sup>)</i> |                           |
|------------------|-------------------------|---|---------------------------|--|---------------------------|---|---------------------------|
|                  |                         | <i>1990's</i>                                   | <i>Century<br/>change</i> | <i>1990's</i>                                | <i>Century<br/>change</i> | <i>1990's</i>   | <i>Century<br/>change</i> |
| <i>Temperate</i> | Total                   | 679   | -59                       | 221  | 22                        | 325   | 56                        |
|                  | Wide streams<br>(>60m)  | 18  | -6                        | 28   | -1                        | 1552  | 308                       |
|                  | Small streams<br>(<60m) | 19  | -5                        | 46   | -6                        | 2348  | 260                       |
|                  | Lakes                   | 65  | -10                       | 10   | 1                         | 160   | 32                        |
|                  | Reservoirs              | 56  | 56                        | 26   | 25                        | 458   | -612                      |
|                  | Flooded areas           | 521   | -94                       | 111  | 3                         | 214   | 38                        |
| <i>Arctic</i>    | Total                   | 100   | 0                         | 7  | 0                         | 71  | 1                         |
|                  | Wide streams<br>(>60m)  | 11  | 0                         | 2  | 0                         | 170   | -22                       |
|                  | Small streams<br>(<60m) | 12  | 0                         | 3  | 0                         | 268   | -3                        |
|                  | Lakes                   | 53  | 0                         | 1  | 0                         | 11  | 2                         |
|                  | Reservoirs              | 1   | 1                         | 0  | 0                         | 343   | -1970                     |
|                  | Flooded areas           | 49  | 0                         | 1  | 0                         | 49  | 1                         |

**Figure SI1: Year average observations of alkalinity (a), DOC (b), pCO<sub>2</sub> (c) pH (d) and TOC (e) versus model results**

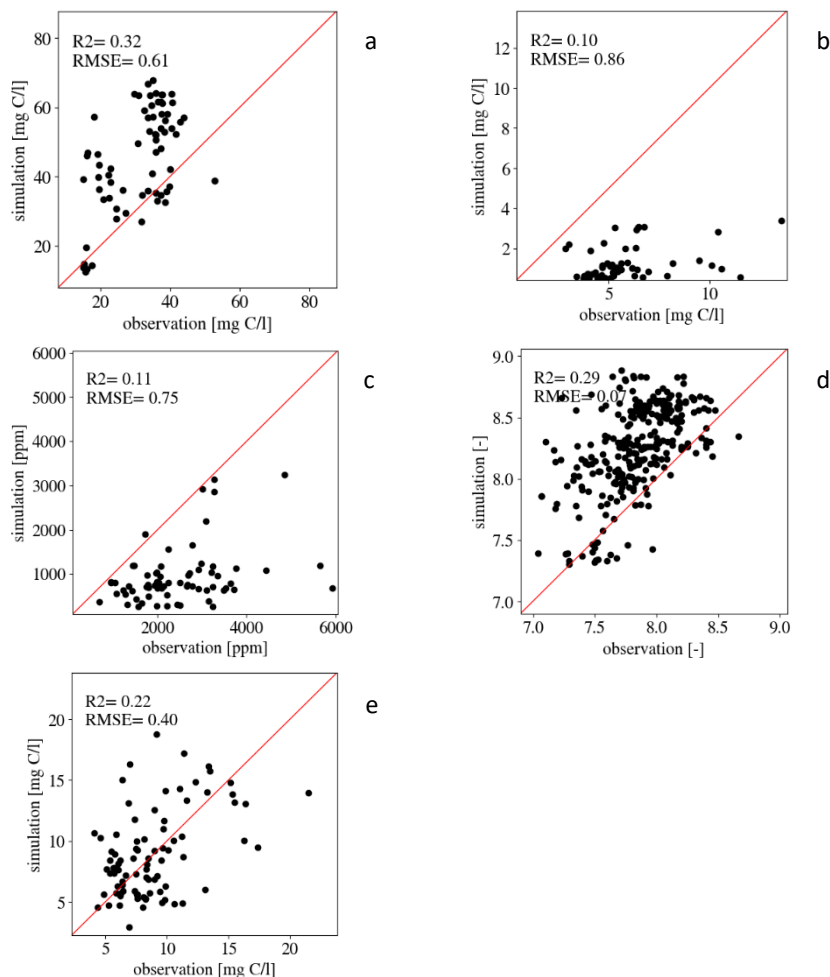


**Figure SI1. Representation of all available matching datapoints in time and space (observation data versus simulation data) for the entire Mississippi basin. DISC-CARBON simulations agree with measurements (Aulenbach et al., 2007) of alkalinity, DOC, pCO<sub>2</sub>, pH and TOC realistically. The RMSE shows that DISC-CARBON simulates the order of magnitude within acceptable margins and is able to simulate the spatio-temporal variety of a large basin as a whole. More long term measurements for other basins are needed to further assess DISC-CARBON performance.**

## LHS

We used the Latin Hypercube sampling method to conduct a sensitivity analysis. This method enables to quantify the spatial distribution of sensitivity of CO<sub>2</sub> emissions to any model parameter, constraint or input with a limited number of runs (750) with a uniformly randomized combined set of all model parameters, external constraints and external inputs. In each run, each model parameter, constraint and input is randomly multiplied with a factor between 0.95 and 1.05 and assembled as a setting for one run. For temperature, the randomization is applied between -1K and +1K around the default temperature.

The contribution of each parameter ( $X_i$ ) to model outcome  $Y$  is then calculated with linear regression (Saltelli, 2000: in Beusen et al 2015):

$$Y = \beta_0 + \beta_1 X_1 + \beta_2 X_2 \dots + \beta_n X_n + e$$

with  $\beta_i$  as the ordinary regression coefficient of parameter  $i$  and  $e$  the error of the approximation of  $Y$ . The linear regression model can be evaluated for parameter contribution analysis if the coefficient of determination ( $R^2$ ) is close to 1, i.e. when there is no variation of  $Y$  that is not explained with the linear regression model. A standardized regression coefficient ( $SRC_i$ ) is used to scale  $\beta_i$  to the relative contribution of variation of  $Y$ , by using the standard deviations of  $X_i$  and  $Y$  as follows:

$$SRC_i = \beta_i \frac{\sigma_{X_i}}{\sigma_Y}$$

$SRC_i$  is independent of units and scale of parameters. The  $SRC_i$  has a value between -1 and 1. A positive  $SRC_i$  value indicates that an increased parameter value leads to an increased output  $Y$ . A negative  $SRC_i$  indicates a decreased output  $Y$  with an increased parameter value.  $SRC_i^2 / R^2$  yields the contribution of each parameter  $X_i$  to model outcome  $Y$ .

## LHS results

The key results of the LHS sensitivity analysis for the parameters / inputs to which basin total CO<sub>2</sub> emissions are most sensitive are presented in Table SI2. For clarity purposes, we only show  $SRC$ -values which are smaller than -0.2 or exceeding 0.2. If a parameter or input has a positive  $SRC$  value, it indicates that when the input parameter increases, the output parameter increases. A negative  $SRC$  value indicates that when the input parameter increases, the output parameter decreases.

Within the set of conditions in the sensitivity analysis, the most dominant contributor to CO<sub>2</sub> emissions variability for 4 out of 5 basins is terrestrial C delivery. However, there is some difference amongst the tested rivers. At this moment, quantitative attribution of basin characteristics to parameter / input responsiveness is unknown; as such, exploration of LHS results is of indicative nature and largely speculative.

**Table S12: SRC values of LHS sensitivity analysis for total CO<sub>2</sub> emissions from the Amazon, Mississippi, Nile, Lena and Yangtze rivers (max\_pp<sub>ALG</sub>\_rate: maximum primary production rate of pelagic algae).**

| <i>parameter / C Input</i>              | <i>Amazon</i> | <i>Miss.</i> | <i>Nile</i> | <i>Lena</i> | <i>Yangtze</i> |
|---|---------------|--------------|-------------|-------------|----------------|
| <i>Discharge</i>                        | -0.06         | -0.10        | -0.02       | -0.30       | -0.11          |
| <i>Temperature</i>                      | 0.28          | 0.34         | 0.65        | 0.20        | 0.39           |
| <i>Depth</i>                            | 0.00          | -0.06        | 0.22        | 0.02        | 0.00           |
| <i>max_pp<sub>ALG</sub>_rate</i>        | -0.13         | -0.36        | 0.05        | -0.03       | -0.36          |
| <i>alkalinity flux from groundwater</i> | 0.00          | -0.40        | -0.06       | -0.25       | -0.35          |
| <i>DIC flux from groundwater</i>        | 0.42          | 0.50         | 0.14        | 0.82        | 0.59           |
| <i>POC litterfall in flooded areas</i>  | 0.85          | 0.39         | 0.58        | 0.14        | 0.20           |

---

---

## Chapter 4

### **DISC-CARBON: A five decade (1950-2000) carbon cycle simulation of the stream network of the Rhine basin**

Wim Joost van Hoek<sup>1</sup>, Lauriane Vilmin<sup>1,2</sup>, Arthur H.W. Beusen<sup>1,2</sup>, José M. Mogollón<sup>4</sup>, Xiaochen Liu<sup>1</sup>, Joep J. Langeveld<sup>1</sup>, Alexander F. Bouwman<sup>1,2</sup>, Jack J. Middelburg<sup>1</sup>

<sup>1</sup> Department of Earth Sciences, Utrecht University, P.O. Box 80021, 3508TA Utrecht, the Netherlands.

<sup>2</sup> Deltares, P.O. Box 177, Delft, the Netherlands. Postcode: 2600 MH.

<sup>3</sup> PBL Netherlands Environmental Assessment Agency, P.O. Box 30314, 2500GH the Hague, the Netherlands.

<sup>4</sup> Department of Industrial Ecology, Leiden University, P.O. Box 9518, 2300RA Leiden, the Netherlands.



**ABSTRACT**

This paper presents the application of the coupled hydrology-biogeochemistry model IMAGE-DGNM with 0.5 by 0.5-degree resolution for the river Rhine, with simulations of the concentrations, transformations and transfer fluxes of dissolved inorganic C (DIC), dissolved organic C (DOC) and terrestrial and autochthonous particulate organic C (POC) from headwaters to river mouth with a time step of 1 month for the period 1950-2000. Simulations of DIC, DOC and TOC concentrations are in the same order of magnitude as observation (RMSE's of respectively -46%, +33%, +147%). Sensitivity analysis shows that in-stream chemistry and CO<sub>2</sub> emissions are weakly correlated with discharge in contrast to recent regression approaches. The dominant driver of total C export, being mainly DIC export, is the weathering input from groundwater. CO<sub>2</sub> emissions are strongly responsive to temperature variability and POC dynamics.

## 1 Introduction

Only recently, Cole et al. (2007) identified rivers as significant components of the global carbon (C) cycle and recognized that river systems function as globally important sources of CO<sub>2</sub>. Since then, multiple studies have confirmed the significance of freshwater systems in global C cycling, but the magnitude of fluxes and the influence human perturbation are uncertain (Cole et al., 2007; Battin et al., 2009; Tranvik et al., 2009; Bastviken et al., 2011; Raymond et al., 2013; Regnier et al., 2013; Borges et al., 2015a; Holgerson and Raymond, 2016; Sawakuchi et al., 2017).

Carbon in freshwater originates from terrestrial (allochthonous) sources and from aquatic within-system (autochthonous) production (Prairie and Cole, 2009). Allochthonous C is delivered to surface water as dissolved or particulate organic C (plant litter, leached material) or dissolved inorganic C (carbonates produced during weathering or soil respiration) (Cole et al., 2007) and particulate inorganic C (Meybeck, 1982; Mueller et al., 2022). After delivery to streams, rivers, lakes or reservoirs, organic C is metabolized to inorganic C, buried in sediment or laterally transported towards oceans. The inorganic C delivered or generated within the system is transported downstream or emitted to the atmosphere as CO<sub>2</sub> since aquatic systems are predominantly supersaturated in CO<sub>2</sub> relative to the atmosphere (Kempe, 1984; Frankignoulle et al., 1998; Duarte and Prairie, 2005).

Many studies have been published on local C processing in headwaters, rivers, lakes, reservoirs and floodplains (Tranvik et al., 2009; Crawford et al., 2013, 2016; Wallin et al., 2013; Hotchkiss et al., 2015; Wollheim et al., 2015; Holgerson and Raymond, 2016). These local assessments have identified the key governing processes and their sensitivity to perturbations. Global assessments of riverine C cycling, and in particular CO<sub>2</sub> partial pressure and global CO<sub>2</sub> effluxes have been very important to quantify the role of rivers in the global C cycle. However, these budgeting approaches fail to describe the rapid changes in the global C-cycle (Ciais et al., 2013b) and are not appropriate for hindcasting or making informed projections. Many existing river biogeochemistry models lack spatio-temporal input and hydrological constraints. Moreover the models usually lump the various compartment of the aquatic continuum and regress modelled and observed C export at the scale of whole river basins (Beusen et al., 2005; Mayorga et al., 2010a; Kroeze et al., 2012). After upscaling, such approaches yield a first order quantification of C fluxes to the coastal ocean. However, they contribute little to advance our understanding of the C cycle

in river basins. To describe the interactions between land-use changes, interventions in the hydrology (dam construction, reservoirs, water extraction), and wastewater discharge, and their consequences for riverine C cycling, we need a model that spatio-temporally resolves the biogeochemical processes coupled to hydrology.

In this paper we present an application of the Dynamic Integrated Model to Assess the Global Environment (IMAGE) Global Nutrient Model (DGNM) (Vilmin et al., 2020) with the DISC-CARBON module for simulating freshwater C cycling (van Hoek et al., 2021). This new model describes the spatial and temporal variability of C concentration and fluxes based on the river basin hydrology from headwaters to mouth and C cycling processes. DISC-CARBON was developed for global applications, but, in this chapter, we apply and test the model to the stream network of the Rhine basin without parameter tuning. The river Rhine drains an important part of Western Europe with an area of 185,620 km<sup>2</sup> and a length of 1,250 km (van der Weijden and Middelburg, 1989). The annual average discharge is 2,300 m<sup>3</sup>/s. The hydrology of the Rhine is strongly impacted by dams. Furthermore, with a population of 58 million inhabitants, it drains strongly urbanized landscapes with intensive agricultural systems (Uehlinger et al., 2009).

To test the results, we validated the model against observations for a series of monitoring stations throughout the main branch of the river Rhine, and performed a sensitivity analysis. Furthermore, to analyse the performance of the full production-respiration DISC-CARBON module (biology scheme), two other numerical schemes are presented, including an abiotic system excluding any in-stream processing of *DOC* and autochthonous production, and an extended abiotic system including heterotrophic respiration, but excluding production.

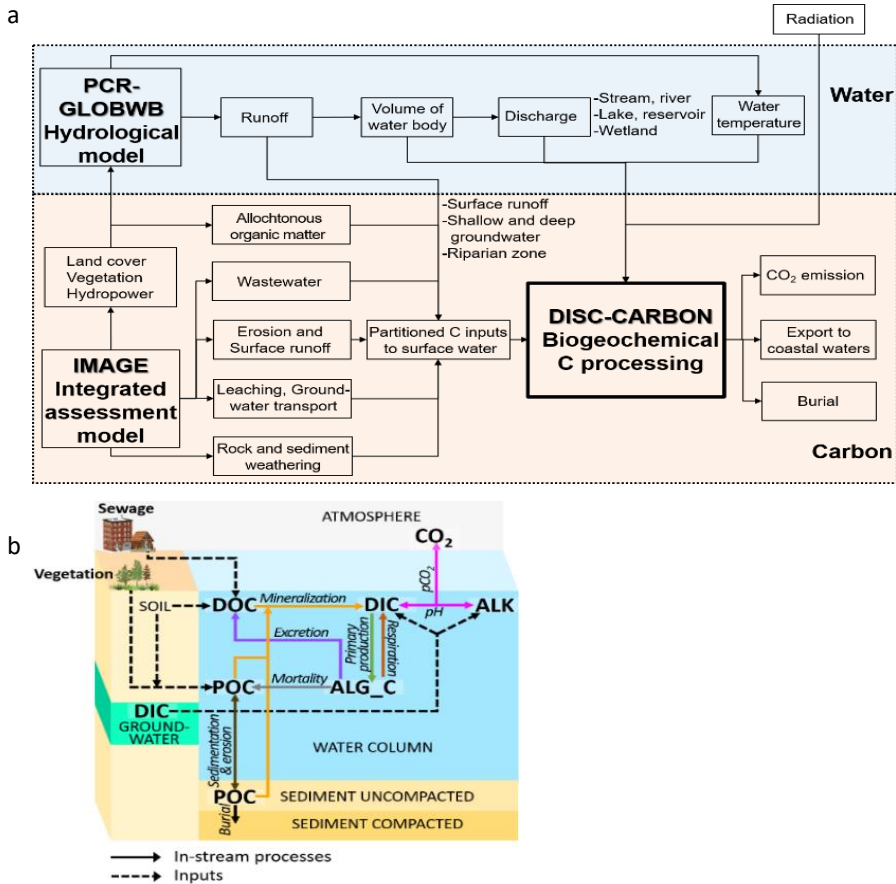
## **2 Data and methods**

### **2.1 Model description**

Here we provide a brief model description, and for details on model equations, parameters and values of constants we refer to van Hoek et al. (2021). The IMAGE-DGNM model framework integrates the PCRaster Global Waterbalance (PCR-GLOBWB) dynamic global hydrology model (Sutanudjaja et al., 2018) with the IMAGE model (Stehfest et al., 2014) that provides C delivery to inland waters (streams, rivers, lakes, reservoirs, floodplains) for the period 1900-2000. The biogeochemistry within the streams, rivers, lakes, reservoirs and floodplains is modelled using the Dynamic In-Stream Chemistry (DISC) module, which is part of the IMAGE-DGNM

framework (Vilmin et al., 2020) (figure 1a). IMAGE-DGNM has a global coverage with a 0.5 degree spatial resolution and includes spatially resolved biogeochemical input data (Beusen et al., 2015a; Vilmin et al., 2020). IMAGE-DGNM uses ancillary information of air temperature from a CRU dataset (Mitchell and Jones, 2005) as a 1:1 proxy for the water temperature. Minimum timestep is limited by hydrological constraints and biogeochemical data. In the presented study, hydrological constraints and biogeochemical data provide monthly data; results are presented in a monthly timestep. The framework is, however, able to process any timestep.

IMAGE provides land cover data to PCR-GLOBWB and wastewater, suspended particulate matter (SPM) and allochthonous organic C loads to DISC-CARBON; PCR-GLOBWB provides water flows, depth and volume of water bodies for streams of Strahler order > 5. The hydrology for smaller streams and rivers is parameterized in IMAGE-DGNM using the approach proposed by (Wollheim et al., 2008), as described in Beusen et al. (2015). DGNM explicitly accounts for spatio-temporal distribution of external sources for the different forms of C. These include wastewater (from (Bouwman et al., 2013) erosion and vegetation in riparian areas and floodplains (based on (Beusen et al., 2015a), weathering (Langeveld et al., 2020). After delivery of C in the form of particulate organic C (*POC*), dissolved organic C (*DOC*), dissolved inorganic C (*DIC*, the sum of  $\text{CO}_2$ ,  $\text{HCO}_3^-$  and  $\text{CO}_3^{2-}$ ) and alkalinity (*ALK*) to streams and rivers, the DISC model numerically calculates in-stream biogeochemistry and transport from Strahler order 1 to the mainstream for each grid cell, and from upstream cells to the coastal ocean (van Hoek et al., 2021) (figure 1b).



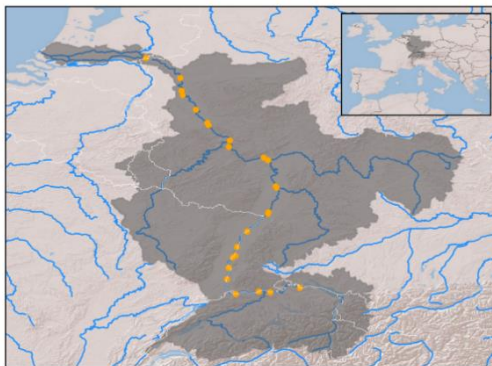
**Figure 3. (a) Scheme of the IMAGE-DGNM framework including the DISC-CARBON module for the in-stream biogeochemical C transformation processes and (b) scheme of C sources, forms and biogeochemical transformations in all simulated waterbodies in the DISC-CARBON module. The formulae for each transformation process are listed in Table S12.**

IMAGE-DGNM numerically resolves the mass and fluxes of suspended particulate matter (*SPM*) and sedimented particles. The pool of sedimented particles represents the mass of particles that have settled that can be resuspended as a result of exposure of the sediment surface to flowing waters. *SPM* is an important factor for light attenuation in the water column. (Kirk, 2011). *SPM* is delivered from land to

surface waters through soil erosion and from litterfall by terrestrial vegetation and during transport, it is produced within the water column through primary production and removed through mineralization. *SPM* consists of non-reactive, particulate inorganic matter (*PIM*) and reactive particles, particulate organic matter (*POM*). All suspended particulate species also exist in the sediment form. Calcium carbonate particles are not identified as a distinct unit. In non-endoreic watersheds, water residence time is considered too short for  $\text{CaCO}_3$  precipitation/dissolution to be relevant. The framework does not provide estimates for endoreic waterbodies.

The DISC-CARBON module describes the biogeochemical transformations of *DOC* and *POC* to *DIC*. These instream processes depend on hydrology, temperature and radiation. *POC* comprises hundreds of different compounds varying from easily decomposable to recalcitrant (Middelburg, 1989; Bianchi, 2011). To account for the diversity in *POC* reactivity, we distinguish among allochthonous, terrestrial *POC* (*POC<sub>terre</sub>* and *SEDOC<sub>terre</sub>*) and aquatic, autochthonous *POC* (*POC<sub>auto</sub>* and *SEDOC<sub>auto</sub>*), because the mineralization of terrestrial organic matter with structural carbohydrates and lignins is slower than that of aquatic organic matter, rich in N and P (Middelburg, 2019). Physical dynamics of *POC* are governed by simplified deposition and resuspension equations.

Alkalinity (*ALK*) is generated by weathering of soils and rocks and delivered to streams. Although *ALK* is the sum of excess bases in solution in natural environments, carbonate alkalinity ( $\text{HCO}_3^- + 2 \text{CO}_3^{2-}$ ) tends to make up most of the total alkalinity. *ALK* is delivered to surface water and combined with model generated *DIC* to calculate  $\text{pCO}_2$  and pH, but it is not modified by chemical reactions within the river. Consequently, DISC-CARBON ignores *ALK* production and consumption by primary production, respiration, nitrification and calcium carbonate precipitation and dissolution within the stream network (Soetaert et al., 2007), since we assume that large scale alkalinity concentrations are



**Figure 4. Map of Rhine basin with available in-stream carbon measurement locations (yellow dots) for GLORICH (Hartmann et al., 2014b).**

governed by weathering of soils and rocks. Also, although the hyporheic zone may be an important component in the production/removal of alkalinity (Boulton et al., 1998b), spatio-temporal data is not sufficient to constrain processes within. In addition, total *DIC* is governed by biological processes such as primary production and mineralization of *DOC* and *POC*.

## 2.2 Testing and validation of DISC-CARBON

The performance of the model is validated by comparing simulation results of *DIC*, *ALK*, *pCO<sub>2</sub>*, *pH*, *DOC* and *TOC* with literature data along the main stream (Figure 2). Literature data were acquired from the GLORICH database (Hartmann et al., 2014b). We compare monthly simulations and once every two weeks measurements of *DIC*, alkalinity, *pCO<sub>2</sub>*, *pH*, *DOC* and *TOC* for the station in Lobith, located on the German-Dutch border. The model can do simulations at any temporal resolution, but here we discuss the monthly aggregated results.

To further evaluate the model performance, we calculated the sensitivity of the modelled 5-year average (1995-2000) *CO<sub>2</sub>* emissions, total C export and POC retention to the variation of 45 parameters, 8 environmental constraints and 8 C sources using Latin Hypercube Sampling (Saltelli, 2000). The method allows to quantify sensitivity of model outcomes to varying parameters values with a relatively limited number of runs. We ran the model 750 times with a uniformly randomized combined set of all model parameters, external constraints and external inputs. In each run, each model parameter, constraint and input is randomly multiplied with a factor between 0.95 and 1.05 and combined into a setting for one run. For temperature, the randomization is applied between -1K and +1K of the default temperature. Values used for the parameters, constraints and inputs are presented in the supplementary material.

The contribution of each parameter ( $X_i$ ) to model outcome  $Y$  is assessed with linear regression (Saltelli, 2000: in Beusen et al 2015):

$$Y = \beta_0 + \beta_1 X_1 + \beta_2 X_2 \dots + \beta_n X_n + e$$

with  $\beta_i$  as the ordinary regression coefficient of parameter  $i$  and  $e$  the error of the approximation of  $Y$ . The linear regression model can be evaluated for parameter contribution analysis if the coefficient of determination ( $R^2$ ) is close to 1, i.e. when there is no variation of  $Y$  that is not explained with the linear regression model.

A standardized regression coefficient ( $SRC_i$ ) is used to scale  $\beta_i$  to the relative contribution of variation of  $Y$ , by using the standard deviations of  $X_i$  and  $Y$  as follows:

$$SRC_i = \beta_i \frac{\sigma_{X_i}}{\sigma_Y}$$

$SRC_i$  is independent of units and scale of parameters. The  $SRC_i$  has a value between -1 and 1. A positive  $SRC_i$  value indicates that an increased parameter value leads to an increased output  $Y$ . A negative  $SRC_i$  indicates a decreased output  $Y$  with an increased parameter value.  $SRC_i^2 / R^2$  yields the contribution of each parameter  $X_i$  to model outcome  $Y$ .

### 3 Results and discussion

#### 3.1 Model results for 1950-2000 for the three schemes

Basin-average  $DIC$  concentrations are higher by a few mg liter<sup>-1</sup> in the respiration and biology scheme compared to the abiotic one, as an effect of in-stream production of  $DIC$  by respiration. Alkalinity concentrations are identical among the different schemes, since the imported bicarbonate is not biogeochemically active during its transport through the aquatic continuum. Simulated  $DIC$  and alkalinity concentrations in the biology scheme are on average respectively 46% and 43% lower than observations (Figure 3be) and are also weakly correlated with measurements (bicarbonate  $r^2=0.01$ ;  $DIC$  abiotic:  $r^2=0.05$ ;  $DIC$  respiration:  $r^2=0.07$ ;  $DIC$  biology:  $r^2=0.07$ ). The weak correlation is likely related to the parameterization of the riverine alkalinity flux (Jansen, 2010), which depends on the coarse spatial distribution of the lithology and riverine discharge. The lithological data (Dürr et al., 2005) used here show only the dominant lithological class in 0.5 by 0.5-degree resolution. Furthermore, runoff calculated by PCR-GLOBWB is prone to uncertainty and may be systematically underestimated in source areas of alkalinity.



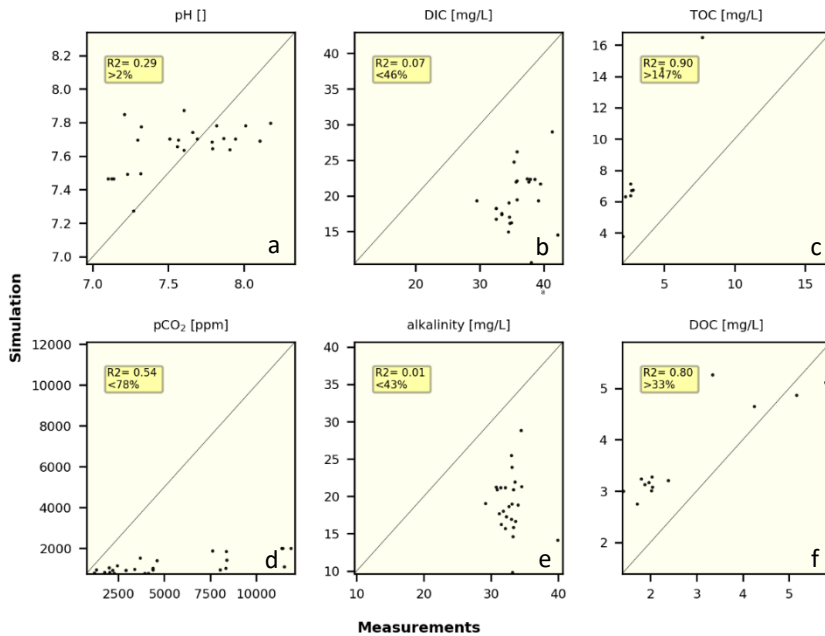


**Figure 3. Comparison between average measurements (x-axis) and average simulations (biology scheme) for all available stations in the Rhine basin. Measurements are from the GLORICH database (Hartmann et al., 2014)**

Simulated average values of pCO<sub>2</sub> in the respiration-only and biology schemes are high (Figure 3d: 1399 and 1183 ppm, respectively), but much lower than average values of 5261 ppm from the GLORICH database (Hartmann et al., 2019). This underestimation can be partly attributed to underestimated *DIC* and alkalinity, but values based on indirect measurements may also be strongly biased (Abril et al., 2015). Moreover, direct pCO<sub>2</sub> measurement in the Rhine using an equilibrator device vary from 545 to 1990 ppm (Frankignoulle et al., 1998)

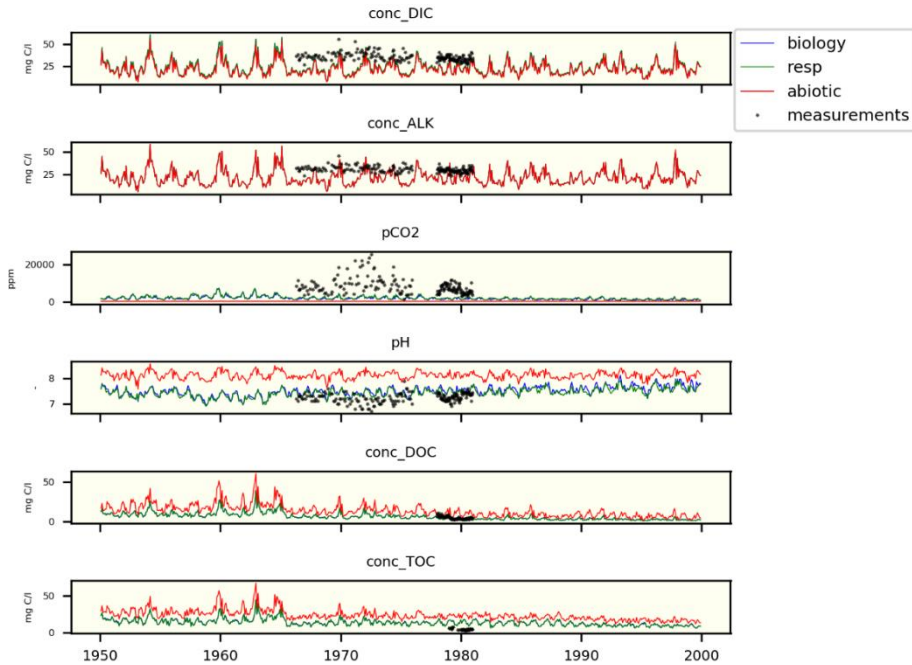


**Figure 4. Timeseries of measurements and simulations at Bimmen/Lobith, Germany. Measurements are from the GLORICH database (Hartmann et al., 2014)**

The average simulated abiotic (8.0), respiration-only (7.6) and biology (7.7) pH values (Figure 3a) show a fairly good agreement with average measurements (pH=7.6), with a low  $r^2$  for the abiotic run ( $r^2=0.04$ ), and higher ones for the respiration and biology schemes ( $r^2=0.31$  and  $r^2=0.29$  respectively). The simulated *DOC* (Figure 3f) and *TOC* (Figure 3c) concentrations compare well with measurements (*DOC* [abiotic:  $r^2=0.73$ ; respiration:  $r^2=0.79$ ; biology:  $r^2=0.81$ ]; *TOC* [abiotic:  $r^2=0.88$ ; respiration:  $r^2=0.95$ ; biology:  $r^2=0.95$ ]), with the abiotic scheme leading to overestimated *TOC* and *DOC* compared to measurements (*DOC*\_measurements: 2.8 mg liter<sup>-1</sup>. and *DOC*\_abiotic: 7.4 mg liter<sup>-1</sup> [>159%]; *TOC*\_measurements: 3.6 mg liter<sup>-1</sup> and *TOC*\_abiotic: 14.3 mg liter<sup>-1</sup> [>297%]) and the respiration and biology scheme underestimating *DOC* and *TOC* (*DOC*\_respiration: 3.6 mg liter<sup>-1</sup> [>29%] and *DOC*\_biology: 3.7 mg liter<sup>-1</sup> [>31%]; *TOC*\_respiration: 8.8 mg liter<sup>-1</sup> [>144%] and *TOC*\_biology: 9.0 mg liter<sup>-1</sup> [<150%]).

Figure 4 shows a 50-year simulation (for the abiotic, respiration-only and biology schemes) and measurement time series for station Bimmen/Lobith at the German/Dutch border. Differences among simulation results of the different schemes are most apparent for the organic forms of C (*DOC* and *TOC*). In the abiotic

simulations all delivered organic C remains organic and concentrations are high, whereas in the other two schemes, organic forms are mineralized to *DIC*, resulting in lower concentrations of organic forms and elevated  $p\text{CO}_2$ . Time series of all other available measurement locations are found in the supplementary material section E (validation data).

### 3.2 Sensitivity analysis

The influence of a range of parameters on simulated  $\text{CO}_2$  emissions, C export and C retention was investigated, but we discuss only those parameters that have an influence of more than 20% on the variation of simulated  $\text{CO}_2$  emissions, C export or C retention. Table 1 shows the most important outcomes of the sensitivity analysis. The entire table, containing all assessed parameters and SRC results is available in the supplementary materials section F (sensitivity analysis).

Simulated total basin  $\text{CO}_2$  emissions are strongly influenced by many model parameters. Total basin  $\text{CO}_2$  exchange is positively influenced by litter input in floodplains (SRC = 0.45), *DIC* fluxes from groundwater (SRC = 0.43), the organic sediment mineralization rate (SRC = 0.28) and temperature (SRC = 0.27). The  $\text{CO}_2$  exchange is negatively influenced by alkalinity flux from groundwater (SRC = -0.42), global radiation (SRC = -0.24) and burial rate (SRC = -0.22).

Except for the floodplains,  $\text{CO}_2$  emissions are largely governed by *DIC* and *ALK* inputs that originate from groundwater.  $\text{CO}_2$  emissions from floodplains are predominantly sensitive to temperature, global radiation, organic sediment mineralization rate, burial rate, minimum sediment thickness and most dominantly by input of POC from terrestrial vegetation.

The sensitivity analysis shows that variability of total C export (of which *DIC* is the dominant C species) is almost entirely governed by variability of alkalinity delivery from groundwater, i.e. weathering (SRC = 0.9). Almost all other C eventually escapes to the atmosphere.

The most important controlling factor of the modelled retention of  $\text{POC}_{\text{terre}}$  is the mineralization rate of  $\text{SEDOC}_{\text{terre}}$ ,  $k_{\text{SEDOC}_{\text{terre\_min}}}$ , which is governed by temperature. More mineralization enables more C to escape from the system as *DIC*. As expected, the burial rate also strongly affects *POC* retention. Furthermore, an increased input of  $\text{POC}_{\text{terre}}$  from litterfall leads to an increased total retention fraction.

Many regression models use discharge as a driver of river C export at the river basin scale (Beusen et al., 2005; Mayorga et al., 2010a; Kroeze et al., 2012; Stokal et al., 2016), our sensitivity analysis suggests that discharge has a minor direct influence on the C biogeochemistry, retention and emissions and only total C export was strongly influenced by discharge (SRC=0.34). This concerns the river Rhine, and analysis of the results for other rivers is needed to assess if this is a general or local feature.

**Table 1: Results of sensitivity analysis for the Rhine river to variation in model parameters, expressed as the standard regression coefficient**

| parameter                           | CO <sub>2</sub> exchange |            |             |       |            |             | TC     | POC       |
|-------------------------------------|--------------------------|------------|-------------|-------|------------|-------------|--------|-----------|
|                                     | total                    | headwaters | main stream | lakes | reservoirs | floodplains | export | retention |
| <i>Q</i>                            | -0.01                    | -0.06      | -0.11       | -0.18 | -0.11      | 0.06        | 0.34   | -0.06     |
| <i>T</i>                            | 0.27                     | 0.00       | 0.04        | 0.11  | 0.08       | 0.32        | -0.07  | -0.50     |
| <i>l<sub>o</sub></i>                | -0.24                    | 0.00       | -0.08       | -0.04 | -0.07      | -0.28       | 0.10   | 0.03      |
| <i>kSEDOCT<sub>erre,min</sub></i>   | 0.28                     | 0.00       | 0.03        | 0.04  | 0.05       | 0.34        | -0.02  | -0.36     |
| <i>k<sub>sed,bur</sub></i>          | -0.22                    | 0.00       | -0.02       | -0.03 | -0.05      | -0.28       | 0.02   | 0.23      |
| <i>k<sub>sed,lim</sub></i>          | 0.16                     | 0.00       | 0.01        | 0.01  | 0.02       | 0.21        | -0.02  | -0.15     |
| <i>WEA<sub>DIC</sub></i>            | 0.43                     | 0.72       | 0.71        | 0.69  | 0.69       | 0.07        | 0.01   | 0.00      |
| <i>WEA<sub>ALK</sub></i>            | -0.42                    | -0.70      | -0.68       | -0.67 | -0.67      | -0.07       | 0.90   | 0.00      |
| <i>LITPOC<sub>floodplains</sub></i> | 0.45                     | 0.00       | 0.03        | 0.02  | 0.00       | 0.57        | 0.09   | 0.55      |

### 3.3 Importance of biological processes

Irrespective of the complexity of the biological processing, represented by the levels of complexity in the three applied numerical schemes, the river Rhine represents a source of CO<sub>2</sub> to the atmosphere (Figure 5). In the abiotic scheme (Figure 5a), CO<sub>2</sub> emissions are very low (0.02 Tg C year<sup>-1</sup>), while emissions in the respiration-only scheme (Figure 5b) and in the biological scheme (Figure 5c) are 118 (2.36 Tg C year<sup>-1</sup> or 41% of total C inputs) and 93 times higher (1.85 Tg C year<sup>-1</sup> or 32% of total C inputs), respectively. This indicates that outgassing of delivered CO<sub>2</sub> from external sources is very limited compared to within system generation of CO<sub>2</sub> by respiration. Furthermore, the difference between the respiration-only and biology scheme with respect to the basin CO<sub>2</sub> emissions suggests that in-stream biological processing is an important aspect in regulating CO<sub>2</sub> emissions from the aquatic continuum. The export of DIC is only 7% and 6% higher in the respiration-only (1.35 Tg C year<sup>-1</sup> or +0.9 Tg C year<sup>-1</sup>) and biology scheme (1.33 Tg C year<sup>-1</sup> or +0.7 Tg C year<sup>-1</sup>) respectively, than in the abiotic scheme (1.26 Tg C year<sup>-1</sup>), while in-stream production of DIC is

2.42 and 3.71 Tg C year<sup>-1</sup> for respectively the respiration and the biology scheme versus 0 Tg C year<sup>-1</sup> in the abiotic scheme (Figure 4). Nearly all CO<sub>2</sub> that is produced and consumed through in-stream biogeochemistry is emitted to the atmosphere in both the respiration-only and the biology schemes.

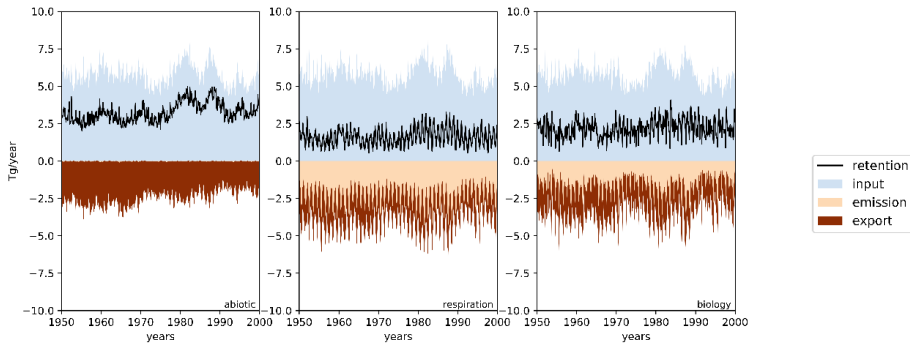


**Figure 5. Time series of total basin aggregated C budget for the abiotic (a), respiration (b) and biology (c) schemes**

In the abiotic scheme, about 3.25 Tg C year<sup>-1</sup> (57%) is retained in the Rhine basin, while total C retention in the respiration-only and biological schemes is 1.66 Tg C year<sup>-1</sup> (29% of total C input) and 2.07 Tg C year<sup>-1</sup> (36% of total C input), respectively (Figure 5). The difference in C retention between the respiration-only and the biology scheme implies that in-stream biological processing is a necessary element to consider when quantifying basin retention of C.

Total C delivery is 5.8 Tg C year<sup>-1</sup> in all schemes, but total C export to the ocean in the abiotic scheme is 2.48 Tg C year<sup>-1</sup> (43% of total C input), and 1.78 Tg C year<sup>-1</sup> (31% of total C input) and 1.88 Tg C year<sup>-1</sup> (32% of total C input) in the respiration and biology schemes, respectively.

*DIC*, *DOC* and *POC<sub>terre</sub>* average inputs into freshwaters of the Rhine basin are 1.3, 0.96 and 3.51 Tg C year<sup>-1</sup>, or 23, 17 and 60 % of the total C input, respectively (Figure 6). In the abiotic scheme, *DOC* delivery is fully balanced by export. In the respiration-only and biology schemes, *DOC* delivered to the aquatic system is partly exported (0.27 Tg C year<sup>-1</sup>, 28% *DOC* of input, and 0.34 Tg C year<sup>-1</sup>, 35% *DOC* of input, respectively). In-stream removal of *DOC* through mineralization is 0.69 Tg C year<sup>-1</sup> (72% of *DOC* input) and 0.82 Tg C year<sup>-1</sup> (85% of input). In the biology scheme, an additional 0.2 Tg C year<sup>-1</sup> (21% of *DOC* input) of *DOC* is produced in-stream by algal excretion. Export of *DOC* for the abiotic, respiration-only and biology schemes is 0.96, 0.27 and 0.34 Tg C year<sup>-1</sup>, respectively.

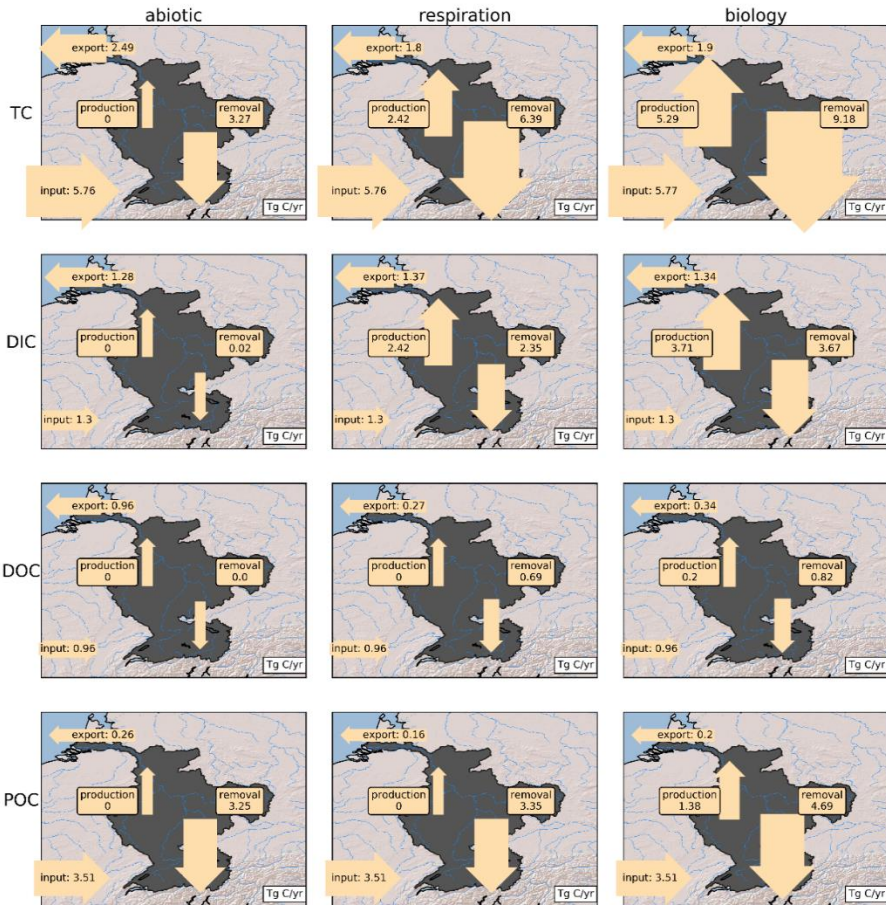


**Figure 6. 50 year (1950-2000) average modelled input, production, removal and export fluxes of the Rhine basin of total C (TC) and C species for the three biogeochemical schemes (i.e., abiotic, respiration and biology).**

About  $0.26 \text{ Tg C year}^{-1}$  (7% of POC input) of the POC delivered to the freshwater system ( $3.51 \text{ Tg C year}^{-1}$ ) is exported in the abiotic scheme. In the respiration-only and biology scheme, export of POC is  $0.16 \text{ Tg C year}^{-1}$  (5% of POC input) and  $0.2 \text{ Tg C year}^{-1}$  (6% of POC input), respectively. For the biology scheme, POC includes  $POC_{\text{terre}}$  and  $POC_{\text{auto}}$ . POC removal is  $3.25 \text{ Tg C year}^{-1}$  (93% of total POC input) in the abiotic scheme, and  $3.35 \text{ Tg C year}^{-1}$  (95% of POC input) and  $4.69 \text{ Tg C year}^{-1}$  (134% of POC input) in the respiration-only and full biology respectively. In-stream production of POC ( $1.38 \text{ Tg C year}^{-1}$ ) in the biology scheme through primary production results in a higher POC removal rate than POC input.

## Conclusions

The DISC module of IMAGE-DGNM is a major step forward in basin scale modelling of river systems. Results show that process-based modelling is essential to assess the fate of C in river basins. Biogeochemical production and consumption of C within its lifetime in the river basin are in the same order of magnitude as the inputs without calibration. The sensitivity analysis showed that in-stream chemistry and CO<sub>2</sub> emissions are weakly correlated with discharge in contrast to recent regression approaches. The dominant driver of total C export, being mainly *DIC* export, is the weathering input from groundwater. CO<sub>2</sub> emissions are strongly responsive to temperature variability and *POC* dynamics. The sensitivity analysis also suggests that if we want to understand CO<sub>2</sub> emissions from river systems, floodplains are a pivotal component to consider, as increases in CO<sub>2</sub> emissions originate for 45% from terrestrial vegetation litter delivery to floodplains/wetlands. This may be higher for tropical floodplains, as floodplains/wetlands contribute relatively much to the total water area of river basins.

Our results show that improvement in some model formulations could result in a better match of simulations with observations. Firstly, a better description of the hydrology in low-order streams to replace the current parameterization will improve our C cycle model in headwaters. The HydroSheds dataset (Lehner and Grill, 2013) is a good candidate to improve our PCR-GLOBWB model. The HydroLakes dataset (Messenger et al., 2016) will improve the current data on lake and reservoir water volume. Secondly, C inputs are an important source of uncertainty in terms of their spatial distribution, organic/inorganic ratios and form (dissolved or particulate). For example, an improved estimate of terrestrial *POC* input from litterfall and its variation between headwaters to wider mainstreams is necessary to provide a more robust quantification and spatial estimate of CO<sub>2</sub> emissions from freshwaters. Similarly, alkalinity input from groundwater is important but uncertain and can be improved by a better model for weathering and *DOC* input to aquifers and transformation to *DIC*. A future major challenge to be tackled in global biogeochemical modelling frameworks is to introduce limitations to primary production imposed by nutrients (nitrogen, phosphorus and silicium) and oxygen availability.

## **Associated content**

### **Code and data availability**

The presented version of DISC-CARBON is archived on Zenodo (van Hoek et al., 2020) under the Gnu Public License, GPL v3, in the form of input data and scripts to run the model and the raw output data for all the simulations presented in this study. Python scripts containing the source code of DISC-CARBON 1.0 are available in section A (source code). All used input data is found in section B (model input). Raw output data for the model runs shown in the results section are found in section C (raw output data). Data specifically to reproduce the figures are found in section D (data for figures). For further information about the IMAGE-DGNM framework and the data used to produce the presented results, please contact Alexander F. Bouwman ([lex.bouwman@pbl.nl](mailto:lex.bouwman@pbl.nl)).

### **Author contributions**

W.J. van Hoek prepared the original draft, developed the DISC-CARBON module and ran the model simulations. A.H.W. Beusen and J.M. Mogollón integrated the IMAGE-GNM and PCR-GLOBWB to construct the IMAGE-DGNM framework in which the DISC-CARBON was developed. J.J. Middelburg, A.F. Bouwman, L. Vilmin, X. Liu and J.J. Langeveld contributed to formulate concepts and research aims.

### **Acknowledgements**

This work is part of The New Delta 2014 ALW project project nr 869.15.014, which is financed by the Netherlands Organisation for Scientific Research (NWO). Alexander F. Bouwman and Arthur H. W. Beusen received support from PBL Netherlands Environmental Assessment Agency through in-kind contributions to The New Delta 2014 ALW project. Lauriane Vilmin received funding from part of the Earth and life sciences (ALW) Open Programme 2016 project no. ALWOP.230, which is financed by the Netherlands Organisation for Scientific Research (NWO). Joep J. Langeveld received funding from The New Delta 2014 ALW project project nr 869.15.015, which is financed by the Netherlands Organisation for Scientific Research (NWO).



---

## References

- Abril, G., Bouillon, S., Darchambeau, F., Teodoru, C. R., Marwick, T. R., Tamoooh, F., Ochieng Omengo, F., Geeraert, N., Deirmendjian, L., Polsenaere, P. and Borges, A. V.: Technical note: Large overestimation of pCO<sub>2</sub> calculated from pH and alkalinity in acidic, organic-rich freshwaters, *Biogeosciences*, 12(1), 67–78, doi:10.5194/bg-12-67-2015, 2015.
- Aulenbach, B. T., Buxton, H. T., Battaglin, W. A. and Coupe, R. H.: Streamflow and nutrient fluxes of the Mississippi-Atchafalaya River Basin and subbasins for the period of record through 2005., 2007.
- Bastviken, D., Tranvik, L. J., Downing, J. A., Crill, P. M. and Enrich-Prast, A.: Freshwater methane emissions offset the continental carbon sink, *Science* (80-. ), 331(6013), 50, 2011.
- Battin, T. J., Luysaert, S., Kaplan, L. A., Aufdenkampe, A. K., Richter, A. and Tranvik, L. J.: The boundless carbon cycle, *Nat. Geosci.*, 2(9), 598–600, 2009.
- Beusen, A. H. W., Dekkers, A. L. M., Bouwman, A. F., Ludwig, W. and Harrison, J.: Estimation of global river transport of sediments and associated particulate C, N, and P, *Global Biogeochem. Cycles*, 19(4), 2005.
- Beusen, A. H. W., Van Beek, L. P. H., Bouwman, L., Mogollón, J. M. and Middelburg, J. B. M.: Coupling global models for hydrology and nutrient loading to simulate nitrogen and phosphorus retention in surface water—description of IMAGE–GNM and analysis of performance, *Geosci. Model Dev.*, 8(12), 4045–4067, 2015.
- Bianchi, T. S.: The role of terrestrially derived organic carbon in the coastal ocean: A changing paradigm and the priming effect, *Proc. Natl. Acad. Sci.*, 108(49), 19473–19481, doi:10.1073/pnas.1017982108, 2011.
- Borges, A. V., Abril, G., Darchambeau, F., Teodoru, C. R., Deborde, J., Vidal, L. O., Lambert, T. and Bouillon, S.: Divergent biophysical controls of aquatic CO<sub>2</sub> and CH<sub>4</sub> in the World’s two largest rivers, *Sci. Rep.*, 5, 1–10, doi:10.1038/srep15614, 2015.
- Boulton, A. J., Findlay, S., Marmonier, P., Stanley, E. H. and Valett, H. M.: The functional significance of the hyporheic zone in streams and rivers, , 59–81, 1998.
- Bouwman, A. F., Beusen, A. H. W., Griffioen, J., van Groenigen, J. W., Hefting, M. M., Oenema, O., van Puijenbroek, P. J. T. M., Seitzinger, S. P., Slomp, C. P. and Stehfest, E.: Global trends and uncertainties in terrestrial denitrification and N<sub>2</sub>O emissions, *Philos. Trans. R. Soc. London B Biol. Sci.*, 368(1621), 20130112, 2013.
- Ciais, P., Sabine, C., Bala, G., Bopp, L., Brovkin, V., Canadell, J., Chhabra, A., DeFries, R., Galloway, J. and Heimann, M.: Carbon and other biogeochemical cycles, in *Climate Change 2013: The Physical Science Basis. Contribution of Working*

- Group I to the Fifth Assessment Report of the Intergovernmental Panel on Climate Change, pp. 465–570, Cambridge University Press., 2013.
- Cole, Prairie, Y. T., Caraco, N. F., McDowell, W. H., Tranvik, L. J., Striegl, R. G., Duarte, C. M., Kortelainen, P., Downing, J. A. and Middelburg, J. J.: Plumbing the global carbon cycle: integrating inland waters into the terrestrial carbon budget, *Ecosystems*, 10(1), 172–185, 2007.
- Crawford, J. T., Striegl, R. G., Wickland, K. P., Dornblaser, M. M. and Stanley, E. H.: Emissions of carbon dioxide and methane from a headwater stream network of interior Alaska, *J. Geophys. Res. Biogeosciences*, 118(2), 482–494, doi:10.1002/jgrg.20034, 2013.
- Crawford, J. T., Loken, L. C., Stanley, E. H., Stets, E. G., Dornblaser, M. M. and Striegl, R. G.: Basin scale controls on CO<sub>2</sub> and CH<sub>4</sub> emissions from the Upper Mississippi River, *Geophys. Res. Lett.*, 1–7, doi:10.1002/2015GL067599. Received, 2016.
- Duarte, C. M. and Prairie, Y. T.: Prevalence of heterotrophy and atmospheric CO<sub>2</sub> emissions from aquatic ecosystems, *Ecosystems*, 8(7), 862–870, doi:10.1007/s10021-005-0177-4, 2005.
- Dürr, H. H., Meybeck, M. and Dürr, S. H.: Lithologic composition of the Earth's continental surfaces derived from a new digital map emphasizing riverine material transfer, *Global Biogeochem. Cycles*, 19(4), 1–23, doi:10.1029/2005GB002515, 2005.
- Frankignoulle, M., Abril, G., Borges, A., Bourge, I., Canon, C., Delille, B., Libert, E. and Théate, J.-M.: Carbon Dioxide Emission from European Estuaries, *Science* (80-. ), 282(5388), 434–436, doi:10.1126/science.282.5388.434, 1998.
- Hartmann, J., Lauerwald, R. and Moosdorf, N.: A Brief Overview of the GLObal River Chemistry Database, GLORICH, *Procedia Earth Planet. Sci.*, 10, 23–27, doi:10.1016/j.proeps.2014.08.005, 2014.
- Hartmann, J., Lauerwald, R. and Moosdorf, N.: GLORICH-Global river chemistry database, PANGAEA <https://doi.org/10.1594/PANGAEA.902360>, 520, 2019.
- van Hoek, W. J., Vilmin, L., Beusen, A., J., M., Langeveld, J., Bouwman, A. F. and Middelburg, J. J.: Release version 1 of the CARBON-Dynamic In Stream Chemistry model, , doi:10.5281/zenodo.3738140, 2020.
- van Hoek, W., Wang, J., Vilmin, L., Beusen, A., Mogollon, J., Müller, G., Pika, P., Liu, X., Langeveld, J., Bouwman, A. and Middelburg, J.: Exploring spatially explicit changes in carbon budgets of global river basins during the 20th century, *Environ. Sci. Technol.*, 2021.
- Holgerson, M. A. and Raymond, P. A.: Large contribution to inland water CO<sub>2</sub> and CH<sub>4</sub> emissions from very small ponds, *Nat. Geosci.*, 9(3), 222–226, doi:10.1038/ngeo2654, 2016.

- 
- Hotchkiss, E. R., Hall Jr, R. O., Sponseller, R. A., Butman, D., Klaminder, J., Laudon, H., Rosvall, M. and Karlsson, J.: Sources of and processes controlling CO<sub>2</sub> emissions change with the size of streams and rivers, *Nat. Geosci.*, 8(9), 696–699, 2015.
- Jansen, N.: Chemical rock weathering as source of dissolved silica and sink of atmospheric CO<sub>2</sub>, *Intitute Biogeochem. Mar. Chem., Dr rer. na*, 125, 2010.
- Kempe, S.: Sinks of the anthropogenically enhanced carbon cycle in surface fresh waters, *J. Geophys. Res.*, 89(D3), 4657, doi:10.1029/JD089iD03p04657, 1984.
- Kirk, J. T. O.: *Light and photosynthesis in aquatic ecosystems*, Third Edit., Cambridge University Press., 2011.
- Kroeze, C., Bouwman, A. F. and Seitzinger, S. P.: Modeling global nutrient export from watersheds, *Curr. Opin. Environ. Sustain.*, 4(2), 195–202, 2012.
- Langeveld, J., Bouwman, A. F., van Hoek, W. J., Vilmin, L., Beusen, A. H. W., Mogollón, J. M. and Middelburg, J. J.: Estimating dissolved carbon concentrations in global soils: a global database and model, *SN Appl. Sci.*, 2(10), 1–21, 2020.
- Lehner, B. and Grill, G.: Global river hydrography and network routing: Baseline data and new approaches to study the world’s large river systems, *Hydrol. Process.*, 27(15), 2171–2186, doi:10.1002/hyp.9740, 2013.
- Mayorga, E., Seitzinger, S. P., Harrison, J. A., Dumont, E., Beusen, A. H. W., Bouwman, A. F., Fekete, B. M., Kroeze, C. and van Drecht, G.: Global nutrient export from WaterSheds 2 (NEWS 2): model development and implementation, *Environ. Model. Softw.*, 25(7), 837–853, 2010.
- Messenger, M. L., Lehner, B., Grill, G., Nedeva, I. and Schmitt, O.: Estimating the volume and age of water stored in global lakes using a geo-statistical approach, *Nat. Commun.*, 7, 1–11, doi:10.1038/ncomms13603, 2016.
- Meybeck, M.: Carbon, nitrogen, and phosphorus transport by world rivers, *Am. J. Sci.*, 282(4), 401–450, 1982.
- Middelburg, J. J.: A simple rate model for organic matter decomposition in marine sediments, *Geochim. Cosmochim. Acta*, 53(7), 1577–1581, doi:https://doi.org/10.1016/0016-7037(89)90239-1, 1989.
- Middelburg, J. J.: Organic Matter is more than CH<sub>2</sub>O BT - Marine Carbon Biogeochemistry : A Primer for Earth System Scientists, edited by J. J. Middelburg, pp. 107–118, Springer International Publishing, Cham., 2019.
- Mitchell, T. D. and Jones, P. D.: An improved method of constructing a database of monthly climate observations and associated high-resolution grids, *Int. J. Climatol.*, 25(6), 693–712, doi:10.1002/joc.1181, 2005.
-

- Prairie, Y. T. and Cole, J. J.: Carbon , Unifying Currency, *Encycl. Inl. Waters*, 2(December), 743–746, doi:<http://dx.doi.org/10.1016/B978-012370626-3.00107-1>, 2009.
- Raymond, P. A., Hartmann, J., Lauerwald, R., Sobek, S., McDonald, C., Hoover, M., Butman, D., Striegl, R., Mayorga, E. and Humborg, C.: Global carbon dioxide emissions from inland waters, *Nature*, 503(7476), 355–359, 2013.
- Regnier, P., Friedlingstein, P., Ciais, P., Mackenzie, F. T., Gruber, N., Janssens, I. A., Laruelle, G. G., Lauerwald, R., Luysaert, S. and Andersson, A. J.: Anthropogenic perturbation of the carbon fluxes from land to ocean, *Nat. Geosci.*, 6(8), 597–607, 2013.
- Saltelli, A.: Chan. K., Scott EM (ed.), *Sensitivity Analysis*, 2000.
- Sawakuchi, H. O., Neu, V., Ward, N. D., Barros, M. D. L. C., Valerio, A., Gagnemaynard, W., Cunha, A. C., Fernanda, D., Diniz, J. E., Brito, D. C., Krusche, A. V and Richey, J. E.: Carbon dioxide emissions along the lower Amazon River, *Front. Mar. Sci.*, 4(March), 1–12, doi:[10.3389/fmars.2017.00076](https://doi.org/10.3389/fmars.2017.00076), 2017.
- Soetaert, K., Hofmann, A. F., Middelburg, J. J., Meysman, F. J. R. and Greenwood, J.: Reprint of “The effect of biogeochemical processes on pH,” *Mar. Chem.*, 106(1), 380–401, doi:<https://doi.org/10.1016/j.marchem.2007.06.008>, 2007.
- Stehfest, E., van Vuuren, D., Kram, T., Bouwman, L., Alkemade, R., Bakkenes, M., Biemans, H., Bouwman, A., den Elzen, M., Janse, J., Lucas, P., van Minnen, J., Muller, C. and Prins, A. G.: Integrated Assessment of Global Environmental Change with IMAGE 3.0. Model description and policy applications. [online] Available from: <http://www.pbl.nl/en/publications/integrated-assessment-of-global-environmental-change-with-IMAGE-3.0>, 2014.
- Strokal, M., Kroeze, C., Wang, M., Bai, Z. and Ma, L.: The MARINA model (Model to Assess River Inputs of Nutrients to seAs): Model description and results for China, *Sci. Total Environ.*, 562, 869–888, doi:[10.1016/j.scitotenv.2016.04.071](https://doi.org/10.1016/j.scitotenv.2016.04.071), 2016.
- Sutanudjaja, E. H., Beek, R. van, Wanders, N., Wada, Y., Bosmans, J. H. C., Drost, N., Ent, R. J., De Graaf, I. E. M., Hoch, J. M. and Jong, K. de: PCR-GLOBWB 2: a 5 arcmin global hydrological and water resources model, *Geosci. Model Dev.*, 11(6), 2429–2453, 2018.
- Tranvik, L. J., Downing, J. A., Cotner, J. B., Loiselle, S. A., Striegl, R. G., Ballatore, T. J., Dillon, P., Finlay, K., Fortino, K., Knoll, L. B., Kortelainen, P. L., Kutser, T., Larsen, S., Laurion, I., Leech, D. M., McCallister, S. L., McKnight, D. M., Melack, J. M., Overholt, E., Porter, J. A., Prairie, Y., Renwick, W. H., Roland, F., Sherman, B. S., Schindler, D. W., Sobek, S., Tremblay, A., Vanni, M. J., Verschoor, A. M., von Wachenfeldt, E. and Weyhenmeyer, G. A.: Lakes and reservoirs as regulators of carbon cycling and climate, *Limnol. Oceanogr.*, 54(6), 2298–2314, doi:[10.4319/lo.2009.54.6\\_part\\_2.2298](https://doi.org/10.4319/lo.2009.54.6_part_2.2298), 2009.

- Uehlinger, U., Wantzen, K. M., Leuven, R. S. E. W. and Arndt, H.: The Rhine River Basin., 2009.
- Vilmin, L., Mogollón, J. M., Beusen, A. H. W., Van Hoek, W. J., Liu, X., Middelburg, J. J. and Bouwman, A. F.: Modeling process-based biogeochemical dynamics in surface fresh waters of large watersheds with the IMAGE-DGNM framework, *J. Adv. Model. Earth Syst.*, 12(11), e2019MS001796, 2020.
- Wallin, M. B., Grabs, T., Buffam, I., Laudon, H., Ågren, A., Öquist, M. G. and Bishop, K.: Evasion of CO<sub>2</sub> from streams - The dominant component of the carbon export through the aquatic conduit in a boreal landscape, *Glob. Chang. Biol.*, 19(3), 785–797, doi:10.1111/gcb.12083, 2013.
- van der Weijden, C. H. and Middelburg, J. J.: Hydrogeochemistry of the river rhine: long term a n d seasonal variability, elemental budgets, base levels a n d pollution, , 23(10), 1247–1266, 1989.
- Wollheim, W. M., Vörösmarty, C. J., Bouwman, A. F., Green, P., Harrison, J., Linder, E., Peterson, B. J., Seitzinger, S. P. and Syvitski, J. P. M.: Global N removal by freshwater aquatic systems using a spatially distributed, within-basin approach, *Global Biogeochem. Cycles*, 22(2), 1–14, doi:10.1029/2007GB002963, 2008.
- Wollheim, W. M., Stewart, R. J., Aiken, G. R., Butler, K. D., Morse, N. B. and Salisbury, J.: Removal of terrestrial DOC in aquatic ecosystems of a temperate river network, *Geophys. Res. Lett.*, 42(16), 6671–6679, 2015.

## Chapter 5

### **Carbon in inland waters; integrating freshwater systems into the global anthropogenic carbon budget**

Wim Joost van Hoek<sup>1</sup>, Joep J. Langeveld<sup>1</sup>, Alexander F. Bouwman<sup>1,2</sup>, Jack J. Middelburg<sup>1</sup>

<sup>1</sup> Department of Earth Sciences, Utrecht University, P.O. Box 80021, 3508TA Utrecht, the Netherlands.

<sup>2</sup> PBL Netherlands Environmental Assessment Agency, P.O. Box 30314, 2500GH the Hague, the Netherlands.

**ABSTRACT**

Inland waters play an important role in the global C cycle. However, the magnitude and long-term changes of inland carbon fluxes are uncertain. Particularly in global studies, the dynamics of freshwater C cycling are not explicitly included in the global C budget. Moreover, it is unknown how the global freshwater C budget changes as an effect of human perturbation of the global C cycle. This hampers understanding of the global C budget and provides an additional uncertainty in how global C cycle evolves. A recently developed spatially and temporally explicit process-based modelling approach enables quantification of different C forms in freshwater systems in the river continuum from headwaters to estuaries during the full 20th century. Model estimates of the global C fluxes during the 1990s and C budgets for several large river basins are consistent with literature. The C storage in the global atmosphere (+431%), ocean (+275%) and land (+495%) compartments increased rapidly during the 20th century. Our results show that net organic C burial in aquatic systems increased by only ~20% and other fluxes in the aquatic system changed even less during the 20th century, i.e. C inputs (+6%), CO<sub>2</sub> emissions (+8%) and C export (no change). However, on a basin scale, there are major differences among individual river basins. Our study suggests that freshwaters are a significant component of the global C budget, but much less sensitive than terrestrial systems to human interferences.

## 1 Introduction

The global climate is changing (IPCC, 2021), as the global carbon (C) budget is perturbed through anthropogenic influences (Houghton and Nassikas, 2017; Friedlingstein et al., 2022). Natural ecosystems play a key role in the global C cycle, as they are commonly thought to act as a net C sink (Keenan and Williams, 2018). Unlike terrestrial systems, freshwaters are not explicitly included in the global C budget (Drake et al., 2018; Friedlingstein et al., 2022). Cole et al., (2007) highlighted that the impact of these aquatic systems as active components on the global C budget is poorly known, potentially causing an incorrect appreciation of future feedback processes. Subsequent studies showed that freshwaters may play an important role in the global C cycle, e.g. by burying organic C and emitting substantial amounts of CO<sub>2</sub> (Battin et al., 2009; Tranvik et al., 2009; Aufdenkampe et al., 2011; Raymond et al., 2013). Moreover, C cycling in freshwater systems may also be impacted by anthropogenic influences, for example directly through damming and canalization, or indirectly through human-induced climate change, however, the extent of these impacts is uncertain (Regnier et al., 2013).

In existing global freshwater C budget studies, the global C input into freshwaters is only indirectly estimated. Total C delivery to global freshwaters is the closing term of the freshwater C budget after estimating C export to the ocean, C emissions to the atmosphere and C burial (Drake et al., 2018). The most recent global estimate of CO<sub>2</sub> evasion from inland waters (2.1 Pg C year<sup>-1</sup>) is based on spatially extrapolated freshwater pCO<sub>2</sub> values and exchange rates (Raymond et al., 2013), although more recent regional studies suggest this number may be higher (Borges et al., 2015b; Holgerson and Raymond, 2016; Sawakuchi et al., 2017). Global organic C burial in freshwaters (0.6 Pg C year<sup>-1</sup>) is estimated through spatially extrapolated lake areas and burial rates (Tranvik et al., 2009), while export to the ocean (0.9 Pg C year<sup>-1</sup>) is based on in-stream measurements (Cole et al., 2007). None of these freshwater fluxes are estimated spatiotemporally distributed, which inhibits the analysis of fluxes over time and the assessment of future feedback processes within the global C cycle. To improve our understanding of the C delivery to global freshwaters, there is a need for quantitative mechanistic approaches (Regnier et al., 2013) to describe the C linkage of terrestrial and aquatic systems (Tank et al., 2018), particularly the delivery of C to freshwaters via different pathways (vegetation, groundwater, and through autochthonous production in the water column).



To address this gap, a novel generation of large-scale freshwater C models is emerging, that couple land and freshwater systems (Lauerwald et al., 2017b; Nakayama, 2017; van Hoek et al., 2021). In this study, we apply the mechanistic process-based Integrated Model to Assess the Global Environment - Dynamic Global Nutrient Model framework (IMAGE-DGNM). DGNM (Vilmin et al., 2020; van Hoek et al., 2021) describes the mobilization, delivery and instream biogeochemistry of C and nutrients in the land-ocean-aquatic continuum, including spatial and temporal variability, within the consistent framework of the IMAGE assessment model (Stehfest et al., 2014). We use this model to quantify C fluxes to, in and from global freshwaters systems and integrate these into the global C budget. In addition, the temporal resolution of IMAGE-DGNM enables to quantify changes in the freshwater C budget during the 20<sup>th</sup> century and thus estimate the anthropogenic impact on C in freshwaters during this period in perspective of the changing global C budget.

## **2 Materials and Methods**

For quantification of C in global freshwaters we used the DGNM model, including the latest DISC-CARBON module, within the IMAGE framework (Vilmin et al., 2020; van Hoek et al., 2021). This model integrates the IMAGE integrated assessment model (Stehfest et al., 2014), which provides climatic-environmental constraints such as land use and wastewater input to inland waters, with the PCR-GLOBWB dynamic global hydrology model (Van Beek et al., 2011; Sutanudjaja et al., 2018). The IMAGE model is consistently coupled (Stehfest et al., 2014) to the Dynamic Global Vegetation Model with managed Land (LPJmL, v3.5) (Sitch et al., 2003, 2008; Bondeau et al., 2007) to provide terrestrial C dynamics such as litterfall and soil respiration. Erosion of soil POC (Langeveld et al., 2020; van Hoek et al., 2021) and delivery of DOC and DIC via groundwater and surface runoff (Langeveld et al., 2020) are spatially resolved in a consistent process-based approach. DGNM calculates transport, retention, atmospheric exchange and processing of DOC, POC and DIC species within a river basin from the lower order to the river mouth, including lakes, reservoirs and floodplains. Modelled C dynamics in freshwaters are globally distributed with a 0.5 degree spatial resolution and a yearly timestep. This study covers the first and final decades of the 20<sup>th</sup> century. Freshwater C budgets are presented both on a global scale and for a range of individual basins.

The integration of freshwater C cycling budget terms into the global C budget by Friedlingstein et al., (2022) was done by adopting the same relatively well-constrained atmospheric and oceanic sinks, as well as the emissions due to both land use change and the use of fossil fuel. Our estimate for C export to the ocean ( $0.86 \text{ Pg C year}^{-1}$ ) is similar to the C export ( $0.78 \text{ Pg C year}^{-1}$ , (Resplandy et al., 2018)) used in the global C budget (Friedlingstein et al., 2022). We corrected the seawater-air interface flux accordingly with our terms in the C budget. Also, the atmosphere-land flux was set to balance the atmospheric sink and all net fluxes to and from the atmosphere, similar to the approach by Friedlingstein et al., (2022). Finally, the residual land sink is the difference between the atmosphere-land flux and the C delivery from the land to global freshwaters.

### 3 Results and discussion

#### 3.1 Estimating C budget terms in global watersheds in a hydrology- and process-based transport model

We simulated C processing in global freshwater systems during the 1990s with a process-based model (Figure 1a; *freshwaters* block; Table 1). Our estimate of delivery of C to inland waters from terrestrial systems in the 1990s is  $3.53 \text{ Pg C year}^{-1}$ , close to  $3.35 \text{ Pg C year}^{-1}$  found in the latest global study that uses a spatially resolved large database of observed  $p\text{CO}_2$  values (Raymond et al., 2013). Some regional estimates suggest a regionally higher input (Sawakuchi et al., 2017), which may increase global values up to  $5.35 \text{ Pg C year}^{-1}$ . If we include simulated in-stream C capture through gross primary production, which in the DISC-CARBON simulation means an additional  $2.5 \text{ Pg C year}^{-1}$  of input, our total input estimate would be  $6 \text{ Pg C year}^{-1}$ . However, in our simulation only a negligible amount of organic C of autotrophic origin (including living phytoplankton and POC that originates from dead autochthonous phytoplankton and periphyton) ends up in export to oceans or ends up being buried; which means that in the DISC-CARBON simulation all autotrophic material is completely balanced by autotrophic respiration and the  $2.5 \text{ Pg C year}^{-1}$  taken up by gross primary production is emitted as  $\text{CO}_2$  before freshwaters export to the ocean. The net autotrophic C budget of global freshwaters as simulated by DISC-CARBON is therefore  $0 \text{ Pg C year}^{-1}$ , in contrast to the  $0.3 \text{ Pg C year}^{-1}$  suggested by Regnier et al. (2013). The autotrophic C cycle is a closed budget on its own, therefore the following results only consider the net interactions of the freshwater C cycle with the interfaces to the global C cycle.

The majority of terrestrial C input in our simulation is in the form of organic C (~63%), which is largely litterfall in flooded areas (van Hoek et al., 2021). Net erosion only plays a minor role (Langeveld et al., n.d.; van Hoek et al., 2021). About 37% is DIC (Table 1), which is mainly from CO<sub>2</sub>-supersaturated groundwater (Langeveld et al., n.d.; This thesis Chapter 3). Net global CO<sub>2</sub> emissions (2.24 Pg C year<sup>-1</sup>) equal the estimate by Raymond *et al.*, (2013) of 2.1 Pg C year<sup>-1</sup>. Tropical inland waters are the prime evasion hotspot, contributing ~82% of the global CO<sub>2</sub> emissions (Figure 2c; SI Table 2) (This thesis Chapter 3). Freshwater methane emissions, though only minor (Bastviken et al., 2011), are not included in our simulation.

Currently, burial of C is poorly constrained (Drake et al., 2018). In our simulation, about 0.36 Pg C year<sup>-1</sup> is buried in global freshwaters, which is within the range of estimates of 0.23 Pg C year<sup>-1</sup> (Cole et al., 2007) and 0.6 Pg C year<sup>-1</sup> (Tranvik et al., 2009). A recent study compiled a large database of organic C burial rates in lakes and reservoirs, finding a global burial rate of 185 Tg C year<sup>-1</sup> for the 1990s (Anderson et al., 2020), only slightly higher than our global annual burial rate for lakes and reservoirs of 153 Tg C year<sup>-1</sup> (van Hoek et al., 2021).

Finally, 0.86 Pg C year<sup>-1</sup> is exported to the ocean, which is close to other estimates of total C export 0.9-0.95 Pg C year<sup>-1</sup> (Cole et al., 2007; Regnier et al., 2013; Drake et al., 2018). Simulated freshwater inorganic C export (0.49 Pg C year<sup>-1</sup>; Figure 1, Table 1) is in the upper part of the range of previous estimates (Cole et al., 2007). About 43% (0.37 Pg C year<sup>-1</sup>) of the exported C is organic, similar to other studies (Schlünz and Schneider, 2000; Cole et al., 2007), but the amounts of dissolved and particulate species are respectively lower and higher than expected, with a simulated DOC: POC ratio of ~1:3 (Table 1). This is mainly caused by an oversimplified parameterization of the organic C production in floodplains, which strongly overestimates POC compared to DOC. For the total C budget however, this has no impact. Finally, we recognize that the contribution of organic C to the total C export to the ocean in our estimation may actually be smaller due to oxidation in estuaries (Borges et al., 2004; Sawakuchi et al., 2017). Estuaries and their biogeochemistry are not included in our model.

The simulated fate of the C delivered to global inland waters, is net emission (64%) and burial (10%) in the aquatic continuum, while a remaining 24% is exported to estuaries (1990s; Figure 1a; Table 1

Table 1). This exported percentage is close to recent estimates (18-28%) (Raymond et al., 2013; Regnier et al., 2013). Also, ~83% of the organic C input is removed within the system, either mineralized to DIC or buried as sediment (Table 1), highlighting freshwaters as biodynamically active systems.

The C flux estimates in freshwaters according to our first global integrated terrestrial-aquatic process-based approach agree with the most recent global study (Raymond et al., 2013). Our mechanistic model provides the first consistent estimates on the delivery of specific species of C via different pathways including autochthonous production to inland waters independently of the emissions, export and burial, while integrating the C budget across land and freshwater systems. Being able to implement this process-based approach is a major step forward (Regnier et al., 2013; Tank et al., 2018). The capability of making spatial distributions (Figure 2c; SI Table2) and simulating long-time periods (Figure 1a; Table 1) allows for e.g. identifying hotspots and analyzing changes during 20th century due to climate changes and interference in hydrology by humans. For example, a study by Lauerwald *et al.*, (2015) estimated that 78% of global freshwater CO<sub>2</sub> emissions occur at latitudes between 25°N and 25°S, similar to 82% for tropical waters in our model simulation (This thesis, Chapter 3). We acknowledge that, based on later regional studies (Drake et al., 2018), global C flux estimates may be somewhat conservative. For example, our study and Raymond *et al.*, (2013) do not explicitly resolve wetlands (van Hoek et al., 2021) which may be a substantial source of inorganic C (Borges *et al.*, 2015). Also, including estuaries, coasts and river mouths may have a significant impact (Borges et al., 2004; Bauer et al., 2013; Sawakuchi et al., 2017) and a next step in quantifying C in the land-ocean aquatic continuum (LOAC), bridging terrestrial-aquatic systems and the ocean.

### **3.2 Aquatic systems in the global C budget in the late 20<sup>th</sup> century**

Freshwaters are not explicitly included as a component in global C budgeting (Friedlingstein et al., 2022) (SI Table 2). We integrated global inland waters into the global C budget, linking the land and the ocean, balancing the global budget in a consistent approach by assuming the atmospheric and oceanic sinks by Friedlingstein et al., (2022) and assigning the budget residual to atmosphere-land flux, similar to earlier Global Carbon Projects (up to Le Quéré *et al.*, 2016) (Figure 1a). The seawater-air interface flux (AO) is almost unchanged compared to Friedlingstein *et al.*, (2019), because our freshwater C flux to the ocean (0.86 Pg C year<sup>-1</sup>; Figure 1a; Table 1

---

Table 1) is close to that of Resplandy *et al.*, (2018) ( $0.78 \text{ Pg C year}^{-1}$ ) which is used in the global C budget (Friedlingstein *et al.*, 2022). This implies the freshwater export can consistently be integrated in the global C budget. (Resplandy *et al.*, 2018; Borges *et al.*, 2004; Sawakuchi *et al.*, 2017) In the global C budget, the residual net atmosphere-land flux ( $2.6 \text{ Pg C year}^{-1}$ ; SI Table 2) is conventionally used to balance the other fluxes from, to and in the atmosphere, and often attributed to C uptake by terrestrial systems (Ciais *et al.*, 2013b; Huntzinger *et al.*, 2017; Keenan and Williams, 2018). When specifically including freshwaters into the late 20<sup>th</sup> century global C budget (Figure 1a), this residual net atmosphere-land flux (AL) more than doubles to  $5.73 \text{ Pg C year}^{-1}$  to compensate for emissions from freshwaters (FA) (Figure 1a; Table 1). This implies that, when including freshwaters into the global C budget, the net C flux from the atmosphere to terrestrial systems (thus, only considering the land, not freshwaters) is much larger than previously estimated, though required to close the global C budget. This  $5.73 \text{ Pg C year}^{-1}$  atmosphere to land flux is much larger than the net C flux from the atmosphere to terrestrial systems as estimated by terrestrial models ( $2.4 \text{ Pg C year}^{-1}$ ; SI Table 2), while these models commonly do not include lateral C removal through the LOAC in their C budgets (Ciais *et al.*, 2008; Drake *et al.*, 2018; Abril and Borges, 2019).

It has been suggested that terrestrial C cycling models implicitly include freshwater  $\text{CO}_2$  emissions in terrestrial respiration and consequently the net atmosphere-land flux, thus only being translocated spatially (Drake *et al.*, 2018). This would only partly explain the discrepancy, as in our integrated C budget about 34% of the C to inland waters is not emitted but exported or buried (Figure 1a). In addition, our residual AL flux may yet be conservative compared to other (non-dynamic) estimates for global C in freshwater systems (Sawakuchi *et al.*, 2017; Drake *et al.*, 2018), which would imply an AL flux of up to  $\sim 7.5 \text{ Pg C year}^{-1}$ . Also, other smaller net C fluxes are ignored currently, but may be of relevance in the global C budget (Randerson *et al.*, 2002; Ito, 2019; Kirschbaum *et al.*, 2019). Regardless, we advocate that the C flux from the land to freshwater systems, with a net flux of a similar size as the annual increase of the atmospheric sink, should explicitly be included in terrestrial models that are used to estimate the terrestrial C sink.

Finally, the land sink is  $2.20 \text{ Pg C year}^{-1}$ , calculated as the difference between the AL flux and the terrestrial input into freshwater systems LF (Figure 1a). Figure 1a shows that  $\text{CO}_2$  emissions in inland water are  $\sim 39\%$  of the net C flux from the atmosphere to the land, indicating that a significant amount of C initially sequestered on the land is translocated and emitted elsewhere. Moreover, globally  $\sim 62\%$  of the net

sequestered terrestrial C is laterally exported to aquatic systems particularly in tropical regions (Figure 2), where high water flows and high terrestrial productivity induce an increased lateral C flow to aquatic systems (Langeveld et al., n.d.; Borges et al., 2015b; Abril and Borges, 2019).

The land sink of 2.20 Pg C year<sup>-1</sup> in our integrated global C budget is slightly lower than the current residual estimate by Friedlingstein et al., (2022) of 2.6 Pg C year<sup>-1</sup> (SI Table 2). Note however that this residual estimate equals the combined terrestrial-aquatic burial of C which is 2.56 Pg C year<sup>-1</sup> (Figure 1a; Table 1). In other words; our study explicitly distinguishes the two main C compartments of the terrestrial-aquatic continuum, while being entirely consistent with previous top-down based estimations of the global C budget (Friedlingstein et al., 2022), including the terrestrial C sink. We show that the active pipe (Cole et al., 2007; Abril and Borges, 2019), receiving and processing a similar magnitude of C as the annual increase of the atmospheric C pool, is a relevant component of the global C cycle and should be included in the global C budget.

### **3.3 Changes of freshwaters in the global C budget during the 20<sup>th</sup> century**

Human activities have changed inland waters, with several studies indicating interference with the C cycle in freshwater systems (e.g. Raymond *et al.*, 2008; Van Cappellen and Maavara, 2016; Maavara *et al.*, 2017). We simulated C in freshwater systems as part of the global C budget (Friedlingstein et al., 2022) both for the first (Figure 1b) and final (Figure 1a) decade of the 20<sup>th</sup> century in a consistent approach, subsequently attributing the difference between both decades to anthropogenic perturbation during this era (Figure 1c; Table 1

Table 1). During the 1900s, anthropogenic emissions are only ~24% compared to the late 1990s, indicating an increase of the human C input of 5.86 Pg C year<sup>-1</sup> in the global C budget during the 20<sup>th</sup> century (Figure 1c).

Figure 1b shows that freshwater systems in the 1900s played an important role in the global C cycle, as the C flux from terrestrial to aquatic systems (3.32 Pg C year<sup>-1</sup>) is one of the largest flows in the C budget, only second to the atmosphere-land flux (3.69 Pg C year<sup>-1</sup>). Meanwhile, when considering perturbation effects during the 20<sup>th</sup> century, freshwaters seem to play a limited role (Figure 1c). While other compartments show a substantial increase of annual C storage, with ~434% (atmosphere), ~274% (ocean) and ~204% (land), the increase of net burial in aquatic systems is only ~20% (0.06 Pg C year<sup>-1</sup>). In a recent study, organic C burial rates in lakes and reservoirs during the 20<sup>th</sup> century were found to increase from 50 Tg C year<sup>-1</sup> to 185 Tg C year<sup>-1</sup> (Anderson et al., 2020). This is close to the values in our simulation, where burial in lakes and reservoirs increase from 69 Tg C year<sup>-1</sup> to 153 Tg C year<sup>-1</sup> (van Hoek et al., 2021). Note that these burial fluxes in lakes and reservoirs exceed the net global burial change, which is due to decreased burial in flooded areas (van Hoek et al., 2021).

Even more than the perturbation of the freshwater burial sink, changes in C fluxes in aquatic systems during the 20<sup>th</sup> century (Figure 1c) are minor for input (+0.21 Pg C year<sup>-1</sup>; +6.3%), emissions (+0.16 Pg C year<sup>-1</sup>; +7.7%) and export (-0.01 Pg C year<sup>-1</sup>; +1.2%). This indicates that, in particular compared to changes of other fluxes and reservoirs in the global C budget during the 20<sup>th</sup> century, C fluxes in freshwater systems on a global scale are not very sensitive to 20<sup>th</sup> century anthropogenic perturbations. However on a basin scale, there are major differences among basins. Carbon delivery to Amazon freshwaters increased by 15% and emissions by 16%. In the Mississippi, C delivery increased by 29% and burial increased by 20%. Also in the Yangtze basin we see strongly increased burial of ~60%. (Table S11) due to reservoir construction (van Hoek et al., 2021).

About 10% (0.21 of 2.04 Pg C year<sup>-1</sup>) of the increased C uptake by terrestrial systems ends up as an additional C source to aquatic systems, of which the major part (0.16 Pg C year<sup>-1</sup>) is returned to the atmosphere, illustrating that the land is more sensitive to perturbations of the C cycle than the inland waters, i.e. the land sink increases much more than the freshwater sink (Figure 1c). Regardless, the global percentages for freshwaters still indicate that freshwater systems have increased the C cycling rate in response to perturbations of the global C budget.

Regnier *et al.*, (2013) made a first estimate of anthropogenic perturbations of freshwaters in the global C cycle and concluded that the flux of C to inland waters has increased by  $\sim 1.0 \text{ Pg C year}^{-1}$  (+67%) since pre-industrial times, mainly due to enhanced C export from soils to freshwaters. This strong sensitivity to human interference is not seen in our simulation, neither is there a strong increase in *net* POC erosion (Langeveld *et al.*, n.d.) from soils during the 20<sup>th</sup> century ( $+ 6 \text{ Tg C year}^{-1}$ ). Although our process-based estimates from a robust integrated framework do not include pre-20<sup>th</sup> century anthropogenic perturbations of  $\sim 1.6 \text{ Pg C year}^{-1}$  (Friedlingstein *et al.*, 2022) and thus do not represent the full perturbation of C in freshwater systems, they do show that the response of C in inland waters to human activities may be much smaller than previously estimated.

The new IMAGE-DGNM modelling approach now enables to integrate C cycling dynamics in freshwater systems and lateral C fluxes from the land to the ocean into the global C budget. It enables to better understand the global C budget by differentiating the C exchange with the atmosphere amongst explicitly terrestrial and freshwater systems, while also further constraining the C flux from the land to the ocean in a process-based approach. Moreover, future feedback processes regarding the role of freshwaters in reaction the perturbation of the global C budget can now be better estimated. Our simulations suggests that while freshwater systems are shown to be a significantly important component of the global C budget, their response to human interference with respect to C cycling is less so.



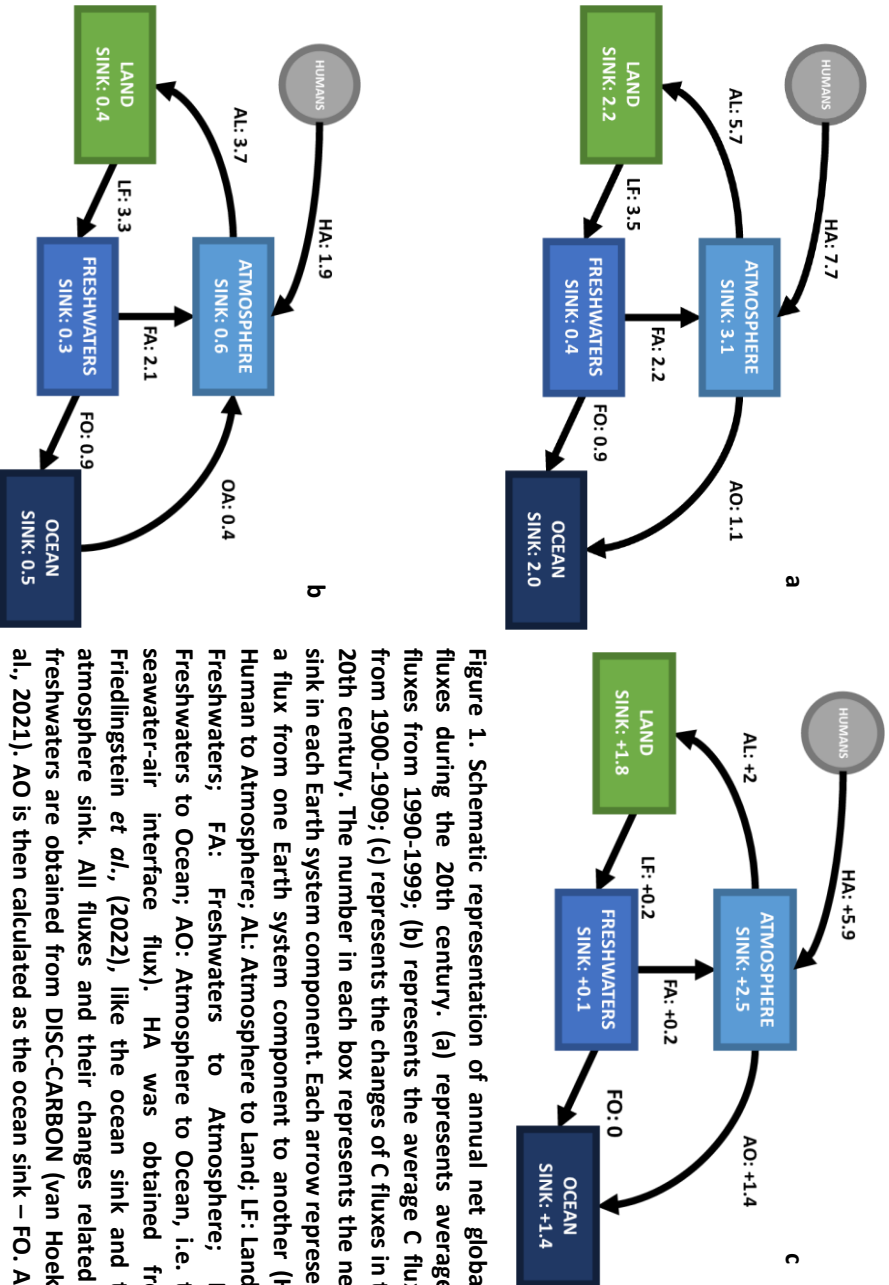
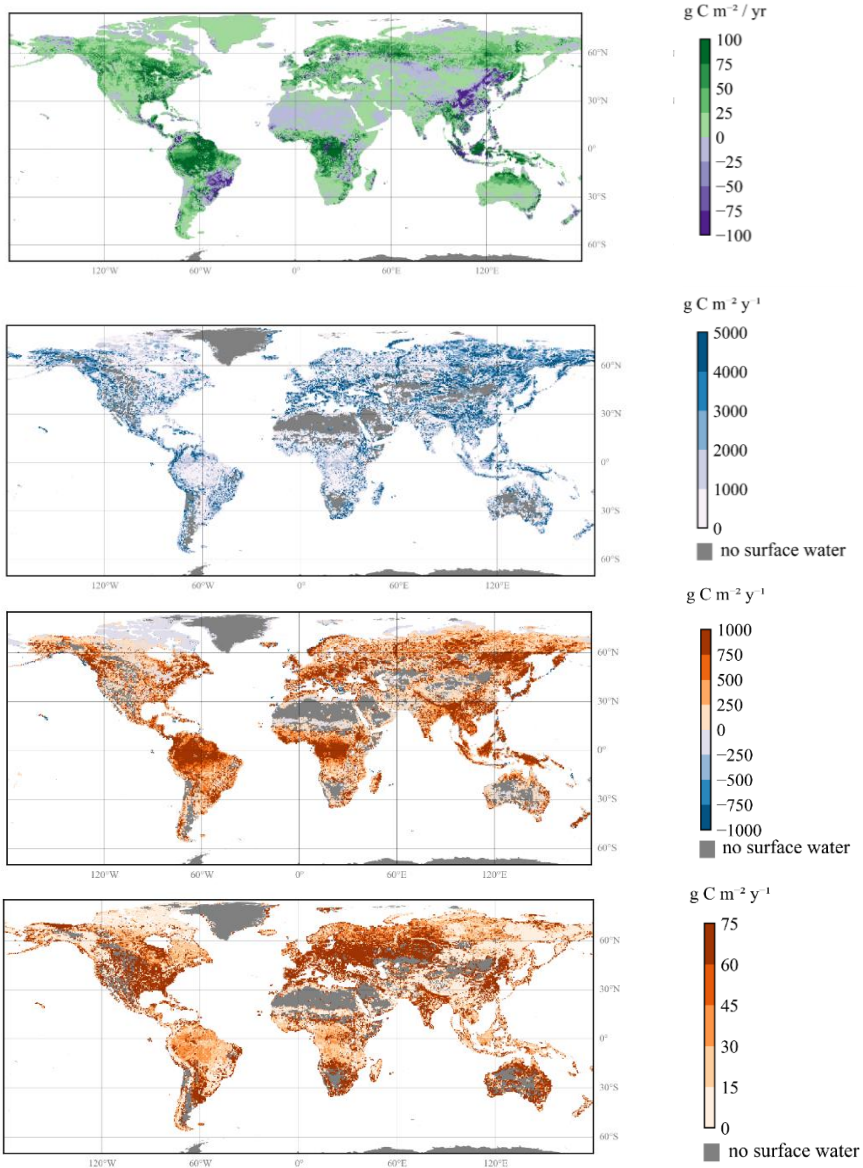


Figure 1. Schematic representation of annual net global C fluxes during the 20th century. (a) represents average C fluxes from 1990-1999; (b) represents the changes of C fluxes in the 20th century. (c) represents the net C fluxes in the 20th century. The number in each box represents the net C sink in each Earth system component. Each arrow represents a flux from one Earth system component to another (HA: Human to Atmosphere; AL: Atmosphere to Land; LF: Land to Freshwaters; FA: Freshwaters to Atmosphere; FO: Freshwaters to Ocean; AO: Atmosphere to Ocean, i.e. the seawater-air interface flux). HA was obtained from Friedlingstein *et al.*, (2022), like the ocean sink and the atmosphere sink. All fluxes and their changes related to freshwaters are obtained from DISC-CARBON (van Hook *et al.*, 2021). AO is then calculated as the ocean sink – FO. AL is calculated as HA+FA-(atmospheric sink+AO). Finally, the land sink was calculated as AL-LF.

Table 1. C budgets of global freshwaters during the 20th century ( $\text{Pg C y}^{-1}$ ).

| <i>Period</i>     | <i>Input</i> |            |            |              | <i>Emission</i> |            | <i>Burial</i> |            |            |              | <i>Export</i> |            |            |              |
|-------------------|--------------|------------|------------|--------------|-----------------|------------|---------------|------------|------------|--------------|---------------|------------|------------|--------------|
|                   | <i>DIC</i>   | <i>DOC</i> | <i>POC</i> | <i>Total</i> | <i>DIC</i>      | <i>DOC</i> | <i>DIC</i>    | <i>DOC</i> | <i>POC</i> | <i>Total</i> | <i>DIC</i>    | <i>DOC</i> | <i>POC</i> | <i>Total</i> |
| <i>1900- 1909</i> | 1.22         | 0.19       | 1.91       | 3.32         | 2.08            | 0.3        | 0.48          | 0.09       | 0.3        | 0.87         |               |            |            |              |
| <i>1990-1999</i>  | 1.3          | 0.21       | 2.02       | 3.53         | 2.24            | 0.36       | 0.49          | 0.09       | 0.28       | 0.86         |               |            |            |              |
| <i>difference</i> | 0.08         | 0.02       | 0.11       | 0.21         | 0.16            | 0.06       | 0.01          | 0          | -0.02      | -0.01        |               |            |            |              |



**Figure 2.** From top to bottom the average spatial distribution of net Biome Production (NBP) (Stehfest et al., 2014), C delivery to freshwaters (LF) (Langeveld et al., n.d.; van Hoek et al., 2021), CO<sub>2</sub> emissions from freshwaters (FA) (This thesis Chapter 3) and C burial in freshwaters (van Hoek et al., 2021).

## References

- Abril, G. and Borges, A.: Ideas and perspectives: Carbon leaks from flooded land: do we need to replumb the inland water active pipe?, 2019.
- Anderson, N. J., Heathcote, A. J. and Engstrom, D. R.: Anthropogenic alteration of nutrient supply increases the global freshwater carbon sink, *Sci. Adv.*, 6(16), eaaw2145, 2020.
- Aufdenkampe, A. K., Mayorga, E., Raymond, P. A., Melack, J. M., Doney, S. C., Alin, S. R., Aalto, R. E. and Yoo, K.: Riverine coupling of biogeochemical cycles between land, oceans, and atmosphere, *Front. Ecol. Environ.*, 9(1), 53–60, 2011.
- Bastviken, D., Tranvik, L. J., Downing, J. A., Crill, P. M. and Enrich-Prast, A.: Freshwater methane emissions offset the continental carbon sink, *Science* (80-. ), 331(6013), 50, 2011.
- Battin, T. J., Luysaert, S., Kaplan, L. A., Aufdenkampe, A. K., Richter, A. and Tranvik, L. J.: The boundless carbon cycle, *Nat. Geosci.*, 2(9), 598–600, 2009.
- Bauer, J. E., Cai, W.-J., Raymond, P. A., Bianchi, T. S., Hopkinson, C. S. and Regnier, P. A. G.: The changing carbon cycle of the coastal ocean, *Nature*, 504(7478), 61–70, 2013.
- Van Beek, L. P. H., Wada, Y. and Bierkens, M. F. P.: Global monthly water stress: 1. Water balance and water availability, *Water Resour. Res.*, 47(7), 2011.
- Bondeau, A., Smith, P. C., Zaehle, S., Schaphoff, S., Lucht, W., Cramer, W., Gerten, D., Lotze-campen, H., Müller, C., Reichstein, M. and Smith, B.: Modelling the role of agriculture for the 20th century global terrestrial carbon balance, *Glob. Chang. Biol.*, 13(3), 679–706, doi:10.1111/j.1365-2486.2006.01305.x, 2007.
- Borges, A. V., Delille, B., Schiettecatte, L., Gazeau, F., Abril, G. and Frankignoulle, M.: Gas transfer velocities of CO<sub>2</sub> in three European estuaries (Randers Fjord, Scheldt, and Thames), *Limnol. Oceanogr.*, 49(5), 1630–1641, 2004.
- Borges, A. V., Darchambeau, F., Teodoru, C. R., Marwick, T. R., Tamoo, F., Geeraert, N., Omengo, F. O., Guérin, F., Lambert, T., Morana, C., Okuku, E. and Bouillon, S.: Globally significant greenhouse-gas emissions from African inland waters, *Nat. Geosci.*, 8(8), 637–642, doi:10.1038/ngeo2486, 2015a.
- Borges, A. V., Abril, G., Darchambeau, F., Teodoru, C. R., Deborde, J., Vidal, L. O., Lambert, T. and Bouillon, S.: Divergent biophysical controls of aquatic CO<sub>2</sub> and CH<sub>4</sub> in the World's two largest rivers, *Sci. Rep.*, 5, 15614, 2015b.
- Van Cappellen, P. and Maavara, T.: Rivers in the anthropocene: Global scale modifications of riverine nutrient fluxes by damming, *Ecohydrol. Hydrobiol.*, 2016.

- 
- Ciais, P., Borges, A., Abril, G., Meybeck, M., Folberth, G., Hauglustaine, D. and Janssens, I. A.: The impact of lateral carbon fluxes on the European carbon balance, *Biogeosciences*, 5, 1259–1271, 2008.
- Ciais, P., Sabine, C., Bala, G., Bopp, L., Brovkin, V., Canadell, J., Chhabra, A., DeFries, R., Galloway, J. and Heimann, M.: Carbon and other biogeochemical cycles, in *Climate Change 2013: The Physical Science Basis. Contribution of Working Group I to the Fifth Assessment Report of the Intergovernmental Panel on Climate Change*, pp. 465–570, Cambridge University Press., 2013.
- Cole, Prairie, Y. T., Caraco, N. F., McDowell, W. H., Tranvik, L. J., Striegl, R. G., Duarte, C. M., Kortelainen, P., Downing, J. A. and Middelburg, J. J.: Plumbing the global carbon cycle: integrating inland waters into the terrestrial carbon budget, *Ecosystems*, 10(1), 172–185, 2007.
- Drake, T. W., Raymond, P. A. and Spencer, R. G. M.: Terrestrial carbon inputs to inland waters: A current synthesis of estimates and uncertainty, *Limnol. Oceanogr. Lett.*, 132–142, doi:10.1002/lol2.10055, 2018.
- Friedlingstein, P., Jones, M. W., O’Sullivan, M., Andrew, R. M., Bakker, D. C. E., Hauck, J., Le Quéré, C., Peters, G. P., Peters, W., Pongratz, J., Sitch, S., Canadell, J. G., Ciais, P., Jackson, R. B., Alin, S. R., Anthoni, P., Bates, N. R., Becker, M., Bellouin, N., Bopp, L., Chau, T. T. T., Chevallier, F., Chini, L. P., Cronin, M., Currie, K. I., Decharme, B., Djeutchouang, L. M., Dou, X., Evans, W., Feely, R. A., Feng, L., Gasser, T., Gilfillan, D., Gkritzalis, T., Grassi, G., Gregor, L., Gruber, N., Gürses, Ö., Harris, I., Houghton, R. A., Hurtt, G. C., Iida, Y., Ilyina, T., Luijckx, I. T., Jain, A., Jones, S. D., Kato, E., Kennedy, D., Klein Goldewijk, K., Knauer, J., Korsbakken, J. I., Körtzinger, A., Landschützer, P., Lauvset, S. K., Lefèvre, N., Lienert, S., Liu, J., Marland, G., McGuire, P. C., Melton, J. R., Munro, D. R., Nabel, J. E. M. S., Nakaoka, S.-I., Niwa, Y., Ono, T., Pierrot, D., Poulter, B., Rehder, G., Resplandy, L., Robertson, E., Rödenbeck, C., Rosan, T. M., Schwinger, J., Schwingshackl, C., Séférian, R., Sutton, A. J., Sweeney, C., Tanhua, T., Tans, P. P., Tian, H., Tilbrook, B., Tubiello, F., van der Werf, G. R., Vuichard, N., Wada, C., Wanninkhof, R., Watson, A. J., Willis, D., Wiltshire, A. J., Yuan, W., Yue, C., Yue, X., Zaehle, S. and Zeng, J.: Global Carbon Budget 2021, *Earth Syst. Sci. Data*, 14(4), 1917–2005, doi:10.5194/essd-14-1917-2022, 2022.
- van Hoek, W. J., Langeveld, J. J., Vilmin, L., Liu, X., Beusen, A. H. W., Mogollón, J. M., Bouwman, A. F. and Middelburg, J. J.: Global Freshwater CO<sub>2</sub> Emissions Are Increasing As A Result Of Rising Terrestrial Carbon Inputs, Chapter 3 van Hoek PhD thesis, 2022.
- van Hoek, W., Wang, J., Vilmin, L., Beusen, A., Mogollón, J., Müller, G., Pika, P., Liu, X., Langeveld, J., Bouwman, A. and Middelburg, J.: Exploring spatially explicit changes in carbon budgets of global river basins during the 20th century, *Environ. Sci. Technol.*, 2021.
-

- Holgerson, M. A. and Raymond, P. A.: Large contribution to inland water CO<sub>2</sub> and CH<sub>4</sub> emissions from very small ponds, *Nat. Geosci.*, 9(3), 222–226, doi:10.1038/ngeo2654, 2016.
- Houghton, R. A. and Nassikas, A. A.: Global and regional fluxes of carbon from land use and land cover change 1850–2015, *Global Biogeochem. Cycles*, 31(3), 456–472, 2017.
- Huntzinger, D. N., Michalak, A. M., Schwalm, C., Ciais, P., King, A. W., Fang, Y., Schaefer, K., Wei, Y., Cook, R. B. and Fisher, J. B.: Uncertainty in the response of terrestrial carbon sink to environmental drivers undermines carbon-climate feedback predictions, *Sci. Rep.*, 7(1), 1–8, 2017.
- IPCC, 2021: *Climate Change 2021: The Physical Science Basis. Contribution of Working Group I to the Sixth Assessment Report of the Intergovernmental Panel on Climate Change* [Masson-Delmotte, V., P. Zhai, A. Pirani, S.L. Connors, C. Péan, S. Berger, N. Caud, Y. Chen, L. Goldfarb, M.I. Gomis, M. Huang, K. Leitzell, E. Lonnoy, J.B.R. Matthews, T.K. Maycock, T. Waterfield, O. Yelekçi, R. Yu, and B. Zhou (eds.)]. Cambridge University Press, Cambridge, United Kingdom and New York, NY, USA, In press, doi:10.1017/9781009157896
- Ito, A.: Disequilibrium of terrestrial ecosystem CO<sub>2</sub> budget caused by disturbance-induced emissions and non-CO<sub>2</sub> carbon export flows: a global model assessment, *Earth Syst. Dyn.*, 10(4), 685–709, 2019.
- Keenan, T. F. and Williams, C. A.: The terrestrial carbon sink, *Annu. Rev. Environ. Resour.*, 43, 219–243, 2018.
- Kirschbaum, M. U. F., Zeng, G., Ximenes, F., Giltrap, D. L. and Zeldis, J. R.: Towards a more complete quantification of the global carbon cycle, *Biogeosciences*, 16(3), 831–846, 2019.
- Langeveld, J., Bouwman, A. F., van Hoek, W. J., Vilmin, L., Beusen, A. H. W., Mogollón, J. M. and Middelburg, J. J.: Estimating dissolved carbon concentrations in global soils: a global database and model, *SN Appl. Sci.*, 2(10), 1–21, 2020.
- Langeveld, J., Bouwman, A. F., van Hoek, W. J., Vilmin, L., Beusen, A. H. W., Liu, X., Mogollón, J. M. and Middelburg, J. J.: Estimating global dissolved carbon flows from soils to surface waters (in preparation), 2021a.
- Langeveld, J., Bouwman, A. F., van Hoek, W. J., Vilmin, L., Beusen, A. H. W., Liu, X., Mogollón, J. M. and Middelburg, J. J.: Towards a balanced budget? Including lateral carbon removal in the global terrestrial C budget (in preparation), 2021b.
- Lauerwald, R., Laruelle, G. G., Hartmann, J., Ciais, P. and Regnier, P. A. G.: Spatial patterns in CO<sub>2</sub> evasion from the global river network, *Global Biogeochem. Cycles*, 29(5), 534–554, doi:10.1002/2014GB004941. Received, 2015.

- Lauerwald, R., Regnier, P., Camino-Serrano, M., Guenet, B., Guimberteau, M., Ducharne, A., Polcher, J. and Ciais, P.: ORCHILEAK (revision 3875): a new model branch to simulate carbon transfers along the terrestrial–aquatic continuum of the Amazon basin, *Geosci. Model Dev.*, 10, 3821–3859, 2017.
- Maavara, T., Lauerwald, R., Regnier, P. and Cappellen, P. Van: Global perturbation of organic carbon cycling by river damming, *Nat. Commun.*, accepted(May), 1–10, doi:10.1038/ncomms15347, 2017.
- Nakayama, T.: Development of an advanced eco-hydrologic and biogeochemical coupling model aimed at clarifying the missing role of inland water in the global biogeochemical cycle, *J. Geophys. Res. Biogeosciences*, 122(4), 966–988, 2017.
- Le Quéré, C., Andrew, R., Canadell, J. G., Sitch, S., Korsbakken, J. I., Peters, G. P., Manning, A. C., Boden, T. A., Tans, P. P. and Houghton, R. A.: Global carbon budget 2016, 2016.
- Le Quéré, C., Andrew, R. M., Friedlingstein, P., Sitch, S., Hauck, J., Pongratz, J., Pickers, P. A., Korsbakken, J. I., Peters, G. P. and Canadell, J. G.: Global carbon budget 2018, *Earth Syst. Sci. Data*, 10(4), 2141–2194, 2018.
- Randerson, J. T., Chapin, F. S., Harden, J. W., Neff, J. C. and Harmon, M. E.: Net ecosystem production: a comprehensive measure of net carbon accumulation by ecosystems, *Ecol. Appl.*, 12(4), 937–947, 2002.
- Raymond, P. A., Hartmann, J., Lauerwald, R., Sobek, S., McDonald, C., Hoover, M., Butman, D., Striegl, R., Mayorga, E. and Humborg, C.: Global carbon dioxide emissions from inland waters, *Nature*, 503(7476), 355–359, 2013.
- Raymond, P. a, Oh, N.-H., Turner, R. E. and Broussard, W.: Anthropogenically enhanced fluxes of water and carbon from the Mississippi River., *Nature*, 451(7177), 449–52, doi:10.1038/nature06505, 2008.
- Regnier, P., Friedlingstein, P., Ciais, P., Mackenzie, F. T., Gruber, N., Janssens, I. A., Laruelle, G. G., Lauerwald, R., Luysaert, S. and Andersson, A. J.: Anthropogenic perturbation of the carbon fluxes from land to ocean, *Nat. Geosci.*, 6(8), 597–607, 2013.
- Resplandy, L., Keeling, R. F., Rödenbeck, C., Stephens, B. B., Khatiwala, S., Rodgers, K. B., Long, M. C., Bopp, L. and Tans, P. P.: Revision of global carbon fluxes based on a reassessment of oceanic and riverine carbon transport, *Nat. Geosci.*, 11(7), 504–509, 2018.
- Sawakuchi, H. O., Neu, V., Ward, N. D., Barros, M. D. L. C., Valerio, A., Gagne-maynard, W., Cunha, A. C., Fernanda, D., Diniz, J. E., Brito, D. C., Krusche, A. V and Richey, J. E.: Carbon dioxide emissions along the lower Amazon River, *Front. Mar. Sci.*, 4(March), 1–12, doi:10.3389/fmars.2017.00076, 2017.

- Schlünz, B. and Schneider, R. R.: Transport of terrestrial organic carbon to the oceans by rivers: re-estimating flux and burial rates, *Int. J. Earth Sci.*, 88, 599–606, doi:10.1007/s005310050290, 2000.
- Sitch, S., Smith, B., Prentice, I. C., Arneth, A., Bondeau, A., Cramer, W., Kaplan, J. O., Levis, S., Lucht, W. and Sykes, M. T.: Evaluation of ecosystem dynamics, plant geography and terrestrial carbon cycling in the LPJ dynamic global vegetation model, *Glob. Chang. Biol.*, 9(2), 161–185, 2003.
- Sitch, S., Huntingford, C., Gedney, N., Levy, P. E., Lomas, M., Piao, S. L., Betts, R., Ciais, P., Cox, P. and Friedlingstein, P.: Evaluation of the terrestrial carbon cycle, future plant geography and climate-carbon cycle feedbacks using five Dynamic Global Vegetation Models (DGVMs), *Glob. Chang. Biol.*, 14(9), 2015–2039, 2008.
- Stehfest, E., van Vuuren, D., Kram, T., Bouwman, L., Alkemade, R., Bakkenes, M., Biemans, H., Bouwman, A., den Elzen, M., Janse, J., Lucas, P., van Minnen, J., Muller, C. and Prins, A. G.: Integrated Assessment of Global Environmental Change with IMAGE 3.0. Model description and policy applications. [online] Available from: <http://www.pbl.nl/en/publications/integrated-assessment-of-global-environmental-change-with-IMAGE-3.0>, 2014.
- Sutanudjaja, E. H., Beek, R. van, Wanders, N., Wada, Y., Bosmans, J. H. C., Drost, N., Ent, R. J., De Graaf, I. E. M., Hoch, J. M. and Jong, K. de: PCR-GLOBWB 2: a 5 arcmin global hydrological and water resources model, *Geosci. Model Dev.*, 11(6), 2429–2453, 2018.
- Tank, S. E., Fellman, J. B., Hood, E. and Kritzbberg, E. S.: Beyond respiration: Controls on lateral carbon fluxes across the terrestrial-aquatic interface, *Limnol. Oceanogr. Lett.*, 3(3), 76–88, 2018.
- Tranvik, L. J., Downing, J. A., Cotner, J. B., Loiselle, S. A., Striegl, R. G., Ballatore, T. J., Dillon, P., Finlay, K., Fortino, K., Knoll, L. B., Kortelainen, P. L., Kutser, T., Larsen, S., Laurion, I., Leech, D. M., McCallister, S. L., McKnight, D. M., Melack, J. M., Overholt, E., Porter, J. A., Prairie, Y., Renwick, W. H., Roland, F., Sherman, B. S., Schindler, D. W., Sobek, S., Tremblay, A., Vanni, M. J., Verschoor, A. M., von Wachenfeldt, E. and Weyhenmeyer, G. A.: Lakes and reservoirs as regulators of carbon cycling and climate, *Limnol. Oceanogr.*, 54(6), 2298–2314, doi:10.4319/lo.2009.54.6\_part\_2.2298, 2009.
- Tranvik, L. J., Cole, J. J. and Prairie, Y. T.: The study of carbon in inland waters—from isolated ecosystems to players in the global carbon cycle, *Limnol. Oceanogr. Lett.*, 3(3), 41–48, 2018.
- Vilmin, L., Mogollón, J. M., Beusen, A. H. W., Van Hoek, W. J., Liu, X., Middelburg, J. J. and Bouwman, A. F.: Modeling process-based biogeochemical dynamics in surface fresh waters of large watersheds with the IMAGE-DGNM framework, *J. Adv. Model. Earth Syst.*, 12(11), e2019MS001796, 2020.



---

---

## Supporting Information: Carbon in inland waters; integrating freshwater systems into the global anthropogenic carbon budget

**SI Table 1. Carbon budgets of aquatic systems during the 20th century (Tg C year<sup>-1</sup>)**

| <i>Basin</i>       | <i>Period</i> | <i>Input</i> |            |            | <i>Emission</i> |            |            | <i>Export</i> |              |    |    |
|--------------------|---------------|--------------|------------|------------|-----------------|------------|------------|---------------|--------------|----|----|
|                    |               | <i>DIC</i>   | <i>DOC</i> | <i>POC</i> | <i>Total</i>    | <i>DIC</i> | <i>DOC</i> | <i>POC</i>    | <i>Total</i> |    |    |
| <i>Amazon</i>      | 1900-1909     | 197          | 18         | 694        | 911             | 798        | 34         | 39            | 1            | 37 | 77 |
|                    | 1990-1999     | 306          | 18         | 722        | 1046            | 930        | 34         | 49            | 1            | 32 | 82 |
|                    | difference    | 109          | 0          | 28         | 137             | 131        | 0          | 10            | 0            | -5 | 5  |
| <i>Mississippi</i> | 1900-1909     | 15           | 2          | 31         | 48              | 19         | 15         | 12            | 0            | 1  | 13 |
|                    | 1990-1999     | 23           | 3          | 36         | 61              | 22         | 18         | 19            | 0            | 2  | 21 |
|                    | difference    | 8            | 1          | 5          | 14              | 3          | 3          | 7             | 0            | 1  | 8  |
| <i>Nile</i>        | 1900-1909     | 7            | 1          | 34         | 42              | 28         | 11         | 3             | 0            | 0  | 3  |
|                    | 1990-1999     | 6            | 1          | 33         | 40              | 28         | 9          | 3             | 0            | 0  | 3  |
|                    | difference    | -1           | 0          | -1         | -2              | 0          | -2         | 0             | 0            | 0  | 0  |
| <i>Lena</i>        | 1900-1909     | 11           | 4          | 11         | 26              | 12         | 1          | 4             | 2            | 7  | 13 |
|                    | 1990-1999     | 12           | 5          | 12         | 29              | 13         | 1          | 5             | 3            | 7  | 15 |
|                    | difference    | 1            | 1          | 1          | 3               | 1          | 0          | 1             | 1            | 0  | 2  |
| <i>Yangtze</i>     | 1900-1909     | 21           | 5          | 20         | 47              | 18         | 10         | 14            | 1            | 3  | 18 |
|                    | 1990-1999     | 21           | 7          | 25         | 54              | 21         | 16         | 13            | 1            | 3  | 17 |
|                    | difference    | 0            | 2          | 5          | 7               | 3          | 6          | -1            | 0            | 0  | -1 |

**SI Table 2. The global C budget during the 20<sup>th</sup> century (adapted from Friedlingstein et al. (2022))**

| Activity  | Flux 1900-1909<br>(Pg C year <sup>-1</sup> ) | Flux 1990-1999<br>(Pg C year <sup>-1</sup> ) | Difference<br>(Pg C year <sup>-1</sup> ) |
|---|--|--|--|
| <b>Sources</b>  |  |  |  |
| 1. Fossil fuel combustion and cement production emissions | 0.66 ± 0.03                                  | 6.4 ± 0.3                                    | + 5.7                                    |
| 2. Land-use change emissions                              | 1.2 ± 0.7                                    | 1.3 ± 0.7                                    | + 0.13                                   |
| <b>Sinks</b>  |  |  |  |
| 1. Atmospheric CO <sub>2</sub> growth rate                | 0.59 ± 0.02 <sup>1</sup>                     | 3.1 ± 0.02                                   | + 2.5                                    |
| 2. Oceanic CO <sub>2</sub> growth rate                    | 0.52 ± 0.5 <sup>1</sup>                      | 2.0 ± 0.6                                    | +1.4                                     |
| Residual sink (land-attributed)                           | 0.74 ± 0.9 <sup>2</sup>                      | 2.6 ± 0.9                                    | + 1.9                                    |
| Land sink estimated by DGVMs                              | 0.78 <sup>3</sup>                            | 2.4 ± 0.4                                    | + 1.6                                    |
| C budget difference residual sink vs land sink DGVMs      | -0.03  | 0.27   | + 0.31                                   |

<sup>1</sup> general modelling uncertainty given in dataset description by Friedlingstein et al. (2022).

<sup>2</sup> calculated based on the uncertainties of the individual sinks and sources.

<sup>3</sup> uncertainty unknown, though by Friedlingstein et al. (2022) for other decades report uncertainties in the range of 0.3 - 0.6 Pg C year<sup>-1</sup>.

## Synthesis

This thesis explored the global C budget of freshwaters and its spatiotemporal variations in the 20th century using the mechanistic IMAGE-Dynamic Global Nutrient Model extended with the newly developed Dynamic In-stream Chemistry Carbon module (DISC-CARBON). This model couples river basin hydrology, environmental conditions and C delivery and generates C flows from headwaters to mouths. DISC-CARBON is a spatially explicit global model with 0.5 by 0.5-degree resolution that simulates the concentrations, transformations and transfer fluxes of dissolved inorganic C (*DIC*), dissolved organic C (*DOC*) and terrestrial and autochthonous particulate organic C (*POC*) from headwaters to river mouth in a single integrated model. Chapters 2 and 3 of this thesis show that the simulations of spatiotemporal river export and CO<sub>2</sub> emissions are in good agreement with observations and literature, and Chapter 4 shows that the model also properly simulates the C cycle for an individual river, the Rhine. With the DISC-CARBON model developed, the long-term C budget of freshwaters can now be estimated with confidence. Below the results for the freshwater C budget terms C inputs, emissions, export and burial are summarized and compared with other studies with a range of completely different approaches, and subsequently the consequence of including the freshwater C budget in the overall global C budget is discussed. The last part discusses the shortcomings of the model, and possible improvements needed to better quantify the C budget of global freshwaters.

### The freshwater C budget

For the first time, DISC-CARBON enables to make a spatiotemporally consistent assessment of the global C concentrations and C budgets of freshwaters. It allows to qualify why, and quantify how much and where, input, emission, export and storage have changed over the course of the 20<sup>th</sup> century. Budget studies published so far have limitations because (1) a “static” C budget was based on aggregated data covering long periods, (2) data with limited spatial coverage was extrapolated to the global scale and (3) the C budgets were not quantified using a globally consistent methodology.

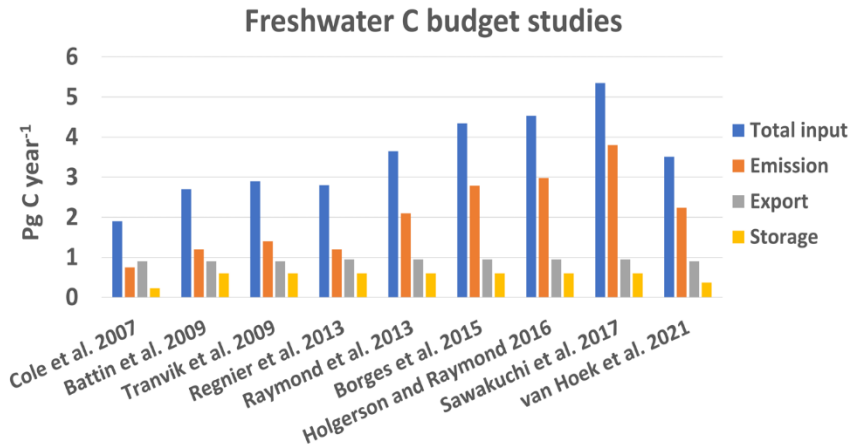


**Figure 1. Comparison of DISC-CARBON van Hoek et al., 2021) results with other global freshwater C budget studies in chronological order**

At the end of the 20<sup>th</sup> century, total global C inputs from land to freshwaters add up to 3.5 Pg C year<sup>-1</sup>, burial is 0.4 Pg C year<sup>-1</sup> and CO<sub>2</sub> emission is 2.2 Pg C year<sup>-1</sup>. Increasing global C inputs, burial and CO<sub>2</sub> emissions reported in the literature are confirmed by DISC-CARBON. Global river C export to oceans has been stable around 0.9 Pg C year<sup>-1</sup>. This indicates that global river basins have been balancing the increased inputs through enhanced in-stream retention and emission to the atmosphere. The long-term changes and spatial patterns of concentrations and fluxes of different C forms in the global river network result from many parallel and simultaneous processes, including the combined influence of the lithology, climate, hydrology of river basins, terrestrial and biological C sources, in-stream C transformations, and human interferences such as damming. The increased C retention in inland waters, from 0.3 Pg C year<sup>-1</sup> in the first decade of the 20<sup>th</sup> century to 0.4 Pg C year<sup>-1</sup> in the last decade of the 20<sup>th</sup> century may be closely related to the increasing number of dams constructed. CO<sub>2</sub> emissions from inland water systems showed an increase of 0.2 Pg C year<sup>-1</sup> from an average of 2.1 Pg C year<sup>-1</sup> in the 1900's to an average of 2.3 Pg C year<sup>-1</sup> in the 1990's, mainly as a result of an increase in terrestrial carbon (C) delivery.

Most CO<sub>2</sub> emissions originate from floodplains 1.4 Pg C year<sup>-1</sup>, where CO<sub>2</sub> is produced through mineralization of terrestrial organic C. Rivers contribute 0.8 Pg C year<sup>-1</sup> to total CO<sub>2</sub> emissions, mainly due to the influx of CO<sub>2</sub> supersaturated groundwater. Lakes and reservoirs emit 0.2 Pg C year<sup>-1</sup>. Although delivery of organic C through soil erosion increased from 106 Tg C year<sup>-1</sup> to 168 Tg C year<sup>-1</sup> and the volume of reservoirs increased during the 20<sup>th</sup> century from nearly 0 to more than 3500 km<sup>3</sup>, DISC-CARBON simulations do not indicate a major influence of these changes on global CO<sub>2</sub> emissions from freshwaters, but some key processes such as eutrophication have not been explicitly included.

## The global C budget

In the last chapter of this thesis, the implications of integrating the freshwater C budget in the global C budget were explored. Conventionally, the residual net atmosphere-land flux (2.3 Pg C year<sup>-1</sup> in the late 20<sup>th</sup> century (Friedlingstein et al., 2022)) is used to balance the other fluxes from and to the atmosphere, and often attributed to C uptake by terrestrial systems (Ciais et al., 2013b; Huntzinger et al., 2017; Keenan and Williams, 2018); depicted in figure 2 below. When including freshwaters in the global C budget, this residual net atmosphere-land flux (AL) more than doubles to 5.7 Pg C year<sup>-1</sup> to compensate for emissions from freshwaters (FA); depicted in figure 2 top. This implies that by accounting for the lateral transport and processing in rivers in the global C budget, the net C flux from the atmosphere to terrestrial systems (thus, only considering the land, not freshwaters) is much larger than previously estimated, and leads to a closed global C budget. This 5.7 Pg C year<sup>-1</sup> from atmosphere to land is much larger than the net C flux from the atmosphere to terrestrial systems as estimated by terrestrial models (2.3 Pg C year<sup>-1</sup> (Friedlingstein et al., 2022)), while these models commonly do not include lateral C removal through the LOAC in their C budgets. Therefore, the C flux from the land to freshwater systems, with a net flux of a similar size as the annual increase of the atmospheric sink, should explicitly be included in terrestrial models that are used to estimate the terrestrial C sink.

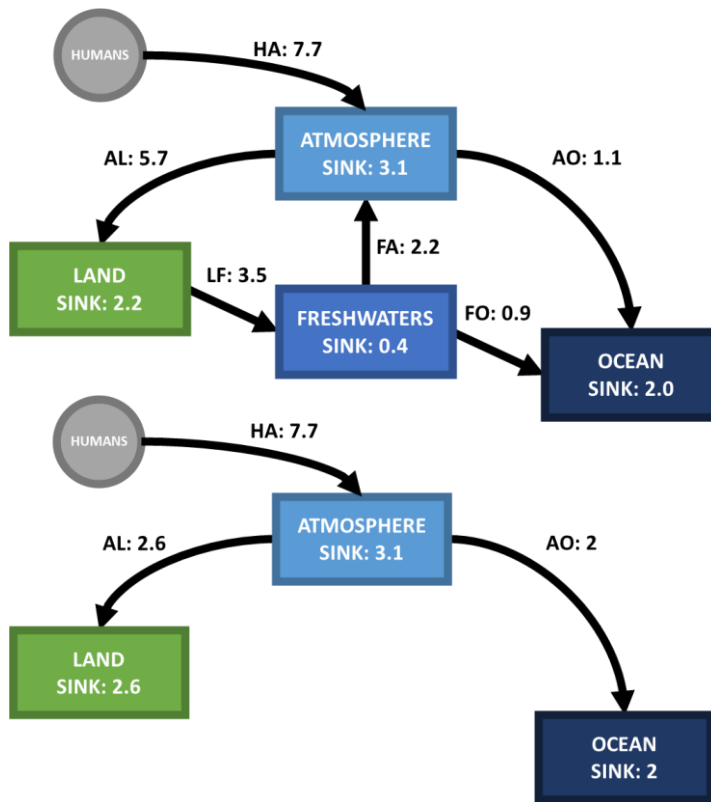


**Figure 2. A global C budget that includes freshwaters (top) and a global C budget that excludes freshwaters (bottom) for 1990's in Pg C year<sup>-1</sup>**

The global C budget has changed dramatically (figure 3, bottom) as a consequence of C emissions from human activities. However, our capabilities to quantify the response of freshwater systems are still rather limited. Several studies indicated that human activities interfere with the C cycle in freshwater systems (e.g. Raymond *et al.*, 2008; Van Cappellen and Maavara, 2016; Maavara *et al.*, 2017). DISC-CARBON suggests that although freshwaters are a significant component of the global C budget, they are much less sensitive to human induced global change interferences than terrestrial systems. Figure 3 shows that the C storage in the global atmosphere ( $2.5 \text{ Pg C year}^{-1}$  or  $\sim 431\%$ ), ocean ( $1.4 \text{ Pg C year}^{-1}$ , or  $\sim 275\%$ ) and land ( $1.8 \text{ Pg C year}^{-1}$ , or  $\sim 495\%$ ) compartments increased rapidly during the 20<sup>th</sup> century. In contrast, net burial in aquatic systems increased by only  $\sim 20\%$  ( $0.1 \text{ Pg C year}^{-1}$ ). Other fluxes in the aquatic system changed even less during the 20<sup>th</sup> century, i.e. C inputs ( $+0.2 \text{ Pg C year}^{-1}$ ;  $+6\%$ ),  $\text{CO}_2$  emissions ( $+0.2 \text{ Pg C year}^{-1}$ ;  $+8\%$ ) and C export  $0 \text{ Pg C year}^{-1}$ . Regnier

*et al.*, (2013) made a first estimate of anthropogenic perturbations of freshwaters in the global C cycle and concluded that the flux of C to inland waters has increased by  $\sim 1.0 \text{ Pg C year}^{-1}$  (+67%) since pre-industrial times, mainly due to enhanced C export from soils to freshwaters. This strong sensitivity to human interference is not observed in our simulation. Moreover, the increase in *net* POC erosion (Langeveld *et al.*, 2021) from soils was also limited during the 20<sup>th</sup> century in our model output ( $+ 6 \text{ Tg C year}^{-1}$ ).

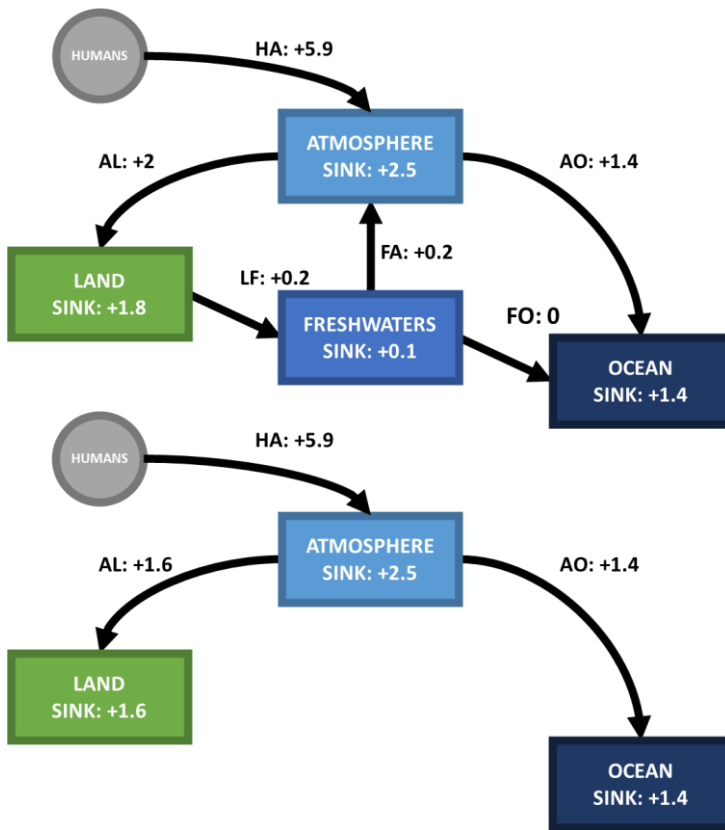


**Figure 3.** The change of the global C budget from the 1900's to 1990's that includes freshwaters (top) and the global C budget change from the 1900's to 1990's that excludes freshwaters (bottom) in  $\text{Pg C year}^{-1}$



## Outlook

This work focused on the historical global C budget of freshwaters, with an annual timestep, for a 0.5 by 0.5 degrees spatial resolution. The main objective was to quantify the long-term C budget of global freshwaters. While keeping this main objective in mind, there are two directions to move from here which are equally relevant.

DISC-CARBON has a number of limitations that can be grouped into those related to the hydrological/hydrodynamical and sedimentological description of water bodies, the spatio-temporal resolution, and C-nutrient stoichiometry.

1. The hydrodynamic and sedimentological representation of floodplains needs a better constrained parameterization. Floodplains are a hydrological dynamic interface between land and freshwaters, a major source for particulate organic C, prime sources of CO<sub>2</sub> emissions and sites with substantial organic carbon burial. Variables and parameters that account for these characteristics are poorly constrained in DISC-CARBON.
2. According to Holgerson & Raymond (2016) small lakes and ponds represent major CO<sub>2</sub> sources. Currently small lakes and ponds are not explicitly represented in DISC-CARBON. It remains unclear if and how they are coupled to the aquatic continuum and how they can be embedded in the DISC framework. Small lakes and ponds account for a large part for CH<sub>4</sub> emissions. CH<sub>4</sub> emissions are not modelled in DISC-CARBON, although they may contribute significantly to the C budget of freshwaters. Improved parameterization of organic C deposition in sediments, and a spatio-temporal representation of redox conditions is needed for mechanistic modelling of CH<sub>4</sub> emissions from freshwaters.
3. The hydrodynamic and morphological characteristics of lakes and reservoirs are not represented in DISC-CARBON, although these have substantial impacts on their C fluxes, through the atmosphere interface by CO<sub>2</sub> / CH<sub>4</sub> emissions (Schilder et al., 2013) or through the sediment interface by OC burial (Forsberg, 1989).
4. More in general, DISC-CARBON represents processes like respiration, production, deposition and resuspension, whereby the model temporal scale (annual) is too coarse to describe these processes. Seasonal discharge, daily and seasonal temperature and light variability may affect the response of the modelled system as a whole. It is yet unclear how sensitive the model

is to increased/decreased temporal resolution. Likewise, these processes depend on C inputs, like groundwater delivery of alkalinity, CO<sub>2</sub> and POC delivery from litterfall, that have a high spatial heterogeneity. It is unclear how sensitive the current model results are to increased/decreased spatial resolution.

5. Finally, C is embedded in a wider stoichiometric context with nitrogen (N), phosphorus (P) and silicon (Si). An important next step for the DISC module in general is to couple these cycles. For example to have a more realistic representation of spatio-temporally distributed primary production nutrient fertilization/limitations. More/less production leads to more/less OC burial, with consequences for C emissions to the atmosphere and impacts for delivery to coastal ecosystems.

The original idea of DISC has always been that different versions for C, N, P and Si are developed separately after which they are merged into a single calculation framework for all nutrients at once. The current development process does not allow for this. Although the code bases for C, N, P and Si all have an identical origin, merging them is challenging due to their completely separated development paths. From a technical perspective, for a successful continued development of the DISC module, the code base needs better embedding in version management, unit testing and some modularization, with each module representing a relevant domain, being developed, tested and documented separately and each with their own code base repository.

Apart from addressing the above limitations, DISC-CARBON needs improved embedding in the IMAGE framework (1) to enable scenario analysis and (2) to enable analysis of the interface of watersheds to the rest of the earth system. The last chapter is a first effort to place river systems in the larger context of the earth system. . Embedding DISC in the IMAGE framework will enable to study how river C fluxes change due to future climate, land-use and other environmental changes and how this will feed back to the global C cycle.

---

---

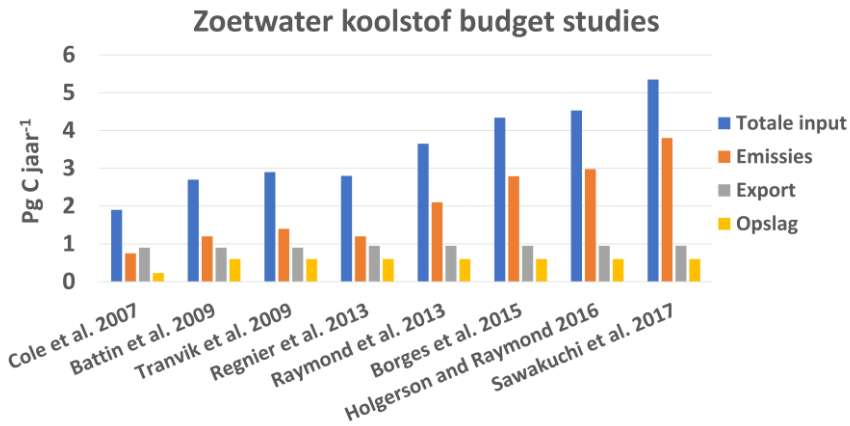
## **Synthese (Dutch translation)**

Deze thesis verkende het mondiale zoetwaterkoolstofbudget en zijn spreiding over ruimte en tijd gedurende de 20<sup>ste</sup> eeuw. Daarbij werd gebruik gemaakt van het mechanistische IMAGE-Dynamic Global Nutrient Model (IMAGE-DGNM) met de nieuw ontwikkelde Dynamic InStream Chemistry Carbon module.(DISC-CARBON). Dit model koppelt rivierafvoerhydrologie, omgevingscondities en koolstofafgifte van land en genereert koolstofstromen van bovenstrooms naar riviermondingen. DISC-CARBON is een ruimtelijk expliciet model met een resolutie van 0.5 graad bij een 0.5 graad die concentraties, transformaties en stromen van opgelost inorganisch koolstof (DIC), opgelost organisch koolstof (DOC) en terrestrische en autochtone koolstof deeltjes (POC) simuleert in één integraaloplossing. In deze samenvatting zijn de resultaten samengevat en worden ze vergeleken met andere studies die allen een andere benadering hebben. Daarnaast wordt besproken hoe relevant het is dat het zoetwaterkoolstofbudget wordt meegenomen in het mondiale koolstofbudget. Het laatste deel van deze samenvatting bespreekt de tekortkomingen van het model en mogelijke verbeterpunten.

### **Het zoetwaterkoolstofbudget**

Over het algemeen zijn de resultaten van DISC-CARBON voor mondiale import, begraving en CO<sub>2</sub> emissies in lijn met andere studies, maar er duidelijke verschillen te vinden die te maken hebben met de gebruikte benadering (Figuur 1).

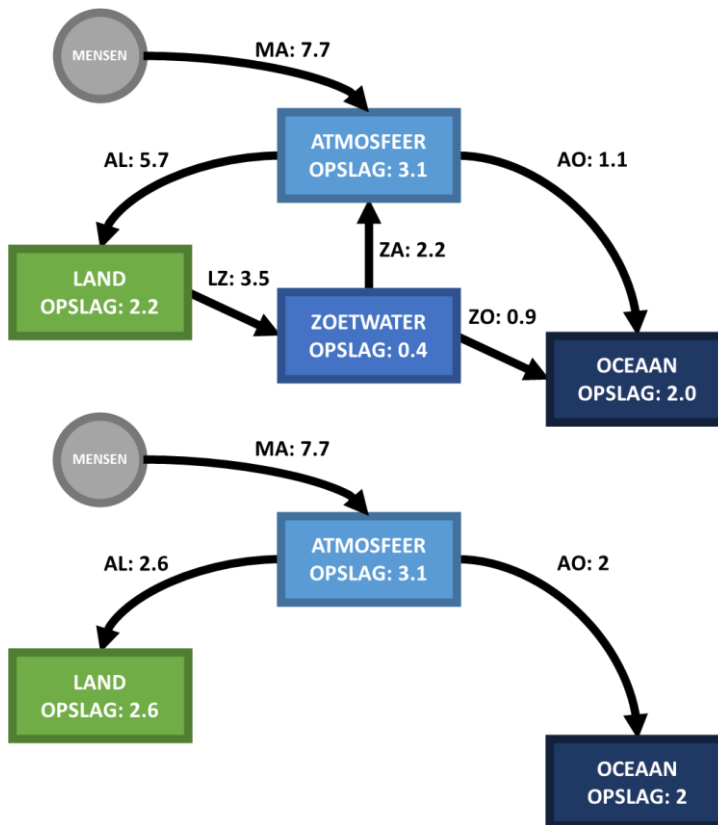
DISC-CARBON heeft een tijdruimtelijk consistente berekening gemaakt van mondiale koolstofconcentraties en koolstofbudgetten van zoetwatersystemen. De module maakt het mogelijk om te kwalificeren waarom en kwantificeren hoeveel en waar import, emissies, export en opslag zijn veranderd gedurende de twintigste eeuw. Budgetstudies die tot nu toe waren gepubliceerd hebben de limitaties (1) dat ze statisch koolstofbudgetten zijn gebaseerd op geaggregeerde data over langere periodes, (2) dat ze een gelimiteerde ruimtelijke dekking hebben die is geëxtrapoleerd is naar mondiale schaal en/of (3) dat ze niet met een mondiaal consistente methode gekwantificeerd zijn.



**Figuur 1. Vergelijking van DISC-CARBON resultaten in van Hoek et al., (2021) met andere mondiale zoetwater koolstof budget studies in chronologische volgorde.**

Aan het einde van de 20<sup>e</sup> eeuw is de totale import van koolstof van land naar zoetwatersystemen 3,5 Pg koolstof jaar<sup>-1</sup>, is de begraving 0,4 Pg koolstof jaar<sup>-1</sup> en is de koolstofdioxide emissie 2,2 Pg koolstof jaar<sup>-1</sup>. Toenemende mondiale koolstof import, begraving en koolstofdioxide emissies zoals beschreven in literatuur wordt bevestigd door DISC-CARBON. Mondiale koolstofexport naar oceanen is stabiel rond de 0,9 Pg koolstof jaar<sup>-1</sup>. Dit duidt erop dat mondiale stroomgebieden compenseren voor de toegenomen koolstof inputs door meer koolstof vast te houden en meer koolstofdioxide te emitteren naar de atmosfeer. Lange-termijn veranderingen en ruimtelijke patronen van concentraties en stromen van verschillende koolstof vormen in mondiale riviernetwerken zijn het gevolg van veel verschillende parallelle en tegelijkertijd plaatsvindende processen, zoals door invloeden van lithologie, klimaat, hydrologie van stroomgebieden, terrestrische en biologische koolstofbronnen, koolstoftransformaties in de waterkolom en menselijke interferentie zoals het bouwen van stuwweren. De toegenomen koolstofretentie in zoetwatersystemen, van 0,3 Pg koolstof jaar<sup>-1</sup> in het eerste decennium van de 20<sup>ste</sup> eeuw naar 0,4 Pg koolstof jaar<sup>-1</sup> in het laatste decennium van de 20<sup>ste</sup> eeuw is waarschijnlijk sterk gerelateerd aan het toegenomen aantal dammen. Koolstofdioxide emissies uit zoetwatersystemen namen toe met 0,2 Pg koolstof jaar<sup>-1</sup> van een gemiddelde van 2,1 Pg koolstof jaar<sup>-1</sup> in de 1900's naar een gemiddelde van 2,3 Pg koolstof jaar<sup>-1</sup> in de 1990's, vooral als gevolg van toegenomen terrestrisch koolstofimport. De meest koolstofdioxide emissies ontstaan uit overstromingsvlaktes of uiterwaarden. Zij stoten 1,4 Pg koolstof jaar<sup>-1</sup>. Rivieren stoten 0,8 Pg koolstof jaar<sup>-1</sup> uit, vooral door de instroom van oververzadiging van koolstofdioxide in

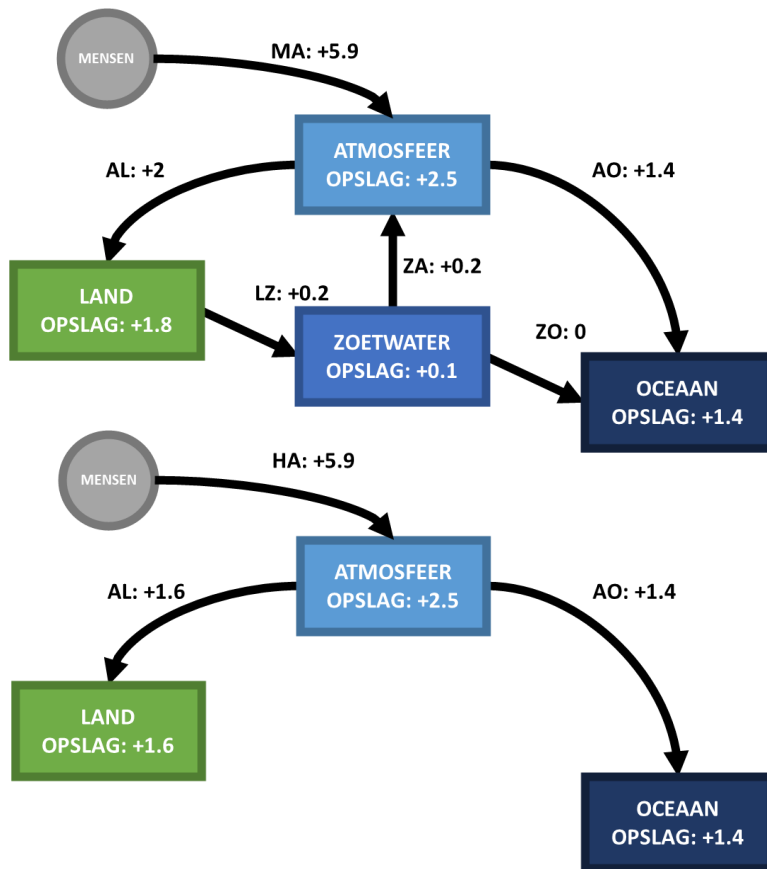
grondwater. (Stuw)meren stoten 0,2 Pg koolstof jaar<sup>-1</sup> uit. Hoewel de import van organisch koolstof door bodemerositie toenam van 106 Tg koolstof jaar<sup>-1</sup> naar 168 Tg koolstof jaar<sup>-1</sup> en het volume van reservoirs toenam van bijna 0 naar meer dan 3500 km<sup>3</sup>, duiden simulaties van DISC-CARBON niet op grote invloed van deze veranderingen op mondiale koolstofdioxide uitstoot van zoetwatersystemen; echter, hierbij is geen rekening gehouden met eutrofiëring.



**Figuur 2. Een wereldwijd koolstofbudget met zoetwatersystemen (boven) en een wereldwijd koolstofbudget zonder zoetwatersystemen (onder) voor de jaren 1990's in Pg koolstof jaar<sup>-1</sup>**

## Het mondiale koolstofbudget

In het laatste hoofdstuk van deze thesis werden de implicaties van het integreren van het zoetwaterkoolstofbudget in het mondiale koolstofbudget verkend. Oorspronkelijk was netto atmosfeer-land flux (2,3 Pg koolstof jaar<sup>-1</sup> (Friedlingstein et al., 2022)) altijd een restflux om andere fluxen van en naar de atmosfeer te verdisconteren, en werd deze flux toegewezen aan koolstofopname door terrestrische systemen (Ciais et al., 2013b; Huntzinger et al., 2017; Keenan and Williams, 2018); weergegeven in figuur 2. Als zoetwatersystemen meegenomen worden in het mondiale koolstofbudget, moet deze rest flux meer dan verdubbeld worden naar 5,7 Pg koolstof jaar<sup>-1</sup> om de emissies van zoetwatersystemen te verdisconteren (figuur 2 boven). Dit impliceert dat als we lateraal transport en de processen in de waterkolom meenemen in het mondiale koolstofbudget, de netto koolstofflux van atmosfeer naar land (daarbij doelend op alleen de terrestrische component, niet de zoetwatersystem) veel groter dan eerder gedacht en tevens leidt tot een gesloten koolstofbudget. Deze 5,7 Pg koolstof jaar<sup>-1</sup> van atmosfeer naar land is daarnaast ook veel groter dan de netto koolstofflux van atmosfeer naar terrestrische systemen zoals geschat door terrestrische vegetatiemodellen (2,3 Pg koolstof jaar<sup>-1</sup> (Friedlingstein et al., 2022)). Deze modellen nemen doorgaans geen laterale koolstofstromen mee in hun budget. Een dergelijke koolstofflux van land naar zoetwatersystemen moet in deze terrestrische vegetatiemodellen meegenomen worden om een betere schatting te maken van de werkelijke terrestrische koolstof opslag. Het mondiale koolstofbudget is sterk veranderd (figuur 3 onder) als gevolg van koolstofemissies door menselijke activiteiten. Echter, de quantitative respons van zoetwater systemen wordt nog altijd slecht begrepen. Verschillende studies tonen aan dat menselijke activiteit interfereren met de koolstofcyclus in zoetwatersystem (e.g. Raymond et al., 2008; Van Cappellen and Maavara, 2016; Maavara et al., 2017). DISC-CARBON geeft aan dat hoewel zoetwatersystemen een belangrijke component in het mondiale koolstofbudget zijn, zoetwaterkoolstofbudgetten veel minder gevoelig zijn voor door mensen veroorzaakte mondiale interferenties dan terrestrische koolstofbudgetten.



**Figuur 3.** De verandering van het mondiale koolstofbudget van de 1900's tot de 1990's. Boven het budget inclusief zoetwatersystemen, onder het budget exclusief zoetwatersystemen in Pg koolstof jaar<sup>-1</sup>.

Figuur 3 laat zien dat de mondiale koolstofopslag in de atmosfeer (+2,5 Pg koolstof jaar<sup>-1</sup> of ~431%), oceanen (+1,4 Pg koolstof jaar<sup>-1</sup> of 275%) en land (+1,8 Pg koolstof jaar<sup>-1</sup> of ~495%) snel zijn toegenomen gedurende de 20<sup>ste</sup> eeuw. Netto begraving daarentegen, nam slechts met 20% toe (+0,1 Pg koolstof jaar<sup>-1</sup>). Andere fluxen in zoetwatersysteem veranderden zelfs nog minder, zoals koolstofimport (+0,2 Pg koolstof jaar<sup>-1</sup> of ~6%), koolstofdioxide emissies (+0,2 Pg koolstof jaar<sup>-1</sup> of 8%) and koolstofexport (0 Pg koolstof jaar<sup>-1</sup>). Regnier et al., (2013) maakte een allereerste schatting van menselijke verstoring van zoetwatersystemen in de mondiale koolstofcyclus en concludeerde dat de flux van koolstof naar zoetwatersystemen is toegenomen met ~1.0 Pg koolstof jaar<sup>-1</sup> (+67%) sinds pre-industriële tijden. Deze



toename werd voornamelijk veroorzaakt door versnelde flux van koolstof in bodems naar zoetwatersystemen. Deze sterke gevoeligheid voor menselijke interferentie is niet terug te zien in simulaties door DISC-CARBON. Daarnaast, de toename van netto erosie van particuliere organische koolstof (Langeveld et al., 2021) door bodems was zeer beperkt in de DISC-CARBON simulatie (+6 Tg koolstof jaar<sup>-1</sup>).

## Outlook

Dit werk richtte zich op het historische mondiale koolstofbudget van zoetwatersystemen, met een jaarlijkse tijdstap, met een resolutie van een 0,5 graad bij een 0.5 graad. Het hoofddoel was om het lange-termijns koolstofbudget te kwantificeren. Met dit in gedachte zijn er twee belangrijke richtingen om mee verder te gaan vanaf de huidige stand van zaken.

DISC-CARBON heeft aantal limitaties, onder te verdelen in beperkingen in hydrologische/hydrodynamische en sedimentologische beschrijving van binnenwateren, de tijdruimtelijke resolutie en de koolstof-nutrient stoichiometrie.

1. Hydrodynamische en sedimentologische representatie van overstromingsgebieden. Overstromingsgebieden zijn een hydrologisch dynamisch raakvlak tussen land en zoetwatersysteem, een grote bron voor particulier organisch koolstof, een belangrijke oorsprong voor koolstofdioxide emissies en plekken met veel begraving van organisch koolstof. Variabelen en parameters die verantwoordelijk zijn voor deze processen zijn heel beperkt tot niet gedefinieerd in DISC-CARBON.
2. Kleine meren en vijvertjes zijn grote bron van koolstofdioxide emissies volgens Holgerson & Raymond (2016). Op dit moment worden kleine meren en vijvertjes niet expliciet benoemd in DISC-CARBON. Het blijft onduidelijk of en hoe deze zijn gekoppeld aan het continuüm en hoe zij kunnen worden ingebed in het DISC raamwerk. Kleine meren en vijvertjes zijn tevens verantwoordelijk voor een groot deel van de methaanemissies. Methaanemissies worden niet gemodelleerd in DISC-CARBON, hoewel zij mogelijk een groot deel van het koolstofbudget van zoetwatersystemen uitmaken. Verbeterde parameterisatie van organische koolstofdepositie in sedimenten en tijdruimtelijke representatie van redox condities is nodig voor mechanistische modelleren van methaanemissies uit zoetwatersysteem.

3. De hydrodynamische en morfologische karakteristieken van (stuw)meren worden niet meegenomen in DISC-CARBON, hoewel deze mogelijk een impact hebben op hun koolstoffluxen, door effecten op emissies van koolstofdioxide en methaan (Schilder et al., 2013) of door effecten op koolstofbegraving (Forsberg, 1989).
4. DISC-CARBON neemt processen zoals respiratie, productie, depositie en resuspensie mee, maar de tijdsresolutie is te grof om deze processen goed te beschrijven. Seizoensafvoer, dag- en seizoensvariatie van temperatuur en licht kan een invloed hebben op de response van het gemodelleerde systeem. Het is onduidelijk hoe gevoelig het model is voor een verhoogde/verlaagde tijdsresolutie. In lijn daarmee, deze zelfde processen hangen af van koolstofimport, door grondwater of door bladval. Deze processen hebben een grote ruimtelijke heterogeniteit. Het is onduidelijk hoe gevoelig de huidige modelresultaten zijn voor verhoogde/verlaagde ruimtelijke resolutie.
5. Tenslotte, koolstof is een onderdeel van een stoichiometrische context met stikstof, fosfor en silicon. Een belangrijke volgende stap voor de DISC module is om deze componenten met elkaar te koppelen. Hiermee kan bijvoorbeeld een realistischere representatie worden gemaakt van de tijdruimtelijke verdeling van nutriëntfertilisatielimitering voor primaire productie. Meer of minder primaire productie leidt tot meer of minder begraving van organisch koolstof en daarmee heeft het ook gevolgen voor koolstofemissies naar de atmosfeer en de export naar oceanen.

Het oorspronkelijke idee van DISC is altijd geweest dat verschillende versies voor koolstof, stikstof, fosfor en silicon apart van elkaar worden ontwikkeld waarna ze kunnen worden samengevoegd in één berekening voor alle nutriënten bij elkaar. Het huidige ontwikkelproces echter staat dat in de weg. Hoewel de code-bases voor koolstof, stikstof, fosfor en silicon allemaal dezelfde oorsprong hebben, is het samenvoegen een enorme uitdaging geworden omdat ze compleet onafhankelijk van elkaar verder ontwikkeld zijn. Vanuit een technisch perspectief is het belangrijk dat verdere ontwikkeling plaatsvindt ingebed in versiebeheer, unit-testing en modularisatie. Elke module binnen DISC neemt een relevant domain binnen zoetwatersysteemberekeningen voor zijn rekening. Deze modules kunnen onafhankelijk van elkaar worden ontwikkeld, getest en gedocumenteerd en hebben elk hun eigen code-base repository.

Los van de hierboven genoemde beperkingen, DISC-CARBON heeft een betere inbedding in het IMAGE-raamwerk (1) voor scenario analyse en (2) voor analyse van de koppeling van biogeochemie in stroomgebieden met de rest van het aardsysteem. Het laatste hoofdstuk van deze thesis was een eerste opzet om stroomgebieden in de bredere context van het aardsysteem te plaatsen. Het inbedden van DISC in het IMAGE raamwerk geeft inzicht in hoe koolstoffluxen in rivieren zullen veranderen door verandering in klimaat, landgebruik en andere omgevingsfactoren en hoe dit terugkoppelt in de mondiale koolstofcyclus.

## References

- Van Cappellen, P. and Maavara, T.: Rivers in the anthropocene: Global scale modifications of riverine nutrient fluxes by damming, *Ecohydrol. Hydrobiol.*, 2016.
- Ciais, P., Sabine, C., Bala, G., Bopp, L., Brovkin, V., Canadell, J., Chhabra, A., DeFries, R., Galloway, J. and Heimann, M.: Carbon and other biogeochemical cycles, in *Climate Change 2013: The Physical Science Basis. Contribution of Working Group I to the Fifth Assessment Report of the Intergovernmental Panel on Climate Change*, pp. 465–570, Cambridge University Press., 2013.
- Forsberg, C.: Importance of sediments in understanding nutrient cyclings in lakes, *Hydrobiologia*, 176(1), 263–277, 1989.
- Friedlingstein, P., Jones, M. W., O’Sullivan, M., Andrew, R. M., Bakker, D. C. E., Hauck, J., Le Quéré, C., Peters, G. P., Peters, W., Pongratz, J., Sitch, S., Canadell, J. G., Ciais, P., Jackson, R. B., Alin, S. R., Anthoni, P., Bates, N. R., Becker, M., Bellouin, N., Bopp, L., Chau, T. T. T., Chevallier, F., Chini, L. P., Cronin, M., Currie, K. I., Decharme, B., Djeutchouang, L. M., Dou, X., Evans, W., Feely, R. A., Feng, L., Gasser, T., Gilfillan, D., Gkritzalis, T., Grassi, G., Gregor, L., Gruber, N., Gürses, Ö., Harris, I., Houghton, R. A., Hurtt, G. C., Iida, Y., Ilyina, T., Luijkx, I. T., Jain, A., Jones, S. D., Kato, E., Kennedy, D., Klein Goldewijk, K., Knauer, J., Korsbakken, J. I., Körtzinger, A., Landschützer, P., Lauvset, S. K., Lefèvre, N., Lienert, S., Liu, J., Marland, G., McGuire, P. C., Melton, J. R., Munro, D. R., Nabel, J. E. M. S., Nakaoka, S.-I., Niwa, Y., Ono, T., Pierrot, D., Poulter, B., Rehder, G., Resplandy, L., Robertson, E., Rödenbeck, C., Rosan, T. M., Schwinger, J., Schwingshackl, C., Séférian, R., Sutton, A. J., Sweeney, C., Tanhua, T., Tans, P. P., Tian, H., Tilbrook, B., Tubiello, F., van der Werf, G. R., Vuichard, N., Wada, C., Wanninkhof, R., Watson, A. J., Willis, D., Wiltshire, A. J., Yuan, W., Yue, C., Yue, X., Zaehle, S. and Zeng, J.: *Global Carbon Budget 2021*, *Earth Syst. Sci. Data*, 14(4), 1917–2005, doi:10.5194/essd-14-1917-2022, 2022.
- Holgerson, M. A. and Raymond, P. A.: Large contribution to inland water CO<sub>2</sub> and CH<sub>4</sub> emissions from very small ponds, *Nat. Geosci.*, 9(3), 222–226, doi:10.1038/ngeo2654, 2016.
- Huntzinger, D. N., Michalak, A. M., Schwalm, C., Ciais, P., King, A. W., Fang, Y., Schaefer, K., Wei, Y., Cook, R. B. and Fisher, J. B.: Uncertainty in the response of terrestrial carbon sink to environmental drivers undermines carbon-climate feedback predictions, *Sci. Rep.*, 7(1), 1–8, 2017.
- Keenan, T. F. and Williams, C. A.: The terrestrial carbon sink, *Annu. Rev. Environ. Resour.*, 43, 219–243, 2018.

- Langeveld, J., Bouwman, A. F., van Hoek, W. J., Vilmin, L., Beusen, A. H. W., Liu, X., Mogollón, J. M. and Middelburg, J. J.: Towards a balanced budget? Including lateral carbon removal in the global terrestrial C budget (in preparation), n.d.
- Maavara, T., Lauerwald, R., Regnier, P. and Cappellen, P. Van: Global perturbation of organic carbon cycling by river damming, *Nat. Commun.*, accepted(May), 1–10, doi:10.1038/ncomms15347, 2017.
- Raymond, P. a, Oh, N.-H., Turner, R. E. and Broussard, W.: Anthropogenically enhanced fluxes of water and carbon from the Mississippi River., *Nature*, 451(7177), 449–52, doi:10.1038/nature06505, 2008.
- Regnier, P., Friedlingstein, P., Ciais, P., Mackenzie, F. T., Gruber, N., Janssens, I. A., Laruelle, G. G., Lauerwald, R., Luyssaert, S. and Andersson, A. J.: Anthropogenic perturbation of the carbon fluxes from land to ocean, *Nat. Geosci.*, 6(8), 597–607, 2013.
- Schilder, J., Bastviken, D., van Hardenbroek, M., Kankaala, P., Rinta, P., Stötter, T. and Heiri, O.: Spatial heterogeneity and lake morphology affect diffusive greenhouse gas emission estimates of lakes, *Geophys. Res. Lett.*, 40(21), 5752–5756, 2013.

---

## Acknowledgements

Working on my PhD has been an amazing journey and experience which would not have been possible without the help of many colleagues, friends and family. In the very first place I would like to thank my promotors professor Jack Middelburg and professor Lex Bouwman; without you, this work wouldn't be here. Jack, you are truly a walking encyclopedia, not only filled with knowledge but also with a lot of wisdom. Thank you for always being supportive and also always seeing the good things in my work. I never forget our shared happiness when I had a first stable run of the full biology version of my model. Thank you for your everlasting preciseness and new angles. Lex, thank you so much for your patience! There were many struggles on my way, but I always felt you kept believing in me. You have been reading my texts over and over again with always new helpful comments. I want you to know that your help is being incredibly appreciated. Also thank you for taking me and the rest of the group to Amsterdam for beers on the water, two times. Unforgettable memories! Many thanks to Arthur Beusen as well, you are always available for an open discussion, for my questions on your computer science insights, and for setting up the foundation for the CARBON-DISC model. You are always around with a jolly vibe!

The Utrecht team is dear to me. First, my office companion Joep. Joep, thank you a lot for bearing with me through this exploration. Thank you for sharing the difficult times we faced during development and to keep giving me that pat on the back when I had some tough times. You were a fantastic companion to have during our travels to Brussels, Paris and Hamburg. Also, I will always be open for another “potje tafeltennis”. Xiaochen, I never forget when our friendship started. Ever since we are tuned to the same frequency. Thank you for joining to solve another ODE solution exception. Thank you for our great conversations during our carpooling. Lauriane, thank you for being a great companion and sparring partner altogether. Thanks for reading through my writings and your valuable comments. José, thank you for reading and always providing razor-sharp insights. Junjie, thank you a lot for helping me finalizing the writing. Philip, many thanks for listening to my frustrations in tough times. Marijn and Lisa, students that worked with me, thank you for joining me in your learning journey. Itzel, Caroline, thanks for helping me with your Linux desktop when I was in dire need! The team of C-CASCADES, thank you for sharing your views and ideas in Brussels, Hamburg and Paris. Laurens Ganzeveld, thank you for introducing me to this PhD position

---

Thanks to the reading committee and dissertation committee I am able to make this life chapter come to an end. Thank you prof. Dekker, prof. Soetaert, prof. Regnier, prof. Friedlingstein, prof van Vuuren and prof. de Bresser. Thank you to Margot Stoete for designing the cover and bookmark.

I would like to thank my close friends. Mart, thank you for always being supportive. You helped me out in very dark personal times, I will never forget that. Max, Yorick, Leon, Jonne, we understand each others deep emotions through music. I wish we will always keep doing that, it keeps me going. Jeroen, thank you for being my cycling mate. We speak through our legs, you get the best out of me on the bike, always beyond new limits. I can't wait for a new crazy challenge. Art, you must know how important you have been for me in the past few years. You were the best colleague for me to start to professionalize in IT. Jonathan, thank you for all the discussions and gaming hours in Gran Turismo.

Nathalie, you have seen from very close how hard this endeavour was for me. Thank you for being on my side for many years through good and bad times. You will always have a special place in my heart.

Shirin, without your endless energy and support, I would never have been able to finish this work. Thank you for your light and thank you for your warmth. Thank you for leading me and for following me. Thank you for reading me and for writing me. Thank you for being a lovely partner. Your smile and happiness keeps me going.

Homayoon and Massi, Negar, Amin and Nazanin, thank you too for thinking of me. Although you are geographically so far away, I can feel your love and support very close.

Last, but not definitely not least, I want to thank my close and dear family, mam Wilma, vader Wim, sister Marijn, brother Thijs Jan for being the stable backbone during my entire PhD. I always found you by my side through highs and lows. This booklet is dedicated to you.

---

## Curriculum Vitae

Wim Joost van Hoek was born at July 5, 1987, in Vlaardingen, the Netherlands. After graduating at Udens College in Uden, he started his bachelor Soil, Water and Atmosphere at Wageningen University in 2006. In 2009, he started his Master Climate Studies at Wageningen University. He graduated in 2012. During his thesis project he explored the potential connection between ozone deposition and a declining CO<sub>2</sub> uptake through photosynthesis on the basis of a single column model supervised by dr. Laurens Ganzeveld. After that, during an internship at ECN, Petten, he derived under supervision of dr. Arnoud Frumau fluxes of ozone from gradient tower measurements and calculated attributions different removal processes to the total deposition flux. After graduation Wim Joost was employed at EARS E2M in Delft to develop climate and agriculture related remote sensing data products on the basis of MeteoSat data. In March 2016 he started at Utrecht University. During this project he developed together with colleagues a numerical scheme for carbon chemistry, ecology, CO<sub>2</sub> emissions, deposition/resuspension processes and transport (DISC-CARBON) coupled to an existing global hydrological model (PCR-GLOBWB) and a global terrestrial earth system model (IMAGE). The results of that work are presented in this thesis.

During his PhD candidacy, Wim Joost found his passion in programming; To pursue a professional career in IT, he decided to make a career switch towards software development. As from June 2020 until November 2022 he was employed by Keylane BV as Java developer. Per February 2023 he is employed as software engineer at Nederlands Forensisch Instituut (NFI).